



The conference series INTERCOH is dedicated to improving our understanding of the physical processes of cohesive sediment in the natural environment, which are still poorly understood, though research into this topic started almost half a century ago. Yet, this understanding is important, as the earth's surface is almost entirely covered with larger or smaller amounts of cohesive sediment, or mud as it is generally known, with the exception perhaps of some deserts and some parts of the ocean seabed. It is, and has

been throughout time, both a blessing and a curse to mankind.

The conference series INTERCOH, initiated by Dr. Reg Parker and Prof. Ashish Mehta, offers an international platform where young, experienced and world leading scientists and engineers can meet and discuss the latest progress in the area of cohesive sediment properties, dynamics and modeling.

This book of abstracts contains contributions on the basis of theoretical and numerical studies, and on the basis of field and laboratory measurements, as well as contributions on chemico-biological processes affecting the physical behavior of cohesive sediment.

www.INTERCOH.org

Book of abstracts

13th International Conference on Cohesive Sediment Transport Processes

7-11 September 2015
Leuven, Belgium

Erik Toorman, Tina Mertens,
Michael Fettweis & Joris Vanlede (Editors)



INTERCOH2015

LEUVEN BELGIUM

VLIZ SPECIAL PUBLICATION 74

BOOK OF ABSTRACTS

13th International Conference on
Cohesive Sediment Transport Processes

7-11 September 2015
Leuven, Belgium

Erik Toorman, Tina Mertens,
Michael Fettweis & Joris Vanlede (Editors)



INTERCOH2015

LEUVEN BELGIUM

VLIZ SPECIAL PUBLICATION 74

INTERCOH2015 – 13th International Conference on Cohesive Sediment Transport Processes is organised by the KU Leuven Hydraulics Laboratory (Department of Civil Engineering), in collaboration with: Flanders Marine Institute (VLIZ), Flanders Hydraulics Research (FHR), and the Royal Belgian Institute of Natural Sciences - OD Nature (RBINS) (former MUMM).

STEERING COMMITTEE

- Joe Gailani, ERDEC, US Army Corps of Engineers, USA
- Qing He, East China Normal University, China
- Romaric Verney, IFREMER, France
- Yasuyuki Nakagawa, PARI, Japan
- Guan-Hong Lee, Inha University, Korea
- Jerome Maa, VIMS, USA
- Larry Sanford, University of Maryland, USA (**chair**)
- Jez Spearman, HR Wallingford, UK
- Mohsen Soltanpour, K. N. Toosi University of Technology, Iran
- Erik Toorman, KU Leuven, Belgium
- Susana Vinzon, Federal University of Rio de Janeiro, Brazil
- Johan Winterwerp, Deltares & Delft University of Technology, The Netherlands

LOCAL ORGANISING COMMITTEE

- Dr Matthias Baeye (RBINS - OD Nature [former MUMM])
- Prof. Jean Berlamont (KU Leuven)
- Prof. Margaret Chen (Vrije Universiteit Brussel)
- Prof. Tom Demulder (Universiteit Gent)
- Ingrid Dobbelaere (VLIZ)
- Dr Michael Fettweis (RBINS - OD Nature [former MUMM]), core team member
- Ir. Tina Mertens (VLIZ), core team member
- Prof. Jaak Monbaliu (KU Leuven)
- Marc Sas (IMDC)
- Prof. Sandra Soares-Frazão (UCL: Université catholique de Louvain)
- Prof. Stijn Temmerman (Universiteit Antwerpen)
- Prof. Erik Toorman (KU Leuven), **chair**
- Danny Uten (KU Leuven), website
- Dr Dries Van den Eynde (RBINS - OD Nature [former MUMM])
- Joris Vanlede (Flanders Hydraulics Research), core team member
- Dr Tomas Van Oyen (Flanders Hydraulics Research)
- Anita Vermunicht (KU Leuven), conference secretariat

INTERCOH website: www.intercoh.org

WITH FINANCIAL SUPPORT OF:



**Fonds Wetenschappelijk Onderzoek
Vlaanderen**
Opening new horizons



DEME
Dredging, Environmental
& Marine Engineering

www.deme-group.com



www.asicon.be/en



www.nortek-as.com



www.imdc.be

Cover photo: Upwelling of sediments by waves along the Belgian coast. © Erik Toorman

This publication should be quoted as follows:

Toorman Erik, Tina Mertens, Michaël Fettweis & Joris Vanlede (Eds). 2015. INTERCOH2015. 13th International Conference on Cohesive Sediment Transport Processes. Leuven, Belgium, 7-11 September 2015. Hydraulics Division, Department of Civil Engineering, KU Leuven. VLIZ Special Publication 74 – Flanders Marine Institute (VLIZ). Oostende, Belgium. xii+224p.

ISSN 1377-0950

ISBN 978-94-920430-8-5

Reproduction is authorized, provided that appropriate mention is made of the source.

PREFACE

INTERCOH2015 is the 13th edition of an international gathering of scientists and engineers facing challenges posed by the presence of cohesive sediments (“mud”) in the aquatic environment. Even though for the first time organized in Belgium, it is not the first international meeting of this kind. In November 1990 (25 years ago) an International Workshop on Cohesive Sediments, entitled *Towards a definition of “mud”*, was organized by the Royal Belgian Institute for Natural Sciences in Brussels, in collaboration with many national partners, under the chair of Prof. Stanislas Wartel. This very likely triggered the further internationalization of Prof. Ashish Mehtha’s workshops in the US, resulting in the first edition under the title INTERCOH, which was organized in 1994 for the first time outside the US by HR Wallingford in the UK.

For further information on INTERCOH, visit the website www.intercoh.org.

Even though Belgium is small, the problems caused by the presence of mud in the major ports of Antwerp and Zeebrugge and their access channels, have triggered scientific mud research, a challenge taken up by Prof. Jean Berlamont of the KU Leuven in the early 1980s. Belgium is also the home to two of the largest dredging companies in the world.

This book of abstracts gives an impression of the scientific questions and practical problems that are faced by scientists and engineers today. Sediment research is difficult; cohesive sediment behavior is more complex than that of non-cohesive sediments. Some of the questions are (very) old and have not found adequate solutions for many years. Whether this edition succeeds in presenting progress and innovation is left to the judgment of the participants.

The submitted abstracts have been evaluated by members of the Local Organizing Committee (LOC). The compilation of the book and its lay-out has been carried out by VLIZ under the excellent coordination of Ingrid Dobbelaere.

Full papers will be published in the journal *Ocean Dynamics* (Springer) after peer-review, forming a Topical Collection.

This conference would not have been possible without the efforts of many people. The help and advice from the other members of the core team of the LOC, consisting of Tina Mertens (VLIZ), Michael Fettweis (RBINS) and Joris Vanlede (Flanders Hydraulics) have been invaluable. The conference secretariat was well taken care of by Anita Vermunicht (KU Leuven, Hydraulics Division). Many members of the KU Leuven Hydraulics research staff have been helping out for all kinds of logistic tasks.

Finally, I would also like to thank the sponsors for supporting this conference: FWO Vlaanderen, DEME, ASICON-Geometius, Nortek and IMDC.

Prof. Dr Erik A. Toorman
Chairman INTERCOH2015

TABLE OF CONTENTS

PREFACE	iii
----------------------	------------

ORAL PRESENTATIONS

Attari Morteza Jedari, Arash Bakhtiari, S. Abbas Haghshenas, J. Ebrahim Hamidian and Jun Sasaki. Long-term suspended sediment transport patterns over the North-Western part of the Persian Gulf, applying a three-dimensional hydrodynamic model	3
Barciela Rial Maria, Johan C. Winterwerp, Jasper Griffioen and Thijs van Kessel. Consolidation and strength development of soft mud deposits by horizontal drainage	5
Benson Tom and John Baugh. Modelling the effects of water injection dredging on water quality	7
Bi Qilong and Erik Toorman. On two-phase/mixture modelling of sediment transport and turbulence modulation due to fluid-particle interactions	9
Cartwright Grace M., Kelsey A. Fall and Carl T. Friedrichs. Identification of suspended resilient pellets in particles tracked by a Particle Image Camera System (PICS) in a muddy estuary	11
Chassagne Claire, Maria E. Ibanez and Andy Manning. Flocculation in natural environment: from the lab to the field	13
Chen Margaret. Flocculation in turbulent flow – a view into particle network	15
Chou Tzu-Yin, Che-Yuan Liu, Hao-Cheng Yu, Jason C.S. Yu, Quinten Vanhellemont and Michael Fettweis. Surface SPM concentration in Taiwan Strait during summer and winter monsoon	17
Claeys S., P. Staelens, J. Vanlede, M. Heredia, T. Van Hoestenbergh, T. Van Oyen and E. Toorman. A rheological lab measurement protocol for cohesive sediment	20
Cronin Katherine, Claire Jeuken, Julia Vroom, Thijs van Kessel and Jamie Lescinski. Modelling investigations on deep sea mine tailing plume dispersion on the Chatham Rise	22
Dale Jonathan, Paul Kilkie and Heidi Burgess. Spatial and temporal variations of <i>in situ</i> erosion shear strength of newly inundated inter-tidal sediment	24
de Linares Matthieu, Régis Walther, Julien Schaguene, Cayrol Cyrielle and Luc Hamm. Development of an hydro-sedimentary 3D model with sand-mud mixture - calibration and validation on 6 years evolution in the Seine Estuary	25
de Lucas Pardo Miguel, Thijs van Kessel and Johan C. Winterwerp. The role of biota in fine sediment transport processes in the Markermeer: a synthesis	27
Decrop Boudewijn, Tom De Mulder, Erik Toorman and Marc Sas. A parameter model for dredge plume sediment source terms	28

Dujardin Arvid, Joris Vanlede, Thomas Van Hoestenbergh, Luc Van Poucke, Michael Fettweis, Claudio Cardoso, Carlos Velez, Renaat De Sutter and Chantal Martens. Factors influencing top sediment layer and SPM concentration in the Zeebrugge harbor	30
Fall Kelsey A., Carl T. Friedrichs, Grace M. Cartwright and David G. Bowers. Controls on suspended particle properties and water clarity along a partially-mixed estuary, York River, Virginia, USA	32
Fettweis Michael, Matthias Baeye and Romaric Verney. Uncertainty of <i>in situ</i> SPM concentration measurements	34
Forsberg Pernille L., Verner B. Ernstsens, Ulrik Lumborg, Klavs Bundgaard and Aart Kroon. Modelling of sediment dynamics and the effect of mussel bioengineering in a non-tidal coastal lagoon, Rødsand lagoon, Denmark	36
Gailani Joseph, S. Jarrell Smith and Mathew Taylor. Physical process measurements of sediment suspension by vessel operations at Pearl Harbour, Hawaii	38
Hellmich Franziska, Achim Kopf and Peter Staelens. Benchmarking of three penetrometers for identification of fluid mud layers	40
Herrero Albert, Céline Berni and Benoit Camenen. Laboratory experiments on silt infiltration into a gravel bed	42
Hope Julie A., Andrew J. Manning, Rebecca J. Aspden, Jaco Baas and David M. Paterson. The roles of physical mixing and biochemical composition on the depositional characteristics of flocculated suspended sediment in the Eden Estuary, Scotland	44
Ibikunle Olugbenga, Alan Cuthbertson, John McCarter and Farzin Samsami. Measurement of density and porosity profiles within mixed sediment deposits using an electrical resistivity technique	46
Ibrahim Elsy, Kim Wonkook, Melba Crawford and Jaak Monbaliu. The impact of bio-physical thresholds on sediment analysis through field reflectance spectra and hyperspectral imagery	49
Janry Sébastien and Philippe Monnet. Rheological properties of cohesive sediments from Garonne Estuary	51
Kim Yong Hoon, Gi Young Bang, Tae In Kim, Yong Sik Song and Jong Seong Ryu. Relative effect of wind waves and tidal currents on sediment resuspension in the Saemangeum region, west coast of Korea	53
Kurtenbach Andreas, Tom Gallé and Reinhard Bierl. Analysing fluvial transport and deposition of kaolinite-clay during steady and unsteady flow	55
Le Hir Pierre, Florence Cayocca and Julie Vareilles. Estuarine morphodynamics: simulating schematic configurations with a process-based 3D model with focus on the evolution of tidal marshes under climate change	56
Lee Byung Joon and Mark Schlautman. Adsorption and flocculation mediated by polymeric substances in cohesive sediment suspensions: experimental study	58
Lee Guan-hong, Hyun-Jung Shin and Hyo-Bong Park. Evaluation of ADCP backscatter inversion to suspended sediment concentration in estuarine environments	60
Lichtman I.D., P.D. Thorne, J.H. Baas, L. Amoudry, J. Hope, R.D. Cooke, P.S. Bell, J. Malarkey, D.R. Parsons, J. Peakall, S.J. Bass, R.J. Schindler, L. Ye, R.J. Aspden, D.M. Paterson, A.G. Davies and A.J. Manning. The effects of mixed cohesive and non-cohesive sediment properties on bedform and suspended sediment dynamics in the intertidal Dee Estuary	62
Lumborg Ulrik and Klavs Bundgaard. Studies of the relationship between suspended sediment concentration and light attenuation	64

Maa J.P.-Y., Y.Y. Shao, X.T. Shen and J. Shen. Simulating extremely high ebb current velocities in the Changjing Deep-water Navigation Channel	66
MacDonald Lain T. and Julia C. Mullarney. Sediments in motion.....	68
Manning Andrew J. and David H. Schoellhamer. Quantifying and comparing settling velocity within the San Francisco Bay-Delta Estuary, northern California, USA.....	70
Marroig Patrícia and Susana Vinzon. Fluid mud transport from Patos Lagoon to Rio Grande Port, RS, Brazil	72
Mehta Ashish J. Small diameter limit of cohesionless particle erosion	75
Mengual Baptiste, Florence Cayocca, Pierre Le Hir, Thierry Garlan and Pascal Laffargue. Physical impacts induced by bottom trawling in the 'Grande-Vasière' area (Bay of Biscay)	76
Moriarty Julia, Courtney Harris, Christophe Rabouille and Flora Toussaint. Resuspension and sediment bed oxygen consumption: developing and testing a coupled model	78
Mosquera Rodrigo and Francisco Pedocchi. Yield strength determination from slump tests	80
Nakagawa Yasuyuki, Takumi Shinozawa, Yuji Matsumoto and Michiyuki Watanabe. Field measurement of fluid mud layer in dredged navigation channel at river mouth	82
Naulin Marie and Andreas Malcherek. Combining turbulence and mud rheology in a numerical 3D-model of the Ems Estuary.....	84
Orseau Sylvain, Sandric Lesourd, Nicolas Huybrechts and Antoine Gardel. Geomorphologic evolution of subtidal mud bank area through an estuary mouth. The case of Kaw mud bank (French Guiana).....	86
Riethmüller Rolf, Markus Schartau, Götz Flöser and Wolfgang Schönfeld. Deriving space-time information of the organic fraction of suspended particular matter in a coastal environment.....	89
Samiksha S.V., P. Vethamony, M.T. Babu and K. Sudheesh. Attenuation of 'short waves' in the mudbank region off Alleppey, Kerala coast, India.....	91
Saremi Sina, Nils Drønen and Hans Jacob Vested. Multiscale modelling of dispersive plumes	93
Schoellhamer David H. and Andrew J. Manning. Erosion characteristics and horizontal variability for small erosion depths in the Sacramento - San Joaquin River Delta, California, USA.....	95
Shen Xiaoteng and Jerome P.-Y. Maa. A conceptual one-dimensional flocculation model for floc size distributions of suspended kaolinite in a cylindrical tank	97
Sherwood Christopher R., Alfredo Aretxabaleta, Romaric Verney, Emmanuel Boss and Peter Thorne. Modeling floc dynamics observed during the OASIS experiment	99
Smith S. Jarrell, David Perkey and Anthony Priestas. Erosion thresholds and rates for sand-mud mixtures	100
Soltanpour Mohsen, Sami Saeideh and Hejazi Kouros. Numerical modelling of wave and non-Newtonian mud interaction.....	102
Sottolichio Aldo, Isabel Jalon Rojas and Sabine Shmidt. Calibration of sediment parameterizations to simulate the turbidity maximum in a highly turbid estuary: integration of model, field and satellite data	104

Spearman Jez. Flocculation, self-similarity and the rheology of aqueous clay suspensions.....	105
Tarhini Zaynab, Sébastien Jarny and Alain Texier. Rheology and local study of a transparent model cohesive sediment.....	107
Thorne Peter D., Iain T. MacDonald and Christopher E. Vincent. Examining flocculation processes using multi-frequency acoustics.....	110
Tokuzo Hosoyamada, Ayurzana Badarch and Takeshi Ohtake. Interaction of suspended sediment and salt wedge in a river estuary.....	112
Toorman E.A., I. Vandebeek, M. Liste-Muñoz, M. Heredia, I. Rocabado, J. Vanlede, G. Delefortrie, M. Vantorre and Y. Meersschaut. Drag on an object towed through a fluid mud layer: CFD versus experiment.....	114
Van den Eynde Dries, Matthias Baeye, Michael Fettweis, Frederic Francken and Vera Van Lancker. Validation of modelled bottom shear stress under the influence of currents and waves, using long-term measurements.....	116
van der Wegen Mick, Bruce Jaffe, Amy Foxgrover, Edwin Elias and Dano Roelvink. The impact of sea level rise on tidal mudflats: modelling decadal time scale mudflat morphodynamics in South San Francisco Bay.....	118
van Holland Gijsbert, Davy Depreiter, Han Winterwerp and Michael De Beukelaer-Dossche. Sediment management in the Seaschedt - risk of hyper turbidity.....	120
van Kessel Thijs, Katherine Cronin and Luca van Duren. On the impact of human activities on the SPM dynamics of the Dutch Wadden Sea.....	122
van Maren Bas, T. van Kessel, K. Cronin and L. Sittoni. The impact of channel deepening and dredging on the sediment concentration of the Ems Estuary.....	124
van Prooijen Bram C. and Qin Zhu. Horizontal coherent structures between channel and mudflat.....	126
Verney Romaric, Florent Grasso, Virginie Lafon, Emmanuelle Mulamba-Guilhemat, David Doxaran, Flavie Druine, Julien Deloffre, Jean Philippe Lemoine and Pierre Le Hir. Evaluating turbidity maximum patterns and their variability in the Seine Estuary from metrics: associating observations and model results.....	128
Walther Régis, Pierre Lehir and Florence Cayocca. Evaluation of the effect of climate change on the muddy deposits in the flood plain of the Loire Estuary and on the turbidity maximum (C3E2 Project- French research program).....	130
Wan Yuanyang, Dano Roelvink and Fengfeng Gu. Modeling of seasonal variations of fine-grained suspended sediment dynamics in the Yangtze Estuary.....	132
Winterwerp Johan C., Claire Chassagne, Maria Ibanez, Miguel de Lucas Pardo, Thijs van Kessel, Walther van Kesteren and Bram van Prooijen. Fine sediment properties: determination, interpretation and use.....	133
Xu Chunyang and Ping Dong. Mud flocculation model considering the effects of distribution of fractal dimension ns and yield strength.....	135

POSTER PRESENTATIONS

Achete Fernanda, Mick van der Wegen, Dano Roelvink and Bruce Jaffe. Modelling estuarine sediment budget impacts: anthropogenic or natural?	141
Bass S.J., J. Hope, A.J. Manning, R.J. Aspden, T. Downs, H.S. Eccles, P.L. Forsberg, I.D. Lichtman, R.J. Schindler, P.D. Thorne, J.H. Baas, A.G. Davies, J. Malarkey, D.R. Parsons, D.M. Paterson, J. Peakall and L. Ye. Physical and biogenic influences on sediment dynamics in a mixed sediment intertidal environment	143
Brunier-Coulin Florian, Pablo Cuellar and Pierre Philippe. Local mechanisms of cohesive soil erosion.....	146
Bundgaard Klavs, Ulrik Lumborg and Pernille Forsberg. Online monitoring, conceptual model of sediment dynamics and numerical modelling of non-tidal lagoon system.....	148
Chao Guo, He Qing, Bram van Prooijen and Wang Xianye. Flocculation characteristics on a muddy tidal flat.....	150
Chassagne Claire and Maria E. Ibanez. Zeta potential: a new tool for assessing the properties of clays?	152
Cuchiara Debora, Gustavo Cuchiara, José Francisco de Souza and Elisa Fernandes. The relationship between waves, mud deposition and meteorological events in the Rio Grande do Sul state coastal area (Brazil).....	154
Dankers Petra. Creating wetlands with cohesive sediment.....	156
De Maerschack Bart, Maarten Van Esbroeck, Stefaan Ides and Yves Plancke Monitoring sludge spill of the AMORAS underwater cell	158
Delgado Rosalia, Anne-Lise Montreuil, Sebastian Dan and Margaret Chen Contribution of waves and currents to observed suspended sediment distribution patterns in a macro-tidal beach	160
Druine Flavie, Robert Lafite, Julien Deloffre, Romaric Verney and Jean-Philippe Lemoine. Suspended solid concentration in the Seine Estuary based on the SYNAPSES turbidity monitoring network: quantification and variability.....	162
Fettweis Michael, Matthias Baeye, Thomas Van Hoesteberghe, Luc Van Poucke, Arvid Dujardin and Chantal Martens. <i>In situ</i> measurements of SPM concentration to evaluate the impact of the disposal of fine grained sediments from maintenance dredging	163
Fossati Mónica, Rodrigo Mosquera, Francisco Pedocchi and Ismael Piedra-Cueva. Self-weight consolidation tests of the Río de la Plata sediments.....	165
Friedrichs Carl T., Grace M. Cartwright, Patrick J. Dickhudt, Kelsey A. Fall and Lindsey M. Kraatz. Controls on bed erodibility in a muddy, partially-mixed estuary: York River, Virginia, USA.....	167
Gourgue Olivier, Joris Vanlede and Margaret Chen. Pre- and post-processing unstructured grids for estuary and coastal sea models with the PUG Matlab toolbox	170
Griffiths Joshua, David Bowers, Francis Gohin, Romaric Verney, Timothy Clarke and Carole Nahum. Estimations of settling speed using remotely sensed suspended material concentrations	172
Haghshenas S. Abbas and Mohsen Soltanpour. Study of spectral wave transformation over muddy beds.....	173

Harris Courtney K., Justin J. Birchler, Tara Kniskern and D. Reide Corbett. Linking sediment transport and geochemical processes in a numerical model with application offshore of the Mississippi River	175
Hillebrand G., P. Heininger, T. Krämer, C. Möhlenkamp, J. Pelzer, D. Schwandt and E. Claus. Estimating the amount of erodible contaminated sediments within the groyne fields of the Elbe River	176
Ibanez Maria, Claire Chassagne and Johan C. Winterwerp. Assessment of flocculation, settling and consolidation of cohesive sediments using the zeta potential	178
Jong-Wook Kim, Ha Ho Kyung and Woo Seung-Buhm. Effect of discharge on hydrodynamics and sediment transport by the operation of tidal power plant.....	180
Kilkie Paul, Heidi Burgess, Callum Firth and Phillip Teasdale. The influence of clay mineralogy on the erosion thresholds of estuarine cohesive sediments	182
Kyunghoi Kim, Lee In-Cheol and Hibino Tadashi. An effect of pore water flow on the re-suspension of cohesive sea bottom sediment	183
Landuyt Sydney, Stijn Claeys, Thomas Van Hoestenbergh, Meshkati Shahmirzadi, Peter Staelens and Tomas Van Oyen. Experimental investigation of the variability of the peak shear stress within consolidating cohesive sediment	185
Lee Byung Joon, Qilong Bi, Erik Toorman, Michael Fettweis and Holger Weilbeer. Two-class flocculation kinetic model: development and application to large-scale, multi-dimensional cohesive sediment transport	187
Leiping Ye, D.R. Parsons, R.J. Schindler, A.J. Manning and COHBED Project Team. Bedform dynamics in mixed sand-clay-EPS substrates.....	189
Lu Hai-yan, He Qing, Pan Cun-hong and Cao Ying. Analysis on variations of water/sediment and morphodynamics response in Hangzhou Bay in recent 50 years	191
Meshkati Shahmirzadi M.E., S. Claeys, T. Van Hoestenbergh, P. Staelens, T. Van Oyen, J. Vanlede and R. De Sutter. The effect of different physico-chemical parameters on the rheological behavior of consolidating mud	193
Pang Qixiu and Ruibo Zhang. Factors affecting the rheological characteristics of mud	195
Pedocchi Francisco, Valentina Groposso, Rodrigo Mosquera, Marcos Gallo and Susana Vinzón. Measuring mud properties with a tuning-forks device	198
Qin Zhu, Bram C. van Prooijen and Cynthia D. Maan. High resolution bed level changes on an intertidal mudflat	200
Razavi Arab Azadeh, S. Abbas Haghshenas, Farzin Samsami and Michael John Risk. Traces of sediment origin in rheological behaviour of mud samples taken from the North-Western Persian Gulf	202
Rehman Khawar and Cho Yong-Sik. Numerical simulation of sediment transport in shallow-water flows	204
Ruiz Gerardo. Sensitivity analysis for suspended load formulae in sediment transport	205
Samsami Farzin, Alan Cuthbertson and Olugbenga Ibikunle. Experimental investigation of flocculation in mixed sediments.....	206
Shao Y.Y., Z.L. Zhu and X.T. Shen. <i>In situ</i> observations of sediment dynamics in Tongzhou Bay, China: in response to wave-current interaction and strong wind forcing.....	208

Shin Hyun-Jung, Guan-hong Lee, Soongji Lee, Jeong Shin Lee, Tim Dellapenna, Josh Williams, Young Taeg Kim and Ho Kyung Ha and Jae Il Kwon. Mud siltation in the north harbour of Incheon, Korea	210
Thant Silvy, Matthias Baeye, Michael Fettweis, Frederic Francken, Jaak Monbaliu and David Van Rooij. Extreme values of suspended particulate matter concentration and their relation to swell and wind sea in the Belgian coastal zone	213
Todd David, Alex J. Souza and Colin F. Jago. Seasonal variations in SPM and floc characteristics in a hypertidal estuary	215
van der Hout Carola, Rob Witbaard and Theo Gerkema. Observed residual transport of SPM within a coastal turbidity maximum zone.....	217
Verney Romaric, Gael Many, Aurelien Gangloff, François Bourrin, David Doxaran, Ivane Pairaud, Matthias Jacquet and David Le Berre. A glider in the plume: an innovative approach to investigate and simulate the fate of Rhône River sediment in the Gulf of Lions during the 2014 winter flood	219
Wang Xianye, Bram van Prooijen, Qin Zhu and Qing He. Influence of hydrodynamics on sediment characteristics: comparison between two tidal flats	221
Zhang Jinfeng, Qinghe Zhang and Jerome P.-Y. Maa. The paradigm of coagulation processes of polystyrene latex particles.....	223

ORAL PRESENTATIONS

Long-term suspended sediment transport patterns over the North-Western part of the Persian Gulf, applying a three-dimensional hydrodynamic model

Attari Morteza Jedari¹, Arash Bakhtiari², S. Abbas Haghshenas¹, J. Ebrahim Hamidian¹ and Jun Sasaki³

¹ Institute of Geophysics, University of Tehran
North Kargar Ave., Tehran PC 1439951113, Iran
E-mail: sahaghshenas@ut.ac.ir and mortezajedariattari@yahoo.com

² Faculty of Civil Engineering, K. N. Toosi University of Technology
No. 1346, Vali-Asr St., Tehran PC 1996715433, Iran

³ Graduate School of Frontier Sciences, The University of Tokyo
5-1-5 Kashiwanoha, Kashiwa, Chiba 277-8563, Japan

The North-West part of the Persian Gulf is covered with mud deposits, partly originating from the Arvand River. On the Iranian coastline, Deylam Bay is the western margin of the affected area by the mud. Mud deposits up to 20 meters thickness are observed at the very shallow coast between Shah-Abdollah Port and the Arvand River mouth; it is why very fine sand with oolitic origin is dominant in Deylam port on the south eastern corner of the bay. Near the most northern point of the bay there is a small village with a newly constructed port, called Shah-Abdollah, where repeating sequences of soft mud and fine sand could be observed on the beach, indicating that this location maybe a marginal point of the sandy and muddy sediments. Hence, it is believed that the long-term pattern of suspended mud transport in the North-Western Persian Gulf is the main cause for determination of mud affected margins in this area (Khaleghi et al., 2014). Concurrently with the development of coastal and marine areas in this mentioned body of water, a need for understanding of sediment transport patterns and sediment constituents in the sea-bed increasingly arises in order to clarify the effects of anthropogenic activities and ensure more accurate planning. This research was performed in order to offer a sophisticated response for the arisen needs via providing a better understanding of coastal and gulf-scale processes in the North-Western Persian Gulf, where fine deposits govern the general sediment environment. We applied a quasi-three-dimensional hydrodynamic model to the Persian Gulf and simulated the current field for a 1-year period. The results were compared to a very precious velocity field data which had been collected inside the Persian Gulf in 2012. Using the results, we focused on the north-western part and simulated the sediment transport which is mostly coming from: 1) the Arvand River catchment area and 2) chemical precipitation from the water. The phenomenon was tracked through investigations and a clear border can be distinguished on the sea-bed near the Shah-Abdollah Port where upper-left region is mostly covered by mud and downer-right region is covered by the original sand. The model has a bed module which is capable of simulating the accumulation of sediment constituents including deposition and resuspension considering bed shear stresses induced by bottom currents and wind waves. Wave hindcast is performed using a module based on JONSWAP method.

As it is well established in this field, the proposed hydrodynamic model considers all meteorological driving forces of a general hydrodynamic model including: tide, wind, precipitation, river load, solar radiation, air pressure and air temperature. We note that, even though the Persian Gulf is a semi enclosed water body, tide is the dominant driving force of the water circulation. This was developed in the frame of a quasi-three-dimensional hydrodynamic model. The model is capable of simulation of the velocity field as well as consequent pollutant (dissolved and suspended) transport and oil slick dissemination.

The hydrodynamic model (Sasaki and Isobe, 1999) is based on Navier-Stokes equations with the hydrostatic and Boussinesq approximations. In the water body, the conservation equation for any water quality parameter is given by a three-dimensional transport equation with the source term. A comprehensive water quality model and a multi-layer-material bed module was added to the model.

Through this numerical experience the collected velocity data which clarifies the vertical profile of the velocity in the North-Western Persian Gulf has been reproduced and comparisons show that the model was successfully applied and the model results are in consistency with the observed data. The variation of the horizontal velocity in vertical direction was sophisticatedly reproduced and verifies that the results of this research are of help to understand the gulf-scale processes of the Persian Gulf.

Through applying the boundary condition for several years successively, long-term pattern of suspended mud transport and consequent spatial pattern of formed bed constituent in the study area were extracted and compared with morpho-dynamic evidences in the study area. The main parameters which had to be focused on were the river load and precipitation rate which were comprehensively investigated.

References

- Khaleghi A., M. Soltanpour and S.A. Haghshenas. 2014. A study on the sand-mud mixture at north-west of the Persian Gulf. 34th Coastal Engineering Conference (ICCE 2014), ASCE, Seoul, Korea.
- Sasaki J. and M. Isobe. 1999. Development of a long-term predictive model of water quality in Tokyo Bay. Proceedings of Estuarine and Coastal Modelling, ASCE 6:564-580.

Consolidation and strength development of soft mud deposits by horizontal drainage

Barciela Rial Maria¹, Johan C. Winterwerp^{1,2}, Jasper Griffioen^{3,4,5} and Thijs van Kessel²

¹ Faculty of Civil Engineering and Geosciences, Delft University of Technology, Stevinweg 1, 2628 CN Delft, the Netherlands
E-mail: m.barcielarial@tudelft.nl

² Deltares, PO Box 177, 2600 MH Delft, the Netherlands

³ Deltares, PO Box 85467, 3508 AL Utrecht, the Netherlands

⁴ Department of Innovation, Environmental and Energy Sciences, Faculty of Geosciences, Utrecht University, PO Box 80115, 3508 TC Utrecht, the Netherlands

⁵ TNO, PO Box 80015, 3508 TA Utrecht, the Netherlands

Introduction

The management of fine sediments will be increasingly important. Large amounts of mobilised sediments will progressively be used for nature building projects. Existing literature extensively covers the building properties of traditional materials, yet natural ones, because of their diverse properties, present a greater challenge. In this paper, this challenge is addressed by determining the strength behaviour of fresh mud through consolidation experiments with horizontal drainage, performed in cylindrical columns.

A series of experiments, which determine the consolidation and strength development of fresh mud deposits from Markermeer Lake (the Netherlands), is described. This novel approach mimics land and crust formation with soft soils. The influence of crust formation and sediment variability on the consolidation process is carefully studied, as well as the physical-chemical interactions. The results provide engineering rules for wetland creation and contribute to the understanding of the dominant mechanisms for soil formation from soft sediments.

Methods

Consolidation experiments are conducted in 1.3m high PMMA transparent columns, of which the inner diameter is 10.0cm. To allow horizontal drainage, a porous pipe equipped with a filter only permeable for water is placed in the centre of the column and the water is slowly pumped out.

All columns are equipped with an impermeable base. On their walls, a scale bar allows the measurement of the consolidation development. The settlement of the water-mud interface, and the subsequent wet-dry and dry mud-air interfaces, are monitored by video. In addition, ten pore water pressure ports are installed at intervals of 5.0cm each, starting at 5.0cm from the base. An extra reference pressure port, which is always located above the sediment, is placed at 1.1m from the bottom. All the entries are provided with a Vyon plastic filter to prevent sediment leaking. This method was previously used by Bowden (1988), Merckelbach (2000) and Te Slaa et al. (2013). Every pressure port is connected to its pressure transducer, which is connected to a variable water table for calibration. The accuracy of the pore water pressure values is 1mm water head or 10 Pa, as determined by calibration.

The bulk density is measured using electrical conductivity. This is done via a Conductivity Concentration Meter (CCM). All columns have 10 conductivity probes situated at 5, 15, 20, 25, 30, 35, 40, 45, 50 and 65cm from the base, as shown in Fig. 1. The top probe is placed at a higher level as a reference magnitude in the overlying clear water. Each double platinum electrode probe, 1cm vertically spaced, is connected to a port. The probes are aligned with the wall curvature to reduce their influence on the deposition process.

Since conductivity measurements are sensitive to temperature fluctuations, and to reduce algae formation, the columns are placed in a climate room without light. Nevertheless, small temperature fluctuations are still possible. For the purpose of correcting temperature fluctuations, the temperature inside the columns is determined with a 50cm long probe with a resolution of $\pm 0.1^\circ\text{C}$.

At the same time, a parallel non-drained series of experiments is performed utilizing columns also equipped with pressure ports, but with a segmented lower part (see Fig. 1). The aim of this setup is to obtain different sections of the column, which are used to take samples for further geochemical analysis and submitted to the shear vane test. Thus, we acquire, for example, the strength profiles of the mud bed and the changes experienced by transformation of sedimentary organic matter from the starting point of the experiment. With the aim of estimating the evolution of the proportion of

components with different thermal stability, the Rock-Eval pyrolysis (Hetényi *et al.*, 2005) is applied at different phases of the consolidation process. The redox potential is also measured.

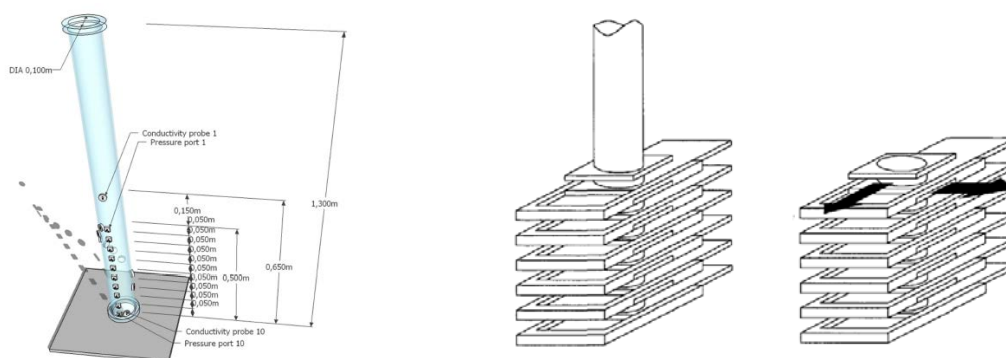


Fig. 1. On the left, the original columns adapted to get horizontal (courtesy of Steven te Slaa). On the right, the segmented columns used in the second series (Merckelbach, 2000).

The interaction between clay minerals and organic matter plays a decisive role at the consolidation process. Thus, the sediment is also characterised in detail before starting both series of experiments and an X-Ray diffraction analysis is performed to characterize the mineralogy of the clay as well as other fine-grained minerals.

An environmental scanning electron microscope (ESEM) is used to analyse two different mud samples. Humidities between 0% and 99% are applied for prolonged periods of time, while observing the changes in microstructure. In this way, the fabric of the clay can be studied in its most natural state (Cheng *et al.*, 2004).

The particle size distribution is first determined for an untreated sample using laser diffraction with a Malvern particle sizer. We observe that, according to the lithological classification, the type of sediment studied is in the range of silt. Therefore, the sample is pretreated to allow the dispersion of primary particles. The cementing materials are removed; organic matter by H_2O_2 and carbonates by HCl. As a result, the clay distribution of the individual particles is obtained.

Conclusions

With the experiments performed, the difference in consolidation behaviour is studied with and without horizontal drainage. Moreover, crust formation and how this crust affects the chemistry in the mud is measured. The Rock-Eval analysis reveals relatively high contents of organic matter and the ESEM yields insight into the presence of clay minerals versus other fine-grained particles within the clay and silt fraction. We also confirm that the organic matter material consists of humic substances, mainly fulvic acids.

References

- Bowden R.K. 1988. Compression behaviour and shear strength characteristics of a natural silty clay sedimented in the laboratory. PhD. thesis, Oxford University.
- Cheng X., H. Janssen, F.B. Barends and E.J. denHaan. 2004. A combination of ESEM, EDX and XRD studies on the fabric of Dutch organic clay from Oostvaardersplassen (Netherlands) and its geotechnical implications. *Applied Clay Science* 25(3-4):179-185.
- Hetényi M., T. Nyilas and T.M. Tóth. 2005. Stepwise Rock-Eval pyrolysis as a tool for typing heterogeneous organic matter in soils. *Journal of Analytical and Applied Pyrolysis* 74(1-2):45-54.
- Merckelbach L.M. 2000. Consolidation and strength evolution of soft mud layers. PhD. thesis, Delft University of Technology.
- Te Slaa S., Q. He, D.S. Van Maren and J.C. Winterwerp 2013. Sedimentation processes in silt-rich sediment systems. *Ocean Dynamics* 63(4):399-421.

Modelling the effects of water injection dredging on water quality

Benson Tom and John Baugh

HR Wallingford, Howbery Park, Wallingford, Oxon, OX8 10BA, UK
E-mail: t.benson@hrwallingford.com; j.baugh@hrwallingford.com

Some estuaries around the world have historically been subjected to unregulated releases of industrial effluent and untreated sewage. Contaminants associated with these discharges have a tendency to adsorb to the natural mud particles in suspension which themselves tend to flocculate and sink rapidly to the bed. As a result, estuary deposits can contain high levels of pollutants.

An example of this problem is the Mersey Estuary (UK) which in recent years has undergone an extensive programme of regeneration to the docks and infrastructure. In the latest phase of works, the regeneration of old ship berths close to the mouth of the estuary was proposed to facilitate a new container terminal. The sediments in the Mersey are highly contaminated with heavy metals and Polycyclic Aromatic Hydrocarbons (PAHs). Dredging of these deposits is therefore tightly regulated, requiring the material to be removed to designated landfill sites. The potential cost of the operations to the developer has led to other dredge methodologies being considered.

This paper describes a study undertaken to assess the feasibility of using Water Injection Dredging (WID) to clear the berths. This method offers considerable saving in terms of efficiency and cost but, since it introduces the contaminants back into the water column, raises concerns over water quality. In the assessment, a fully coupled 3D hydrodynamic, sediment transport and newly developed water quality model of the Mersey Estuary is described. This TELEMAC model simulates the advection and dispersion of dredged material and includes the process of partitioning of contaminants to and from adsorbed (particulate) and dissolved (water) phases. The effect of flocculation on settling velocity of the suspended particulates is included in the model using a recently developed model (Soulsby *et al.*, 2013) which is found to improve the calibration against *in situ* ADCP derived sediment flux measurements (Land and Jones, 2001).

Results for four locally significant contaminants are described, with two heavy metals (mercury and lead) and two polycyclic aromatic hydrocarbons (anthracene and naphthalene) being considered. After due consideration of the findings of the study the statutory regulators and other stakeholders permitted the use of WID for the dredging of the berths, thus highlighting the usefulness of the methodology.

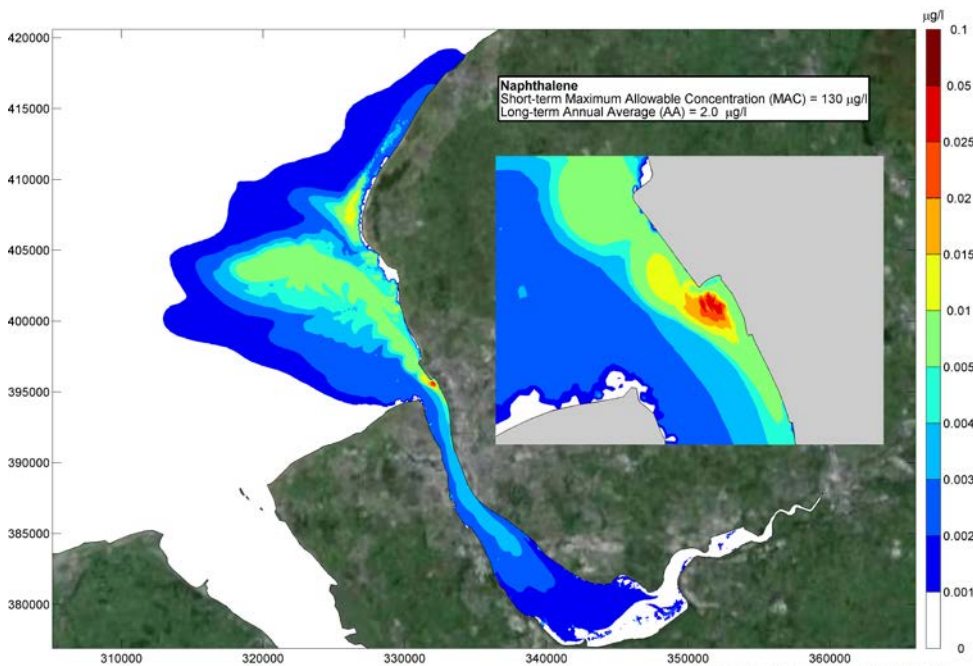


Fig. 1. Maximum predicted concentrations of dissolved Naphthalene released during 4 weeks of dredging in the Mersey Estuary.

References

- Land J.M. and P.D. Jones. 2001. Acoustic measurement of sediment flux in rivers and near-shore waters. p.127-134. In: Proceedings of the Seventh Federal Interagency Sedimentation Conference. Vol. III. Fed. Interagency Subcomm. on Sediment., Washington, DC.
- Soulsby R.L., A.J. Manning, J. Spearman and R.J.S. Whitehouse. 2013. Settling velocity and mass settling flux of flocculated estuarine sediments. *Marine Geology* 339:1-12.

On two-phase/mixture modelling of sediment transport and turbulence modulation due to fluid-particle interactions

Bi Qilong and Erik Toorman

Hydraulics Laboratory, Department of Civil Engineering, KU Leuven
Kasteelpark Arenberg 40, PO Box 2448, B-3001 Leuven, Belgium
E-mail: qilong.bi@bwk.kuleuven.be and erik.toorman@bwk.kuleuven.be

A fundamental issue in modelling sediment transport is to understand the complex mechanism that involves fluid-particle interactions. When the suspension concentration becomes significantly high near the bottom, interactions between particles also play an important role in turbulence modulation as well as affecting the suspension capacity in the above water column. These insights have been provided by using two-phase flow theory to analyse the four-way coupling effects in the high concentrated benthic layer, which cannot be done with traditional sediment transport models. In the work of Toorman and Bi (2013), the fundamental equations have been reconstructed from two-phase flow/mixture theory by expressing mixture theory equations in terms of fluid variables, combined with a drift closure. Following the previous work, the relative particle movement is solved separately with a force balance equation for completing the equations. In addition, a modified low-Reynolds $k-\varepsilon$ turbulence model has been developed by Toorman (2011). For application to the two-phase flow/mixture theory, an extended version is proposed as turbulence closure.

Fundamental equations of two-phase/mixture theory

Unlike the two-fluid model, the mixture theory usually chooses volume- and/or weight- averaged variables for the mixture, which is the sum of carrier and dispersed phase. The additional complexity regarding momentum exchanges between phases temporarily can be circumvented in this way (but returns at a later stage). By employing ensemble-averaged fluid velocity U_i and solids velocity V_i , related to Reynolds-averaged properties proposed by Toorman (2008):

$$U_i = \overline{u_i} + \frac{\overline{-u'_i \phi'}}{1 - \overline{\phi}} = \overline{u_i} + U_{Di} \quad \text{and} \quad V_i = \overline{v_i} + \frac{\overline{v'_i \phi'}}{\overline{\phi}} = \overline{v_i} + V_{Di} \quad (1)$$

where: $\overline{u_i}$ and $\overline{v_i}$ = the respective Reynolds-averaged fluid and solids velocities, U_{Di} and V_{Di} = the respective fluid and solids drift velocities, $\overline{\phi}$ = the Reynolds-averaged solids volume fraction, $\overline{-u'_i \phi'}$ and $\overline{v'_i \phi'}$ = the respective Reynolds averaged fluid and solids turbulent flux. Substitution of (1) into the Reynolds-averaged equations leads to the following basic equations (where the overbar is dropped). The suspension continuity equation reads:

$$\frac{\partial(U_j + W_j \phi)}{\partial x_j} = 0 \quad (2)$$

where: x_j = the location coordinate and $W_i = V_i - U_i$ = the (ensemble-averaged) slip velocity. The exact suspension momentum equation becomes:

$$\begin{aligned} \rho \left(\frac{\partial U_i}{\partial t} + U_j \frac{\partial U_i}{\partial x_j} \right) = & -\frac{\partial p}{\partial x_i} + \rho g \delta_{iz} + \frac{\partial(\sigma_\mu + \sigma_{Tij} + \sigma_{Dij})}{\partial x_j} \\ & - \rho_s \phi \left(\frac{\partial W_i}{\partial t} + U_j \frac{\partial W_i}{\partial x_j} + W_j \frac{\partial(U_i + W_i)}{\partial x_j} \right) \end{aligned} \quad (3)$$

with: $\rho = \rho_s \phi + \rho_w (1 - \phi)$ = the suspension bulk density, ρ_s and ρ_w = the particle and fluid density, p = pressure, g = gravity constant, σ_μ = the viscous stress, σ_T = the turbulent Reynolds stress:

$$\sigma_{Tij} = \rho_s \phi \left(-\overline{v'_i v'_j} \right) + \rho_w (1 - \phi) \left(-\overline{u'_i u'_j} \right) \approx -\overline{\rho u'_i u'_j} \approx \rho v_i \left(\frac{\partial U_i}{\partial x_j} + \frac{\partial U_j}{\partial x_i} \right) \quad (4)$$

and σ_D = the drift diffusion stress:

$$\begin{aligned} \sigma_{Dij} &= \rho_s \phi (V_{Di} V_{Dj}) + \rho_w (1 - \phi) (U_{Di} U_{Dj}) \\ &\approx \left(\frac{v_t}{Sc} \right)^2 \left(\rho_s \phi \frac{\partial \ln \phi}{\partial x_i} \frac{\partial \ln \phi}{\partial x_j} + \rho_w (1 - \phi) \frac{\partial \ln(1 - \phi)}{\partial x_i} \frac{\partial \ln(1 - \phi)}{\partial x_j} \right) \end{aligned} \quad (5)$$

using the Boussinesq approximation. The slip velocity W can be obtained either from a simplified particle force balance (e.g. Kim *et al.*, 1998) or the suspension momentum balance equation.

Low-Reynolds turbulence modelling

It is observed that in benthic suspension layers high suspended sediment concentrations above the saturation limit are found (resulting in “fluid mud” or sheet flow conditions; Toorman, 2002) and turbulence is no longer fully developed (because the four-way particle-particle-fluid interactions consume much energy). Therefore, it is necessary to determine the eddy viscosity in the above equations from low-Reynolds turbulence models (Patel *et al.*, 1985). In order to reduce the necessary high grid resolution for this type of turbulence closure a two-layer approach (Rodi, 1991) is applied where a low-Reynolds $k-\varepsilon$ model for the outer layer is combined with a low-Reynolds mixing-length model for the bottom layer (Toorman, 2011). Besides semi-empirical damping functions, the $k-\varepsilon$ model also contains extra terms originating from the extra terms in the momentum equation (eq.3). Since the exact $k-\varepsilon$ model for suspensions (Elghobashi and Abou-Arab, 1983) cannot be solved, simplified models (e.g. Chauchat and Guillou, 2008) are investigated and new closures are proposed based on the analysis of experimental data in combination with dimensional analysis and theoretical considerations. The model is first evaluated with the simulation of flume experiments for sand suspensions. Next, the model is combined with a non-Newtonian rheological closure for the viscosity of fluid mud (based on Toorman, 1997) to simulate (steady and unsteady) shear flow over a muddy bottom.

References

- Chauchat J. and S. Guillou. 2008. On turbulence closures for two-phase sediment-laden flow models. *Journal of Geophysical Research: Oceans* (1978–2012): 113(C11).
- Elghobashi S.E. and T.W. Abou-Arab. 1983. A two-equation turbulence model for two-phase flows. *Phys. Fluids* 26:931– 938.
- Kim I., S. Elghobashi and W.A. Sirignano. 1998. On the equation for spherical-particle motion: effect of Reynolds and acceleration numbers. *Journal of Fluid Mechanics* 367:221-253.
- Patel V.C., W. Rodi and G. Scheuerer. 1985. Turbulence models for near-wall and low-Reynolds number flows: a review. *AIAA J.* 23(9):1308-1319.
- Rodi W. 1991. Experience with two-layer models combining the $k-\varepsilon$ model with a one-equation model near the wall. AIAA-91-0216, 29th Aerospace Sciences Meeting, (7-10 January 1991, Reno, Nevada, USA).
- Toorman E.A. 1997. Modelling the thixotropic behaviour of dense cohesive sediment suspensions. *Rheologica Acta* 36(1):56-65.
- Toorman E.A. 2002. Modelling of turbulent flow with cohesive sediment. p.155-169. In: *Proceedings in Marine Science, Vol.5: Fine Sediment Dynamics in the Marine Environment*. Winterwerp J.C. and C. Kranenburg (Eds). Elsevier Science, Amsterdam.
- Toorman E.A. 2008. Vertical mixing in the fully-developed turbulent layer of sediment-laden open-channel flow. *Journal of Hydraulic Engineering* 134(9):1225-1235.
- Toorman E.A. 2011. Low-Reynolds modelling of high-concentrated near-bottom suspended sediment transport. IAHR Symposium on Two-phase Modelling for Sediment Dynamics in Geophysical Flows (THESIS-2011, Paris, April 26-28, 2011), Abstract, 4p.
- Toorman E.A. and Q. Bi. 2013. Hybrid two-phase/mixture modelling of sediment transport as a tool for large-scale morphological model development. Internal Research Paper, presented at THESIS2013 (Chatou, FR), Hydraulics Laboratory, KU Leuven.

Identification of suspended resilient pellets in particles tracked by a Particle Image Camera System (PICS) in a muddy estuary

Cartwright Grace M., Kelsey A. Fall and Carl T. Friedrichs

College of William and Mary, Virginia Institute of Marine Science, Gloucester Pt., VA 23062, USA
E-mail: gracec@vims.edu, kafall@vims.edu, carl.friedrichs@vims.edu

The Particle Imaging Camera System (PICS) was designed to allow for the measurement of the settling velocity of individual particles *in situ* by using the smaller particles (<30 microns) to remove the effects of water velocity due to boat/water motion (Smith, 2010). Smith and Friedrichs (2011) took advantage of this system to identify the *in situ* size and settling velocities of cohesive flocs and suspended sediment aggregates in a trailing suction hopper dredge plume. They characterized the particles of each 30s video into three groups: flocs (density $\leq 1150\text{kg/m}^3$), primary mineral particles (density $\geq 1800\text{kg/m}^3$) and bed aggregates ($1150\text{mg/m}^3 < \text{density} < 1800\text{kg/m}^3$). This classification system, while adequate for suspended dredge plumes, needs to be revisited when the PICS is used in a muddy estuary, such as the York River Estuary, Virginia. Fig. 1B shows the settling velocities of particles tracked within a video captured 2.5m from the surface in the Clay Bank region of the York River, plotted against their equivalent spherical diameters. While most of the particles are classified as flocs, as indicated by the blue dots in Fig. 1C and the peak in the relative number of particles in Fig. 1E, there is still a large number of particles classified as “bed aggregates” (red dots). This number of higher density particles may be unexpected, as this video was captured 4.25m over a “muddy bed” in a natural system with a flood current of 40cm/s. However, biologically compacted mud in the form of resilient pellets (see Fig. 2) may be the answer. Bed sediments from five sediment cruises during this study period (Aug. 2012 – Nov. 2014) were found to be comprised of 86-96% mud (Fig. 3A). However, 9-14% of the mud was packaged as resilient pellets (Fig. 3B). Sediment captured 38cm above the bed by traps deployed on tripods were found to have 92-98% mud, with 4-14% of the mud packaged as resilient pellets (Fig. 3A and B). Pellets isolated from the Apr. to Jul. 2014 trap were sampled with the PICS to determine the distribution of settling velocities (W_s), particle densities, and the ratio of the long and short axis of the particles. This will be used to identify the pellets in PICS videos captured during the five 6h anchor stations (black lines in Fig. 3) where three depths were sampled each hour.

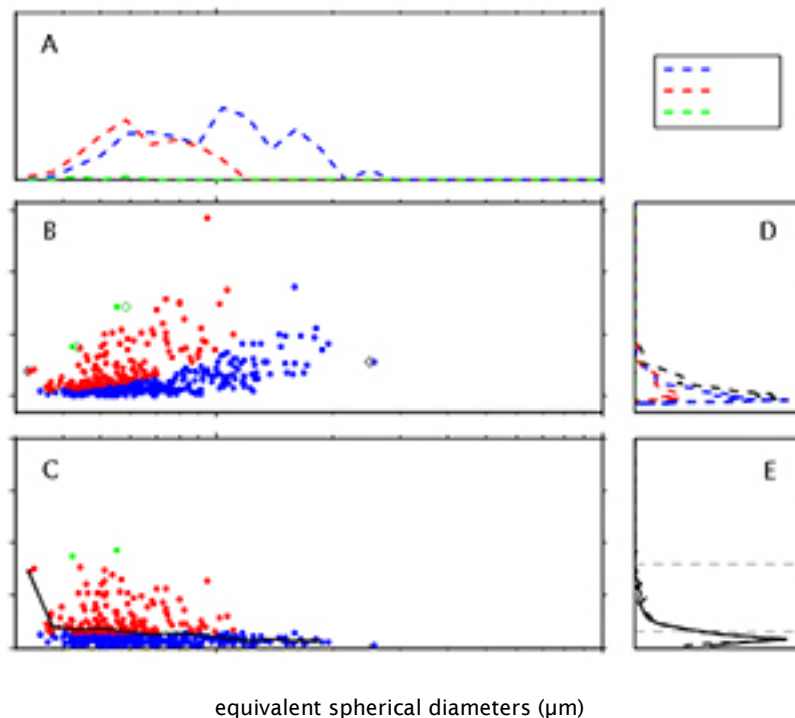


Fig. 1. 489 particles tracked from video captured *in situ* at 2.5m (4.25mab) during a flood tide (40cm/s) at Clay Bank, York River, VA using a PICS settling camera.

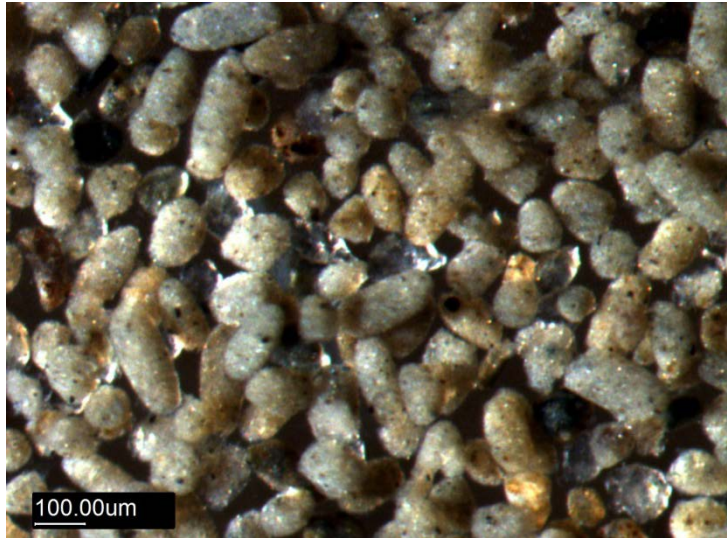


Fig. 2. Pellets, sand and debris captured on 63-micron mesh from sediment trap deployed April 2 - July 21, 2014.

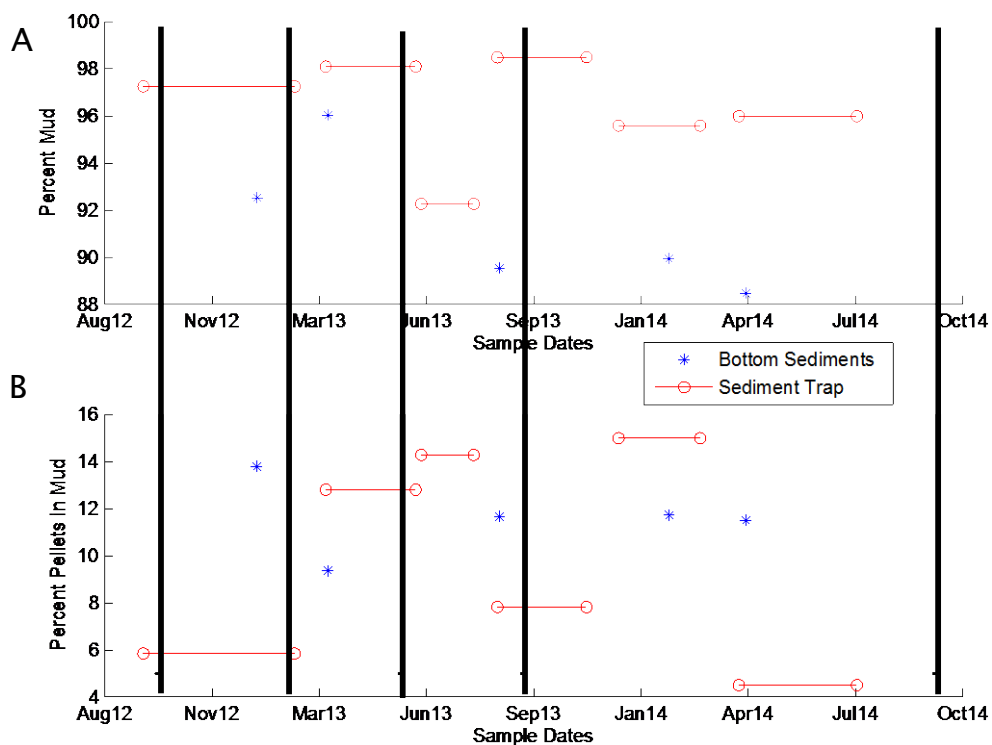


Fig. 3. A) Percent mud analysed from bottom sediment (blue stars) and sediment traps deployed on tripods in Clay Bank region of the York River Estuary, VA. B) Percent pellets in mud fraction in bottom sediment and sediment traps. Black lines indicate PICS 6-hr anchor station periods.

References

- Smith S.J. 2010. Fine sediment dynamics in dredge plumes. PhD Thesis. School of Marine Science, College of William & Mary. Gloucester Point, VA.
- Smith S.J. and C.T. Friedrichs. 2011. Size and settling velocities of cohesive flocs and suspended sediment aggregates in a trailing suction hopper dredge plume. *Continental Shelf Research* 31(10S):S50-S63.

Flocculation in natural environment: from the lab to the field

Chassagne Claire¹, Maria E. Ibanez¹ and Andy Manning^{2,3,4}

¹ Section of Environmental Fluid Mechanics, Civil Engineering and Geosciences, Delft University of Technology, PO Box 5048, 2600 GA, Delft, the Netherlands
Email: C.Chassagne@tudelft.nl

² HR Wallingford, Howbery Park, Wallingford, Oxfordshire, OX10 8BA, UK

³ Department of Geography, Environment and Earth Sciences, University of Hull, Kingston Upon Hull, Humberside, HU6 7RX, UK

⁴ School of Marine Science and Engineering, Plymouth University, Drake Circus, Plymouth, Devon, PL4 8AA, UK

Flocs are constituted of an aggregation of clays and polymers in the presence of ions of variable concentration. Their structure and strength are not only depending on the properties of the constituents, but also on the history of their formation.

A few scenarios for the formation of flocs were investigated in the laboratory, based on the availability of polymers and/or salt at the onset of aggregation and on the shear stresses present during the growth of the flocs. Flocculated suspensions were created using established laboratory jar testing protocols (Mietta, 2010). The structure of the created flocs was analysed using version 2 of the LabSFLOC - Laboratory Spectral Flocculation Characteristics - instrument (Manning, 2006) by recording their floc size, density, settling velocity, and strength. A systematic investigation of the changes in floc structure after resuspension of the flocs was performed. The flocs thus obtained were compared with the flocs obtained in natural environments, for which data has been collected recently in the southern North Sea, more specifically in the Rhine ROFI at a depth of 12m, close to the Sand Motor between Hook of Holland and Scheveningen, the Netherlands.

By integrating the results of these studies, a new model for floc formation was developed. This model is based on the Population Balance Equation (PBE) which describes how a particle size distribution is evolving in time, under influence of shear stresses (Mietta, 2010; Mietta *et al.*, 2011). The new model differs from the standard PBE in the following ways:

- 1) The aggregation/break-up parameters of the model will integrate more measurable data to limit the amount of empiricism, following the work initiated in our group (Mietta *et al.*, 2009)
- 2) The model will consist of a mathematical (analytical) function which reproduces the results of the PBE derivations, but which can be more easily implemented into larger scale numerical models like Delft3D.
- 3) The model will be extended compared to the standard PBE model, so as to include the interaction of particles with the sediment bed, for which no model currently exists.

An example is given below, illustrating the possibility of using analytical functions, with a limited number of parameters to reproduce the time evolution of floc formation. These parameters can in turn be linked with parameters such as collision efficiency, break-up rate, etc. appearing in the PBE model, and to measurable parameters such as salinity, shear stresses and organic matter content.

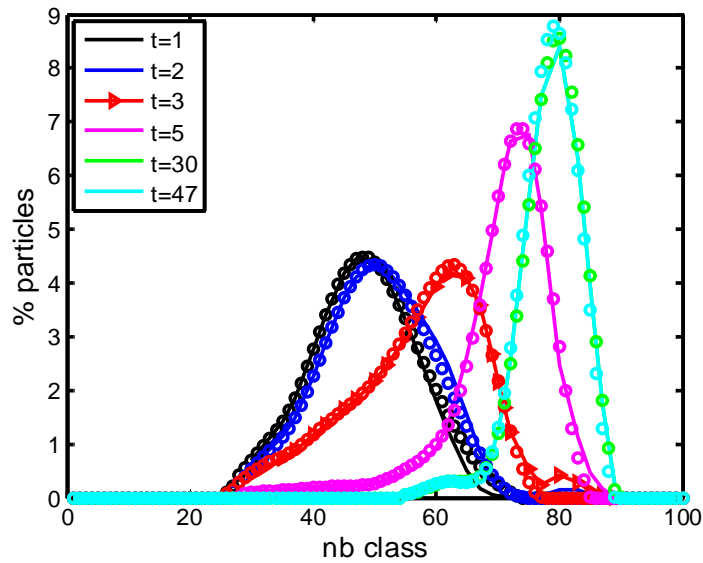


Fig. 1. Test case: River clay in presence of cationic flocculant; Evolution of the Particle Size Distribution (% particles in each class) in time; the size (in microns) of a particle in a given class (nbclass) is given by $10^{(0.05 \cdot \text{nbclass})}/50$; The symbols correspond to the measurements and the lines to the theoretical model; the time $t = 1$ corresponds to the time where the cationic flocculant is added, $t = n$ to the situation $(n-1) \times 30$ s later.

In this example, the stirring time in the jar, and the pumping through the Light Scattering measuring device was low enough to ensure that the flocs only grow, and would not break-up. In this simple case, we found that given 3 constant parameters a_1 , a_2 , b_1 , and two exponentially increasing in class number parameters $t_a(i)$ and $t_b(i)$, we could integrate analytically the PBE. The time evolution of the number N_i of particles in class i was then found to be:

$$N_i(t) = \frac{a_1}{1 + a_2 \exp\left(-\frac{t}{t_a(i)}\right)} \left[b_1 + \exp\left(-\frac{t}{t_b(i)}\right) \right]$$

This function could be used to model the PSD over the entire flocculation period (full lines in the figure).

References

- Manning A.J. 2006. LabSFLOC - A laboratory system to determine the spectral characteristics of flocculating cohesive sediments. HR Wallingford Technical Report, TR 156.
- Mietta F., C. Chassagne, A.J. Manning and J.C. Winterwerp 2009. Influence of shear rate, organic matter content, pH and salinity on mud flocculation. *Ocean Dynamics* 59(5):751-763.
- Mietta F. 2010. Evolution of the floc size distribution of cohesive sediments. Ph.D. Thesis, TU Delft press
- Mietta F., C. Chassagne, R. Verney *et al.* 2011. On the behavior of mud floc size distribution: model calibration and model behaviour. *Ocean Dynamics* 61:2-3.

Flocculation in turbulent flow – a view into particle network

Chen Margaret

Department of Hydrology and Hydraulic Engineering, Vrije Universiteit Brussel (VUB), Pleinlaan 2, 1050 Brussels, Belgium
E-mail: Margaret.Chen@vub.ac.be

Introduction

Cohesive sediment is prone to form aggregated particle network, and consequently its transport, settling, deposition, resuspension, and interaction between fine particles and flow are to large extent determined by intrinsic strength of particle network. In the estuarine environment suspended particles are mostly flocculated, and are continuously moving through estuarine zones of varying salinity, suspended sediment concentration and turbulence intensity, and as a result, they are subject to a continuous process of flocculation and de-flocculation. The aim of this study is to investigate floc formation at various locations within the Scheldt Estuary (Belgium, the Netherlands) through field measurements and laboratory experiments and to get insight into the longitudinal variability of flocculation and to contribute to improved understanding of sediment transport dynamics.

Field investigation and laboratory simulation experiment

Flocculation *in-situ* field measurements were carried out following the salinity gradient along the Scheldt Estuary. *In-situ* benthic camera, floc-sampler and Environmental Scanning Electron Microscope Wet-mode (ESEM-WM) were used to sample and observe flocs. Simulation experiments were performed in an attempt to reproduce the observed natural phenomena in terms of the variability of floc formation with respect to the suspended particle locality from areas varying in salinity and situated above, within, and below the estuarine turbidity maximum (ETM) zone. These simulation experiments were focused on three main influential parameters: suspended sediment concentrations (SSC), salinity and temperature, and were completed on natural estuarine suspension under controlled turbulence.

Every individual floc image acquired from ESEM-WM was analysed using the image software to determine the floc size (length, width and height) and the floc median length. Floc volume is presented as parts per thousand (ppt), which represents the volume units of flocs per thousand volume units of suspension. The *in-situ* floc shape is described by the floc sphericity that is determined by the floc length to width ratio.

In situ suspended particle flocculation and characteristics

Direct field investigations in the Scheldt Estuary show that suspended particles are intensively flocculated. Evolution of floc formation within a tidal cycle is governed by different phases of tidal related current velocity and suspended particle concentration. The longitudinal *in-situ* particle-size spectra demonstrate an important pattern. Large flocs (up to 1400 μ m) are repeatedly found at low or no salinity areas and further upstream. Flocs become smaller toward downstream showing least size, with average floc size around 50 μ m, in a zone where the most important ETM locates. This persistent pattern of average floc-size distribution in the Scheldt Estuary suggests that the increment of SSC to a certain extent leads to a probable increment of the particle collision frequency resulting in floc break-up or floc abrasion within the ETM. In this study no evidence was found for an intensified flocculation in the low salinity transitional zone where fresh and salt water meets and is conventionally considered as the most favourable locality for flocculation because of the optimal salinity range. An overview of aggregated particle network shows distinctive differences of floc structure from the freshwater zone to the downstream high salinity zone (Fig. 1).

Flocculation capability

Observations from the simulation experiments reveal that in a low turbulent flow field flocculation takes place on 3-hour time scales with estuarine reality SSC (around and below 300mg/l). The SSC affects the flocculation at different scales and is particle source dependent. Some intrinsic particle properties such as primary grain compositions, specific surface area and cation exchange capacity as well as biological factors indispensably determine the ultimate size and settling behaviour of floc. Increment in floc size is not necessarily accompanied by an enhanced floc settling behaviour. Floc shape is a significant parameter determining floc settling, and spherical shape is favourable. Introducing particles from the freshwater part of the estuary into a saline environment yields a two-stage effect on floc formation. An initial stage of dense and spherical floc formation associated with fast settling and a second stage of large low-density organic floc growth and very slow settling. The effect of water property (including salinity) on flocculation is particle property dependent. The

impact of temperature increment on flocculation is SSC dependent. High temperature limits floc size but positively affects the formation of spherical-shaped floc.

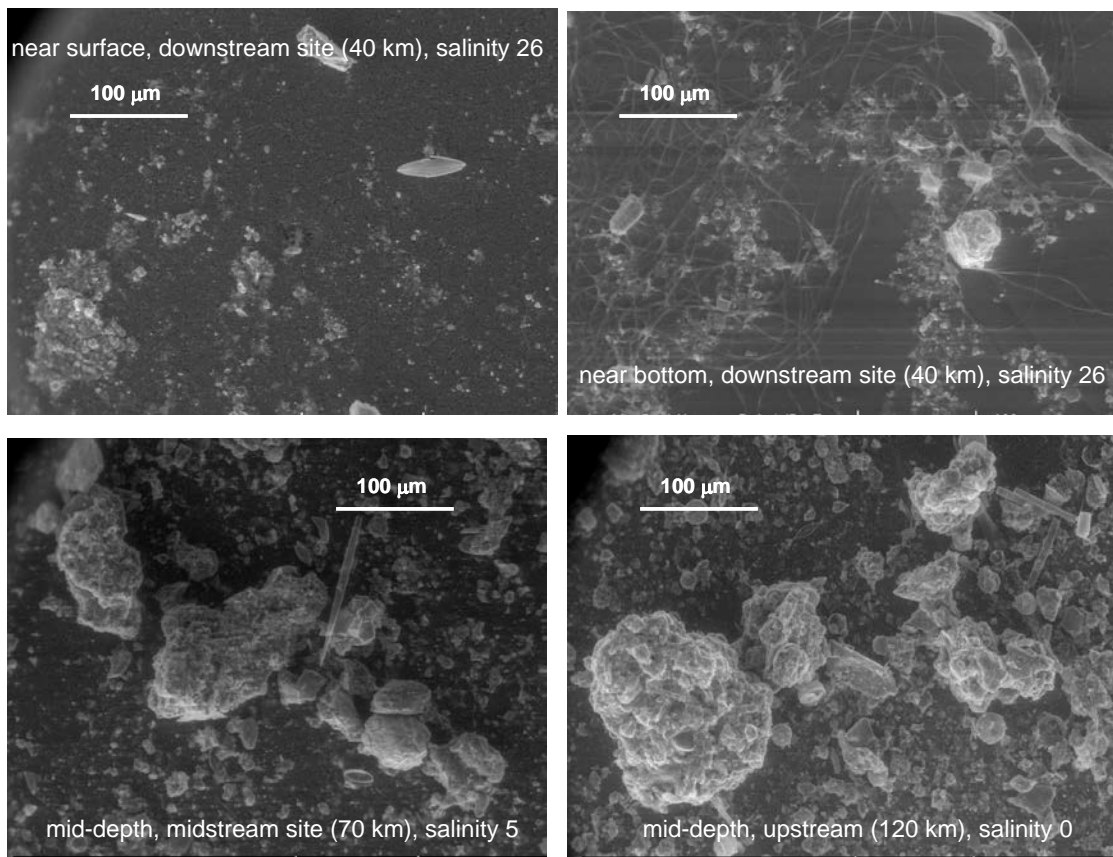


Fig. 1. Particle networks representing flocculated sediments with irregular form and open structure.

Conclusions

The findings of this study show the effect of process parameters on flocculation and floc characteristics as well as compatibility between *in-situ* observations and simulation experiments. Direct field investigations demonstrate an important pattern of longitudinal *in-situ* particle-size spectra. Flocculation simulation experiments have successfully reproduced the observed spatial variation pattern of floc size in nature. Suspended particles from different localities even within the same estuary do show different variability in flocculation. In this study, suspended particles from the upstream of ETM show the strongest flocculation capability, while those from within the ETM show the least capability in floc forming. In addition to local hydraulic flow and local SSC, the biological, physical and chemical components associated with the particle locality are at the root of the variability of flocculation and the resulting floc distribution and settling.

Surface SPM concentration in Taiwan Strait during summer and winter monsoon

Chou Tzu-Yin¹, Che-Yuan Liu¹, Hao-Cheng Yu¹, Jason C.S. Yu¹, Quinten Vanhellemont² and Michael Fettweis²

¹ Department of Marine Environment and Engineering
National Sun Yat-Sen University, Lien-Hai Road 70, 80424 Kaohsiung, Taiwan
E-mail: jasonyu@mail.nsysu.edu.tw

² Operational Directorate Natural Environment, Royal Belgian Institute of Natural Sciences,
Gulledelle 100, B-1200 Brussels, Belgium

The Taiwan Strait, situated in the East China Sea between Taiwan and China is shallow, relatively turbid and characterized by strong tidal currents and a winter and a summer monsoon season, (Jan *et al.*, 2002; Chen and Wang, 2006; Liao *et al.*, 2008). During winter winds are generally blowing from the NE and the hydrodynamics are characterised by the China coastal current that flows towards the SW following the China Coast and a weak Kuroshio branch current along the west coast of Taiwan that flows towards the north. During summer the weather pattern changes, the winds are blowing from the south and the warm water from the South China Sea current is advected into the Strait. The changes in weather pattern influences rainfall and thus river run-off. The riverine discharge in Taiwan during flood season often carries huge amounts of fine-grained sediments into the Strait that are rapidly dispersed in the sea (Dadson *et al.*, 2005; Liu *et al.*, 2006; Chien *et al.*, 2011). These sediment inputs occur during the short time periods of heavy rains often associated with typhoons. Variations in SPM concentration are typically caused by resuspension, mixing, settling and deposition of fine-grained sediments, by advection due to subtidal flows and by the input of fine-grained sediments through river run-off. The aim of the study is to use images from the Moderate Resolution Imaging Spectroradiometer (MODIS) on the Aqua satellite, in order to investigate how local sediment sources together with the seasonality in wind, oceanographic currents and waves influence the SPM dynamics in Taiwan Strait.

In total 4094 MODIS images, covering the period between July 2002 and September 2013, have been processed from Level 1A to Level 2, using the SeaDAS software. Images were collocated on a common rectangular grid using nearest neighbor resampling, and multiple overpasses combined to a single daily composite (Vanhellemont *et al.*, 2011; Vanhellemont and Ruddick, 2011). Surface SPM concentration is then retrieved from remote sensing reflectance at the MODIS band centered at wavelength 667nm, using the algorithm of Nechad *et al.* (2010). Finally, Level 2 processing flags, (Patt *et al.*, 2003) are used to mask out the land and cloud pixels and any bad quality pixels. The SPM concentration data together with wind, wave and current data from numerical models (Yu *et al.*, 2014) have been used to reconstruct the SPM dynamics. The data have been ensemble averaged according to winter and summer monsoon weather type. The use of atmospheric circulation patterns to describe different situations has proven to be very useful in climate and oceanographic studies (Demuzere *et al.*, 2009; Fettweis *et al.*, 2012). Each weather type has a distinct distribution of surface SPM concentrations, which is explained by differences in hydrodynamics, river run-off and wave conditions (see Fig. 1). During the summer monsoon season (June-September) the winds are blowing from the south and warm water with low SPM concentration is entering the Strait from the South China Sea. Higher SPM concentrations are found along the coasts and in the shallow areas of the Strait. These high turbidity areas are generated by local resuspension and by the river runoff. During winter (November-March) the NE winds are stronger. The SPM concentration is higher, which is due to higher waves and thus a higher resuspension, but also due to the higher import of SPM from the Chinese coastal Current into the Strait. The mixing of ocean water with low SPM concentration and coastal waters with high SPM concentration by wind stress is clearly visible in some images where eddies are visible. The results shed new light on the surface SPM concentration variability on seasonal and monthly time scales and allowed to better understand the large scale geographical variability of high turbidity zones in Taiwan Strait induced by meteorological and climatological variations using remote sensing data.

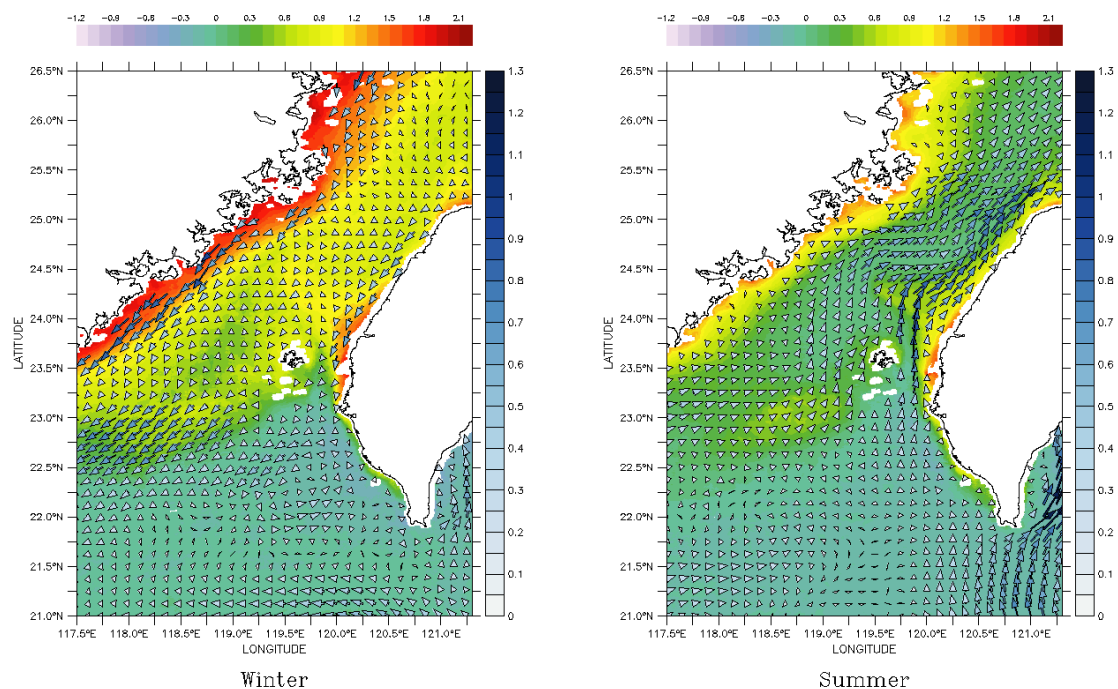


Fig. 1. Winter and summer averaged surface SPM concentration (in log [mg/L]) together with residual current pattern [m/s].

References

- Chen C.-T.A. and S.-L. Wang. 2006. A salinity front in the southern East China Sea separating the Chinese coastal and Taiwan Strait waters from Kuroshio waters. *Continental Shelf Research* 26:1636-1653.
- Chien H., W.-S. Chiang, S.-J. Kao, J.T. Liu, K.-K. Liu and P.L.-F. Liu 2011. Sediment dynamics observed in the Jhoushuei River and adjacent coastal zone in Taiwan Strait. *Oceanography* 24:122-131.
- Dadson S., N. Hovius, S. Pegg, W.B. Dade, M.J. Horng and H. Chen 2005. Hyperpycnal river flows from an active mountain belt. *Journal of Geophysical Research* 110:F04016.
- Demuzere M., M. Werner, N.P.M. van Lipzig and E. Roeckner. 2009. An analysis of present and future ECHAM5 pressure fields using a classification of circulation patterns. *International Journal of Climatology* 29:1796-1810.
- Fettweis M., J. Monbaliu, B. Nechad, M. Baeye and D. Van den Eynde. 2012. Weather and climate related spatial variability of high turbidity areas in the North Sea and the English Channel. *Methods in Oceanography* 3-4:25-29.
- Jan S., J. Wang, C.-S. Chern and C.-Y. Chao. 2002. Seasonal variation of the circulation in the Taiwan Strait. *Journal of Marine Systems* 35:249-268.
- Liao H.-R., H.-S. Yu and C.-C. Su. 2008. Morphology and sedimentation of sand bodies in the tidal shelf sea of eastern Taiwan Strait. *Marine Geology* 248:161-178.
- Liu J.T., H.-L. Lin and J.-J. Hung 2006. A submarine canyon conduit under typhoon conditions off southern Taiwan. *Deep Sea Research I* 53:223-240
- Nechad B., K. Ruddick and Y. Park. 2010. Calibration and validation of a generic multisensor algorithm for mapping of total suspended matter in turbid waters. *Remote Sensing of Environment* 114:854-866.
- Patt F.S., R.A. Barnes, R.E. Eplee, B.A. Franz and W.D. Robinson. 2003. Algorithm updates for the fourth SeaWiFS data reprocessing. NASA Technical Memorandum 22.
- Vanhellemont Q., B. Nechad and K. Ruddick. 2011. GRIMAS: gridding and archiving of satellite-derived ocean colour data for any region on earth. *Proc. CoastGIS 2011 Conf. (Ostend, Belgium)*, 5-8.

Vanhellemont Q. and K. Ruddick. 2011. Generalized satellite image processing: eight years of ocean colour data for any region on earth. Proc. SPIE 8175, Remote Sensing of the Ocean, Sea Ice, Coastal Waters, and Large Water Regions 81750Q.

Yu H.C., C.S. Yu, C.H. Chu and C.T. Terng. 2014. A regional ocean current forecast operational system for the sea around Taiwan. EGU General Assembly, 27 April - 2 May, Vienna, id. 5613.

A rheological lab measurement protocol for cohesive sediment

Claeys S.¹, P. Staelens², J. Vanlede¹, M. Heredia³, T. Van Hoestenbergh³, T. Van Oyen¹ and E. Toorman⁴

¹ Flanders Hydraulics Research, Ministry of Mobility and Public Works, Berchemlei 115, B-2140 Antwerpen, Belgium
E-mail: Stijn.claeys@mow.vlaanderen.be

² DOTOcean NV, Pathoekeweg 9B02, B-8000 Brugge, Belgium

³ Antea Group, Buchtenstraat 9, B-9051 Gent, Belgium

⁴ Hydraulics Laboratory, Department of Civil Engineering, KU Leuven, Kasteelpark Arenberg 40, box 2448, B-3001 Leuven, Belgium

Flanders Hydraulics, together with Antea Group, DOTOcean and KU Leuven, executed a long-term research project to obtain the necessary tools and method to map the (true) yield stress, dynamic viscosity and thixotropy of cohesive sediments for nautical and dredging applications.

This paper describes a method to map the rheological behaviour of cohesive sediment. The protocol is designed to give a minimum set of rheological parameters to characterize a mud sample. It should be practical (can be completed in a limited amount of time) and robust (give reproducible results). This should allow for comparative research, in which the rheological characteristics of mud samples at different stages of consolidation, or mud samples of different origin or composition can be compared.

The protocol is designed to be used with a vane-type rotational rheometer that can perform both shear stress and shear rate controlled experiments. It is important to note that the proposed type of rheometer is not equipped with a spring, but with air or magnetic bearings instead.

The full measurement protocol with its different stages is illustrated in Fig. 1. In the first stage of the experiment, the undisturbed sample is subjected to a stress growth test [1], applying a constantly increasing strain at a constant shear rate, and monitoring the stress build-up over time. Shear stress at a deformation rate of 1 rev/min is recorded for 30 seconds, and the maximum stress value is recorded. This value is reported as the 'peak yield stress at x rev/min', which is related to the undrained shear strength.

Before executing any other tests, the mud sample has to be fully sheared, which is done by shearing the mud sample at the highest possible speed (1000 rev/min) for 15 seconds [2]. This step creates a fully homogenised disturbed sample. A structural equilibrium is obtained and can be used as a reproducible reference stage to execute the next steps.

This is followed by an applied rotation speed for 100 seconds to reach an equilibrium 'instrument' shear stress (or torque) [3]. The necessary time trajectory of the instrument shear stress (calculated out of the measured torque and the dimensions of the vane) to maintain the applied rotational speed leading to an equilibrium is recorded. The shear stress equilibrium values will be used for dynamic viscosity modelling (see below) and the time-trajectory for thixotropic modelling.

Directly after an equilibrium is obtained in the previous stage, a 'Dullaert test' (Dullaert, 2005) is applied [4]. During this test a minimal rotation speed of 0,001 rev/sec is applied for 6 seconds. A very quick sampling rate of 200 samples/second is recorded. Hereafter, the sample is pre-sheared again and a lower rotation speed is applied for 100 seconds. Nine cycles of decreasing rotation speeds are used. The equilibrium shear stress values will be used to construct the Equilibrium Flow Curve (EFC). This EFC describes the dynamic viscosity behaviour of the cohesive sediment at structural equilibrium.

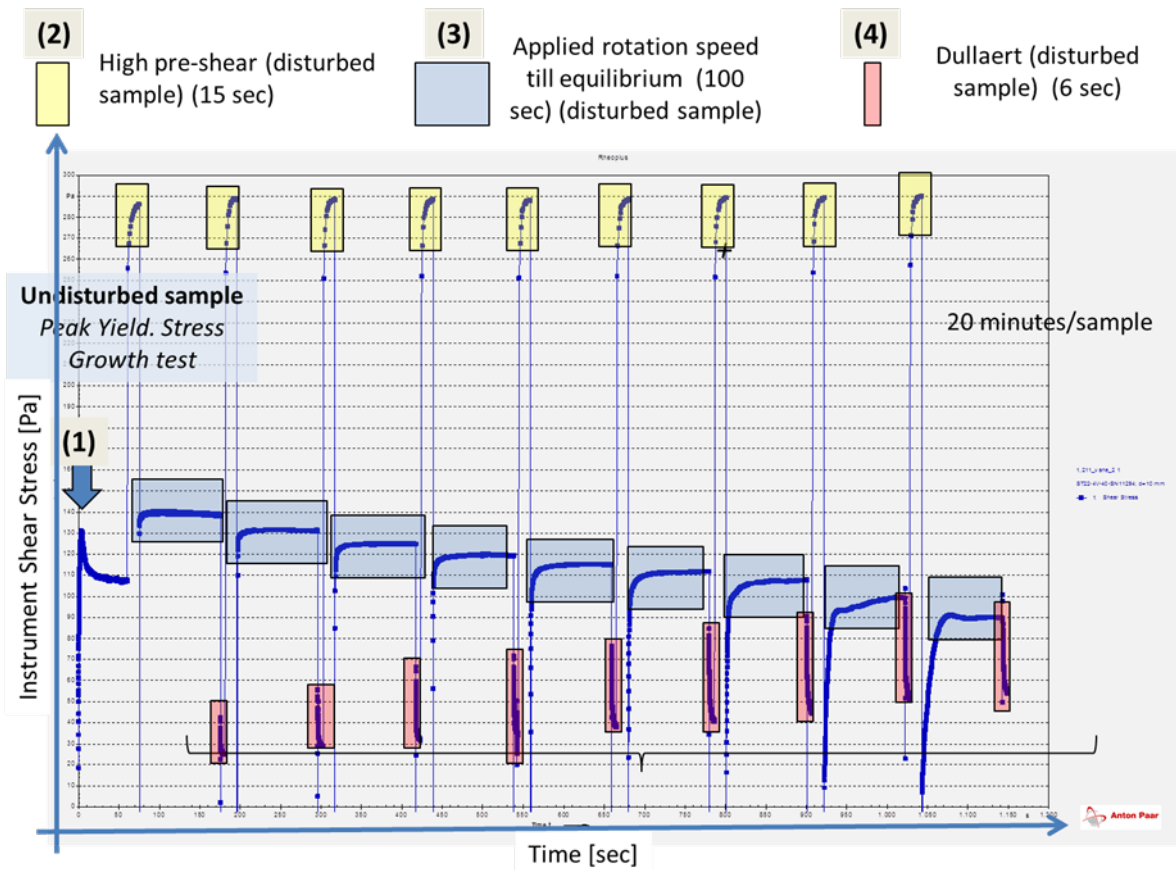


Fig. 1. Full measurement protocol.

Based on the iterative procedure to build an EFC described by Toorman (1994), a Matlab Toolbox is developed for automatic processing of vane test measurements. It is important to note that the shear rate distribution in the cup of the rheometer is non-linear and unknown, because it is dependent on the unknown EFC and because the yield radius (i.e. the distance, relative to the rotating surface, where the flow stagnates when the stress falls below the yield stress) is not known a priori. An iterative procedure is used to obtain the corrected shear rate and the resulting shear stress.

References

- Dullaert K. 2005. Constitutive equations for thixotropic dispersions. PhD Dissertation. Department of Chemical Engineering, KU Leuven. 197p.
- Toorman E.A. 1994. An analytical solution for the velocity and shear rate distribution of non-ideal Bingham fluids in a concentric cylinder viscometer. *Rheologica Acta* 33:193-202.

Modelling investigations on deep sea mine tailing plume dispersion on the Chatham Rise

Cronin Katherine¹, Claire Jeuken¹, Julia Vroom¹, Thijs van Kessel¹ and Jamie Lescinski²

¹ Deltares, PO Box 177, 2600 MH Delft, the Netherlands
E-mail: katherine.cronin@deltares.nl

² Hydronomic, Koninklijke Boskalis Westminster N.V, Rosmolenweg 20, Papendrecht, the Netherlands

Introduction

This paper describes a study that was conducted to investigate the dispersion behaviour of fine sediments in water depths of ~ 350m released during a mining tailings return process in the framework of the Chatham Rise Rock Phosphates (CRP) Mining Project. The Chatham Rise is a submarine feature that is approximately 1000km in length, extending eastward from the South Island of New Zealand. The rise has water depths that range from roughly 80m to 500m, with the Chatham Islands near the eastern extent of the submarine feature. Just north and south of the Rise, water depths quickly approach 3000m. The main purpose of the modelling study was to investigate the turbidity generated in the water column and the deposition footprint on the seabed resulting from the mining discharge.

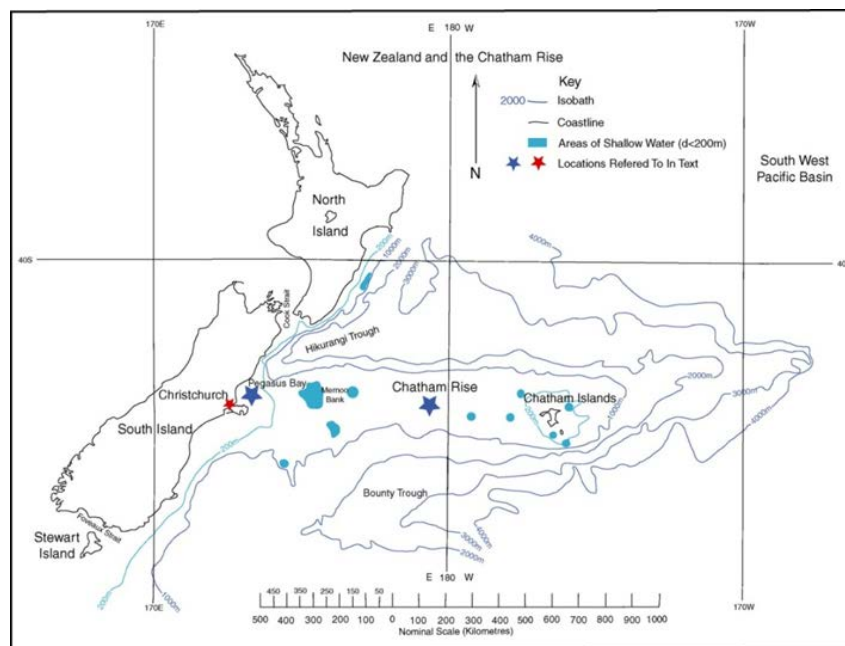


Fig. 1. Map of New Zealand and the Chatham Rise (Wikipedia: Ngatimozart, 2010).

Methodology

This study used a dedicated modelling approach to assess the near and far-field dispersion, resuspension and sedimentation behaviour of sediments. The study consisted of a far-field assessment using a Delft3D model with seasonal forcing: spring, summer and winter periods in 2011 to investigate the impact different hydrodynamic forcing had on the plume dispersion. The near-field mine tailing plume development was first investigated using a JET3D model which models the near-field plume dimensions of the spill as a result of excess density; initial momentum and ambient sea water density. The plume dimensions were then supplied to the far-field model which only considers the behaviour of the silt- and clay fractions. The models were used to examine the impact of releasing the plume at different heights above the bed on turbidity and sedimentation as well as assessing the impact of different oceanographic processes e.g. internal tides on the plume dispersion and dilution. Sensitivity tests were also performed on parameters such as the settling velocity of the fine sediments.

Results

Results of the far field modelling showed that during active mine tailings disposal, high sediment concentrations occur along the mining track. Most of these sediments (both the clay and silt) directly deposit along the track line. Plume dispersion patterns for silt in spring and winter look similar and display dispersion in a north-western direction. In the summer scenario the silt plume dispersion is somewhat larger. Maps of clay dispersion reveal considerable intra-seasonal variation in plume spreading that is similar to the predicted seasonal variation. Outside the mining area (2km-wide and 5km long region, oriented northwest-southeast) the fine sediment concentrations decrease due to plume dispersion. Both inside and outside the mining area, suspended sediment concentrations decay rapidly to values below 0.1mg/l, once mining stops; limited resuspension of deposited sediment occurs over the course of one cycle.

Both horizontal and vertical dispersion in combination with settling velocity determine the time scale over which sediment from an injected plume (re-) deposits. Dispersion is dependent on the degree of stratification therefore dispersion of the sediment plume in horizontal direction will be greater during periods of stronger stratification (but smaller in vertical direction).

The comparison of the sedimentation footprints from the different simulations point at limited effects of intra-seasonal hydrodynamic variations and cumulative effects, due to resuspension and delayed settling. Therefore the temporal variation in sedimentation pattern is much smaller than the variation observed in the suspended plume behaviour. Only data on current velocities were available for model verification but the main implications of the model performance in terms of hydrodynamics for the plume dispersion is also discussed.

Spatial and temporal variations of *in situ* erosion shear strength of newly inundated inter-tidal sediment

Dale Jonathan, Paul Kilkie and Heidi Burgess

School of the Environment and Technology, University of Brighton,
Lewes Road, Brighton BN2 4GJ, UK
E-mail: j.dale2@brighton.ac.uk

Modelling the evolution of intertidal cohesive sediment systems requires accurate estimates of the near bed sediment dynamics including the rate of surface erosion and erosion thresholds (Grabowski *et al.*, 2010). The surface shear strength of cohesive sediment has been recognised to vary both spatially and temporally (e.g. Black *et al.*, 2002; Tolhurst *et al.*, 2006) in response to the physical, chemical and biological properties of the sediment (Winterwerp and van Kesteren, 2004; Grabowski *et al.*, 2011). Ongoing research is increasing the understanding of intertidal biogeochemical sediment properties (e.g. Paterson, 1989; Grabowski *et al.*, 2011), however relatively little is understood about the changes in surface sediment properties when terrestrial land is inundated by the sea, as occurs at managed realignment sites.

Situated on the south coast of England, the Medmerry Managed Realignment site (breached September 2013) is the largest (183 hectares) open coast realignment project in Europe. Regular *in-situ* measurements of sediment surface shear strength were taken using a Cohesive Strength Meter (Paterson, 1989; Tolhurst *et al.*, 1999). Correlated with the variation in geochemical and physical conditions at each sample position, these results further the understanding of factors controlling sediment stability (e.g. Winterwerp and van Kesteren, 2004; Grabowski *et al.*, 2011).

This paper provides an insight into the temporal and spatial variability of cohesive sediment properties in open coastal managed realignment sites, where fluvial influence is limited. As a result there will be improved understanding of the dynamics of sediment with implications for the management and design of anthropogenically created intertidal environments.

References

- Black K.S., T.J. Tolhurst, D.M. Paterson and S.E. Hagerthey. 2002. Working with natural cohesive sediments. *Journal of Hydraulic Engineering-Asce* 128:2-8.
- Grabowski R.C., I.G. Droppo and G. Wharton. 2010. Estimation of critical shear stress from cohesive strength meter-derived erosion thresholds. *Limnology and Oceanography-Methods* 8:678-685.
- Grabowski R.C., I.G. Droppo and G. Wharton. 2011. Erodibility of cohesive sediment: The importance of sediment properties. *Earth-Science Reviews* 105:101-120.
- Paterson D.M. 1989. Short-term changes in the erodibility of intertidal cohesive sediments related to the migratory behaviour of epipelagic diatoms. *Limnology and Oceanography* 34:223-234.
- Tolhurst T.J., K.S. Black, S.A. Shayler, S. Mather, I. Black, K. Baker and D.M. Paterson. 1999. Measuring the *in situ* erosion shear stress of intertidal sediments with the Cohesive Strength Meter (CSM). *Estuarine Coastal and Shelf Science* 49:281-294.
- Tolhurst T.J., P.L. Friend, C. Watts, R. Wakefield, K.S. Black and D.M. Paterson. 2006. The effects of rain on the erosion threshold of intertidal cohesive sediments. *Aquatic Ecology* 40:533-541.
- Winterwerp J.C. and W.G.M. van Kesteren. 2004. *Introduction to the Physics of Cohesive Sediment in the Marine Environment*. Elsevier, Amsterdam.

Development of an hydro-sedimentary 3D model with sand-mud mixture - calibration and validation on 6 years evolution in the Seine Estuary

de Linares Matthieu, Régis Walther, Julien Schaguene, Cayrol Cyrielle and Luc Hamm

Artelia Eau & Environnement, 6 rue de Lorraine, 38120 Echirolles, France
E-mail: matthieu.delinares@arteliagroup.com

Context

Scientific monitoring of the rehabilitation program of the mudflats of the Seine Estuary conducted between 2005 and 2010 revealed the hydro-sedimentary evolution of the mudflats. Furthermore, the biological surveys undertaken make it easier to identify the relationships between physical and biological environments and therefore appreciate the ecological impact of possible additional facilities. That is why the Grand Port Maritime du Havre (GPMH) has called for a study:

- to better understand the current hydro-sedimentary dynamics of mudflats and estuary, based on a hydro-sedimentary 3D modelling, including the dynamics of sand and mud, calibrated on the observations performed since 2005 (Step 1);
- to predict what might be their evolution without new work (Step 2);
- to design and test several hypotheses for further works and assess their impacts (Step 3);
- to define the preliminary project stage for works selected (Step 4).

This is the step 1 that is developed in this paper.

Description of the hydrodynamic 3D model

The Telemac-3D model of the Seine Estuary extends from the Poses dam upstream boundary to the maritime area downstream. Initial bathymetry of the model is representative of the year 2005. The horizontal mesh size of the model ranges from 20 to 100m (for the North channel and associated mudflat) to 5km (for maritime area). The model is forced with the daily discharge of the Seine River, the astronomical tide level, variation of mean sea level due to meteorological conditions, waves and wind conditions.

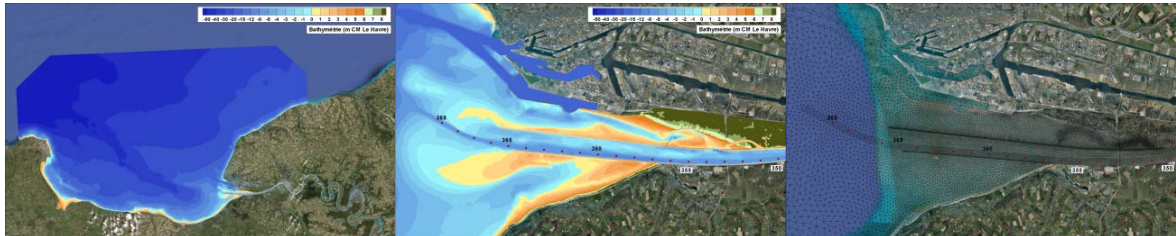


Fig. 1. General view of the 3D model, focus on bathymetry and mesh in interest area.

Calibration of the hydrodynamic model was achieved using measured levels of 19 tide gauges installed between Le Havre and Poses for different flow rates. The hydrodynamic model was then validated by comparison of 3D current results with several measurement campaigns (SHOM, GPMR, GPMH). Model validation for salinity was conducted using data from the network MAREL during one year (2006) at the Honfleur station but also from measurements (MODEL project of GIP Seine Aval program) made at the bottom and the surface at Tancarville Station during 6 months in 2010.

Calibration of the mud dynamic

At first, only mud was taken into consideration in the model. Calibration of the mud transport model consists primarily in the adjustment of different parameters in the model of consolidation, the laws of erosion and deposition and the fall velocity of the sediment. Most of the parameters have been calibrated using measurements from research programs Seine Aval 3 and 4. The model is now able to simulate a turbidity maximum in the range of 100,000 to 400,000 tonnes, which can be expelled after a flood and can grow again in the following months, as shown by turbidity measurements in Honfleur for several years. Seasonal dynamics is correctly reproduced as well as the shape of the turbidity plume.

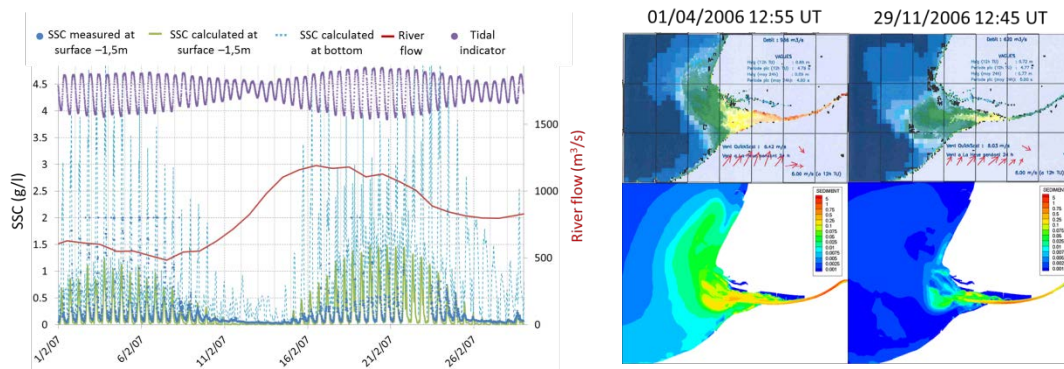


Fig. 2. Comparison of SSC at Honfleur station and comparison of turbidity plumes.

Calibration of mud-sand mixture dynamics

The hydro-sedimentary modeling used to calculate the morphological evolution of the Seine Estuary is based on the following principles:

- representation of sediment mixing with three classes of sand and a class of cohesive sediment ('mud');
- bed load transport and suspension of sand, suspended mud;
- temporal and spatial variation (horizontally and vertically) of the composition of the sediment mixture (% class% sand and mud);
- consolidation of silt deposited;
- consideration of the surface composition of the mixture of the sediment bed for the calculation of the critical stress for erosion.

A 3D model of the initial composition of the bed was made and adapted with measurements and results of simulation. Dredged process and dumping of Havre harbor and Rouen Harbor are included in the simulation. Many comparisons were made with measurement and sensitivity of the model was tested. The calibration of the model is the result of 2 years of work.

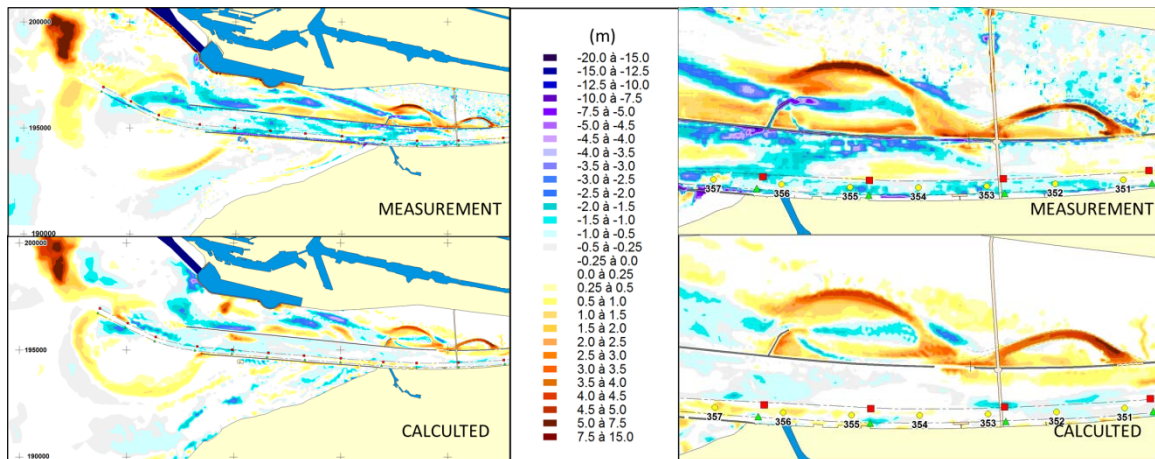


Fig. 3. Comparison of bathymetry evolution (2005-2011) between measurements and 3D model.

The role of biota in fine sediment transport processes in the Markermeer: a synthesis

de Lucas Pardo Miguel¹, Thijs van Kessel¹ and Johan C. Winterwerp^{1,2}

¹ Marine and Coastal Management, Deltares, PO Box 177, 2600 MH, Delft, the Netherlands
E-mail: Miguel.deLucasPardo@deltares.nl

² Section of Environmental Fluid Mechanics, Civil Engineering and Geosciences, Delft University of Technology, PO Box 5048, 2600 GA, Delft, the Netherlands

The very turbid and ecologically deteriorated Lake Markermeer, in the Netherlands, has been subject of many studies over the last decades. A major contribution to the understanding of the lake's dynamics has been accomplished over the last four years, in the context of the PhD study of the first author. We provide an overview of the previous knowledge, as well as elaborate on our most important findings, aiming at the holistic picture of the lake's fine sediment dynamics.

The bed of the lake consists of a muddy layer that is subdivided into an oxic and easily erodible layer and an anoxic and more resistant layer below. Underneath these two layers, very stiff clayey old deposits are found.

Formerly, the turbidity of the lake was considered to be dominated by erosion and deposition of the oxic layer. We corroborated that hypothesis, but we also demonstrated that the oxic layer owes its characteristics not to its oxidized state, but to its bioturbated state. Moreover, we hypothesized that the muddy layer at the bed stems from historic bioturbation of the old deposits on the bed, and after the closure of the lake in 1975.

Furthermore, the turbidity in the water column was formerly regarded as a function of the suspended minerals only. We evaluated the influence of water column biota (algae) in the turbidity, showing that turbidity does not only depend on the amount of suspended minerals, but also on the type of algae present in the water column. In fact, some algae species were found to promote flocculation, whereas some other species inhibit flocculation due to large concentrations of algae yielding steric repulsion. Finally, biota was also found to be relevant for consolidation processes in the lake, accelerating consolidation due to tunnels and burrows created by the fauna. These tunnels result in an increased permeability of the bed, hence in a more rapid dewatering process. Summarizing, the role of biota in the Markermeer has been found to be dominant for the sediment sources (erosion), relevant for sediment transport (inhibition or promotion of flocculation), and relevant for the sediment sinks (consolidation).

During the investigation of these sediment transport processes, we measured a number of sediment transport parameters, either in the field or in the lab. These measurements were then used in a one dimensional modelling exercise. This exercise was performed with the 1DV version of the multi-layer bed module of Delft 3D. The model was coupled externally with Matlab, and thus we could introduce the effect of biota in the relevant sediment transport processes. Below are the main parameters that we measured in the lab and implemented in the model:

- Critical shear stress for erosion and erosion rate for the non-bioturbated anoxic layer and for the bioturbated oxic layer. These parameters were obtained by using a Gust erosion microcosm.
- Settling velocity. Measurements of the settling velocity were performed in the 5 metres large settling column at Delft University of Technology, and with a recently developed measuring chamber.
- Floc sizes were measured in the large scale settling column, with the Malvern Mastersizer used for the small scale flocculation experiments, and in the field with the recently developed floc camera.
- Bioturbation rates were measured by letting fauna bioturbate the bed for a certain time, while measuring the difference in erosion between a non-bioturbated and a bioturbated bed at the Gust erosion microcosm.
- Aggregation rates were measured from the flocculation experiments, from the increased size per time interval between measurements.

All these parameters were used in the sediment transport model, without further calibration. Only the rate at which the sediments in the oxic and bioturbated layer gain strength has to be calibrated for good model results. Our results compare reasonably well with the measurements of turbidity. The latter suggests that our measuring techniques and instruments provide reliable and useful data. Second, turbidity observations cannot be explained without the effect of biota, in particular without the effect of bioturbation. Other biotic effects were found to be relevant as well, as the effect of algae in the aggregation efficiency of flocs or in the settling velocity. Hence, the relevance of biota in Markermeer's fine sediment dynamics has also been established indirectly with the 1DV model.

A parameter model for dredge plume sediment source terms

Decrop Boudewijn^{1,2}, Tom De Mulder², Erik Toorman³ and Marc Sas¹

¹ IMDC (International Marine and Dredging Consultants)
Coveliersstraat 15, B-2600 Antwerp, Belgium
E-mail: boudewijn.decrop@imdc.be

² Hydraulics Laboratory
Dept of Civil Engineering, Ghent University, Sint-Pietersnieuwstraat 41, B-9000 Ghent, Belgium

³ Hydraulics Laboratory
Dept of Civil Engineering, KU Leuven, Kasteelpark Arenberg 40, B-3001 Heverlee, Belgium

Introduction

The work presented in this paper aims at the development of a stochastic model for the fast prediction of the distribution of dredging-induced sediment suspensions in the water column. In recent times, environmental impact assessments of dredging works have been subject to extensive regulation. Methods for the prediction of adverse effects of marine works are permanently being improved. Dredging using Trailer Suction Hopper Dredgers (TSHD) requires discharging of excess water from the vessel's hopper into the sea for optimal efficiency of the operation. The return flow is discharged through a vertical shaft through the dredger's hull, called the overflow. The released material usually contains a fraction of fine sediments for which the residence time in the hopper was insufficient to settle and thus stays in suspension until the overflow shaft is reached. Part of the released material might descend to the sea bed as a density current, another part might be dispersed to form a surface plume. The latter part is bound to stay in the water column for a longer period in case the sediment concentration is too low for a buoyancy-driven descent to the sea bed. The turbidity plume generated in this way can be advected by the sea currents and potentially reaches environmentally sensitive areas.

In the feasibility phases, the fate of these fine sediment plumes needs to be predicted in order to assess the need for mitigation measures. In the operational project phase, plume predictions are needed to assess the timing and location of the works planned for the coming days. The large-scale simulation of the plumes is generally executed with a shallow-water hydrodynamic flow model fitted with a source term for the overflow mixture. The source term which has to be supplied to the large-scale model is the fraction of the released sediments that ends up in the water column. The determination of this source term can be done using time-consuming process-based models, or by means of a parameterised prediction model. The development of the model structure and the fitting of its parameter by means of a large dataset of process-based model output are presented in this paper.

Process-based model

In order to design and fit the coefficients of a stochastic model, a dataset is needed. The dataset in this case has to consist of sediment flux profiles in the vicinity of a TSHD while dredging aggregates containing fine sediment, using the overflow. Decrop *et al.*, (2014a, 2014b) set up a Computational Fluid Dynamics (CFD) framework for the simulation of flow around a TSHD and the detailed turbulent dispersion of the near-field sediment plume, which is actually a buoyant jet-in-crossflow. The CFD model takes into account the effect of mixture bulk density, propeller action and air bubbles. An example of the result of a calculation for relatively shallow water can be seen in Fig. 1. Due to the shallow water in this case, a density current is formed near the sea bed (brown isosurface at sediment volume concentration $C=10^{-5}$) while higher in the water column a surface plume is generated (coloured contours at the water surface).

The liquid discharge and sediment concentration of the overflow discharge can be calculated by means of a hopper model such as by e.g. van Rhee (2002) or Jensen and Saremi (2014). The CFD model is validated using *in situ* measurements of different monitoring campaigns in the field. CFD model output at a fixed distance behind the dredger is transformed to vertical profiles of sediment mass flow rate q_s , which are then stored to serve as a dataset for fitting of the parameter model.

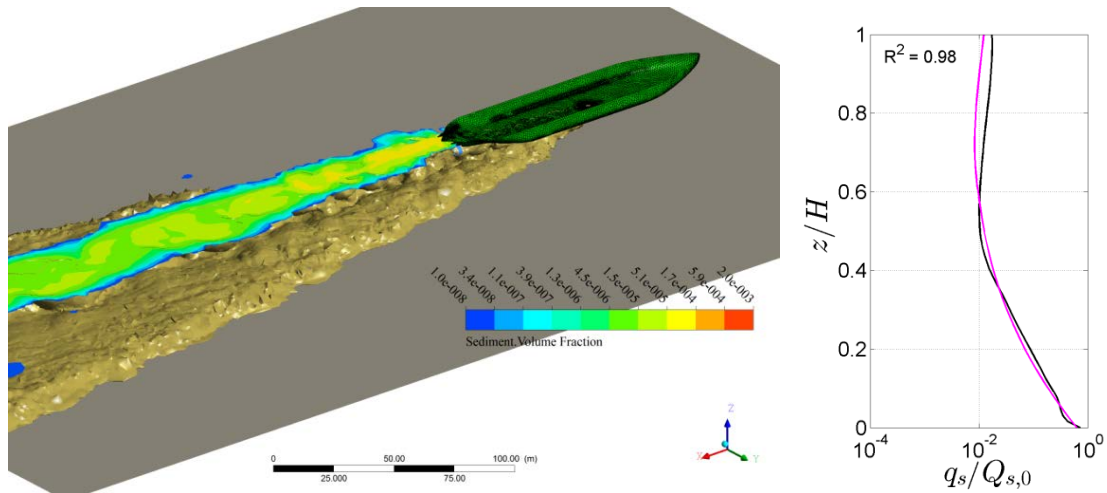


Fig. 1. Left panel: Example of CFD model output used for the fitting of a stochastic model for dredge plume source terms. Right panel: Example of vertical profiles of sediment mass flow rate q_s : a parameter model validation result in magenta and the corresponding CFD output in black line.

Parameter model

Overflow plume profiles extracted from a large number of different CFD simulations were analysed and a parameterisation of the vertical profile of q_s was defined. The different coefficients in the profile shape model were then fitted to the CFD model output dataset using a multivariate general regression model. Subsequently, the CFD model dataset was divided in a training dataset used for the fitting of the coefficients, and a validation dataset. The model includes a predictor step using the parameterisation, and a corrector step to assure the full sediment flux is accounted for. The parameter model provides a vertical profile of q_s in the plume at a given distance behind the ship, which can be directly applied as a source term in a large-scale hydrodynamic/sediment transport model. The result of a validation case for the parameter model is shown in Fig. 1 (right panel). Here, z/H is the distance above the bed divided by the water depth, q_s is the sediment mass flow rate in the plume (in kg/s per meter water depth) and $Q_{s,0}$ is the total solid discharge through the overflow (kg/s). The profile of q_s (normalised by $Q_{s,0}$) from the CFD model is shown in black, the parameter model output in magenta. Error statistics shows that for 75% of the set of validation runs, a coefficient of determination higher than 0.7 is obtained.

The resulting model can thus be implemented in large-scale hydrodynamic model codes, for the online determination of the overflow sediment source term.

References

- Decrop B., T. De Mulder, E. Toorman and M. Sas. 2014a. Large-eddy simulations of a sediment-laden buoyant jet resulting from dredgers using overflow. In: Lehfeldt & Kopmann (Eds). ICHE 2014, Hamburg, Bundesanstalt für Wasserbau. ISBN 978-3-939230-32-8.
- Decrop B., T. De Mulder, E. Toorman and M. Sas. 2014b. Large-eddy simulations of turbidity plumes in crossflow. European Journal of Mechanics B-Fluids. (in press).
- Jensen J.H. and S. Saremi. 2014. Overflow concentration and sedimentation in hoppers. J. Waterway, Port, Coastal, Ocean Eng. 140(6).
- van Rhee C. 2002. On the sedimentation process in a trailing suction hopper dredger. Ph.D. thesis. Technical Univ. Delft, Delft, the Netherlands.

Factors influencing top sediment layer and SPM concentration in the Zeebrugge harbor

Dujardin Arvid¹, Joris Vanlede², Thomas Van Hoestenbergh¹, Luc Van Poucke¹, Michael Fettweis³, Claudio Cardoso¹, Carlos Velez¹, Renaat De Sutter¹ and Chantal Martens⁴

¹ Antea Group, Buchtenstraat 9, B-9051 Gent, Belgium
E-mail: arvid.dujardin@anteagroup.com

² Flanders Hydraulics Research, Department of Mobility and Public Works, Flemish Government, Berchemlei 115, B-2140 Antwerp, Belgium

³ Operational Directorate Natural Environment, Royal Belgian Institute of Natural Sciences, Gulledele 100, B-1200 Brussels, Belgium

⁴ Maritime Access Division, Department of Mobility and Public Works, Flemish Government, Tavernierkaai 3, B-2000 Antwerp, Belgium

The port of Zeebrugge (Belgium) suffers from significant siltation. To safeguard navigation, on average 5 million tons (dry matter) is yearly dredged inside the harbor (Dujardin *et al.*, in progress) and an additional 1.6 million tons (dry matter) in the access channel Pas van het Zand (Lauwaert *et al.*, 2006 & 2008), and disposed on authorized disposal sites in the Belgian part of the North Sea. Numerical model results indicate that a significant part of the disposed sediments recirculates back from the current disposal sites to the dredging areas (Van den Eynde and Fettweis, 2014). A field study, accompanied by an extensive monitoring campaign, was set up in 2013-2014 to verify whether using an alternative disposal site is influencing the SPM concentration and the top sediment layer in the harbor. In addition to the monitoring campaign and in order to better assess the results of the field study, the baseline system behavior was also characterized over a longer period (1999-2012).

The mechanisms causing the sediment from the North Sea to enter the harbor have been intensively studied the last decade (Dujardin *et al.*, 2009; Vanlede and Dujardin, 2014). The sediment dynamics inside of the harbor, however, are still largely unknown. The present study aims to quantify the influence of internal and external factors on the sediment dynamics within Zeebrugge harbor, based on both the 2013-2014 monitoring campaign and the longer period datasets. Possible factors external to the harbor are tide, wind, currents, wave climate, salinity and SPM concentration. The factors internal to the harbor are navigation, dredging operations and fresh water discharge.

For the 2013-2014 campaign, measurements inside and outside the port of Zeebrugge of various oceanographic and sediment parameters (SPM concentration, current velocity, waves, salinity, temperature, tides, wind, bathymetry, density of mud layers) were conducted during the whole duration of the experiment. The measurements outside the port are presented in Fettweis *et al.* (this volume). The monitoring inside the port was carried out at 4 locations. At each location, time series of currents, salinity, temperature, water elevation and SPM concentration were collected near the surface and near the bed. Measurements show for all locations that the maximum SPM concentration reaches more than 4g/l near the bed and up to 2g/l at the surface.

For the characterization of the baseline system behavior, a long-term dataset (1999-2012) is available of the height of the 210kHz and 33kHz reflector, fresh water inflow in the harbor, wind, wave, and tidal data, surface SPM data derived from satellite images (GRIMAS dataset) and dredging quantities. Within this dataset, bathymetric measurements were less frequent than during the 2013-2014 field study, except for the summer of 2012 (Dujardin *et al.*, 2014).

Correlations between different parameters are analyzed, both for the shorter (one year) and longer (13 year) period. Statistical relations were established based on the long-term dataset (Dujardin *et al.*, in progress) and the results from the 2013-2014 study were compared with the findings for the 1999-2012 period. In the harbor, local currents, tidal amplitude and SPM concentrations are significantly correlated. Daily variations in SPM concentrations and bathymetry (210kHz reflector level) are related to tides, storms, seasonal changes, ship movements and dredging operations.

References

- Baeye M., M. Fettweis, G. Voulgaris and V. Van Lancker. 2011. Sediment mobility in response to tidal and wind-driven flows along the Belgian inner shelf, southern North Sea. *Ocean Dynamics* 61:611-622.
- Dujardin A., S. Ides, G. Schramkowski, T. De Mulder and F. Mostaert. 2009. Haven van Zeebrugge – Optimalisatie maritieme toegankelijkheid: Onderzoek naar de water- en sedimentuitwisseling ter hoogte van de havenmond. Versie 3_0. WL Rapporten, 843_01. Waterbouwkundig Laboratorium, Antwerpen, Belgium. (in Dutch).
- Dujardin A., J. Vanlede, S. Vos, T. Verwaest and F. Mostaert. 2014. Invloedsfactoren op de ligging van de top van de sliblaag in het CDNB: Deelrapport 1 – Casestudy “zomer 2012”. Versie 2.0. WL Rapporten, 00_078. Waterbouwkundig Laboratorium & Antea Group, Antwerpen, Belgium. (in Dutch).
- Dujardin A., J. Vanlede, S. Vos, T. Verwaest and F. Mostaert. (in progress). Invloedsfactoren op de ligging van de top van de sliblaag in het CDNB: Deelrapport 2 – Analyse periode 1999 - 2011. Versie 1.0. WL Rapporten, 00_078. Waterbouwkundig Laboratorium & Antea Group, Antwerpen, Belgium. (in Dutch).
- Fettweis M., M. Baeye, F. Francken, B. Lauwaert, D. Van den Eynde, V. Van Lancker, C. Martens and T. Michiels. 2011. Monitoring the effects of disposal of fine sediments from maintenance dredging on suspended particulate matter concentration in the Belgian nearshore area (southern North Sea). *Marine Pollution Bulletin* 62:258-269.
- Fettweis M., M. Baeye, T. Van Hoestenbergh, L. Van Poucke, A. Dujardin and V. Van Lancker. 2015. *In situ* measurements of SPM concentration to evaluate the impact of the disposal of fine grained sediments from maintenance dredging. *Proc. IntercoH 2015* (this issue).
- Lauwaert B., K. Bekaert, D. De Brauwer, M. Fettweis, H. Hillewaert, S. Hoffman, K. Hostens, K. Mergaert, I. Moolaert, K. Parmentier and J. Verstraeten. 2006. Synthesis report on the effects of dredged material disposal on the marine environment (licensing period 2004-'06). MUMM, ILVO Fisheries, Maritime Access Division, and Coast Division. Ostend, Belgium.
- Lauwaert B., K. Bekaert, M. Berteloot, D. De Brauwer, M. Fettweis, H. Hillewaert, S. Hoffman, K. Hostens, K. Mergaert, I. Moolaert, K. Parmentier, G. Vanhoey and J. Verstraeten. 2008. Synthesis report on the effects of dredged material disposal on the marine environment (licensing period 2006-'08). MUMM, ILVO Fisheries, Maritime Access Division, and Coast Division. Ostend, Belgium. 109p.
- Van den Eynde D. and M. Fettweis. 2014. Towards the application of an operational sediment transport model for the optimisation of dredging works in the Belgian coastal zone (southern North Sea). p.250-257. In: Dahlin H., N.C. Flemming, S.E. Petersson (Eds). *Sustainable Operational Oceanography*.
- Vanlede J and A. Dujardin. 2014. A geometric method to study water and sediment exchange in tidal harbors. *Ocean Dynamics*, DOI 10.1007/s10236-014-0767-9.

Controls on suspended particle properties and water clarity along a partially-mixed estuary, York River, Virginia, USA

Fall Kelsey A.¹, Carl T. Friedrichs¹, Grace M. Cartwright¹ and David G. Bowers²

¹ College of William & Mary, Virginia Institute of Marine Science
Gloucester Point, VA 23062, USA
E-mail: kafall@vims.edu, carl.friedrichs@vims.edu, gracec@vims.edu

² School of Ocean Sciences, Bangor University
Menai Bridge, Angelsey, LL595AB, UK
E-mail: d.g.bowers@bangor.ac.uk

The Chesapeake Bay and its associated tidal tributaries, which together form one of the United States' largest and most important estuaries, are among the many coastal systems where degraded water clarity is a major concern. Despite long-term decreases in sediment input, water clarity over the last 20 years has continued to deteriorate in the Bay and its tributaries (Williams *et al.*, 2010). Analysis of long-term monitoring data (Wang *et al.*, 2010) found that the concentration of total suspended solids (TSS), the regulatory indicator of 'suspended sediment pollution', is about as likely to be positively or negatively correlated to sediment loads from the watershed. At the same time, locally suspended sediments are related to water clarity given that the diffuse light attenuation coefficient (K_d) is always positively correlated to TSS. This suggests that even though the suspended sediment in the water column is degrading water clarity, recent sediment input is not determining its concentration.

Gallegos *et al.*, (2011) documented a decade-long change in the Chesapeake Bay in the relationship between surface diffuse light attenuations (K_d) and Secchi disks depth, a visual measurement of the depth at which a standard pattern on a 20cm diameter disk is no longer visible from the surface, which he attributed to the decrease in Secchi disk depths. Secchi depth is more sensitive to scattering of light, and the model for attenuation presented by Gallegos *et al.* (2011) suggested that the most likely explanation for the change in the product of Secchi depths and K_d is due to the increase in the concentration of suspended non-algal organic matter, however no data was available to support his claim. Here it is proposed that the apparent disconnect between water clarity and input of sediment into the Bay and its estuarine tributaries is related to the interaction between organic solids and inorganic sediment. The objective of this study was to investigate the influence of common suspended particle properties (size, concentration, composition) on apparent and inherent optical properties in an estuarine system, specifically K_d as well as beam attenuation (C).

This project focused on observations collected along the York River Estuary, a major tidal tributary of the lower Chesapeake Bay. Vertical profiles through the water column of particle properties (settling velocity, concentration, size, organic content, and density) and physical parameters (salinity, turbidity, light attenuation, and acoustic backscatter) were collected using the Coastal Hydrodynamics & Sediment Dynamics (CHSD) water column profiler (Cartwright *et al.*, 2013). The profiler is equipped with a pump sampler, two Acoustic Doppler Velocimeters (ADVs), a Sequoia Laser In-Situ Scattering and Transmissometry instrument (LISST-100X), and a CTD (conductivity, temperature and depth probe) equipped with a YSI 6136 turbidity sensor, and a high-definition particle imaging camera system (PICS). The pump allows water samples to be collected so that suspended solids can be analysed for organic content. The ADVs provide estimates of mass concentration of suspended particle matter, bottom current velocities, turbulence, and bulk settling velocity (Fugate and Friedrichs, 2002). The LISST measures the suspended particle size distribution in 32 logarithmically spaced size classes over the range 2.5 to 500 μ m, and the PICS system provides direct measurements of particle settling velocities and sizes of particles greater than 30 μ m (Smith and Friedrichs, 2011). Observations of the diffuse light attenuation (K_d) were measured by either a hyperspectral Trios radiometer or LI-COR sensor system (Kirk, 1994). In addition to observations of K_d , LISST optical transmission was used to estimate beam attenuation coefficient (C) following Lund-Hansen (2010).

Preliminary results averaged from along-estuary slack water sampling cruises in the York River in June 2013 and September 2014 are displayed in Fig. 1. Similar spatial and temporal trends are seen in both the inherent (beam attenuation, C) and apparent (diffuse light attenuation, K_d) optical properties (Fig. 1A). The data show an up estuary increase in K_d , c, and TSS and an up estuary decrease in percent organic content. Additionally, these initial results from the York indicate importance of these small, more organic particles on optical properties. Data revealed significant, negative correlations between particle area and organic matter content (i.e. the smaller particles in

suspension are more organic). Additional data will be collected in order to further explore preliminary trends.

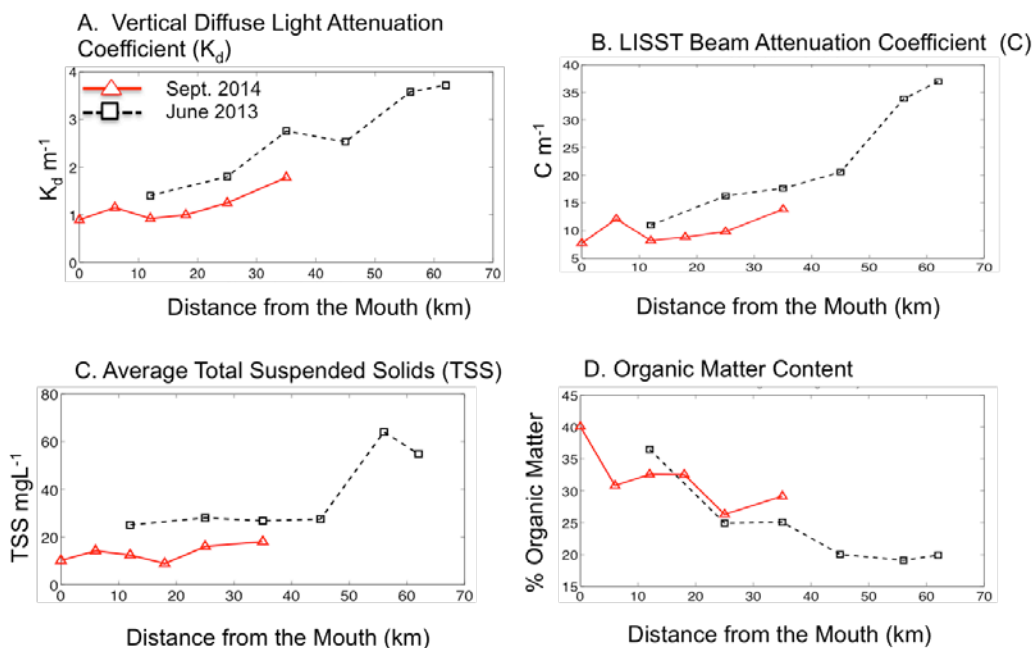


Fig. 1: Averaged K_d (A), C, (B), TSS (C), and Percent Organic Matter (D) from along-estuary slack water sampling cruises in the York River in June 2013 and September 2014.

References

- Cartwright G.M., C.T. Friedrichs and S.J. Smith. 2013. A test of the ADV-based Reynolds-flux method for *in situ* estimation of sediment settling velocity in a muddy estuary. *Geo-Marine Letters* 33:477-484. doi:10.1007/s00367-013-0340-4.
- Fugate D.C. and C.T. Friedrichs. 2002. Determining concentration and fall velocity of estuarine particle populations using ADV, OBS, and LISST. *Continental Shelf Research* 22:1867-1886.
- Gallegos C.L., J.P. Werdell and C.R. McClain. 2011. Long-term changes in light scattering in Chesapeake Bay inferred from Secchi depth, light attenuation, and remote sensing measurements. *Journal of Geophysical Research* 116, doi:10.1029/2011JC007160.
- Kirk J.T.O. 1994. *Light and photosynthesis in aquatic ecosystems*. Cambridge University Press, Cambridge.
- Lund-Hansen L.C. 2010. Suspended matter, Chl-a, CDOM, grainsizes, and optical properties in the Arctic fjord-type estuary, Kangerlussuaq, West Greenland during summer. *Estuaries and Coasts* 33:1442-1451.
- Smith S.J. and C.T. Friedrichs. 2011. Size and settling velocities of cohesive flocs and suspended sediment aggregates in a trailing suction hopper dredge plume. *Continental Shelf Research* 31(10S):S50-S63.
- Wang B.A., L.C. Linker and R.A. Batiuk. 2010. Monitored and modelled correlations of sediment and nutrients with Chesapeake Bay water clarity. *JAWRA Journal of the American Water Resources Association* 49(5):1103-1118.
- Williams M.R., S. Filoso, B.J. Longstaff and W.C. Dennison. 2010. Long-term trends of water quality and biotic metrics in Chesapeake Bay: 1986-2008. *Estuaries and Coasts* 33(6):1279-1299.

Uncertainty of *in situ* SPM concentration measurements

Fettweis Michael¹, Matthias Baeye¹ and Romaric Verney²

¹ Operational Directorate Natural Environment, Royal Belgian Institute of Natural Sciences, Gulledele 100, B-1200 Brussels, Belgium
E-mail: m.fettweis@mumm.ac.be

² Laboratoire Dyneco/Physed, IFREMER, BP 70, F-29280 Plouzané, France

The aim of the study is to assess the state of our understanding, to evaluate the confidence with which SPM concentration can be measured, and to identify human impact in the data series. Direct or indirect measurements of parameters are inherently associated with uncertainties (errors) due to a lack of accuracy of the measuring instruments, inadequate precision of the observations, and the statistical nature of the parameters. When using observations, understanding of the uncertainties is needed, in order to avoid speculative statements. Uncertainty will become an important issue for scientists and decision-makers in the future as they will be used to evaluate GES of the European marine areas and to predict the impact of human activities. Uncertainty in measured data can originate from different sources (Winter, 2007). Those that can be reduced by further study of the system and improving our state of knowledge, and those that are considered unknowable such as variability in the system beyond the existing time series, the chaotic nature of the system, and the indeterminacy of human systems (Dessai and Hulme, 2003).

SPM concentration can be measured using optical or acoustic sensors. The voltage output of Optical Backscatter Sensors (OBS) is converted to Formazine Technical Unit using solutions of formazine and SPM concentration by calibration against filtered water samples. After conversion to decibels, the backscattered acoustic signal strength (from an Acoustic Doppler Profiler) is corrected for geometric spreading, water attenuation, sediment attenuation (Kim *et al.*, 2004) and is calibrated using the OBS-derived SPM concentration estimates (Fettweis, 2008). In general, acoustic backscattering is affected by sediment type, size and composition (Thorne *et al.*, 1991; Hamilton *et al.*, 1998; Bunt *et al.*, 1999; Fugate and Friedrichs, 2002; Voulgaris and Meyers, 2004). OBS signals have primarily been designed to be most sensitive to SPM concentration; size effects are an order of magnitude lower than those of concentration, and flocculation effects are even smaller (Downing, 2006). Compared to optical devices, acoustic devices are more sensitive to coarser grain sizes and thus produce better estimates of the mass concentration of the coarser granular fraction. Changes in colour, size and density of the suspended sediments have been reported to influence the OBS results by a factor 10 to 20 (Sutherland *et al.*, 2000). The latter is especially disturbing when using long-term time series of data of SPM concentration from OBS, as it is collected at a station near Zeebrugge and in the Seine Estuary, and where changes in sediment composition during e.g. a storm or fortnightly cycles have been reported (Baeye *et al.*, 2011; Fettweis *et al.*, 2012; Verney *et al.*, 2013). Therefore a careful analysis of existing calibration data, of LISST data, and of acoustic and optical sensor data, has been carried out. Calibration of sensors (OBS and ADCP) is carried out during 6 tidal cycle measurements in the Belgian nearshore area and the Seine Estuary using *in situ* water samples. The analysis allows to evaluate calibration procedures of sensor output as a function of e.g. seasonal changes in composition and thus on the uncertainty of long-term time series of SPM concentration derived from acoustic and optical measurements of turbidity.

References

- Baeye M., M. Fettweis, G. Voulgaris and V. Van Lancker 2011. Sediment mobility in response to tidal and wind-driven tidal flows along the Belgian inner shelf, southern North Sea. *Ocean Dynamics* 61(5): 611-622.
- Bunt J.A.C, P. Larcombe and C.F. Jago 1999. Quantifying the response of optical backscatter devices and transmissometers to variations in suspended particulate matter. *Continental Shelf Research* 19:1199-1220.
- Dessai S. and M. Hulme 2003. Does climate policy need probabilities? Tyndall Centre for Climate Change Research, Working Paper 34, 42p.
- Downing J. 2006. Twenty-five years with OBS sensors: the good, the bad, and the ugly. *Continental Shelf Research* 26:2299-2318.
- Fettweis M. 2008. Uncertainty of excess density and settling velocity of mud flocs derived from *in situ* measurements. *Estuarine Coastal and Shelf Science* 78:428-436.

- Fettweis M., M. Baeye, B.J. Lee, P. Chen and J.C.R. Yu 2012. Hydro-meteorological influences and multimodal suspended particle size distributions in the Belgian nearshore area (southern North Sea). *Geo-Marine Letters* 32:123-137.
- Fugate D.C. and C.T. Friedrichs 2002. Determining concentration and fall velocity of estuarine particle populations using ADV, OBS and LISST. *Continental Shelf Research* 22:1867-1886.
- Hamilton L.J., Z. Shi and S.Y. Zhang. 1998. Acoustic backscatter measurements of estuarine suspended cohesive sediment concentration profiles. *Journal of Coastal Research* 14:1213-1224.
- Sutherland T.F., P.M. Lane, C.L. Amos and J. Downing 2000. The calibration of optical backscatter sensors for suspended sediment of varying darkness levels. *Marine Geology* 162:587-597.
- Thorne P.D., C.E. Vincent, P.J. Hardcastle, S. Rehman and N.D. Pearson 1991. Measuring suspended sediment concentrations using acoustic backscatter devices. *Marine Geology* 98:7-16.
- Verney R., G. Voulgaris, A. Manning, J. Deloffre and P. Bassoullet 2013. Quantifying suspended particulate matter (SPM) dynamics in estuaries: Combining acoustic and optical approaches. *Proc. of the 12th Int. Conf. on Cohesive Sediment Transport Processes (INTERCOH)*, Gainesville, Florida.
- Voulgaris G. and S. Meyers 2004. Temporal variability of hydrodynamics, sediment concentration and sediment settling velocity in a tidal creek. *Continental Shelf Research* 24:1659-1683.
- Winter C. 2007. Evaluation of Sediment Transport Models. *Sedimentary Geology* 202:562-571.

Modelling of sediment dynamics and the effect of mussel bioengineering in a non-tidal coastal lagoon, Rødsand lagoon, Denmark

Forsberg Pernille L.¹, Verner B. Ernstsén¹, Ulrik Lumborg², Klavs Bundgaard² and Aart Kroon¹

¹ Department of Geosciences and Natural Resource Management
University of Copenhagen, Øster Voldgade 10, DK-1350 Copenhagen K, Denmark
E-mail: pefo@ign.ku.dk

² DHI, Agern Allé 5, DK-2970 Hørsholm, Denmark.

Rødsand lagoon in southeast Denmark (Fig. 1) is a non-tidal coastal lagoon, which is home to a wide range of marine flora and fauna. The lagoon is protected under Natura 2000, which prohibits a permanent disruption of the protected species and natural habitats (Nature Agency, 2014). An increase in turbidity within the lagoon may reduce the ecosystem health due to hindered light penetration. A threat to the lagoonal ecosystem is related to future increasing storm intensities (Olesen *et al.*, 2014), which are presumed to increase the suspended sediment concentration (SSC) within the lagoon. Furthermore the planned construction of a tunnel, the Fehmarnbelt fixed link between Germany and Denmark (FEHY, 2013a), propose a threat to the lagoon due to a possible spill of sediment, which could increase the longshore sediment influx to Rødsand lagoon. Mussels can reduce the SSC in marine environments (Chamberlain *et al.*, 2001; Valeur, 2004; Schröder *et al.*, 2014), why the implementation of a mussel farm has been suggested as a management option. In the present study we developed a module to include mussels as a bioengineering measure in a numerical sediment transport model and investigated how the implementation of an exterior mussel farm affects the sediment dynamics within Rødsand lagoon.

Rødsand lagoon faces Fehmarnbelt to the south and has an open strait to the north (Fig. 1). The lagoon is enclosed from Fehmarnbelt by an elongated spit, named Hyllekrog in the westernmost part of Rødsand lagoon, and by two barrier islands. The lagoon is approximately 30km long and 10km wide. The western part of Rødsand lagoon is shallower (0-5m) than the eastern part (5-10m), and is inhabited by eelgrass, which only grows at shallow depths due to the necessity of light penetration (Middelboe *et al.*, 2003). The sediment bed in Rødsand lagoon is composed of sand and gravel with a medium-fine grained sand and silt layer on top (FEHY, 2013b). The predominant wind and wave direction in the region is from westerly directions leading to a net eastward longshore sediment transport rate of 15,000-20,000 m³/year along the southern coastline of Lolland (FEHY, 2013b).

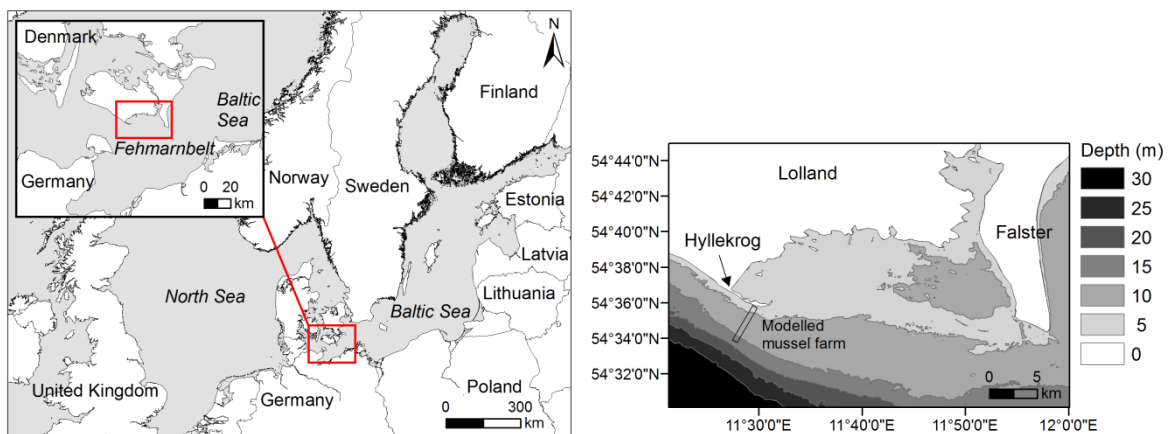


Fig. 1. Left: North-western Europe and the location of Rødsand lagoon. Right: Water depth in Rødsand lagoon and the location of the modelled mussel farm.

On the basis of two-dimensional modelling (MIKE21 by DHI) and field measurements, the flow and sediment dynamics to and from Rødsand lagoon were simulated during a one year period. Particular focus was placed on periods with fair- and gale-force wind speeds from a westerly direction. A mussel farm was numerically modelled through a module extension. The mussel farm reflected a long-line community of blue mussels on the south side of Hyllekrog with an approximate farm size of 4x1km. Blue mussels are native to the Femernbelt region. The sediments that passed the mussel

farm were filtered according to a selected filtration capacity and regenerated as bio-deposits with an optional settling velocity. The local mussel properties for the present study were estimated based on studies conducted by Møhlenberg (2014) and the bio-deposit settling velocity was estimated based on literature reviews (e.g. Chamberlain *et al.*, 2001; Callier *et al.*, 2006; Liutkus *et al.*, 2012).

The numerical model simulations showed that gale-force wind conditions generated a larger sediment transport to Rødsand lagoon than fair weather conditions, and thus typically generated a higher SSC within the lagoon. The SSC within Rødsand lagoon was reduced by 18% with the implementation of a mussel farm within the modelled year. The generated bio-deposits settled within a fan of approximately 400m from the mussel farm, and thereby reduced the sediment transport through the inlets to Rødsand lagoon. The reduction in sediment transport was greatest at the inlet closest to the mussel farm. The effects of the mussel farm on the sediment dynamics were persistent during both fair- and gale-force wind conditions.

This suggests that the implementation of a mussel farm has the potential to reduce the sediment transport to Rødsand lagoon and thereby reduce the turbidity caused by suspended sediments. Apart from biomediation purposes, the mussel module extension can be utilized to improve and develop sediment transport models where known natural patches of mussels are present.

Acknowledgements

This study is part of the project 'SEDILINK - Flow circulation and sediment dynamics in a non-tidal coastal lagoonal system - Rødsand lagoon, Denmark' co-funded by Femern A/S and DHI.

References

- Callier M.D., A.M. Weise, C.W. McKindsey and G. Desrosiers. 2006. Sedimentation rates in a suspended mussel farm (great-entry lagoon, Canada): Biodeposit production and dispersion. *Marine Ecology Progress Series* 322:129-141.
- Chamberlain J., T.F. Fernandes, P. Read, T.D. Nickell and I.M. Davies. 2001. Impacts of biodeposits from suspended mussel (*Mytilus edulis* L.) culture on the surrounding surficial sediments. *ICES Journal of Marine Science* 58:411-416.
- FEHY. 2013a. Fehmarnbelt fixed link EIA. Marine soil - Impact assessment. Sediment spill during construction of the Fehmarnbelt fixed link. Technical report, Femern A/S. Report No. E1TR0059 - Volume II.
- FEHY. 2013b. Fehmarnbelt Fixed Link EIA. Marine Water - Baseline. Suspended Sediment. Technical report, Femern A/S. Report No. E1TR0057 - Volume III.
- Liutkus M., S. Robinson, B. Macdonald and G. Reid. 2012. Quantifying the effects of diet and mussel size on the biophysical properties of the blue mussel, *Mytilus* spp., feces egested under simulated imta conditions. *Journal of Shellfish Research* 31:69-77.
- Middelboe A.L., K. Sand-Jensen and D. Krause-Jensen. 2003. Spatial and interannual variations with depth in eelgrass populations. *Journal of Experimental Marine Biology and Ecology* 291:1-15.
- Møhlenberg F. 2014. Conservatism in impact prediction on eelgrass in Rødsand Lagoon (Memo). DHI - Water and Environment.
- Nature Agency (2014). Overview of the Danish Natura 2000 areas. <http://naturstyrelsen.dk/naturbeskyttelse/natura-2000/natura-2000-omraaderne/>.
- Olesen M., K.S. Madsen, C.A. Ludwigsen, F. Boberg, T. Christensen, J. Cappelen, O.B. Christensen, K.K. Andersen and J.H. Christensen. 2014. Fremtidige klimaforandringer i Danmark. Danmarks Klimacenter rapport. Danmarks Meteorologiske Institut. www.dmi.dk/klimaforandringer.
- Schröder T., J. Stank, G. Schernewski and P. Krost. 2014. The impact of a mussel farm on water transparency in the Kiel Fjord. *Ocean & Coastal Management* 101:42-52.
- Valeur J.R. 2004. Sediment investigations connected with the building of the Øresund bridge and tunnel. *Danish Journal of Geography* 104(2):1-12.

Physical process measurements of sediment suspension by vessel operations at Pearl Harbour, Hawaii

Gailani Joseph, S. Jarrell Smith and Mathew Taylor

U.S. Army Engineer Research and Development Center
3909 Halls Ferry Road, Vicksburg, MS 39056, USA
E-mail: Joe.Z.Gailani@usace.army.mil

Background

Vessel berthing operations generate near-bed flows that are often sufficient to erode and entrain bed sediments. These flows are generated by tugs, bow thrusters, and/or ship propellers providing propulsion and the flows around the ship hull while turning or underway. In addition to erosional stresses, these vessel-induced flows also produce vertical mixing. This process mixes the eroded sediment through entrainment, turbulent mixing, and/or vertical advection. Contaminants are predominately associated with the fine sediments. Therefore the mobilization of fine sediments in ports and harbours by vessel operations is a potentially significant process in describing contaminant transport and fate.

Two key physical parameters that influence the transport and fate of suspended fine sediments are the initial distribution of suspended sediment mass and the settling velocities of the suspended particles. The objectives of the research described herein are: 1) to quantify spatial and temporal distributions of suspended sediment in plumes generated by vessel operations, 2) to determine fine-sediment settling velocities within the vessel-generated plumes, and 3) to assess aggregation states and flocculation of suspended sediments within the plumes.

Methods

Field experiments were conducted on 28, 29, and 31 August 2012. On 28-29 August, a Tiger tug pushed against the pier pilings at Bravo and Oscar Piers, respectively, generating a prop jet which suspended sediments from the bed. In each case, the tug pushed against the pier in three intervals of 5 minutes separated by approximately 15 minutes for observations. During the observational period instrumentation was deployed from a barge. On 31 August, the team conducted measurements in plumes generated by two departing vessels in the vicinity of a pier. During these vessel operations, tugs assisted the departing naval vessels in leaving the pier or berth, turning the vessel, and getting underway during harbour departure.

The general approach in defining the characteristics of the sediment plumes and the suspended sediment within the plume was to first define the initial extent and concentration of the subsurface plume by acoustic backscatter. Then, periodically, a profiling frame was cast through the water column to permit suspended sediment sampling and measurements of temperature, salinity, suspended particle size, and settling velocity. The acoustic mapping and vertical casts of the profiling frame continued alternately until the sediment plume became very diffuse and difficult to discern from ambient conditions by acoustic backscatter.

Settling of cohesive sediments is governed by processes that are difficult to estimate from fundamental sediment properties. Cohesive sediments are known to aggregate (or stick together) to form flocs, composed of fine-grained sediments and organic matter. Floc size is governed by the balance between aggregation and disaggregation processes. Aggregation is influenced by processes causing particles to collide and the efficiency with which these particles stick together. Particle collisions are influenced by turbulence, differential settling, and Brownian motion; whereas aggregation efficiency is largely associated with surface characteristics of the particles (mineralogy, surface coatings, biological polymers, and water chemistry). Disaggregation is influenced by turbulent shear and interparticle bonding strength of the floc.

Flocs formed in suspension have large porosities, and a large fraction of floc volume is occupied by water. After flocs have settled to the sediment bed, the weight of overlying sediments collapses the floc structure and expels pore water. This process, known as consolidation, results in increased bed density and increased interparticle bond strength. If the consolidated bed is later exposed by erosion, a portion of the eroded sediment may not be completely disaggregated and instead is suspended as small fragments of the bed. These bed aggregates differ from the aggregates formed in the water column (flocs) as they are more tightly packed, have stronger interparticle bonds, and have greater particle densities.

The Particle Imaging Camera System (PICS) (Smith and Friedrichs, 2011) was deployed from a profiling frame to determine suspended sediment size, settling velocity, and particle density. Supporting instrumentation was also deployed on the profiling frame to include: 1) a YSI 600XLM sonde for measuring depth, temperature, and salinity, 2) a Laser In-Situ Scattering and Transmissometry particle size analyzer (LISST) for measuring particle size in the range of 7.5 to 1500 μm , and a sampling port for pumped physical samples. The PICS is an ERDC-developed system for *in-situ* measurements of cohesive sediment settling velocities. The PICS collects digital video of particle settling within a small settling column and can be deployed in the field. Sample collection, optical and lighting design, and image acquisition were designed to produce high-quality, *in-situ* image sequences. Image sequences collected by PICS are analysed with automated particle tracking software to produce size, settling velocity, and density (inferred) distributions of particles suspended at the sampling location. Additional details of PICS, including system configuration and measurement uncertainty are provided by Smith and Friedrichs (2011).

Image analysis results in simultaneous measurement of particle size and settling velocity. Using these two measured parameters permits estimation of individual particle densities. This is accomplished by solving the settling balance for spherical particles with the Schiller-Naumann drag approximation (Graf, 1971). The estimated individual particle densities are used to classify particles by their aggregation state. Details of the image processing and analysis methods are provided in Smith (2010). Aggregation states include primary particles (individual mineral grains), bed aggregates (aggregations with density approximating that of the sediment bed), and flocs (lower-density aggregations formed in the water column). Flocs are associated with density between 1010-1200 kg m^{-3} , bed aggregates: 1200-1800 kg m^{-3} , primary particles: 1800-3000 kg m^{-3} . A single 30-second video may have hundreds to thousands of tracked particles.

Results

Periodically during the roving ADCP surveys, the motor barge stopped and held position over the sediment plume for conducting water column casts. During these casts, size and settling velocity data, temperature/salinity data, and physical samples were acquired at approximately 2-3m vertical intervals. The settling velocity data within 20 minutes of plume generation were pooled to evaluate the initial distributions of suspended sediment size, settling velocity, and aggregate state.

The pooled distributions indicate that most particles are aggregated fine sediments. The range of primary, disaggregated particles in the PICS data was 0.1 to 1.0 percent, compared to dense bed aggregates (11 to 41 percent) and low density flocs (57 to 89 percent). The minimum resolvable particle size by PICS is approximately 30 μm , but the LISST can resolve particles as small as 7.5 μm . The LISST data was analysed to determine that 7-9 percent of the suspended particle volume was in the size ranges of 7.5 to 30 μm . The apparent densities of the suspended aggregates suggest that the initial suspension of sediment should not be represented as single, disaggregated sediment grains. Instead, the settling velocities of sediment suspended by the vessel operations should be represented as multiple classes of aggregates with settling velocities consistent with the observations in the plume. The mass-weighted frequency distributions of settling velocity are broadly spread, with the suspended population spanning more than two orders of magnitude in settling velocity. A four sediment class representation was developed. By this representation, a numerical model could represent the diverse population of particles evident in the plume.

References

- Graf W.H. 1971. Hydraulics of sediment transport. Chapter 4. McGraw Hill, New York.
- Smith S.J. 2010. Fine sediment dynamics in dredge plumes. PhD dissertation. School of Marine Science, The College of William and Mary, Gloucester Point, Virginia.
- Smith S.J. and C.T. Friedrichs. 2011. Size and settling velocity of cohesive flocs and suspended sediment aggregates in a trailing suction hopper dredge plume. Continental Shelf Research 31:S60-S63.

Benchmarking of three penetrometers for identification of fluid mud layers

Hellmich Franziska¹, Achim Kopf¹ and Peter Staelens²

¹ MARUM – Center for Marine and Environmental Sciences, University of Bremen,
Leobener Strasse, 28359 Bremen, Germany
E-mail: fhellmich@marum.de

² dotOcean NV, Bedrijvencentrum Brugge, Lieven Bauwensstraat 20, 8200 Brugge, Belgium

Introduction

Fluid mud, a highly concentrated suspension of solids and organic matter, is a known phenomenon which occurs in harbours and waterways worldwide. The nautical bottom lies within the fluid mud layer and is defined by the density or rheological properties of the mud (Wurpts, 2005). Fluid mud is navigable under certain conditions, but consolidating mud layers have to be dredged to ensure a deep enough navigation depth. PIANC defined the critical density for the transition from navigable to non-navigable mud at 1200kg/m^3 (PIANC, 1997). To keep dredging volumes and costs to a minimum it thus is important to distinguish navigable from non-navigable mud layer.

Acoustic echo sounders are commonly used to determine fluid mud deposits but they are not suitable for a detailed resolution of the nautical bottom depth (Wurpts, 2005). Seifert and Kopf (2012) have shown that dynamic cone penetration testing with pore pressure measurements can be a supplementary method for *in-situ* identification, characterization and quantification of fluid and soft mud layers.

Aim of this survey was to deepen the knowledge on penetrometer performance upon impact into fluid mud layers and to compare and correlate the results.

Method

In order to not have to deal with tidal currents and be restricted to the short time span during slack tides for measurements, an artificial environment, provided at a test facility by dotOcean, was chosen for this survey. The test facility is located at Zeebrugge Harbour (Belgium) and consists of a hollow pile filled with water, into which two exchangeable buckets filled with controlled layers of fluid to consolidating mud of two sources were placed consecutively. A layer of sand as a security layer was added before filling one of the buckets with mud. Three differently shaped penetrometers were used during this survey: (i) GraviProbe (dotOcean), (ii) NIMROD (MARUM) and (iii) a dynamic CPTu lance (MARUM). GraviProbe was developed for the special purpose of assessing rheological and density conditions of sediment layers, NIMROD and the dynamic CPTu lance are penetrometers designed for investigation of sediment strength. The penetrometers were deployed into the test environment in various (geometrical) set-ups and in either free-fall mode or via a winch at various velocities.

During deployment and impact into the mud deceleration, pore pressure and tip resistance among other parameters were measured. These primary parameters were used to calculate secondary parameters such as impact velocity, penetration depth, density, sediment resistance force and (dynamic) undrained shear strength. For now the focus mainly lies on the pore pressure and deceleration measurements.

Results

First results show that the pore pressure signal and the density, which is based on pore pressure measurements as well as tip resistance as a function of tip sensitivity and geometry are the most reliable parameters for identifying the impact into the fluid mud layer. Significant deceleration mainly occurs when the penetrometers enter mud or sand layers which are stiff and/or rough enough to slow down the penetrating device.

GraviProbe data gave a good insight into the density of the mud layers. Density increased rapidly from 1020kg/m^3 in the water column to values exceeding 1200kg/m^3 in the first bucket, in the second bucket this increase was less rapid. This implied that in bucket 1 the fluid mud layer was less thick (approx. 0.15m) than in bucket 2 (approx. 0.9m). The underlying consolidating mud was about 1.30m and 2.20m thick, respectively. Maximum density was reached at 1350kg/m^3 .

NIMROD and CPTu data showed partly significantly differing deceleration and pore pressure signals, dependent on set-up geometry and/or deployment velocity.

In bucket 1, NIMROD data showed a distinct deceleration signal upon impact into the mud, especially when using a cylindrical tip on the device in free-fall mode. The overall penetration depth is in good agreement with the GraviProbe results for mud thickness. In bucket 2 the deceleration only occurred in the bottommost layers and is more pronounced in deployments in free-fall mode.

Regardless of tip geometry and deployment velocity, the pore pressure decreased to subhydrostatic values during impact into the mud, but the depth where this decrease sets in is not constant throughout all data sets.

When using the conical tip on the CPTu lance pore pressure decreased to subhydrostatic values as soon as the penetrometer impacts the fluid mud, but for a ball- or disk-shaped tip the pore pressure increased to suprahydrostatic values. The depth of this kink in pore pressure signal is in good agreement with the one for the increase of tip resistance when using a more sensitive tip and was also observed by Seifert and Kopf (2012) before. The deceleration signals only showed the impact into the bucket bottom.

Discussion

The penetrometer type, set-up, tip geometry and sensitivity have a major effect on how the data look. On one hand, pore pressure decreases with NIMROD and the CPTu lance upon impact in the mud if a tip geometry is chosen which displaces the sediment (cone, hemisphere, cylinder). On the other hand, it increases if a so called full-flow tip geometry (ball, disk) is chosen around which the sediment has to 'flow'.

We identified three factors which compromised the data quality: (i) unreliable pore pressure measurements, (ii) variable deployment velocity and (iii) a too slow deployment velocity.

As the pore pressure obviously is a very important parameter in such a study, the pore pressure sensor has to work impeccably. During several deployments in this survey the filter ring sitting in front of the pore pressure port on the MARUM devices got clogged by clayey material and hampered transmission of pressure transients to the sensor. While the absolute values are dampened, the relative evolution of pore pressure with depth was still valuable. To prevent unreliable pore pressure data, the filter ring has to be watched carefully and needs to be exchanged or cleaned even more frequently than usual. This problem does not transfer to GraviProbe, which does not have a filter of porous metal.

The pore pressure evolution is also a matter of deployment velocity. The faster the deployment velocity, the steeper is the gradient of the pore pressure signal. To guarantee that any change in (pore pressure) signal is due to a change of physical properties of the penetrated matter, the penetration velocity needs to be kept constant throughout a single deployment. However, a too slow deployment velocity (< 0.1 m/s) is not advisable. At faster deployment velocities measurements get more pronounced due to the rate effect at dynamically operated cone penetration testing in cohesive sediments (Dayal and Allen, 1975).

In general the results of this survey show that penetrometer can be used to geotechnically characterise fluid and consolidating mud layers, but further refinement of the deployment method is needed for the MARUM devices in order to guarantee good results at the best possible vertical resolution, even in free fall. Moreover a correlation of pore pressure, deceleration and tip resistance values by NIMROD and the CPTu lance to density measurements of GraviProbe has to be set up.

Acknowledgements

The authors would like to thank the German Research Foundation (DFG) for funding this survey. Furthermore, we would like to thank Matthias Lange, Nina Stark and Alois Steiner (MARUM) and the colleagues of dotOcean for support during the fieldwork. We also acknowledge the technical assistance by Christian Zoellner and Matthias Lange (MARUM) for NIMROD and the CPTu lance and by dotOcean for GraviProbe. GraviProbe data has been processed by dotOcean.

References

- Dayal U. and J. H. Allen. 1975. The effect of penetration rate on the strength of remolded clay and sand samples. *Canadian Geotechnical Journal* 12:363-348.
- PIANC 1997. *Approach channels - A guide for design*. Brussels, Belgium. 108p.
- Seifert A. and A. Kopf. 2012. Modified dynamic CPTU penetrometer for fluid mud detection. *American Society of Civil Engineers* 138(2):203-206.
- Wurpts R. 2005. 15 Years experience with fluid mud: definition of the nautical bottom with rheological parameters. *Terra et Aqua* 99:22-32.

Laboratory experiments on silt infiltration into a gravel bed

Herrero Albert, Céline Berni and Benoit Camenen

National Research Institute of Science and Technology for Environment and Agriculture (IRSTEA - Lyon), Rue la Doua 5, Villeurbanne 69100, France
E-mail: albert.herrero@irstea.fr

Introduction

Interaction between sediment fractions with a significantly different size is a common situation in mountain rivers. Deforestation or dam flushing operations are two examples of human activities that affect the sediment dynamics in a mountain catchment. Fine sediments travelling downstream can be deposited on the river bed or infiltrated within it. The infiltration alters dramatically the river habitat by reducing the permeability of the river bed and the oxygen and nutrient exchange at the flow-sediment interface, affecting specifically fish spawning and invertebrate species that inhabit the river bed (Wood and Armitage, 1997). Understanding the dynamics of fine sediment infiltration and the anthropogenic influence on it, is therefore important to minimize the impact of human activities on environment.

Previous studies highlight the influence on fine sediment infiltration of different variables such as fine sediment cohesion (Packman and MacKay, 2003), flow velocity (Cunningham *et al.*, 1987), bed shear stress (Diplas and Parker, 1992), suspended sediment concentration (Khullar *et al.*, 2013), interstitial hydraulic gradient (Schälchli, 1992), the presence of a biofilm (Arnon *et al.*, 2010), bed topography, i.e. occurrence and size of bed forms (Karwan and Saiers, 2012), and the size ratio between the coarse bed sediment and the incoming fine particles (Gibson *et al.*, 2009). Whereas many analyses describe the final equilibrium situation resulting from different flow and sediment conditions, less information is available about the time evolution of the process. Moreover, little work has been carried out concerning gravel and silt interaction, despite being a common situation found in mountain environments. The aim of the present study is to provide useful data to partially fill this gap.

Experimental setup

A series of experiments was performed in the tilting flume of the hydraulics laboratory at Irstea-Lyon (France). This new facility is 18m long and 1m wide and the slope can be varied from 0 to 5 percent. Before each test a 6cm-deep bed formed by clean gravel (5 to 12mm) was installed carefully in such a way that the bed slope coincided with that of the channel. Six cylinders made of a metallic grid with a hole size of 1mm were installed within the bed at three different longitudinal positions ($x = 6, 9$ and 12m) in order to take samples of the bed and measure fine sediment content at different depths. The grid size was chosen so that it retains coarse particles and affects as less as possible the interstitial flow and the fine sediment particles in suspension. Three of the cylinders (one at each longitudinal position) were extracted after 8 hours of experiment whereas the other three were removed at the end of the test.

Water flow with a specified discharge was recirculated along the channel and through a 30m^3 reservoir. Silt size was added and mixed in this chamber to obtain a homogeneous suspended sediment concentration in the flow. As sediment-laden flow recirculates along the flume, part of the fine sediment infiltrates into the bed and suspended sediment concentration decreases. In order to keep an approximately constant concentration, bags of fine sediment were added at the reservoir at the required moment. This operation is based on suspended sediment concentration measurements carried out by two turbidimeters (Hach-Lange, Solitax 0–50 g/L) installed at the upstream and the downstream ends of the channel (Fig. 1). Water samples are taken periodically in order to further control sediment concentration and to calibrate the turbidimeters. Flow velocities are measured at $x = 8\text{m}$ and at the centre line of the channel using an ADV profiler (Nortek, Vectrino II). Water depth is registered at three different longitudinal positions ($x = 3\text{m}$, $x = 8\text{m}$ and $x = 15\text{m}$) by means of ultrasonic sensors. The sediment-laden flow is recirculated until the system reaches an equilibrium with no further fine sediment infiltration.

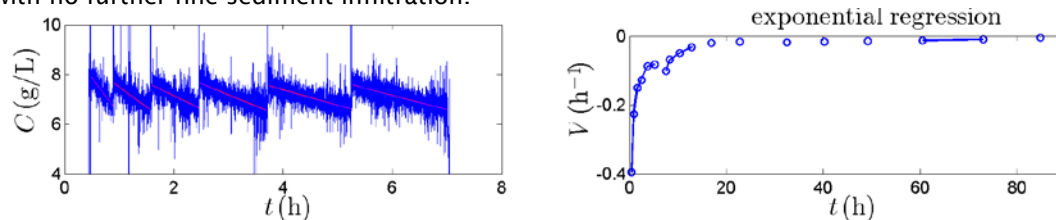


Fig. 2. Time evolution of sediment concentration (left). Infiltration rates are calculated from the time constant of an exponential fitting over each cycle and are plotted versus time (right).

Results

As soon as water and suspended sediment enter into the bed, fine particles start to deposit on the top of the gravel grains generating triangular deposits with a slope equal to the friction angle of the material. Simultaneously, fine sediment accumulates at the impermeable channel base and fills the bed from the bottom upwards. The concentration evolution in time allows evaluating the evolution of fine sediment infiltration rate by fitting each of the cycles separated by the addition of one sediment bag with an exponential curve. Fig. 1 shows how infiltration rate decreases during the experiment. It can be interpreted as the negative correlation of water mass exchange with bed depth (Grant *et al.*, 2012). As fine sediment accumulates at the channel base and develops an almost impermeable layer, the effective bed depth along which water mass exchange takes place decreases and so does the amount of fine sediment that access to and is retained within the bed. The bed evolves to a final state in which almost the whole depth is clogged with fine sediment.

Fig. 2 shows the depth profiles of fine sediment content after eight hours of experiment and at the end of it, for the different tests (Table I). The upwards filling trend can be observed in this comparison. On the other hand, there is a surface bed layer that remains free of sediment.

Fig. 3 shows the final state of tests 1 and 2 highlighting a difference in the thickness of this surface clean layer. The increase of the bed slope causes an augmentation of shear stress and turbulence transfer to the pore spaces close to the bed surface that prevent the deposition of fine particles.

Table I. Variable values for the two laboratory tests

Code	Concentration (g/l)	Slope	Discharge (l/s)
T1	4.0	1	30
T2	4.0	0.1	30



Fig. 4. Side view of the bed at the final state for Test 1 (top) and Test 2 (bottom).

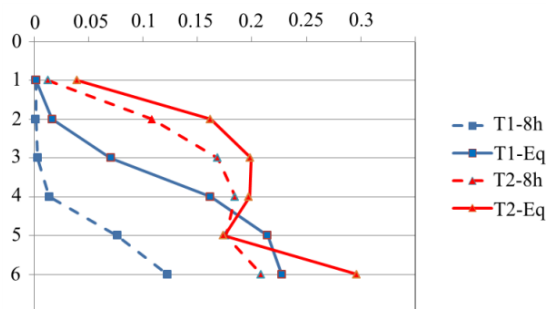


Fig. 3. Fine sediment content profiles after 8h of experiment (dashed lines) and at the equilibrium state (solid lines).

References

- Arnon S., L.P. Marx, K.E. Searcy and A.I. Packman. 2010. Effects of overlying velocity, particle size, and biofilm growth on stream-subsurface exchange of particles. *Hydrological Processes* 24(1):108-114.
- Cunningham A.B., C.J. Anderson and H. Bouwer. 1987. Effects of sediment-laden flow on channel bed clogging. *Journal of Irrigation and Drainage Engineering-Asce* 113(1):106-118.
- Diplas P. and G. Parker. 1992. Deposition and removal of fines in gravel-bed streams. *Dynamics of gravel-bed rivers*. p.313-329.
- Gibson S., D. Abraham, R. Heath and D. Schoellhamer. 2009. Vertical gradational variability of fines deposited in a gravel framework. *Sedimentology* 56(3):661-676.
- Grant S.B., M.J. Stewardson and I. Marusic. 2012. Effective diffusivity and mass flux across the sediment-water interface in streams. *Water Resources Research* 48(5).
- Karwan D.L. and J.E. Saiers. 2012. Hyporheic exchange and streambed filtration of suspended particles. *Water Resources Research* 48.
- Khullar N.K., U.C. Kothiyari and K.G.R. Raju. 2013. Study of deposition of fine sediment within the pores of a coarse sediment bed stream. *International Journal of Sediment Research* 28(2):210-219.
- Packman A.I. and J.S. MacKay. 2003. Interplay of stream-subsurface exchange, clay particle deposition, and streambed evolution. *Water Resources Research* 39(4).
- Schälchli U. 1992. The clogging of coarse gravel river beds by fine sediment. *Hydrobiologia* 235-236(1):189-197.
- Wood P.J. and P.D. Armitage. 1997. Biological effects of fine sediment in the lotic environment. *Environmental Management* 21(2):203-217.

The roles of physical mixing and biochemical composition on the depositional characteristics of flocculated suspended sediment in the Eden Estuary, Scotland

Hope Julie A.^{1,4}, Andrew J. Manning^{2,3,4}, Rebecca J. Aspden¹, Jaco Baas⁵ and David M. Paterson¹

¹ Sediment Ecology Research Group, Scottish Oceans Institute, University of St Andrews, East Sands, St Andrews, Fife, KY16 8LB, UK
E-mail: jah23@st-andrews.ac.uk

² HR Wallingford, Howbery Park, Wallingford, Oxfordshire, OX10 8BA, UK

³ Department of Geography, Environment and Earth Sciences, University of Hull, Kingston Upon Hull, Humberside, HU6 7RX, UK

⁴ School of Marine Science and Engineering, Plymouth University, Drake Circus, Plymouth, Devon, PL4 8AA, UK

⁵ School of Ocean Sciences, Bangor University, Askew St, Isle of Anglesey, LL59 5AB, UK

Sediment load in estuarine waters is generally composed of a mixture of sand, clay and biological matter and it is recognised that there is strong mediation of the physical behaviour of sediment by biological components of the system (Paterson *et al.*, 2000). However the complex flocculation dynamics of this variable material still poses problems for the prediction of transport pathways and depositional behaviour of mixed sediments (Manning *et al.*, 2013). Therefore, understanding the physical and biochemical characteristics of suspended sediment during tidal immersion is of paramount importance when considering transport and deposition in these dynamic environments.

In intertidal mudflats, benthic microalgae can contribute up to half the total autotrophic production in an estuarine system (Underwood and Kromkamp, 1999). The extracellular polymeric substances (EPS) produced by both benthic and pelagic bacteria and algae are a key variable known to influence flocculation processes (Manning *et al.*, 2013). Variation in the nature and concentration of the EPS can alter sediment stability and erosion in mixed sediment beds (Taylor *et al.*, 1999; Black *et al.*, 2002) but these substances can also significantly enhance inter-particle cohesion in the water column and therefore deposition and transport.

This study examined the variation in naturally occurring EPS concentration as well as the composition of sugars and its influence on several physical variables of flocs within the Eden Estuary, Scotland. Samples were collected at 15-30min intervals over a full tidal cycle for total suspended sediment and colorimetric analysis of polymer concentration. Subsamples were transferred to the settling column of the LabSFLOC-2 (Laboratory Spectral Flocculation Characteristics 2), high resolution video floc camera system (Manning, 2006) *in situ* where settling flocs were viewed (resolution~10 μ m) to determine floc size (D) and settling velocity (Ws) characteristics. Additionally, further biochemical analysis of the carbohydrates of the EPS were performed by Gas Chromatography-Mass Spectroscopy (GC-MS) in order to assess the composition of monosaccharides within the samples and linkages.

Preliminary results indicate a wide range of microfloc (D< 160 μ m) and Macrofloc (D>160 μ m) fractions present, with the latter approaching 1mm during flocculation conducive conditions. Correspondingly, when considering all floc samples, floc settling velocities generally spanned three orders of magnitude with floc size and settling velocities correlating with polymer concentrations. These typically ranged from slow settling (Ws of 0.01-0.05mm.s⁻¹) predominantly organically based microflocs to faster settling, significantly larger and more porous Macroflocs settling at ~10-15mm.s⁻¹. The temporal distributions of D and Ws, sediment and polymer concentrations and sugar fractions, are examined in the paper with variation also related to physical and microbiological factors in the bed and the phase of the tidal flow. The relationship between the forcing factors, the bed condition and the source and sinks of EPS material are discussed. The results demonstrate the importance of understanding biological variation in the assessment of sediment transport pathways in estuaries.

References

Black K.S., T.J. Tolhurst, D.M. Paterson and S. Hagerthey. 2002. Working with natural cohesive sediments. *Journal of Hydraulic Engineering* 128(1):2-8.

- Manning A.J. 2006 LabSFLOC - a laboratory system to determine the spectral characteristics of flocculating cohesive sediments. HR Wallingford Technical Report 156.
- Manning A.J., J.R. Spearman, R.J.S. Whitehouse, E.L. Pidduck, J.V. Baugh and K.L. Spencer. 2013. Flocculation Dynamics of Mud: Sand Mixed Suspensions, in *Sediment Transport Processes and Their Modelling Applications*. Dr. Andrew Manning (Ed.).
- Paterson D.M., T.J. Tolhurst, J.A. Kelly, C. Honeywill, E.M.G.T. de Deckere, V. Huet, S.A. Shayler, K.S. Black, J. de Brouwer and I. Davidson. 2000. Variations in sediment properties, Skeffling mudflat, Humber Estuary, UK. *Continental Shelf Research* 20:1373-1396.
- Taylor I.S., D.M. Paterson and A. Mehlert. 1999. The quantitative variability and monosaccharide composition of sediment carbohydrates associated with intertidal diatom assemblages. *Biogeochemistry* 45:303-327.
- Underwood G.J.C. and J. Kromkamp. 1999. Primary production by phytoplankton and microphytobenthos in estuaries. *Advances in Ecological Research* 29:93-153.

Measurement of density and porosity profiles within mixed sediment deposits using an electrical resistivity technique

Ibikunle Olugbenga, Alan Cuthbertson, John McCarter and Farzin Samsami

Infrastructure and Society, Geoscience, School of Energy
Heriot-Watt University, Edinburgh, United Kingdom
E-mail: a.cuthbertson@hw.ac.uk

Introduction

Physical understanding of sedimentation processes in estuaries and nearshore coastal waters is economically important to port facility owners and operators requiring maintenance of navigable depths, and environmentally significant to those bodies charged with maintaining and enhancing these sensitive ecosystems. It is therefore essential that engineers and scientists have fundamental understanding of the physical behaviour of the mixed (sand-mud) sediments that are typically found in estuarine and coastal systems, as well as their role in large-scale morphodynamic evolution (e.g. Torfs *et al.*, 1996; Cuthbertson *et al.*, 2008). However, our ability to predict structural and compositional changes within mixed sediment beds, resulting from mobilisation, transport and deposition processes occurring under combined current and wave actions, remains severely limited by the inadequate knowledge base on the dynamic behaviour of sand-mud mixtures. Additionally, current limitations in the monitoring and characterization of these mixed sediment beds (and specifically the lack of simple, reliable, non-intrusive techniques for measuring bed layer structure and composition) have been identified as a major obstacle to improved understanding of mixed sedimentary environments (e.g. Ha *et al.*, 2010). In this context, the current project has focused on developing an electrical resistivity measurement technique to characterise the spatial and temporal variation in bed structure and composition for saturated sand-clay deposits formed under idealised differential settling conditions. Ongoing development of the technique to test its applicability across a wider range of mixed sediment compositions and to monitor bed changes resulting from more natural erosion/deposition cycles (e.g. under cyclic tidal conditions) is also reported.

Settling column experiments

The resistivity technique was tested initially in a specially designed settling column with plan dimensions 15cm x 15cm and a total height of 50cm (Fig. 1). Two opposite walls of the column incorporated horizontally-aligned arrays of embedded stainless steel electrodes that allowed 4-point electrical measurements to be taken at a vertical resolution of 10mm throughout the column height. These electrode arrays were mounted flush with the inner wall surface to prevent interference with the sand-mud sedimentation process. The horizontal spacing of individual electrode sets was also set at 6mm and 20mm, respectively (Fig. 1), to determine the optimum spacing required for high-resolution characterization of the resulting bed deposits. Pure kaolin clay ($D_{50} = 4\mu\text{m}$; $SG = 2.59$) and fine-medium quartzite sand ($D = 100 - 750\mu\text{m}$; $D_{50} = 250\mu\text{m}$; $SG = 2.64$) were used as cohesive and non-cohesive fractions for the sediment mixtures. These fractions were combined into a slurry with 0.5M NaCl solution to obtain prescribed mixture compositions (% by dry weight) of 100S:0C; 75S:25C; 50S:50C; 25S:75C and 0S:100C. Each mixture was transferred, in turn, into the settling column as a "single shot", agitated by upturning of the column, and then left to settle over a period of 72 hours. The resulting settling and depositional behaviour of the sand-clay mixtures was observed through time-lapsed imaging (Fig. 2) and continuous profiling of the electrical resistivity within the developing bed deposit. Prior calibration for the sand-clay mixtures tested allowed conversion of measured resistivity profiles to more physically-relevant properties such as bulk density or porosity.

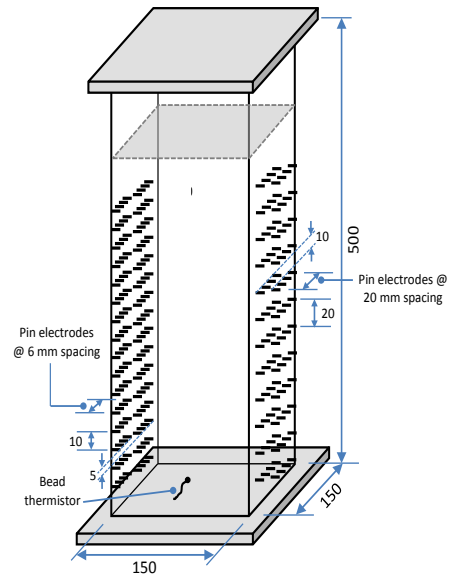


Fig. 1. Settling column arrangement showing 4-point electrode configuration (dimensions in mm).

Results and discussion

Fig. 2. shows the temporal development of the bed deposit for the 50S:50C sediment mixture. The initial rapid settlement of sand was shown to result in the formation of a bottom sand-rich layer, with near-vertical dewatering channels [Fig. 2.(a)]. Above this base layer, a patchier sand-clay layer was deposited [Fig. 2.(b)], followed by a thicker clay-rich layer containing discrete sand patches [Fig. 2.(c)]. The presence of these discrete sand patches suggests trapping within a clay matrix, which would form as the concentration in the clay layer reached the gelling point. Subsequent settlement of these sand patches [Figs. 2.(d) - (f)] also indicated that the clay matrix layer continued to compact (i.e. become denser) through ongoing settlement processes (note: this was also observed from the vertical displacement of the bed deposit surface interface, see Fig. 3). The degree of segregation observed in bed deposits was generally shown to increase with sand content in the settling mixture. Specifically, for the sand-rich 75S:25C mixture, a clearly defined sand-clay interface was shown to form between the lower sand and upper clay dominated layers [Fig. 2.(g)]. Normalised bulk density profiles, derived from electrical resistivity measurements, are shown in Fig. 3. for the 50S:50C and 75S:25C sediment mixtures at elapsed times of 10, 360 and 2880min. As expected, these profiles indicated a general increase in deposit density with elapsed time, due to settlement processes. For the 50S:50C sand-clay mixture [Fig. 3.(a)], the distinct layering structure observed within the deposit was identified by, and matched to, gradient changes within the corresponding measured bulk density profiles [i.e. 2880min, Fig. 3.(a)]. Similarly, the high degree of sand-clay segregation observed in the bed deposit formed by the 75S:25C mixture is also apparent from the sharp transition in bulk density values in the vicinity of the sand-clay layer interface [Fig. 3.(b)].

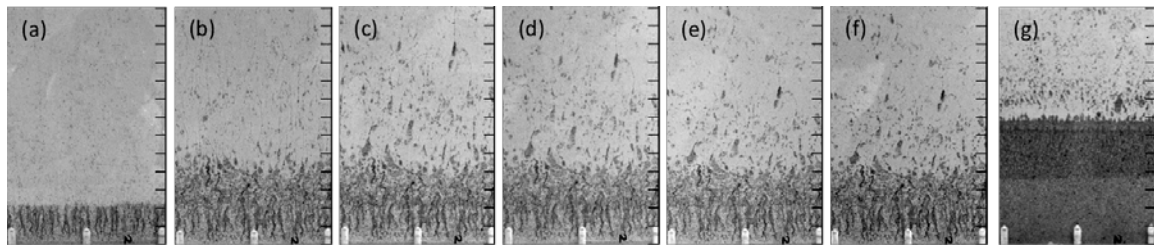


Fig. 2. Time-lapse images of bed deposit formation for the 50S:50C mixture at elapsed times (min.) of (a) 10, (b) 120, (c) 240, (d) 360, (e) 1440, (f) 1800. Fig. 2.(g) shows a corresponding deposit for the 75S:25C mixture after 1800min. (Note: scale divisions shown are 10mm).

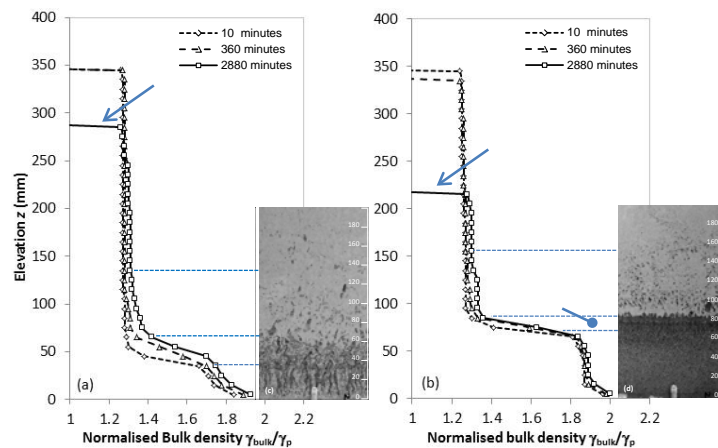


Fig. 3. Normalised bulk density profiles for (a) 50S:50C and (b) 75S:25C mixture deposits after 10, 360 and 2880min (corresponding scaled images also shown at 2880min). Deposit zones (i) - (iv) show sand-rich (>60% sand); sand-clay mix; sandy-clay (<10% sand) and clay layers, respectively.

Next steps

The resistivity technique is currently being utilised in further laboratory tests, employing a benthic annular flume (courtesy of Partrac Ltd.) to investigate sediment bed restructuring under more natural cyclic erosion and deposition events (i.e. more representative of cyclic tidal conditions). Ongoing development of the methodology is also underway to adapt it for a wider range of mixed sediment compositions (e.g. sand-silt-mud, organic matter) and for potential field applications. Preliminary findings from these additional studies will also be discussed in the paper.

References

- Cuthbertson A., P. Dong, S. King and P. Davies. 2008. Hindered settling velocity of cohesive/non-cohesive sediment mixtures. *Journal of Coastal Engineering* 55:1197-1208.
- Ha H., J. Maa and C. Holland. 2010. Acoustic density measurements of consolidating cohesive sediment beds by means of non-intrusive 'Micro-Chirp' acoustic system. *Geo-Marine Letters* 30(6):585-593.
- Torfs H., H. Mitchener, H. Huysentruyt and E. Toorman. 1996. Settling and consolidation of mud/sand mixtures. *Coastal Engineering* 29:27-45.

The impact of bio-physical thresholds on sediment analysis through field reflectance spectra and hyperspectral imagery

Ibrahim Elsy¹, Kim Wonkook², Melba Crawford³ and Jaak Monbaliu⁴

¹ Department of Civil and Environmental Engineering, Notre Dame University - Louaize
PO Box: 72, Zouk Mikael, Zouk Mosbeh, Lebanon
E-mail: eibrahim@ndu.edu.lb

² Korea Ocean Satellite Center (KOSC), Korea Institute of Ocean Science & Technology (KIOST), 787 Haean-ro(st), Sangrok-Gu, Ansan-Shi, Gyunggi-Do, Korea

³ Laboratory for Applications of Remote Sensing (LARS), Purdue University, Neil Armstrong Hall of Engineering, 701 W Stadium Avenue, West Lafayette, IN 47907-2045, USA

⁴ Hydraulics Laboratory, Department of civil engineering, Katholieke Universiteit Leuven, Kasteelpark Arenberg 40, 3001 Heverlee, Belgium

Introduction

The effects of biological, physical, and sedimentological factors and processes play a major role in the fate of an intertidal flat. Non-cohesive sandy particles behave autonomously depending on their diameter and density, while cohesive silt and clay particles aggregate and act in groups (Mitchener and Torfs, 1996). Furthermore, some organisms stabilize the sediment surface against suspension by secreting mucilaginous films (Murphy *et al.*, 2009), while others may destroy the “biostabilizing” structure of the sediment and thus weaken it (Widdows and Brinsley, 2002). The importance of such mechanisms in determining sediment stability leads to a need for frequent and intense field data collection. Remote sensing technology offers an alternative to traditional field sampling. It required a lower amount of typical field samples to obtain sufficient spatial coverage of information. This technology has been successfully utilized to characterize and quantify sediment properties (Rainey *et al.*, 2003; Ibrahim and Monbaliu, 2011; Ibrahim *et al.*, 2014).

Characterization of sediment using remote sensing technology has commonly used supervised classification of imagery, which assembles data into certain groups based on their similarity to pre-defined classes. A successful supervised classification leads to high accuracy and reveals the pre-defined classes of interest. It requires field knowledge to set its training and validation data. Yet, defining the boundaries between classes of sediment properties such as moisture content and mud content have been typically determined using case-specific field data or from experience and intuition. Thus, class boundaries for a sediment property are often defined using an ad-hoc procedure aiming for an equal amount of field samples in each class (Defew *et al.*, 2002). For example, Thomson *et al.*, (2003) used thresholds of 30% mud and 50% mud to distinguish between “Sandy” and “Muddy Sand” classes, and “Muddy Sand” and “Mud” classes, respectively. On the other hand Adam *et al.*, (2006) considered the “Sand” class to include less than 15% mud, “Loamy Sand” has between 15 and 30% mud, and “Clayey Loam” contained more than 30% mud. Mud refers to cohesive particles smaller than 63µm.

The aim of this study is to understand the sensitivity of classification accuracy to the choice of thresholds when classifying intertidal sediment properties. Furthermore, it aims at classifying imagery of the study area using the thresholds that lead to relatively high classification accuracy.

Data and methods

The “Ijzermending”, an intertidal flat located at the outlet of the Ijzer river at the Belgian coast, is used as a case study for this work. It is a nature reserve that consists of dunes, marshes, and mudflats with a total area of 130 hectares. Three flight campaigns took place over the Ijzermending at cloud-free and low-tidal conditions. On the 17th of June 2005, an image was acquired by means of the Airborne Hyperspectral Sensor (AHS) with a 3.4m × 3.4m pixel size. On the 12th of June 2007, an image was obtained by AHS, with a 3m × 3m pixel size. Finally, on the 9th of July 2013, an image was acquired by Airborne Prism EXperiment (APEX) sensor with a 2.3m × 2.3m.

Field campaigns were carried out on the intertidal flat, at low tide, to accompany the acquired images. For each campaign, sampling sites were chosen such that the highest diversity in sediment properties was included. A Differential Global Positioning System (DGPS) determined the coordinates of the sampled sites. Surface sediment samples were collected for pigment analysis, moisture content, mud content, and organic matter content quantification. Surface reflectance was measured by an Analytical Spectral Device (ASD) spectrometer that records reflectance from 350 - 2500nm, i.e. in the visible, near-infrared, and shortwave infrared regions of the spectrum.

The approach in this work can be summarized in the following steps. First, field data that includes field spectra and their corresponding sediment properties are classified using a series of thresholds for each sediment property. This aims at developing a sensitivity analysis to determine the impact

of threshold choice on classification accuracy of the considered sediment properties. The classification is carried out using Support Vector Machines. Then, the thresholds for each sediment property that lead to the best classification accuracy are extracted. Finally, the obtained thresholds are used to classify the hyperspectral images of the IJzermonding.

Conclusions

Given a hyperspectral image accompanied by field data, it is required to classify the image in a supervised manner revealing the distribution of the various sediment properties measured in the data. This paper deals with the choice of classes for each sediment property and the consequential accuracy assessment. The study shows the high sensitivity of classification accuracy on the threshold choices and recommends this finding to be considered in future classification of intertidal sediment.

Acknowledgments

The research presented in this paper is funded by the Belgian Science Policy Office in the frame of the STEREO II programme, project SR/00/109 - ALGASED (remote sensing for characterization of inter-tidal sediments and microphytobenthic algae).

The research pertaining to these results received financial aid by the Belgian Science Policy Office in the frame of the STEREO II programme subsidy number SR/67/167 (BELAIR2013) and SR/XX/168 (BELAIR HESBANIA) / SR/XX/169 (BELAIR LITORA) / SR/XX/170 (BELAIR SONIA).

References

- Adam S., I. Vitse, C. Johannsen and J. Monbaliu. 2006. Sediment type unsupervised classification of the Molenplaat, Westerschelde Estuary, the Netherlands. *EARSel eProceedings* 5:146-160.
- Defew E., T. Tolhurst and D. Paterson. 2002. Site-specific features influence sediment stability of intertidal flats. *Hydrology and Earth System Sciences* 6:971-982.
- Ibrahim E. and J. Monbaliu. 2011. Suitability of spaceborne multispectral data for inter-tidal sediment characterization: A case study. *Estuarine, Coastal, and Shelf Science* 92:437-445.
- Ibrahim E., S. Adam, A. De Wever, A. Govaerts, A. Vervoort and J. Monbaliu. 2014. Investigating spatial resolutions of imagery for intertidal sediment characterization using geostatistics. *Continental Shelf Research* 85:117-125.
- Mitchener H. and H. Torfs. 1996. Erosion of mud/sand mixtures. *Coastal Engineering* 29:1-25.
- Murphy R., T. Tolhurst, M. Chapman and A. Underwood. 2009. Seasonal distribution of chlorophyll on mudflats in New South Wales, Australia measured by field spectrometry and PAM fluorometry. *Estuarine Coastal Shelf Science* 84:108-118.
- Rainey M., A. Tyler, D. Gilvear, R. Bryant and P. McDonald. 2003. Mapping intertidal estuarine sediment grain size distributions through airborne remote sensing. *Remote Sensing of Environment* 86:480-490.
- Thomson A., R. Fuller, M. Yates, S. Brown, R. Cox and R. Wadsworth 2003. The use of airborne remote sensing for extensive mapping of intertidal sediments and saltmarshes in eastern England. *International Journal of Remote Sensing* 24:2717 - 2737.
- Widdows J. and M. Brinsley. 2002. Impact of biotic and abiotic processes on sediment dynamics and the consequences to the structure and functioning of the intertidal zone. *Journal of Sea Research* 48:143-156.

Rheological properties of cohesive sediments from Garonne Estuary

Janry Sébastien and Philippe Monnet

Pprime Institute, UPR 3346 CNRS-University of Poitiers-ISAIE ENSMA,
PO Box 30179, 86962 Futuroscope Chasseneuil Cedex, France
E-mail: sebastien.janry@univ-poitiers.fr

Natural cohesive sediments from the Garonne Estuary are taken and studied in order to determine their rheological properties. The Worall-Tuliani viscoplastic model is used to fit equilibrium flow curves and estimate yield stresses. Thixotropic properties are investigated by following build-up of internal structure of muds.

Introduction

Cohesive sediment behaves as viscoplastic fluids (Migniot, 1989; Van Kessel *et al.*, 1998), with thixotropic properties (Toorman, 1997). In this work, natural cohesive sediments from the Garonne Estuary are studied to determine their complex rheological properties. Equilibrium flow curves are obtained and present a typical double yield stresses evolution (Huang *et al.*, 2009). Moreover thixotropic effects are investigated using specific protocols to follow yield stress evolution as a function of rest time.

Materials

Natural cohesive sediments come from Cambes located in the Garonne Estuary, 15km upstream from Bordeaux. These materials have been taken directly from banks (low tide) for two depths: the first centimetre where muds are very fluid and not consolidated (cream muds) and from 1 to 5cm where muds present higher consistency (muds). Takings have been made manually and muds have been poured in boxes and directly put in an icebox for the travel. Each box has been stored in a refrigerator before measurements to prevent biota and bacterial development. Rheometrical tests have been made during the week following takings period.

Rheological protocols

The rheological characterisation of natural sediments is carried out with an AR1500ex rheometer (TA Instruments) using plate-plate geometry of 4cm diameter. Both surfaces are covered with sand paper with a mean roughness of 82 μ m to prevent slippage effects. Each measurement is realised for a 1mm gap. We check temperature of takings, let inside hermetically boxes to prevent evaporation, was 15°C to reach more quickly the temperature measurements. Muds are manually stirred for 2 minutes and poured within geometry gap. Before measurements and to ensure a reproducible proceeding a preshear is applied with a shear rate of 10s⁻¹ during 120s following by a 600s rest period.

Three protocols have been applied to characterize rheological properties of natural cohesive sediments. First, up and down flow curves are obtained applying shear rate steps ranging from 0.1 to 50s⁻¹ in a logarithmic repartition. Each curve is corrected using Rabinowitch formula to minimize existing error on the estimation of shear rate by using plate-plate geometry. Then two yield stress specific protocols are carried out varying the rest period after preshear to follow thixotropic effects. A shear stress ramp is applied during 60s leading to a parabolic curve of viscosity as a function of shear stress where maximum viscosity corresponds to the yield stress. A shear stress oscillating ramp is applied and averaged on 2 periods at 1Hz. The crossing point between storage and loss modulus is defined as the yield stress.

Rheological results

Down flow curves are fitted with the equilibrium Worall-Tuliani equation (Fig. 1a):

$$\tau = \tau_0 + \eta_\infty \dot{\gamma} + \frac{\eta_0 - \eta_\infty}{1 + \left(\frac{\eta_0 - \eta_\infty}{\tau_\infty - \tau_0} \right) \dot{\gamma}} \quad (1)$$

Where τ_0 is the true yield stress (the stress at $\dot{\gamma} = 0$), τ_∞ the Bingham yield stress, η_0 and η_∞ are the viscosities at low shear rate and high shear rate, respectively.

Worall-Tuliani model is well adapted to our measurements and permits to obtain the two specific yield stresses for equilibrium (Toorman, 1997). Cream muds present yield stresses two times lower

than muds. These differences can be explained by density (1442g/l for cream muds compared to 1493g/l for muds).

Direct measurements of materials yield stresses are plotted as a function of rest time (Fig. 1b). Yield stresses increase as a function of rest time that could be explained by build-up of internal structure of muds. This thixotropic effect seems to evolve for a same constant time for the two materials. Different thixotropic models are then applied to estimate this constant time (Coussot *et al.*, 2002; Cheng *et al.*, 1965). The kinetic of this phenomenon is governed by the same constant time around 2000s which is particularly short compared to tide period. So at the end of tide sediment build-up seems to be complete with a highest resistance to flow.

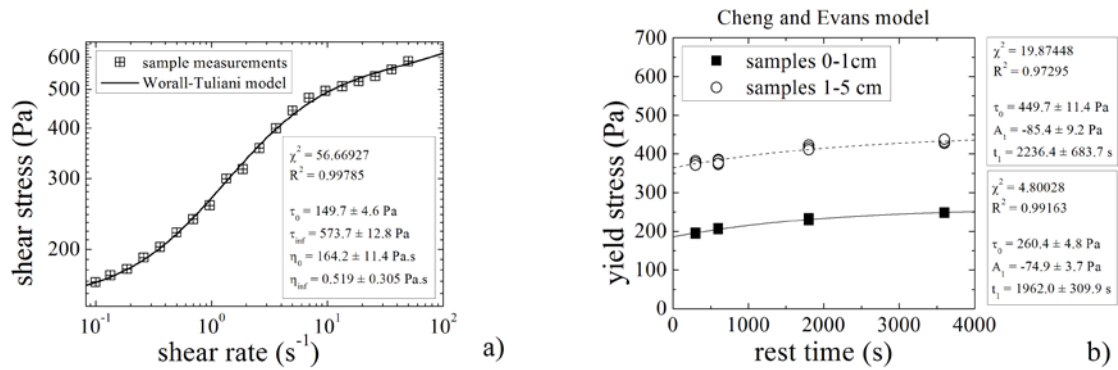


Fig. 1a. Rheogram of muds fitted with Worrall-Tuliani model. Fig. 1b. Yield stresses as a function of rest time for thixotropic Cheng and Evans model.

Conclusion

In this study rheological characterization of natural cohesive sediment is done. Cream muds and muds follow the same viscoplastic behaviour well described by Worrall-Tuliani model. Moreover thixotropic properties are present and a same kinetic is found for the two materials whereas values for cream muds are two times lower than muds linked to densities difference. This work takes place on a research project on tidal bore and these results must be associated to *in situ* measurements for describing erosion processes and sediment transport.

Acknowledgements

The authors acknowledge Pierre Lubin and David Reungoat for their help during muds taking and the Agence Nationale de la Recherche (Projet MASCARET 10-BLAN-0911-01) for financial assistance.

References

- Cheng D.H. and F. Evans. 1965. Phenomenological characterization of the rheological behaviour of inelastic reversible thixotropic and antithixotropic fluids. *British Journal of Applied Physics* 16:1599-1617.
- Coussot P., Q.D. Nguyen, H.T. Huynh and D. Bonn. 2002. Viscosity bifurcation in thixotropic, yielding fluids. *Journal of Rheology* 46:573-589.
- Huang Z. and H. Aode. 2009. A laboratory study of rheological properties of mudflows in Hangzhou Bay, China. *International Journal of Sediment Research* 24:410-424.
- Migniot C. 1989. Tassement et rhéologie des vases - Deuxième partie. *La Houille Blanche* 2 :95-111.
- Toorman E.A. 1997. Modelling the thixotropic behaviour of dense cohesive sediment suspensions. *Rheologica Acta* 36:56-65.
- Van Kessel T. and C. Blom. 1998. Rheology of cohesive sediments: comparison between a natural and an artificial mud. *Journal of Hydraulic Research* 36:591-612.

Relative effect of wind waves and tidal currents on sediment resuspension in the Saemangeum region, west coast of Korea

Kim Yong Hoon¹, Gi Young Bang², Tae In Kim², Yong Sik Song² and Jong Seong Ryu³

¹ Oceanography Division, RPS ASA (Applied Science Associates)
South Kingstown, RI, 02881, USA
E-mail: ykim@asascience.com

² Geosystem Research Corporation
Gunpo, Gyeonggi 435-824, Korea

³ Department of Marine Biotechnology, Anyang University
Ganghwa, Incheon 417-833, Korea

The eastern Yellow Sea is a macro-tidal environment, and tidal currents are known to play a major role in sediment transport in the coastal regions (Hwang *et al.*, 2014). In addition to tide, strong wind waves and wind-driven currents may also influence sediment resuspension and erosion, especially during wintertime when north-westerly winds get stronger. This study presents observation data from the Saemangeum area on the southwest coast of Korea, which demonstrates the temporal and spatial variability in the relative importance of wind waves and tidal currents on sediment resuspension/transport processes. Monitoring programme consists of a month-long continuous measurement on 3 locations using ADCP, pressure sensor, and optical backscatter sensor (AAT TM256-S) on November 2013 (Fig. 1a). Concentration of suspended sediments were measured by both acoustic and optical sensors every 10 minutes, and then calibrated with filtered *in-situ* water samples.

Mooring data show that there exist three distinctive high SSC (suspended sediment concentration) events during the study period (e.g., 10-13, 17-21, and 25-28 Nov.; Fig. 1b). During November, winds were blown mostly from north or northwest, which drives wave propagation toward southwest. Particularly during the events of elevated SSC, wind speeds were higher than 10m/s and significant wave height was larger than 2m. Tidal current speeds were variable during each period, including both flood and ebb as well as neap-spring cycles. The bottommost currents range 0.2-0.6m/s depending on tidal stage and locations. The envelop of tidal currents show a clear trend of fortnight cycle overlaid with several high speed events which are related to high wind periods.

SSC in the bottom boundary layer (~1 m above the bed) showed several episodic events, which were clearly correlated with high wind and wave periods (Fig. 1b), that is consistent with other studies in the eastern coastal zone of Yellow Sea (Lee *et al.*, 2004; Lee and Ryu, 2008). The high SSC events occurred only during the wind speed >10m/s and the significant wave height >2m, which could be considered as critical threshold condition for initiation of resuspension. The highest SSC peak on the PC1 station was observed during the condition of strongest wind period (>15m/s during 11/25 event). It is not surprising to conclude that the resuspension is mainly controlled by wind waves, especially offshore regions of the study area. In such area of >10m water depth, resuspension might be dominated by waves even without the aid of tidal currents. Otherwise, the combined effect of wave and currents is necessary to initiate resuspension.

On the shallower station, PC3, however, the SSC was highest during 11/17 event when the wave height was medium but tidal currents were larger than other events, due probably to spring tidal condition. It indicates that tidal currents could be equally or more important to make sediments resuspended, particularly in the shallower region. Under the similar wave condition of ~2m wave height, SSC during spring tide (11/17) was higher than neap (11/10) on all three stations. Another supporting evidence for the importance of tidal currents on resuspension is that while elevated SSC occurred immediately after increase in wave height during neap, during spring tide SSC was increased after currents velocity was higher than 0.2m/s even under high wave condition (>2m). In addition, the tidal cyclicity of SSC, which is more prominent during spring condition, was almost neglectful during neap.

Even during a single event, the relative importance of waves and currents effect on resuspension occurs in different patterns for different regions. During 11/10 event (neap tide, medium-high wave condition), for instance, the resuspension event was related more to wave activity on PC3 (southern shallow station) while elevated SSC event seemed to be correlated to increased current speed rather than wave offshore station (PC1). Under the wave condition of larger than 2m height, the period of elevated SSC corresponded to approximated 0.2m/s of current speed on PC1.

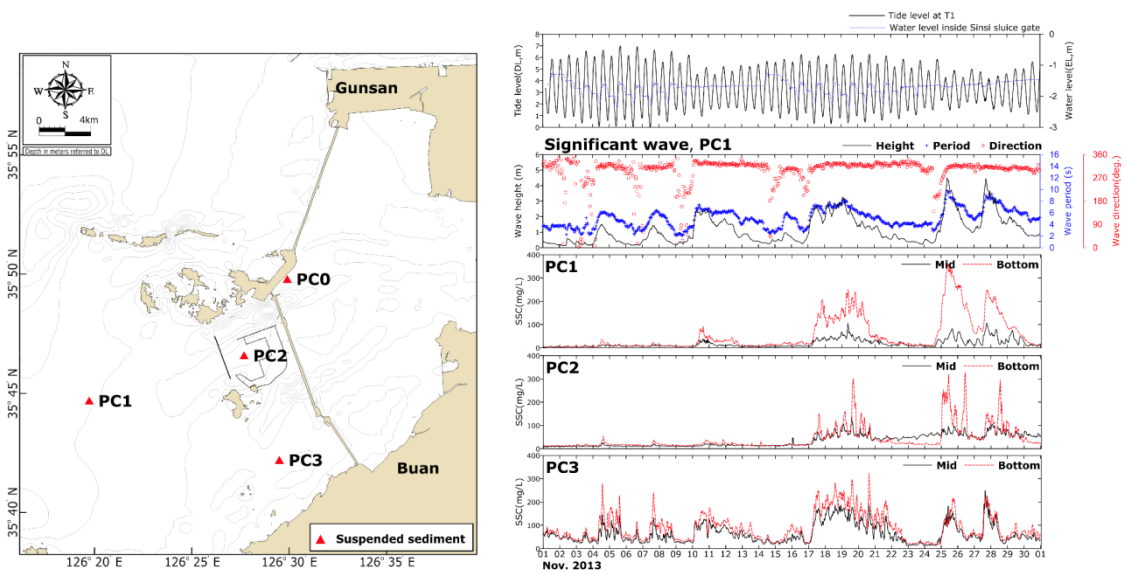


Fig. 1. (a) Study area and 3 mooring locations. (b) Time series of tide level, wave height, direction, and period, and suspended sediment concentration.

References

- Hwang J.H., S.P. Van, B.J. Choi, Y.S. Chang and Y.H. Kim. 2014. The physical processes in the Yellow Sea. *Ocean and Coastal Management*. <http://dx.doi.org/10.1016/j.ocecoaman.2014.03.026>
- Lee H.J., H.R. Jo, Y.S. Chu and K.S. Bahk. 2004. Sediment transport on macrotidal flats in Garolim Bay, west coast of Korea: significance of wind waves and asymmetry of tidal currents. *Continental Shelf Research* 24:821-832.
- Lee H.J. and S.O. Ruy. 2008. Changes in topography and surface sediments by the Saemangeum dyke in an estuarine complex, west coast of Korea. *Continental Shelf Research* 28:1177-1189.

Analysing fluvial transport and deposition of kaolinite-clay during steady and unsteady flow

Kurtenbach Andreas¹, Tom Gallé² and Reinhard Bierl¹

¹ Department of Hydrology, Faculty VI, Trier University, 54286 Trier, Germany
E-mail: kurtenbach@uni-trier.de

² Resource Centre for Environmental Technologies (CRTE), CRP Henri Tudor, 6A, avenue des Hauts-Fourneaux, 4362 Esch-sur-Alzette, Luxembourg

Introduction

Cohesive sediments (<63µm) control several biophysicochemical processes in fluvial systems. They act for instance as carrier for nutrients and contaminants, could induce a reduction of light penetration or provoke severe siltation of reservoirs and benthic habitats. Fluvial transport and deposition of such fine-grained particles are strongly linked to the passage of natural flood events. However, owing to the lack of convenient tracers and detection methods, experimental studies with cohesive sediments in natural river systems and particularly during unsteady flow regimes are rather scarce (Harvey *et al.*, 2012; Krishnappan 2007; Packman *et al.*, 2003; Spencer *et al.*, 2010).

Research approach, material & methods

Two strategies were adopted to study fluvial cohesive sediment phenomena in a natural system and during unsteady boundary conditions: First, artificial floods were released from a reservoir in the Olewiger Bach basin (24km²), a mid-mountain gravel bed river. The outstanding advantage of this artificial flood approach is that some of the governing processes can be excluded or steered by the experimental design. This comprises for instance hydraulic boundary conditions such as maximum discharge and runoff volume, wave form as well as flood duration (Kurtenbach *et al.*, 2006). Second, cohesive sediment dynamics were additionally analysed for comparative purposes during stationary, but variable base flow conditions. Suspended particle dynamics during these field experiments were analysed by introducing the clay mineral kaolinite ($d_{50}=2\mu\text{m}$, $\rho=2.6\text{g/cm}^3$) as a cohesive sediment tracer. During the steady-state field experiments, in-channel transport of kaolinite can be analysed via unspecific analytical methods such as turbidimetry/gravimetry, laser diffraction and photometry. However, during the floods the kaolinite tracer is always conveyed in mixtures with natural suspended matter. Consequently, a specific analytical method is indispensable to accurately quantify tracer fluxes during such unsteady flow regimes. For this purpose, we apply Fourier transform infrared spectroscopy (FTIR) in diffuse reflectance mode (DRIFT) (Gallé *et al.*, 2004).

Results

Our laboratory tests confirm that FTIR-DRIFT spectrometry is capable of detecting the kaolinite tracer even in low percentage solid concentrations. Tracer mass balance calculations during the field experiments reveal significant loss rates of kaolinite both during steady and unsteady flow regimes. Consequently, fluvial retention of fines could be orders of magnitude higher than the expected deposition derived for instance from gravitational settling velocities estimated via the Stokes equation. Potential mechanisms and determining factors of cohesive particle retention such as kinematic wave effects, hyporheic exchange, deposition in riverine dead and channel periphery zones, adhesion on biofilms as well as flocculation will be discussed.

References

- Gallé T., B. Van Lagen, A. Kurtenbach and R. Bierl. 2004. An FTIR-DRIFT study on river sediment particle structure: Implications for biofilm dynamics and pollutant binding. *Environmental Science and Technology* 38:4496-4502.
- Harvey *et al.* 2012. Hydrogeomorphology of the hyporheic zone: Stream solute and fine particle interactions with a dynamic streambed. *Journal of Geophysical Research* 177. doi: 10.1029/2012JG002043.
- Krishnappan B.G. 2007. Recent advances in basic and applied research in cohesive sediment transport in aquatic systems. *Canadian Journal of Civil Engineering* 34:731-743.
- Kurtenbach A., S. Möller, A. Krein and W. Symader. 2006. On the relationship between hydrographs and chemographs. *Hydrological Processes* 20:2921-2934.
- Packman A.I., T.J. Battin and J.D. Newbold. 2003. Coupling of hydrodynamical, biological and geochemical processes in streambeds. *Archives of Hydro-Engineering & Environmental Mechanics* 50:107-123.
- Spencer K.L., A.J. Manning, I.G. Droppo, G.G. Leppard and T. Benson. 2010. Dynamic interactions between cohesive sediment tracers and natural mud. *Journal of Soils and Sediments* 10:1401-1414.

Estuarine morphodynamics: simulating schematic configurations with a process-based 3D model with focus on the evolution of tidal marshes under climate change

Le Hir Pierre, Florence Cayocca and Julie Vareilles

Laboratoire DYNECO/PHYSED, Centre Ifremer de Brest, CS10070, 29280 Plouzané, France
E-mail: plehir@ifremer.fr

Context and objectives

Among the impacts of climate change in estuarine systems, one of the most difficult to tackle is the possible morphological evolution of estuaries, either due to sea level rise downstream, or to changes in both liquid and solid upstream river inputs. In large European estuaries, channel systems are most often constrained by navigation criteria, so that dredging is commonly undertaken in order to maintain the channel depth. On the other hand, lateral zones - especially intertidal flats and tidal marshes - are likely to be strongly impacted by climate change, mainly for two reasons:

- estuarine cross-profiles are essentially convex, so that the upper intertidal flats, most often vegetated (marshes), are only inundated during spring tides high water level; in case of sea level rise, the rate of inundation can increase tremendously, and generate new constraints on the natural marsh ecosystem or on its anthropic use, for instance for extended breeding;
- the tidal marshes elevation depends on the sedimentation rate which is both related to the previously mentioned inundation rate and to the suspended sediment concentration (SSC) in the upper water column in front of marshes; this concentration is strongly dependent on the proximity of the turbidity maximum, the location and intensity of which is related to the river regime.

Methodology

In order to test the estuaries morphological response to climate change and possibly characterize an equilibrium state, a process-based hydrodynamics and sediment transport numerical model, with morphological coupling is applied to schematic geometrical configurations. The morphological coupling requires a rather high horizontal resolution, while the simulation of realistic turbidity maximum location and good range of SSC in the upper layers requires some vertical discretization, so that the interest of schematic cases does not imply any saving in computing time, but an easier interpretation of results, according to the geometry of the estuary, the tidal range and the river regime.

The numerical code is a morphodynamic version of the MARS hydrodynamic code coupled with multilayered bed models. Navier-Stokes equations are solved under the Boussinesq approximation and hydrostatic assumption. Only suspended sediment transport is accounted for, with the possibility of mixing several sand and mud particle classes (Le Hir *et al.*, 2011). The typical horizontal resolution is 100-300m, while the vertical resolution remains crude in order to save computing time. A morphodynamic factor is used to speed up the sediment evolution for given mass exchanges between the bed and the water column. In order to allow meandering and channels divagation or intertidal flats extension, lateral erosion has been implemented for dry cells: lateral erosion is proportional to the tangent velocity components in neighbouring cells. In addition, the deposition of fine suspensions above a given cell can be spread to deeper neighbouring, in order to account for the actual sliding of fluid mud according to the bottom slope. In order to reduce possible artefacts induced by the use of a morphological factor, sediment processes have been strongly simplified: sand and mud have similar erosion behaviours and are mainly distinguished by their settling velocity, which allows for the simulation of sorting processes.

Results

First, the capacity of the model to simulate the long term evolution of an estuary (up to 800 years) has been tested: depending on the upstream sediment input, an equilibrium can be reached, or the estuary evolves into a delta. The banks most often exhibit steep slopes in the lower intertidal zone, while upper flats develop at elevations of realistic marshes. Secondary channels (creeks) can form throughout the marshes provided they are still regularly flooded.

Accounting for sea level rise (SLR=1cm/year during 100 years) leads to strongly non uniform marshes elevation. In the case illustrated on Fig. 1, the SLR is likely to enhance hydrodynamics within the estuary, and then generate meandering.

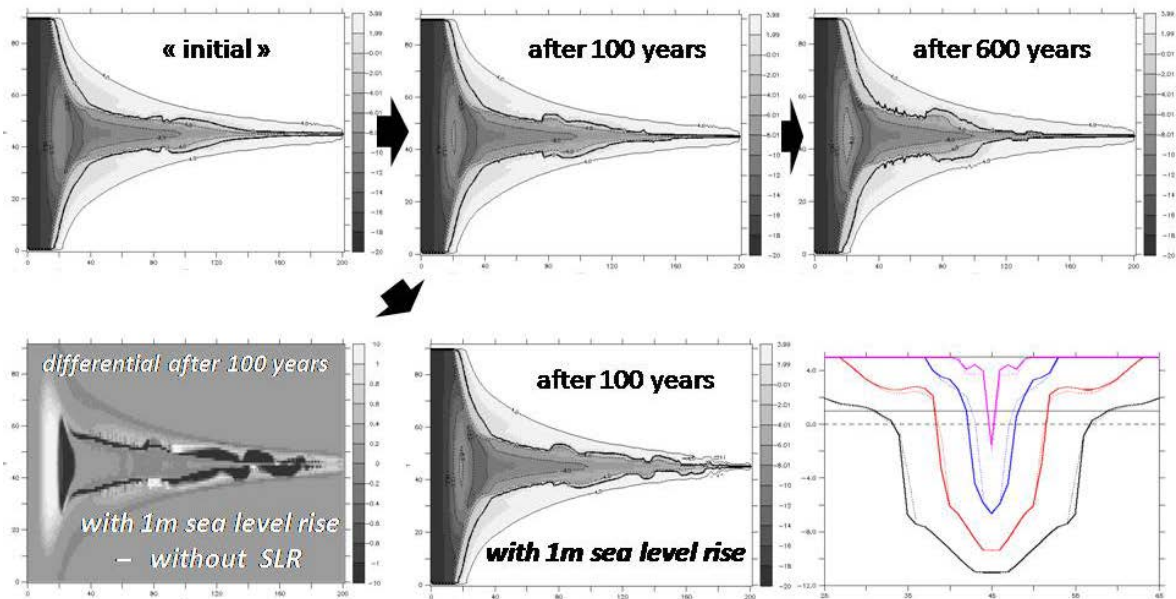


Fig. 1. Topo-bathymetric evolution of a 50km long estuary, with an upstream input of $40\text{m}^3\cdot\text{s}^{-1}$ and $\text{SSC}=0.05\text{kg}\cdot\text{m}^{-3}$. Lower right picture shows cross-sections with and without SLR after 100 y.

Confirming previous results from the literature, it appears that the change of river regime can affect the sedimentation rate on tidal marshes and their response to any sea level rise. In given circumstances the marsh elevation may follow the sea level rise if sedimentation is enough, while in other cases the inundation rate is likely to increase, and lead to other configurations with creeks formation, inducing different vegetation cover and influencing habitats (*e.g.* Temmerman *et al.*, 2012).

Acknowledgements

This work is part of the C3E2 project (Consequence of Climate Change on the Ecogeomorphology of Estuaries) supported by the French ministry of ecology within the GICC programme.

References

- Le Hir P., F. Cayocca and B. Waeles. 2011. Dynamics of sand and mud mixtures : a multiprocess-based modelling strategy. *Continental Shelf Research* 31:S135-S149.
- Temmerman S., M. De Vries and T. Bouma. 2012. Coastal marsh die-off and reduced attenuation of coastal floods: a model analysis. *Global and Planetary Change* 92-93:267-274.

Adsorption and flocculation mediated by polymeric substances in cohesive sediment suspensions: experimental study

Lee Byung Joon¹ and Mark Schlautman²

¹ School of Construction and Environmental Engineering, Kyungpook National University
2559 Gyeongsang-daero, Sangju, Gyeongbuk, 742-711, South Korea
E-mail: bjlee@knu.ac.kr

² Department of Environmental Engineering and Earth Sciences, Clemson University
342 Computer Court, Anderson, SC 29625, USA

Introduction

Polymeric substances are present everywhere in the water environment. They can adsorb cohesive sediments and bind particles together in large flocs, thereby enhancing flocculation. Extracellular polymeric substances (EPS), as natural polymeric substances, enhance flocculation of cohesive sediments in rivers, lakes and estuaries (Droppo, 2001; Chen *et al.*, 2005). As analogues of EPS, synthetic polymeric substances have been widely used as flocculation agents in many engineering systems, for controlling soil erosion and sediment runoff from source sites or removing suspended solids in water and wastewater treatment processes (e.g. Orts *et al.*, 2007). However, not all the polymeric substances can enhance flocculation. The size of a polymeric substance is a critical property to enhance or reduce flocculation. For example, Engel *et al.* (2004) reported that in the marine environment, small polymeric substances (e.g. cell exudates), which initially do not have flocculation capability, aggregate to large polymeric substances, thereby enhancing flocculation. Large polymeric substances in an engineered treatment system also have been reported to enhance flocculation more than small polymeric substances (Green *et al.*, 2000). Thus, this research was conducted to investigate closely the effect of the size of polymeric substances on flocculation, as well as adsorption, in a well-controlled laboratory condition.

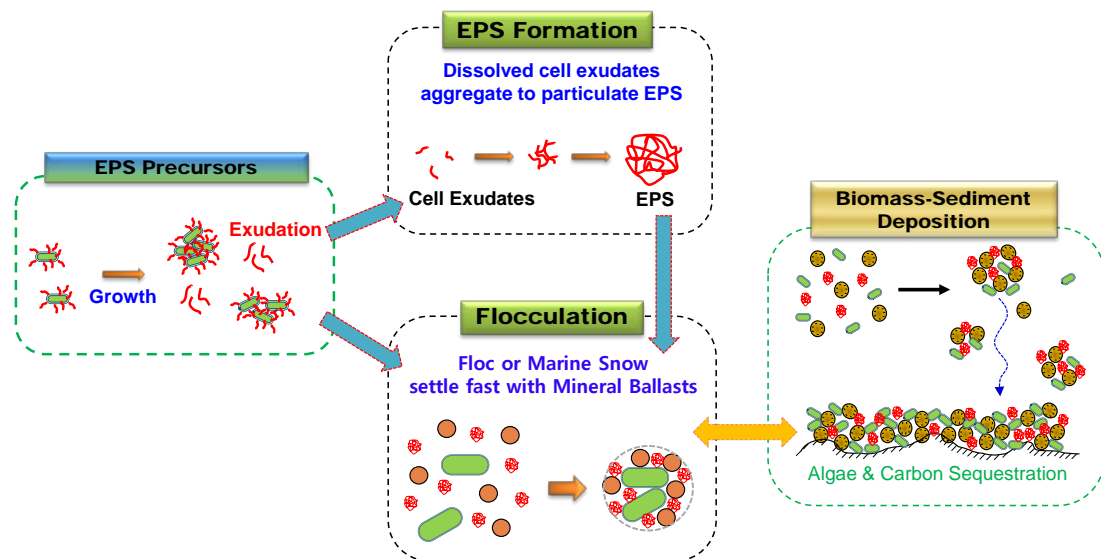


Fig. 1. Conceptual model of EPS formation and bio-mediated flocculation in the marine environment.

Materials and methods

A series of polyacrylamides (PAM) with different molecular weights (MW) (i.e. different sizes) of 1.5kg/mol, 10kg/mol, 0.6–1Mg/mol, and 5–6Mg/mol, which are denoted by 1.5K, 10K, 0.6–1M, and 5–6M PAMs in this paper, were selected and tested as polymeric substances. Those PAMs with different MWs were applied to kaolinite suspensions, to test their adsorption capacity and flocculation capability. The respective bottle-point adsorption test and shear-controlled flocculation test were used to investigate PAMs' adsorption capacity and flocculation capability.

Results and discussion

The bottle-point adsorption tests with kaolinite suspension, dosed with 1.5K, 10K, 0.6–1M, and 5–6M PAMs, indicated that PAM adsorption capacity on kaolinite increases with a higher MW. Especially, 0.6–1M and 5–6M PAMs had 20 to 30 times higher adsorption capacities than 1.5K, 10K

PAMs. In the shear-controlled flocculation tests, 1.5K, 10K PAMs did not enhance flocculation but rather stabilize particles in the kaolinite suspension. The polymeric chains of 1.5K and 10K PAM might be confined within the electrostatic repulsion layer on sediments due to their short polymer chain structure, thereby not being able to develop polymeric bridges between particles and decreasing flocculation (Fig. 1). On the contrary, 0.6~1M and 5~6M PAMs substantially increased flocculation. Especially, 5~6 M PAM was found to have higher flocculation capabilities than 0.6~1M PAM, for being more subject to non-equilibrium flocculation (Pelssers *et al.*, 1989), in which unstable, stretching polymeric structures on sediment surfaces increase particle-particle bridging and flocculation (Fig. 1).

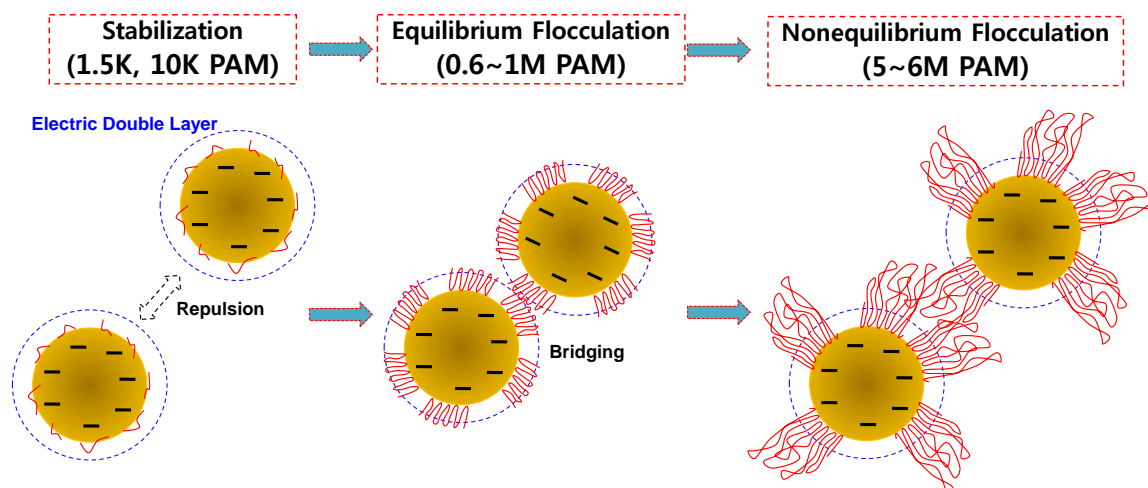


Fig. 2. Schematic diagram for the effect of PAM MWs (i.e. size) on adsorption and flocculation

Conclusion and recommendation

This experimental study revealed that larger polymeric substances are more effective adsorbates and flocculants than smaller polymeric substances. The size (i.e. MW) was found to be an important property of a polymeric substance for determining adsorption capacity and flocculation capability. However, unlike synthetic polymeric substances in a well-controlled laboratory, the functions of natural, biogenic polymeric substances for adsorption and flocculation remain mostly unknown in the natural water environment because they are hardly separated from other factors in such a complex system. This issue might present a challenging task in the scientific community. Hopefully, adopting new physical-chemical-biological analytical techniques, for characterization of polymer substances and quantification of adsorption and flocculation, may help us to get the right answer.

Acknowledgement

This research was supported by Basic Science Research Program through the National Research Foundation of Korea (NRF) funded by the Ministry of Education (No: 2014R1A1A2055622).

References

- Chen M., S. Wartel, B. Van Eck and D. Van Maldegem 2005. Suspended matter in the Scheldt Estuary, *Hydrobiologia* 540:79-104.
- Droppo I.G. 2001. Rethinking What Constitutes Suspended Sediment. *Hydrological Processes* 15:1551-1564.
- Engel A., S. Thoms, U. Riebesell, E. Rochelle-Newall and I. Zondervan 2004. Polysaccharide aggregation as a potential sink of marine dissolved organic carbon. *Nature* 428:929-932.
- Fleer G., M. Cohen Stuart, J. Scheutjens, T. Cosgrove and B. Vincent 1993. *Polymers at interfaces*. Chapman & Hall, London, UK.
- Green V.S., D.E. Stott, L.D. Norton and J.G. Graveel. 2000. Polyacrylamide molecular weight and charge effects on infiltration under simulated rainfall. *Soil Sci. Soc. Am. J.* 64:1786-1791.
- Orts W.J., A. Roa-Espinosa, R.E. Sojka, G.M. Glenn, S.H. Imam, K. Erlacher and J.S. Pederson 2007. Use of synthetic polymers and biopolymers for soil stabilization in agricultural, construction, and military application. *Journal of Materials in Civil Engineering* 19(1):58-66.
- Pelssers E., M. Cohen Stuart and G. Fleer 1989. Kinetic aspects of polymer bridging: equilibrium flocculation and nonequilibrium flocculation. *Colloids Surfaces* 38(1):15-25.

Evaluation of ADCP backscatter inversion to suspended sediment concentration in estuarine environments

Lee Guan-hong, Hyun-Jung Shin and Hyo-Bong Park

Department of Oceanography, Inha University, 100 Inharo, Incheon, 402-751, Korea
E-mail: ghlee@inha.ac.kr

Acoustic Doppler Current Profiler (ADCP), designed for measuring velocity profile, is now widely used for the estimation of suspended sediment concentration from acoustic backscatter intensity, but its application to estuarine environments has not been vigorously tested.

In this study, we examined the inversion capability of two ADCPs with 600 and 1200 kHz at three Korean estuaries: macrotidal Han River Estuary (HRE), microtidal Nakdong River Estuary (NRE), and anthropogenically altered macrotidal Yeongsan River Estuary (YRE) (Fig. 1 and Table I).

Table I. Size composition of bed sediment

Site	Sand (%)	Silt (%)	Clay (%)	d_{50} (μm)	x^a
HRE	11.5	69.8	18.6	13.6	0.022
NRE	41.7	32.8	25.5	30.0	0.078
YRE	2.5	44.0	53.4	4.8	0.012

^a Non-dimensional frequency ($x=k\lambda a$ where k is wave number and a is the particle radius).

In particular, we examined the relative importance of the sound attenuations due to water (α_w) and sediment (α_s) in response to sediment characteristics (size and concentration) as well as changing salinity and temperature (Table II).

Table II. Scenarios for acoustic inversion

Scenario	α_w	α_s
S1	×	×
S2	○ (constant)	×
S3	×	○
S4	○ (constant)	○
S5	○ (varying)	○

The inverted concentration was compared with reference concentrations obtained either water samples or Optical Backscatter Sensors. In NRE and YRE, where suspended sediment concentrations were smaller than 0.2kg/m^3 , the acoustic inversion performed poorly only with α_s ($R^2 = 0.05$ and 0.39 for NRE and YRE, respectively), but well with α_w ($R^2 = 0.99$ and 0.89 for NRE and YRE, respectively) (Fig. 2). Thus, it is important to accurately constrain α_w in low-concentration estuarine environments. However, we did not find that the varying α_w performed considerably better than the constant α_w . On the other hand, the acoustic inversion was poorest at HRE regardless of α_w and α_s ($R^2 = 0.75$ and mean relative error = 45%) (Fig. 2).

The large discrepancy appears to result from the poorly constrained, spatially and temporally varying sediment characteristics (grain size, density and concentration) due to non-local sediment transport at macrotidal HRE.

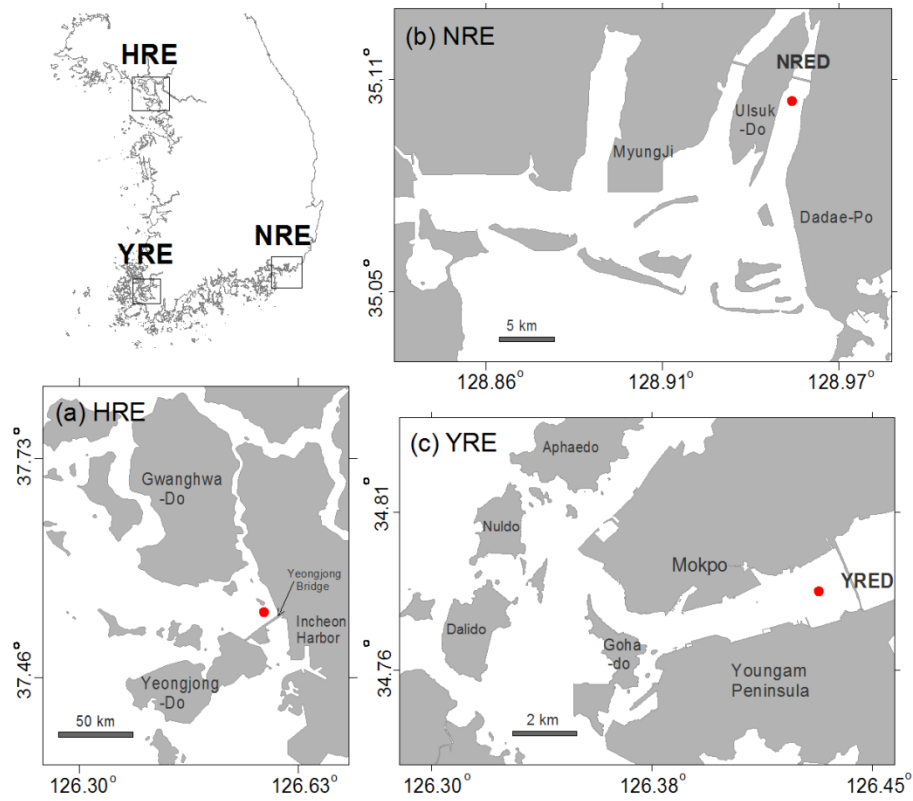


Fig. 1. Study sites: (a) Han River Estuary (HRE), (b) Nakdong River Estuary (NRE), and (c) Yeongsan River Estuary (YRE). Red dot indicates the location of ADCP deployment.

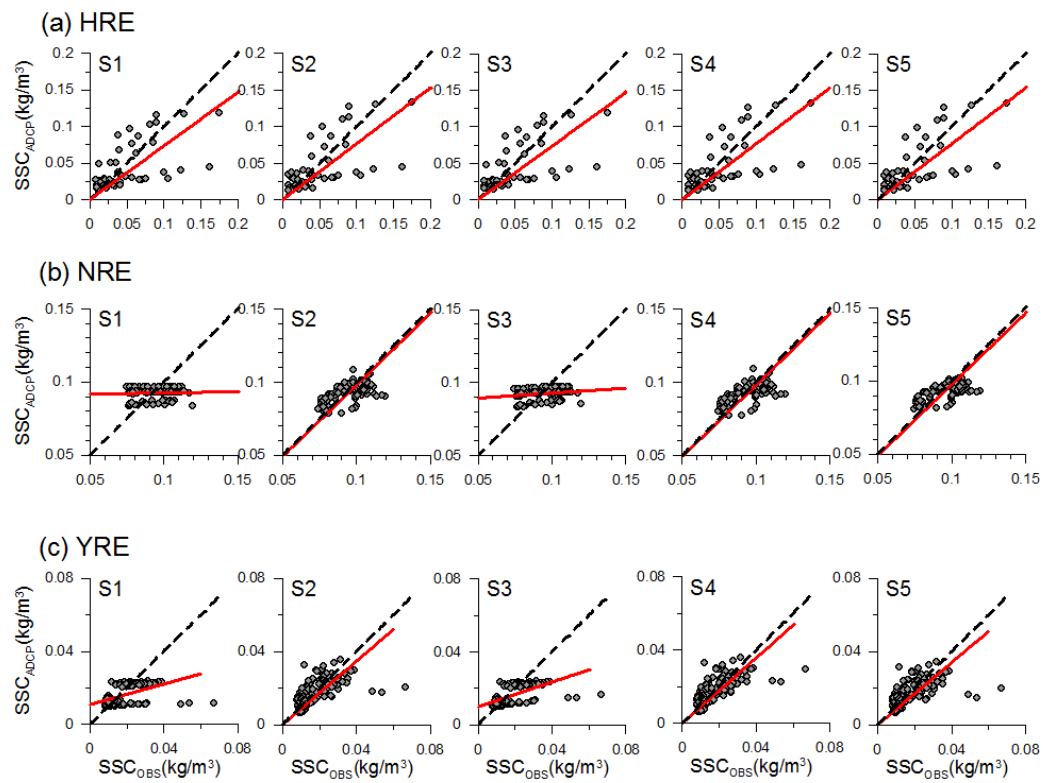


Fig. 2. Comparison between SSC_{ADCP} and SSC_{OBS} for five scenarios. The solid line indicates the regression, while the dashed line represents one-to-one relationship.

The effects of mixed cohesive and non-cohesive sediment properties on bedform and suspended sediment dynamics in the intertidal Dee Estuary

Lichtman I.D.^{1,2}, P.D. Thorne¹, J.H. Baas², L. Amoudry¹, J. Hope³, R.D. Cooke¹, P.S. Bell¹, J. Malarkey², D.R. Parsons³, J. Peakall⁶, S.J. Bass⁴, R.J. Schindler⁴, L. Ye⁵, R.J. Aspden³, D.M. Paterson³, A.G. Davies² and A.J. Manning^{4,5,7}

¹ National Oceanography Centre, Joseph Proudman Building,
6 Brownlow Street, Liverpool L3 5DA, UK
E-mail: doulich@noc.ac.uk

² School of Ocean Sciences, Bangor University, Menai Bridge,
Anglesey, LL59 5AB, UK

³ Sediment Ecology Research Group, Scottish Oceans Institute, University of St Andrews,
East Sands, St Andrews, KY16 8LB, Scotland, UK

⁴ School of Marine Science & Engineering, Plymouth University, Drake Circus, Plymouth, PL4 8AA, UK

⁵ Department of Geography, Environment and Earth Sciences, University of Hull,
Cottingham Road, Hull, HU6 7RX, UK

⁶ School of Earth and Environment, University of Leeds, Leeds, LS2 9JT, UK

⁷ HR Wallingford, OX10 8BA, UK

Introduction

Accurate sediment transport models are essential for the management of coastal erosion, maintenance of navigation channels and understanding the impacts of climate-induced habitat change. Many of these coastal environments are dominated by mixtures of sand and mud. While reasonable sediment transport predictors are available for pure sands, this is not the case for mixed cohesive and non-cohesive sediments. Existing ripple predictors mostly relate bedform dimensions to hydrodynamic conditions and median sediment grain diameter, assuming a narrow unimodal particle size distribution. Under natural conditions, deposited beds may be comprised of mixed sediments affected by both physical and biologically-mediated cohesion (biogenic stabilisation). This natural complexity severely limits the applicability of standard predictors. Indeed, recent laboratory experiments mixing cohesive and non-cohesive sediments and adding bacterial polymers as a proxy for natural biogenic stabilisation have shown that bedform dimensions decrease with increasing bed clay content and that the bedform development rate is reduced by biological action (Baas *et al.*, 2013; Malarkey *et al.*, in press). In the field, it is expected existing predictors will match data for well-sorted sands closely, but will be inaccurate for mixed sediments containing cohesive sediments and natural biota. The paper reports on an extension of laboratory work to examine mixed sediments in the field.

Methodology

Over a two week period, 21 May to 4 June 2013, a field study was carried out on the tidal flats in the Dee Estuary, on the NW coast of England. A range of instrumentation was deployed to measure the sediment properties and hydrodynamics, while sediment samples were collected for laboratory analysis. As part of the fieldwork, a suite of instruments was deployed collecting co-located measurements of the hydrodynamics, suspended sediment properties and bed morphology (Fig. 1). The instruments occupied three sites across the tidal flats collecting data for different bed compositions and morphology. Site 1 was located higher on the intertidal flats than site 3, and site 2 was the lowest and located in a creek. The experiment covered a tidal cycle from springs to neaps, and the weather during the sampling window provided onshore and offshore winds of varying strength.

Bedform measurements were taken every half an hour using an Acoustic Ripple Profiler (ARP) that covered an area of about a 10m². Dynamic measurements of tides and waves were made using an Acoustic Doppler Velocimeter (ADV) at 8Hz. Bed samples were taken when the tidal flats became exposed at low water and a multi-tier sediment trap collected suspended sediment load at five heights during the periods of sufficient inundation. Measurements of the suspended sediment were made using Acoustic Backscatter System (ABS) and LISST (Laser In Situ Scattering and Transmissometry) instruments. Combined bedform and suspended sediment measurements were collected using the BASSI (Bedform and Suspended Sediment Imager). Auxiliary measurements were made by a CTD (Conductivity, Temperature and Depth) with an OBS (Optical Backscatter Sensor).

The bed and multi-tier samples were analysed for particle size distribution (PSD), and separate bed samples were analysed for carbohydrate content as a proxy measure of biological cohesion.



Fig. 5. SEDbed frame deployed at site 1, on the West Kirby tidal flats in the Dee Estuary.

Aims

This paper will present results that show comparisons under different hydrodynamic conditions of ripple dimensions and migration, and suspended sediment size distributions and properties, using measurements of the proportion of mud and content of natural polymers as a proxy for biological stabilisation. Specifically, the following objectives and progression towards these outcomes will be considered and presented:

- compare the field data with laboratory results that showed reduced ripple length due to cohesive sediment content and increased ripple development time caused by biological stabilisation;
- assess how the bed dynamics of ripple migration are affected by cohesion and biological stabilisation;
- assess the performance of a selection of ripple predictors for mixed sediment data, with a view to creating an improved predictor;
- gain a better understanding of how bed and suspended sediment relate to each other using the particle size distribution.

Acknowledgements

This work was funded by the UK Natural Environment Research Council (NERC) under the 'COHBED' project (Realistic Sedimentary Bedform Prediction: Incorporating Physical and Biological Cohesion, NE/1027223/1).

References

- Baas J.H., A.G. Davies and J. Malarkey. 2013. Bedform development in mixed sand-mud: the contrasting role of cohesive forces in flow and bed. *Geomorphology* 182:19-32.
- Malarkey J., J.H. Baas, J. Hope, R.J. Aspden, D.R. Parsons, J. Peakall, D.M. Paterson, R.J. Schindler, L. Ye, I.D. Lichtman, S.J. Bass, A.G. Davies, A.J. Manning and P.D. Thorne. (in press). Beyond biofilms: the pervasive role of biological cohesion in bedform development. *Nature Communications*.

Studies of the relationship between suspended sediment concentration and light attenuation

Lumborg Ulrik and Klavs Bundgaard

DHI, Agern Allé 5, DK-2970 Hørsholm, Denmark
Email: ulu@dhigroup.com

A relationship between suspended sediment concentration (SSC) and light attenuation is not a direct relationship. The relation depends on numerous parameters including sediment grain size distribution, sediment colour and organic content (e.g. Davies-Colley and Smith, 2001). Yet, for many studies and projects, light attenuation is the desired measure when assessing effects of e.g. sediment spill. In this study a measurement campaign was set up with continuous measurements of, among other things, suspended sediment concentration, light attenuation and suspended sediment grain size distribution. Relationships between the individual parameters were obtained.

Introduction

Suspended sediment has impact on the biological communities in near-coastal waters. This is especially true when the concentration range is changed by artificial impacts e.g. dredging. A large part of the impact is related to the light attenuation. Light in the water column and at the sea bed is of major importance for plants ability to undertake photo synthesis, for fish migration and for food seeking by birds. As forecasts for human activities tend to focus on the change in turbidity rather than light attenuation a reliable estimate for a relation between these parameters is desirable.

Monitoring data

In connection with a project in a non-tidal coastal lagoon in Denmark a large data set was collected. The data set consist of numerous parameters including: suspended sediment concentrations, sediment grain size/floc size distributions, light attenuation coefficients and organic content. The data are collected with optical instruments and all was documented by water samples collected in a range of weather conditions. This data set allows for studies of a range of relationships between sediment and light.

Discussion

In order to convert the turbidity data collected in NTU to SSC in mg/l an analysis of the data must be carried out. This is done by comparison of NTU data and concentrations obtained through water samples collected in calm and rough weather. In Fig. 1 an example of such a conversion is provided. The graph clearly shows different classes or populations of sediment with clearly separated conversion formulas. This is dependent on the energy levels. One of the conversions is valid in rough weather (coarse sediment) and one is valid in calm weather (fine sediment). The aim is to introduce a measure of the sediment grain size in the conversion formula and thereby obtaining a more valid measurement of SSC.

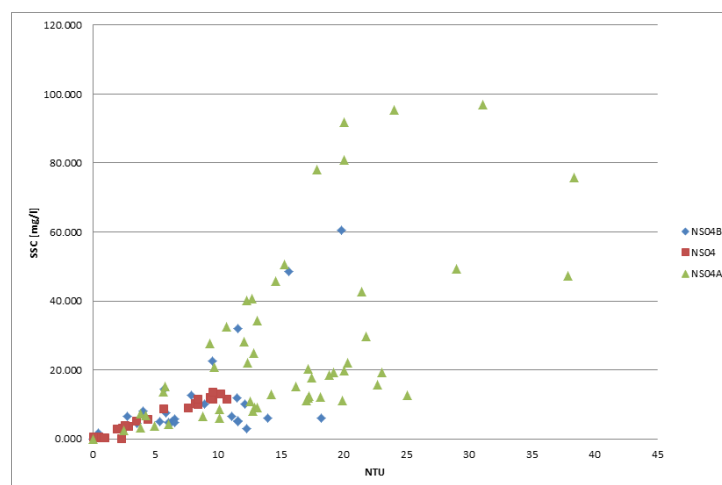


Fig. 1. Obtained conversions between NTU and SSC divided by station. Note the different populations found during different energy levels.

The data set similarly allows for a study of how light attenuation varies with different physical parameters. An example is shown in Fig. 2 where a correlation between NTU and K_d for three sites is provided. It is clear that for one site there is a clear relationship between the two parameters whereas for the two other sites the light attenuation varies extensively while the turbidity is fairly constant. This is because of a variation in grain size distribution. The coarser sediment (non-cohesive) does not dampen the light as much as the finer fractions.

A total of 180 datasets of in situ water samples (SSC), NTU, light intensity and grain size distributions under various weather conditions were collected. The same parameters have likewise been studied in the laboratory. The laboratory tests have used artificial light and sediment collected in the study area. This extensive data set makes it possible to analyse and predict effects of suspended sediment - natural or artificial - with higher accuracy.

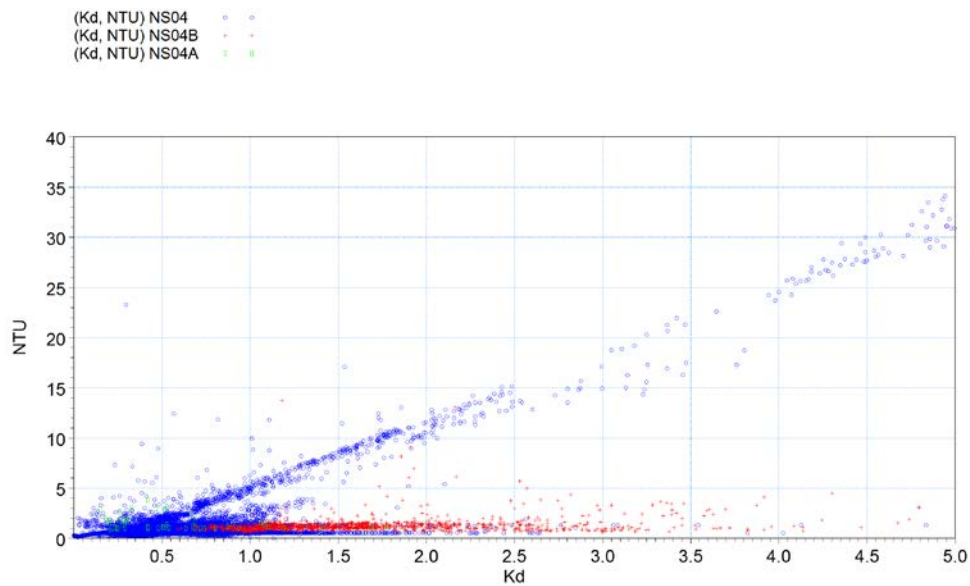


Fig. 2. Relationship between NTU and light attenuation at three different sites.

References

Davies-Colley R. and D. Smith 2001. Turbidity, suspended sediment, and water clarity: a review. *Journal of the American Water Resources Association* 37(5):1085-1101.

Simulating extremely high ebb current velocities in the Changjing Deep-water Navigation Channel

Maa J. P.-Y.¹, Y.Y. Shao², X.T. Shen¹ and J. Shen¹

¹ College of William and Mary, Virginia Institute of Marine Science, USA.
E-mail: maa@vims.edu.

² College of Harbour, Coastal and Offshore Engineering, Hohai, University, Nanjing, P.R. China

Introduction

Along the channel, measured tidal current velocity profiles at stations (from CS1 to CS5 (see Fig. 1) reveal an unusual maximum ebb current velocity (i.e., > 3m/s for a quite large portion of the water column at Sta. CS3 (see Fig. 2), in a survey carried out in 2002 during a wet season. This high velocity, however, has not been successfully simulated by using conventional numerical three-dimensional (3-D) hydrodynamic models. This becomes a problem when details of turbulent (e.g., shear rate, TKE, energy dissipation rate) are needed for simulating flocculation process for floc size distribution. That stimulates this study to explore the possible reasons.

The freshwater discharge in this estuary is high during the wet season (more than 53000 CMS). In general, this attributes to the large ebb current, but that is not the reason of having the observed high ebb velocity. To use an unusually small bottom friction coefficient in any 3-D model may not be the logical choice neither. There are two possible causes that may contribute to the high velocity. The first possible reason comes from the stratification effects, caused by salinity or/and suspended sediment distribution in this channel. A slight stratification in the water column can significantly reduce the eddy viscosity in the water column, and thus, contribute to the increase of current velocity near the surface. The other possible reason is the possible reduction of the constant C_{μ} (= 0.09 when the shear rate is not high) that used to compute the eddy viscosity in the turbulence k - ϵ model. Shih *et al.* (1994) indicated that this constant can be reduced to 0.05 if the shear rate is high.

Methodology

A vertical one-dimensional (1-D) model has been developed to simulate tidal flows. This 1-D model uses a semi-implicit numerical scheme to solve the vertical 1-D momentum equation with the standard k - ϵ model for turbulence. Stratification effect, caused by the vertical gradient of salinity and suspended sediment concentration is included. The model results were verified with data from a non-stratified tidal flow at the Menai Strait, UK (Rippeth *et al.*, 2002) and data from a slightly stratified York River site (Simpson *et al.*, 2005).

The measured time series of salinity and suspended sediment concentration (SSC) profiles for the entire simulation period are part of the input data. These profiles serve the purpose for simulating the change of eddy viscosity profile. Slightly stratified tidal flows will have a nearly linear velocity profile for most of the water column (Anwar, 1983). The possible occurrence of high gradient of SSC near the bed (when the ambient SSC is high) needs to be estimated. This 1-D model experiment found that stratification can significantly alter the eddy viscosity profile for most of the water column, but not near the bed. The salinity stratification contributes to the reduction of eddy viscosity profile, and thus, increases the velocity near the top of the water column.

Modeling results and Conclusions

This study found that the energy loss caused by the change of channel geometry, bathymetry, and bottom roughness is the main reason that causes extremely high ebb current velocity at Sta. CS3. At offshore stations, the effect of channel geometry and bathymetry is diminished, and thus, the maximum ebb current is around 2m/s. It appears that the possible occurrence of high gradient of near-bottom SSC when the ambient SSC is high is not sufficient to alter the near-bed eddy viscosity, and thus, only affects the velocity profile slightly. The reduction of C_{μ} from 0.09 to 0.05 (when the local shear rate is high) does not have much impact on the velocity profile neither.

This study demonstrates the importance of channel geometry and bathymetry that affect the velocity profile. It also shows the importance of having a complete measurement of salinity, suspended sediment concentration, and temperature profiles in order to have a correct understanding of the underlying processes and simulation of the current velocity in estuaries. This will be better prepared for our next-stage study on floc size distribution and the associated settling velocity.

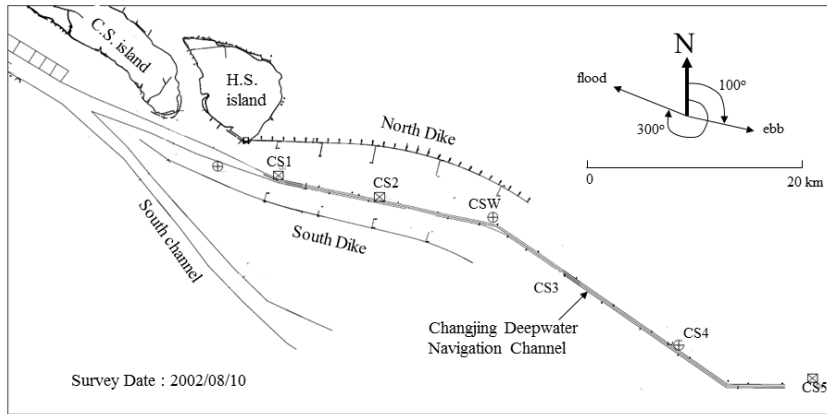


Fig. 1. The six stations along the Changing Deep-water Navigation Channel.

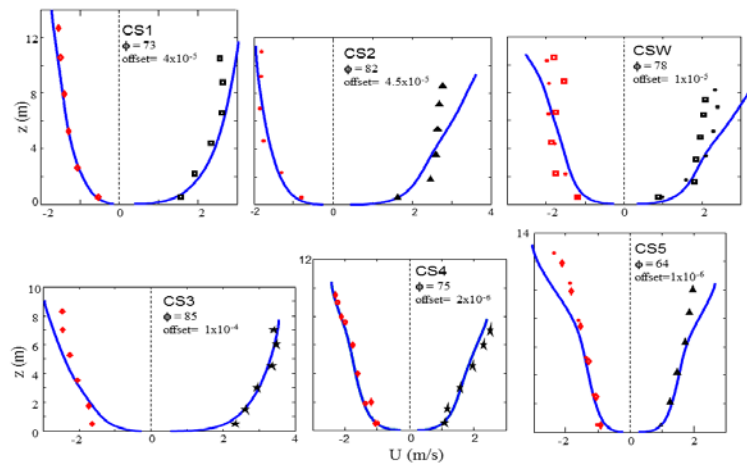


Fig. 2. Measured (symbols) and simulated (lines) maximum flood and maximum ebb velocity profiles at the six stations.

References

- Anwar H.O. 1983. Turbulence measurements in stratified and well-mixed estuarine flows. *Estuarine, Coastal and Shelf Science* 17:243-260.
- Rippeth T.P., E. Williams and J.H. Simpson. 2002. Reynolds Stress and Turbulent Energy Production in a Tidal Channel. *Journal of Physical Oceanography* 32:1242-1251.
- Shih T.H., W.W. Liou, A. Shabbir, Z. Yang and J. Zhu. 1994. A new $k-\epsilon$ eddy viscosity model for high Reynolds number turbulent flows - Model development and validation. Institute for Computational Mechanics in Propulsion and Center for Modeling of Turbulence and Transition. Lewis Research Center, Cleveland, Ohio, NASA., ICOMP-94-21, NASA technical memorandum 106721.
- Simpson J.H., E. Williams, L.H. Brasseur and J.M. Brubaker. 2005. The impact of tidal straining on the cycle of turbulence in a partially stratified estuary. *Continental Shelf Research* 25:51-64.

Sediments in motion

MacDonald Lain T.¹ and Julia C. Mullarney²

¹ National Institute of Water & Atmospheric Research, PO Box 11115, Hamilton, 3251, New Zealand
E-mail: lain.macdonald@niwa.co.nz

² Coastal Marine Group, Faculty of Science and Engineering, University of Waikato, Hamilton, New Zealand

A novel drifter platform was used to measure floc properties, turbulence, suspended sediment concentration (SSC), velocity and salinity in both Lagrangian and Eulerian frames of reference. In Lagrangian mode the system performed well in a heavily sediment-laden river, providing measurements over a large spatial scale. The platform navigated itself through a complex geometry encompassing many bends and significant depth changes. Observed velocities relative to the drifter indicated that the drifter motion was almost Lagrangian with minimal slippage between drifter and water motion. The small amount of slippage that did occur was sufficient to ensure that the drifter oriented itself into the oncoming flow. High-quality in-situ images of flocs were collected using a high-magnification floc camera (FlocCam). An automatic image analysis routine was developed to identify and characterise flocs within each FlocCam image. The results indicated that the FlocCam system had an upper working SSC limit of around 350 to 400mg L⁻¹. The system captured the evolution of floc characteristics over short spatial scales (100s of meters). Median floc size (d₅₀) was found to be positively correlated with SSC. No clear relationship between median floc size and dissipation rate of turbulent kinetic energy could be discerned.

Introduction

Floc size has been successfully measured in both the laboratory and the field in an Eulerian frame of reference using floc cameras and laser diffraction. However, it has been shown that fine sediments have a strong memory of previously encountered upstream conditions (such as turbulence and SSC), which can at least partially overwrite floc response to local conditions. Indeed Braithwaite *et al.* (2012) found that particle size predictions matched well with the Winterwerp (1998) dynamical flocculation model if a phase lag (representing the adjustment time to changes in turbulence conditions) was included. Therefore, quantifying fine-sediment particle dynamics requires following particles in a Lagrangian framework to account for antecedent conditions.

Drifter design

The FlocDrifter body (Fig. 1) consisted of an underwater housing for the FlocCam system which is connected to a stabilising tail which orientates the drifter into the oncoming flow. When deployed in Lagrangian mode, the drifter was tethered to a surface float to keep the drifter at a fixed depth. The design included purpose-built mounts for additional instruments: a Nortek Vector ADV, a 2MHz Nortek Aquadopp ADCP operating in pulse-to-pulse coherent mode. Additionally, a Seabird SBE-37 MicroCAT was mounted vertically at the end of the tail; above the camera housing optical backscatter was measured using a Seapoint turbidity sensor.

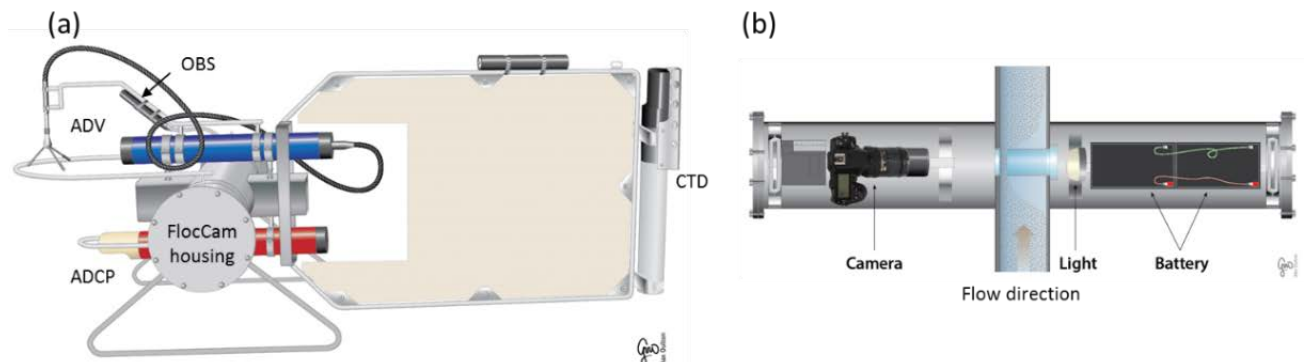


Fig. 1. Schematic of (a) FlocDrifter body and (b) FlocCam system in underwater housing.

Field site

The drifters were tested over multiple days in the heavily sediment-laden Kaipara River on the North Island of New Zealand. The Kaipara River flows into the southern end of the mesotidal Kaipara harbour. The river exhibits large bends, with frequent changes in direction and is characterised by average depths along the thalweg of around 3m. Deployments took place during a period of low

river flows over three days in October 2013. Up to three drifters were released shortly after high tide from varying locations, chosen to be sufficiently close together for sections of tracks to overlap, thus providing multiple measurements during different stages of the ebbing tide. Tracks covered 4.1km (with 3.8km of overlapping sections), 14.9km (6.4km overlapping) and 15.1km (9.2km overlapping) sections of river on days 1, 2 and 3, respectively.

Data analysis

ADCP velocities were recorded at 8Hz over a 0.73m vertical profile (25mm bin spacing) with a burst duration of 512s with a 3s interval between bursts. Estimates of the dissipation rate of turbulent kinetic energy (ϵ) were obtained using the structure function method of Wiles *et al.* (2006). Optical backscatter was recorded continuously at 5Hz, the voltage output by the optical backscatter sensor was related to SSC via a laboratory calibration. An automatic image analysis routine was developed to identify and characterise flocs within each FlocCam image. An Artificial Neural Network was employed to ensure that only in-focus particles were included in the analyses.

Results

The measurements revealed significant along-river variation over scales of a few hundred meters, which would unlikely to have been resolved without a very large array of Eulerian measurements, ϵ ranged from $O(10^{-7})$ to $O(10^{-3.4})$ W/kg (corresponding to Kolmogorov length scales of ~ 200 to $1800\mu\text{m}$). SSC estimates show that the drifters experience considerable variability in SSC as they were advected downstream. The variability in SSC most likely results from the spatial and temporal changes in sediment sources (e.g. erosion) and sediment sinks (e.g. deposition). Preliminary analysis indicates that median floc size is positively correlated with SSC (Fig. 2) although there is some scatter particularly at higher SSCs. No clear relationship between median floc size and ϵ could

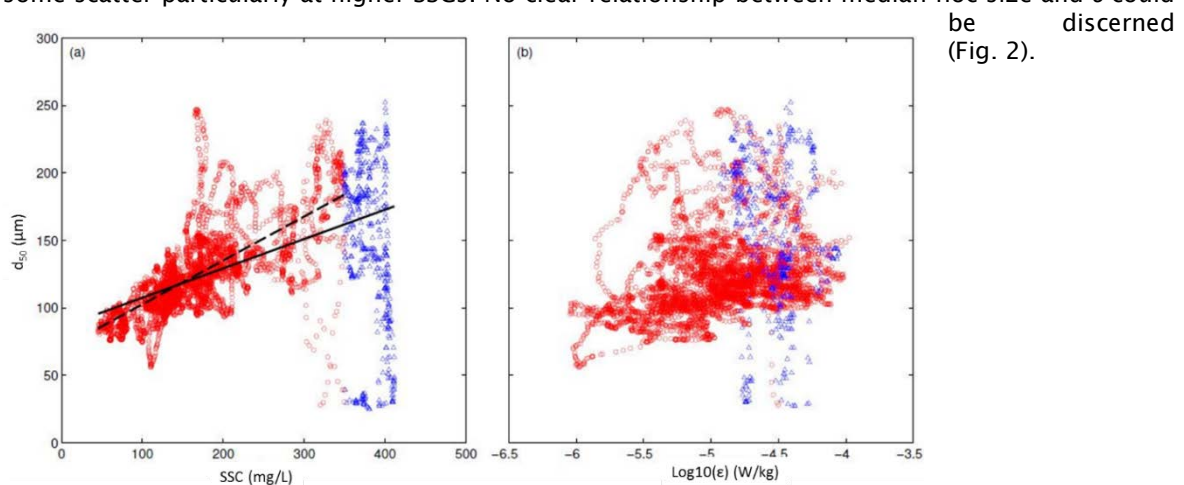


Fig. 2. Median floc sizes d_{50} versus (a) SSC and (b) ϵ .

References

- Braithwaite K.M., D.G. Bowers, W.A.M. Nimmo Smith and G.W. Graham 2012. Controls on floc growth in an energetic tidal channel. *J. Geophys. Res.* 117(C2):C02024.
- Wiles P.J., T.P. Rippeth, J.H. Simpson and P.J. Hendricks 2006. A novel technique for measuring the rate of turbulent dissipation in the marine environment. *Geophys. Res. Lett.* 33(21):L21608.
- Winterwerp J.C. 1998. A simple model for turbulence induced flocculation of cohesive sediment. *Journal of Hydraulic Research* 36(3):309-326.

Quantifying and comparing settling velocity within the San Francisco Bay-Delta Estuary, northern California, USA

Manning Andrew J.^{1,2,3} and David H. Schoellhamer⁴

¹ HR Wallingford, Howbery Park, Wallingford, Oxfordshire, OX10 8BA, UK

² Department of Geography, Environment and Earth Sciences, University of Hull, Kingston Upon Hull, Humberside, HU6 7RX, UK

³ School of Marine Science and Engineering, Plymouth University, Drake Circus, Plymouth, Devon, PL4 8AA, UK
E-mails: andymanning@yahoo.com; a.manning@hrwallingford.com

⁴ United States Geological Survey, Placer Hall, 6000 J Street, Sacramento, CA 95819, USA

The San Francisco Bay-Delta Estuary (Bay-Delta) has a long history with sediment transport and flocculation research, dating back to the classic work of H.A. Einstein, R.B. Krone and E. Partheniades (e.g. Einstein, 1941; Einstein and Krone, 1962; Krone, 1962; Partheniades, 1962; Krone, 1963). The Estuary comprises two distinct regions: San Francisco Bay (SFB) and the Sacramento–San Joaquin River Delta (Delta). The inland Delta region is where the rivers of the Central Valley of California merge to become the San Francisco Estuary. Importantly the rivers deliver fine sediment from the Central Valley watersheds to the Delta. Deposited sediment helps create and sustain the landscape in the Sacramento–San Joaquin River Delta (Delta), including desirable habitats such as tidal marsh, shoals, and floodplains. A key management question is whether the existing Delta landscape can be sustained as sea level rises. The erosion and deposition processes are strongly dependent on the local sediment properties, particularly when cohesion and flocculation are important, as they are in the Delta. Thus, it is important to make local, *in-situ* measurements of erosion rates and settling velocities in order to guide parameterization of a numerical model.

The US Geological Survey collects data that supports the development, calibration, and validation of numerical models of sediment transport and turbidity in the Bay-Delta system. Research questions include: How much flocculation of sediment particles occurs in the Bay-Delta, and what are the settling velocities of the flocs? How do floc settling properties vary spatially and temporally? To address these questions, a Co-operative Agreement was established between the USGS and HR Wallingford (UK).

This abstract presents measurements of floc depositional properties throughout the Bay-Delta during 2008-2011. The floc data were acquired using the INSSEV-LF: IN-Situ Settling Velocity instrument. The LF (LabSFLOC) version of INSSEV is a hybrid system which combines two key components: i) the low intrusive LabSFLOC (version 1) system (a high resolution video-based device to measure the individual floc properties; ii) an *in-situ* estuarine floc sampling acquisition unit (to initially obtain the suspension sample). For the latter, a 2.2L Van Dorn horizontal sampling tube with a 14kg torpedo-shaped weight suspended from the underside of the tube was used to collect a water sample nominally 0.7m above the estuary bed. Manning *et al.*, (2010) provide further details of these floc acquisition procedures. The LabSFLOC– Laboratory Spectral Flocculation Characteristics – instrument (Manning, 2006) was set-up in the various research vessels.

Thirty-one floc population samples were obtained from 21 sites within the Delta, with a similar number of floc samples (30) collected throughout SFB (Manning and Schoellhamer, 2013). Flocculated particles were observed throughout the Delta, including in freshwater. Suspended-sediment concentrations (SSC) in the near-bed region ranged from 4-52mg.l⁻¹ in the Delta, rising to 230mg.l⁻¹ in SFB (South Bay). A combined total of more than 2,200 individual flocs were measured in the Delta, with double the number of flocs observed in the SFB populations. In the Delta, floc sizes (D) ranged from 27µm microflocs (D < 160µm) to macroflocs of 500µm, with flocs 639µm in diameter observed in SFB. Settling velocities (Ws) ranged between 0.04mm.s⁻¹ to 15.8mm.s⁻¹ during a longitudinal transect of SFB. Within the Delta, Macrofloc settling velocities (Ws) were 0.7-5mm.s⁻¹ (mean 2.25mm.s⁻¹) and macroflocs comprised 1-56% (mean 24%) of the suspended mass. Microfloc Ws was smaller (0.3-4.0mm.s⁻¹, mean 1.63mm.s⁻¹), but comprised more (44-99%, mean 76%) of the suspended mass and thus, mass settling fluxes (spanning 0.1-80mg.m⁻²s⁻¹) were dominated by microflocs, albeit an order of magnitude less than depositional fluxes within San Francisco Bay. This presentation will indicate how floc population settling velocities and mass distributions vary throughout the Bay-Delta, and identify characteristic floc dynamical properties and structural composition, at key locations within both SFB and the Delta. The depositional mass settling fluxes

spanned three orders of magnitude, ranging from 4-767mg.m²s⁻¹ in the Bay-Delta. The composition of individual floc population's mass settling flux (MSF in terms of Ws and SSC combinations) will be examined, as will the spatial patterns of the MSF, and findings will be linked to both a new Delta conceptual model for sediment transport and to Ws parameterisations commonly used in numerical sediment transport modelling.

References

- Einstein H.A. 1941. The viscosity of highly concentrated underflows and its influence on mixing. Transactions, American Geophysical Union 22(3):597-603 (Hydrology).
- Einstein H.A. and R.B. Krone. 1962. Experiments to determine modes of cohesive sediment transport in salt water. Journal of Geophysical Research 67(4):1451-1461.
- Gilbert G.K. 1917. Hydraulic-mining debris in the Sierra Nevada. Washington, DC: US Geological Survey Professional Paper 105. 154 p. Available from: <http://pubs.er.usgs.gov/publication/pp105>.
- Krone R.B. 1962. Flume studies of the transport of sediment in estuarial shoaling process: final report. Hydraulic Engineering Laboratory and Sanitary Engineering Research Laboratory, University of California, Berkeley, California. 110p.
- Krone R.B. 1963. A study of rheological properties of estuarial sediments. Report 63-68. Hyd. Eng. Lab. and Sanitary Eng. Lab., University of California, Berkeley.
- Manning A.J. 2006. LabSFLOC - A laboratory system to determine the spectral characteristics of flocculating cohesive sediments. HR Wallingford Technical Report, TR 156.
- Manning A.J. and D.H. Schoellhamer. 2013. Factors controlling floc settling velocity along a longitudinal estuarine transect. Marine Geology 345:266-280.
- Manning A.J., D.H. Schoellhamer, A.J. Mehta, D. Nover and S.G. Schladow. 2010. Video measurements of flocculated sediment in lakes and estuaries in the USA. Proceedings of the Joint Federal Interagency Conference on Sedimentation and Hydrologic Modeling, Riviera Hotel, Las Vegas, Nevada, USA, 27th June-1st July 2010.

Fluid mud transport from Patos Lagoon to Rio Grande Port, RS, Brazil

Marroig Patrícia and Susana Vinzon

Oceanic Engineering Program, Federal University of Rio de Janeiro (UFRJ), Rio de Janeiro, RJ, Brazil
E-mail: pmarroig@oceanica.ufrj.br; susana@oceanica.ufrj.br

Fluid mud is frequently observed in navigational channels. This work aims to contribute to the understanding of the source and transport of fine sediments in the Patos Lagoon system, which may contribute to the silting of Rio Grande Port, southern Brazil. The Patos lagoon receives the contribution of flow and sediments of continental source, which are storage in this large and shallow fresh water body, according to previous studies. On the other hand, huge amounts of fine sediments are dredged annually in the Port channels and basins, which are located in an estuarine portion of the system. This study aims the characterization and mapping of the muddy areas, in the transition from the Lagoon to the mouth, and the main hydrodynamic characteristics of the System. Measurements with OBS, DensiTune, ADCP, AQUADOPP and sampling were carried out in order to obtain the characteristics of the sediment, and the local hydrodynamic in a single campaign. The driving forces responsible for the exchanging of sediments between those two compartments were addressed with the help of a 3D hydrodynamic model.

Keywords

Fluid mud; Patos Lagoon; Port of Rio Grande.

Introduction

The Patos Lagoon system, located in the southern part of Brazil, receives contributions from a continental drainage basin of about 200,000km², with approximately 4.5 million tonnes of suspended particulate matter forming layers of fluid mud in the Lagoon (Hartmann and Schettini, 1996). Baisch (1998) found that only 25% of the total sediment that arrive in the lagoon reach the estuary, the remaining being deposited in the lagoon, where the coarse sediment will be found in the shallow areas exposed to wave action, while silt and clay prevail in the deep channels and in the protected areas from wave action (Toldo *et al.*, 2007). Fluid mud is a high concentration aqueous of well-mixed flocculated suspension of fine-grained sediment. It is frequently related with a sudden change in sediment concentration with depth (luteocline), and typically occurs in near-bottom layers in lakes and estuaries, but also in places that receive plenty fine-sediment supply and have periods of low intensity flow (Wells and Coleman, 1981; Metha *et al.*, 2014). This study presents a first characterization of the bottom composition in the transition from the lagoon to the estuary (Fig. 1). The hydrodynamics of the system is mainly governed by the wind, which is responsible by the set-up and set-down. Vinzon *et al.* (2009) observed that the remote wind have the most influence in the water exchange through the Lagoon's mouth. For example the local NE wind will cause a set-up inside the Lagoon towards the entrance, whereas the NE remote wind will cause a set-down on the Shelf near the Lagoon's mouth by Ekman dynamics. In order to assess the main driven mechanisms which may carry the fine sediments from the lagoon to the navigation channels, a 3D hydrodynamic model was set up and compared with measured data.

Field survey

One survey was conducted in February 2014 aboard R/V Larus to evaluate mud in Patos Lagoon. Profiles of density, suspended sediment concentration, salinity and currents were measured, and bottom sediment samples were collected to determine sediment rheology, shear strength, and grain size, including a box-core. Fig. 1. shows the location of the samplings.

Results and discussion

The distribution of bottom sediments in Patos Lagoon follows the energy gradients and bathymetry, with presence of mud on deeper central regions, and sand banks in the margins. From the analysis of the bottom sediment it was observed that the points are mainly composed by silt (mean of 78%) and clay (mean of 16%), while 3 sampling locations showed a higher percentage of fine sand: 1a, 7a and 9c (91%, 10% and 11%) as shown in Fig. 6. Fig. 2 shows an example of the density profiles, indicating the existence of mud layers, with luteocline height varying from 0.1 to 0.5m. The mean current velocity observed during the period of data collection was 0.4m.s⁻¹, with a maximum of ~1.5m.s⁻¹. The hydrodynamic model was calibrated with a series of 5 months of water levels. Using this tool, and during this period, the series of occurred meteorological events were tested assessing the importance of them for the transport of fine sediments from the Lagoon to the estuarine area.

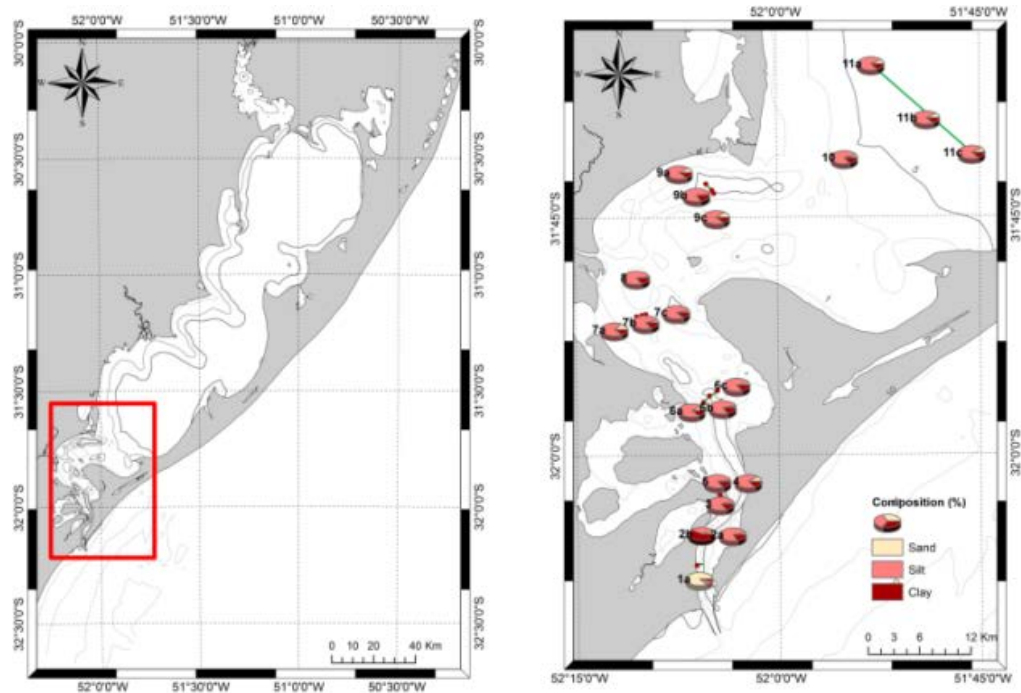


Fig. 6. Patos lagoon and estuary. Port of Rio Grande is located at the entrance, in the estuarine portion of the system. Right panel: % of sand, silt and clay of bottom sediments at sampling points.

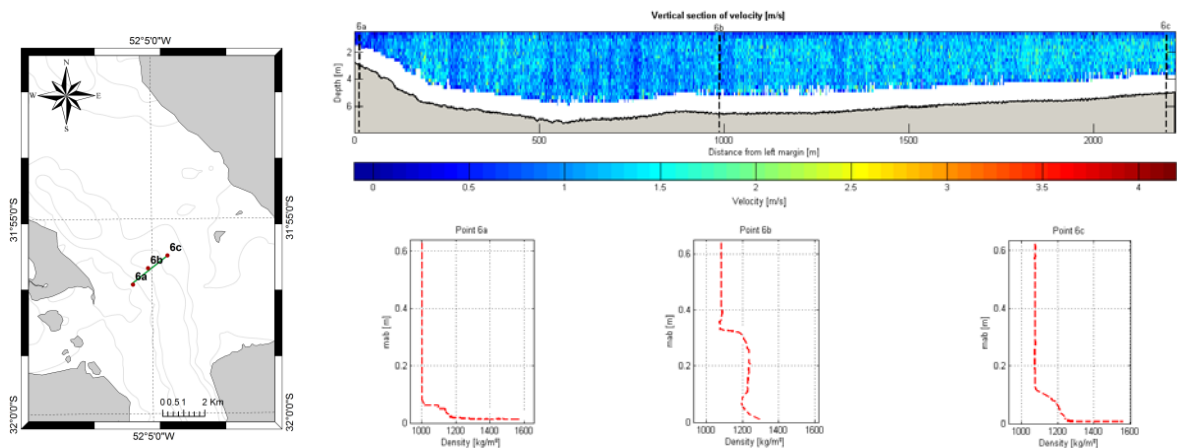


Fig. 7. Vertical section of velocity (m/s), in the transect 6 (left map and also Fig. 1.). During the survey, the velocity direction was leaving the Patos Lagoon. The lines represent the locations of the observed profiles using Densitune, which are depicted below.

References

- Baisch P.R. and J.C. Wasserman. 1998. Chemistry and distribution of trace elements in the Patos Lagoon, South Brazil. p.97-126. In: Environmental geochemistry in the tropics. Springer Berlin Heidelberg.
- Calliari I., N.S. Sperranski, M. Torronteguy and M.B. Oliveira. 2000. The mud banks of Cassino beach, southern Brazil: characteristics, processes and effects. Journal of Coastal Research v. ICS 2000 Proceedings: 318-325.
- Hartmann C. and C. Schettini. 1996. Cronologia sobre o estudo do material em suspensão no sistema lagunar Patos - Mirim e plataforma continental adjacente, RS, Brasil. Technical Notes 9:12-20. LOG/DEGEO/FURG.
- Metha A.J, F. Samsami, Y. Khare and C. Smith. 2014. Fluid mud properties in nautical depth estimation. Journal Waterway, Port. Coastal, Ocean Eng. 140(2):210-222.
- Toldo Jr. E., S. Dillenburg, I. Corrêa, L. Almeida, J. Weschenfelder and N. Gruber. 2007. Sedimentação de Longo e Curto Período na Lagoa dos Patos, Sul do Brasil. Pesquisas em Geociências 33(2):79-86.

- Vinzon S.B., J.C. Winterwerp, R. Nogueira and G.J. de Boer. 2009. Mud deposit formation on the open coast of the larger Patos Lagoon Cassino beach system. *Continental Shelf Research* 29:572-588.
- Wells J.T. and J.M. Coleman. 1981. Physical processes and fine-grained sediment dynamics, coast of Surinam, South America. *Journal of Sedimentary Research* 51(4):1053-1068.

Small diameter limit of cohesionless particle erosion

Mehta Ashish J.

Nutech Consultants, Inc., Gainesville, FL 32606, USA
 E-mail: mehta@coastal.ufl.edu

The critical shear stress for erosion of sand by water-current or waves is commonly obtained from the Shields diagram, and in recent decades the so-called extended Shields diagram (ESD) has been used for the critical stress of finer cohesionless particles (Garcia, 2008). Presently, in mathematical modeling of waters containing both cohesionless and cohesive particles, the lower diameter limit of ESD is commonly taken as a somewhat arbitrary input parameter. As the diameter of the roughly spherical particles decreases below about $15\mu\text{m}$, their flatness represented by the specific surface area increases, along with a concurrent increase in the ratio of the surface force of attraction to particle buoyant weight. At about $1\mu\text{m}$ this ratio is orders of magnitude larger than that at $15\mu\text{m}$, and results in the formation of cohesive microflocs ($d < 100\mu\text{m}$) and/or macroflocs ($d \geq 100\mu\text{m}$) depending on the flow shear rate (Winterwerp and van Kesteren, 2004).

The transition from cohesionless to cohesive particle behavior occurs notionally at a single diameter d_{sc} of about $10\mu\text{m}$. A recent analysis (Mehta and Letter, 2013) suggests that the variation of the critical shear stress of cohesive flocs with particle/floc diameter is useful for deriving a formula for d_{sc} . Above d_{sc} , ESD is a valid representation of cohesionless critical shear stress, whereas below d_{sc} the critical shear stress of cohesive sediment is obtained.

Zones representing cohesionless and cohesive critical shear stress are more conveniently described by the variation of the critical shear stress with diameter d in lieu of ESD, when all cohesionless particles have the same material density. This paper is concerned with the development of such a description, shown in Fig. 1, in which the cohesionless data are limited to quartz and silica particles. Diameters d_1 and d_2 indicate the junctions of segments of the power-law equations (not given) used to approximate the mean trends of cohesionless and cohesive critical shear stresses. The transition diameter d_{sc} makes it convenient to identify diameter ranges of cohesionless particles, dispersed (deflocculated) cohesive particles, microflocs and macroflocs.

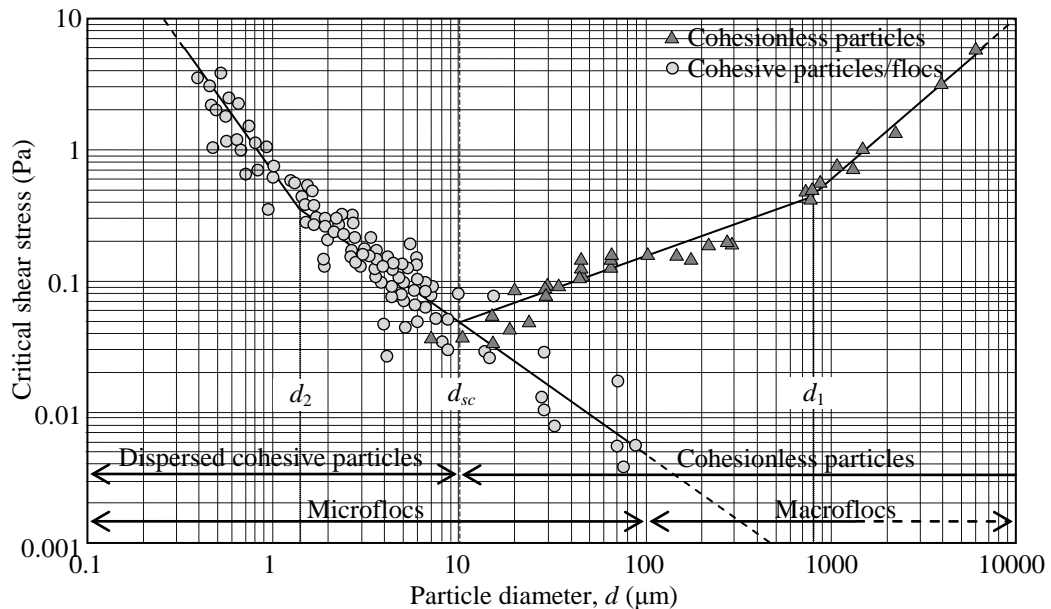


Fig. 1. Transition diameter d_{sc} defined with respect to cohesionless and cohesive sediment particles and critical shear stress for erosion.

References

- Garcia M.H. (Ed.). 2008. Sedimentation engineering: processes, measurements, modeling and practice. American Society of Civil Engineers, Reston, VA. xv+1132p.
- Mehta A.J. and J.V. Letter, jr. 2013. Comments on the transition between cohesive and cohesionless sediment bed exchange. Estuarine, Coastal and Shelf Science 131:319-324.
- Winterwerp J.C. and W.G.M. van Kesteren. 2004. Introduction to the physics of cohesive sediment in the marine environment. Elsevier, Amsterdam. xiii+466p+app.

Physical impacts induced by bottom trawling in the ‘Grande-Vasière’ area (Bay of Biscay)

Mengual Baptiste¹, Florence Cayocca¹, Pierre Le Hir¹, Thierry Garlan² and Pascal Laffargue³

¹ IFREMER, DYNECO/PHYSED, ZI pointe du Diable, CS10070, Plouzané, France
E-mail: <mailto:Baptiste.Mengual@ifremer.fr>

² SHOM, Hydrographic Center, PO Box 146, F-29280, Brest, France

³ IFREMER, EMH, Rue de l'île d'Yeu, PO Box 21105, 44311 Nantes Cedex 03, France

Introduction

Bottom trawling in coastal environments is known to modify the upper sedimentary characteristics and to generate significant local resuspension. The impacts intensity depends on the nature of the substratum (more significant for fine sediment such as mud), the weight of the gear components, the trawl towing velocity, and the local hydrodynamic conditions (Jones, 1992). Some gear components such as doors or footropes can penetrate deep in the surficial sediment (from a few centimetres to a few tens of centimetres; Linnane *et al.*, 2000) and can generate significant local resuspension. Only a few percents of the reworked sediment are really injected into the water column as suspended sediments (Durrieu de Madron *et al.*, 2005). This sediment resuspension is mainly due to doors impact (about 70% to 80% of the total mass resuspended; O'Neill and Summerbell, 2011). This process results in the formation of a turbid plume in the trawl wake. The typical plume vertical height corresponds to 2 to 3 times the vertical opening of the net (Main and Sangster, 1981; Durrieu de Madron *et al.*, 2005) and the resulting near bottom suspended sediment concentrations can reach several hundreds of milligrams per litre (e.g. Durrieu de Madron *et al.*, 2005; Dellapenna *et al.*, 2006; Martin *et al.*, 2013). Palanques *et al.* (2014) showed that the suspended sediment concentration in a trawled area is about three times higher than in a protected area. Concerning bottom impacts, the surficial sediment reworking due to bottom trawling leads to the modification of the sediment properties in terms of grain size, silt content and organic content, which all increase upwards in the upper part (20cm) of the surficial sediment layer (Dellapenna *et al.*, 2006; Palanques *et al.*, 2014). Besides, trawl marks can persist from several months for up to one year for a fine sediment substratum (Palanques *et al.*, 2014; Linnane *et al.*, 2000). The ‘Grande-Vasière’ (G-V) area (about 8000km²) is subjected to deposition and remobilization cycles controlled by river discharges, tidal currents, storms and anthropic factors in particular bottom trawling. The balance between these deposition and erosion factors controls its temporal evolution. Bourillet *et al.* (2006) have proposed a first estimation for the contribution of each factor to the G-V evolution. They suggested that the trawling-induced fine particle remobilization represents about 10% to 30% of the storm-induced erosion. However, this estimation was based on several hypotheses required in order to make up for the lack of quantitative *in situ* measurements. This underlines the necessity of quantifying the physical processes so as to verify these first conclusions and to characterize the local mass of sediment resuspended by bottom trawls.

Methodology and results

This study is based on two field experiments investigating two separate zones and testing two types of trawl (classical versus less damaging one). The two zones differ by the nature of the bottom sediment, with different mud contents (from 25% to 75% respectively). The first set of experiments investigated the typical trawl used by the regional common fleet whereas the last experiments investigated an alternative trawl configuration characterized by an innovative technology for the doors (‘Jumper’). These doors don't have a permanent contact with the seabed, which makes them potentially less damaging for the benthic environment. Measurements located in the water column followed a similar strategy as proposed by Durrieu de Madron *et al.*, (2005) with Conductivity Temperature Depth sensors, turbidity sensors, and a high frequency Acoustic Doppler Current Profiler. Different sensors were also directly fixed to the most impacting parts of the trawl, thus permitting to quantify the turbidity generated just behind the trawl. Finally, bottom impacts were observed in terms of penetration of the different parts of the net thanks to high definition video cameras and laser systems, and the surficial reworking thanks to interface cores.

These experiments allowed quantifying the local resuspension and the surficial sedimentary modifications generated in the trawl wake. Results show a turbid plume 3 to 4 metres high, concentrated very near of the seabed. This observation is consistent with the vertical opening of the net of approximately one metre. Temporal variability of local concentration profiles near the seabed has permitted to estimate the particles settling velocity in the two different zones. Furthermore, the turbid plume transversal dispersion and its turbidity gradients in the trawl wake have been estimated, including just behind the trawl. Turbidity measurements revealed values about 4 times

higher behind the doors than in the clump wake, which confirms the importance of their impact. Sea experiments have also permitted to observe and quantify the trawl furrow depth and the reworking of the surficial sediment layer induced by bottom trawling. The links between furrow volumes and the local quantity of sediment injected in the water column are also investigated.

Conclusions

This study allowed quantifying physical processes induced by bottom trawling in an intensely trawled area of the Bay of Biscay. It also assesses the added value of innovative technologies of doors regarding environmental impacts. The investigation of the turbid plume dynamics during sea trials has permitted to evaluate its three-dimensional behaviour in the trawl wake and the deposition fluxes. These *in situ* measurements allow to better understand the different physical processes at stake and to accurately calibrate a future model. Indeed, this work will be used as the basis of a modelling approach integrated in a pre-existent hydro-sedimentary model so as to quantify the influence of bottom trawling at a regional scale and for long periods.

Acknowledgments

This study was supported by the SHOM (Service Hydrographique et Océanographique de la Marine) and IFREMER (Institut Français de Recherche pour l'Exploitation de la Mer). Sea trials were funded by the BENTHIS project.

References

- Bourillet J.F., J.M. Jouanneau, C. Macher, P. Le Hir and F. Naughton. 2006. 'La Grande Vasière' mid-shelf mud belt: Holocene sedimentary structure, natural and anthropogenic impacts. X International Symposium on Oceanography of the Bay of Biscay, April 19-21 2006. Vigo, Galicia. Spain. <http://archimer.ifremer.fr/doc/00000/6243/>
- Dellapenna T.M., M.A. Allison, G.A. Gill, R.D. Lehman and K.W. Warnken 2006. The impact of shrimp trawling and associated sediment resuspension in mud dominated, shallow estuaries. *Estuarine, Coastal and Shelf Science*, 69 (3-4), 519-530.
- Durrieu de Madron X., B. Ferré, G. Le Corre, C. Grenz, P. Conan, M. Pujo-Pay, R. Buscail and O. Bodiot. 2005. Trawling-induced resuspension and dispersal of muddy sediments and dissolved elements in the Gulf of Lion (NW Mediterranean). *Continental Shelf Research* 25:2387-2409.
- Jones J.B. 1992. Environmental impact of trawling on the seabed: a review. *New Zealand Journal of Marine and Freshwater Research* 26:59-67.
- Linnane A., B. Ball, B. Munday, B.V. Marlen, M. Bergman and R. Fonteyne. 2000. A review of potential techniques to reduce the environmental impact of demersal trawls. *Irish Fisheries Investigations (New Series)* 7:39.
- Main J. and G.L. Sangster. 1981. A study of sand clouds produced by trawl boards and their possible effect on fish capture. *Scottish fisheries Research Report no 20*. Dept of Agriculture and Fisheries for Scotland, 19.
- Martín J., P. Puig, A. Palanques and M. Ribó 2013. Trawling-induced daily sediment resuspension in the flank of a Mediterranean submarine canyon. *Deep-Sea Research II*. <http://dx.doi.org/10.1016/j.dsr2.2013.05.036>.
- O'Neill F.G. and K. Summerbell. 2011. The mobilisation of sediment by demersal otter trawls. *Marine Pollution Bulletin* 62:1088-1097.
- Palanques A., P. Puig, J. Guillén, M. Demestre and J. Martín. 2014. Effects of bottom trawling on the Ebro continental shelf sedimentary system (NW Mediterranean). *Continental Shelf Research* 72:83-98.

Resuspension and sediment bed oxygen consumption: developing and testing a coupled model

Moriarty Julia¹, Courtney Harris¹, Christophe Rabouille² and Flora Toussaint²

¹ the College of William & Mary, Virginia Institute of Marine Science
PO Box 1346 Gloucester Point, Virginia 23062, USA
E-mail: moriarty@vims.edu

² Laboratoire des Sciences du Climat et de l'Environnement, CEA-CNRS-UVSQ, Bât. 12, Avenue de la Terrasse, F-91198 Gif-sur-Yvette Cedex, France

Sediment resuspension in coastal environments is classically seen as a process which entrains deposited organic material and porewater into the overlying water. The alteration of sediment diagenesis due to this transfer is largely understudied. Models representing water column oxygen budgets have usually relied on simplifying assumptions for sediment oxygen demand such as instant remineralization of detritus at the seabed. Model estimates of oxygen concentrations in the Gulf of Mexico, however, have been shown to be very sensitive to parameterizations of sediment oxygen demand. Meanwhile, diagenetic models tend to calculate sediment oxygen demand under an assumption of steady accumulation of organic matter and sediment. Though most diagenetic models neglect resuspension, observations from the Rhone River subaqueous delta indicate that oxygen fluxes increased during resuspension events. To the best of our knowledge, however, no model exists that directly couples diagenetic processes, water column biogeochemistry, and sediment erosion and deposition, and therefore tools for comparing the significance of these processes are lacking.

To evaluate the role of resuspension on sediment oxygen consumption, we implemented a version of the Regional Ocean Modelling System (ROMS) that couples hydrodynamic, sediment transport, and biogeochemical processes. To link the resuspension and biogeochemical modules, a diagenetic model was added to the seabed (Fig. 1). Here, we present a one-dimensional (vertical) version of the coupled model and apply it to the Rhone River subaqueous delta. Preliminary results indicate that resuspension of organic material and reduced porewater constituents produce pulses of oxygen consumption and increase overall sediment oxygen demand.

Model description

The coupled model was developed within the ROMS hydrodynamic model (Haidvogel *et al.*, 2000) and utilized the Community Sediment Transport Modeling System (CSTMS; Warner *et al.*, 2008) and a water column NPZD (nutrient-phytoplankton-zooplankton-detritus) biogeochemical module (Fennel *et al.*, 2006) because this framework is community-based and well-utilized. This study adapted the ROMS-CSTMS-Fennel model by coupling it to a diagenetic model based on Soetaert *et al.* (1996). We also adapted the ROMS-CSTMS seabed layering scheme to resolve millimetre scale features near the seabed surface while maintaining computational efficiency.

This coupled model accounts for processes including diffusive vertical mixing, resuspension, deposition, and burial of particles and dissolved species. Detrital material, created by the water column biogeochemical model, becomes associated and transported with suspended sediment classes, undergoing advection, diffusion, deposition, and erosion. Dissolved constituents (O_2 , NO_3^- , NH_4^+ , etc.) from the biogeochemical model may be exchanged with the seabed through deposition, erosion, and diffusion across the sediment - water interface. Seabed organic material and porewater constituents are subject to diagenetic processes including aerobic, nitrate and anoxic mineralization, and biodiffusion may mix sediment, organic material, and porewater in the seabed.

Implementation for the Rhone River sub-aqueous delta and future work

This coupled one-dimensional vertical model is being implemented for a high-depositional, organic-rich, sub-aqueous delta offshore of the Rhone River (Fig. 2). Model results are being validated using a time series of water column and seabed oxygen profiles described in Toussaint *et al.* (2014). These observations were collected from an *in-situ* benthic station and indicate that increased oxygen consumption in the seabed by a factor of 3 occurs during wave resuspension events compared to quiescent periods. Preliminary results indicate that resuspension events increase oxygen consumption by re-introducing organic matter and reduced porewater species into the water column. Resuspension also erodes the more oxygenated surface sediment from the seabed, exposing the typically-anoxic subsurface to oxygen. Ongoing work includes evaluating the response of seabed-water column fluxes to resuspension events (e.g., frequency and duration), and to less-constrained model parameters (e.g. diffusion and remineralization rates).

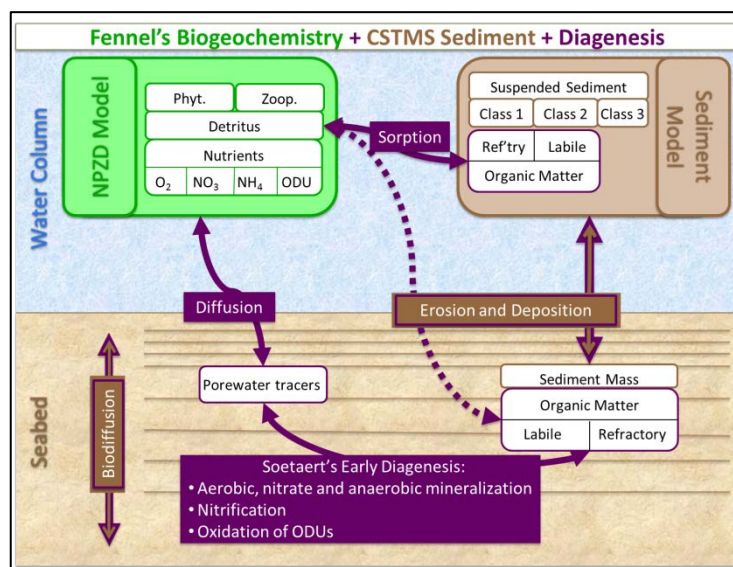


Fig. 1. Schematic illustrating links between the diagenetic, biogeochemistry, and sediment transport modules. Green, brown, and purple outlines indicate for which module (biogeochemistry, sediment transport, and/or the diagenetic model) the process or variable is used. White boxes indicate variables, and coloured boxes indicate processes.

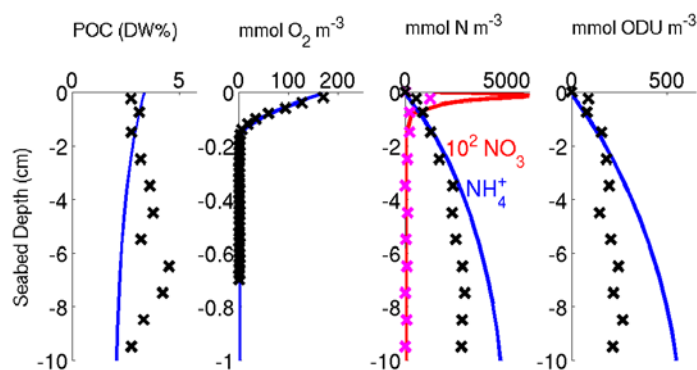


Fig. 2. Profiles of (a) particulate organic material (dry weight, DW), (b) oxygen, (c) nitrate and ammonium, and (d) oxygen demand units (ODUs) for the Rhone River shelf. Lines are preliminary results from a model that neglected resuspension; 'X' shows observations from Pastor *et al.* (2011).

References

- Fennel K., J. Wilkin, J. Levin, J. Moisan, J. O'Reilly and D. Haidvogel. 2006. Nitrogen cycling in the Middle Atlantic Bight: results from a three-dimensional model and implications for the North Atlantic nitrogen budget. *Global Biogeochemical Cycles* 20(3):GB3007.
- Haidvogel D., H. Arango, K. Hedstrom, A. Beckmann, P. Malanotte-Rizzoli and A. Shchepetkin. 2000. Model evaluation experiments in the North Atlantic basin: simulations in nonlinear terrain-following coordinates. *Dynamics of Atmospheres and Oceans* 32(3-4):239-281.
- Pastor L., C. Cathalot, B. Deflandre, E. Viollier, F.J.R. Meysman, C. Ulses, E. Metzger and C. Rabouille. 2011. Modelling biogeochemical processes in sediments from the Rhone River prodelta area (NW Mediterranean Sea). *Biogeosciences* 8:1351-1366.
- Soetaert K., P. Herman and J. Middelburg. 1996. A model of early diagenetic processes from the shelf to abyssal depths. *Geochimica et Cosmochimica Acta* 60(6):1019-1040.
- Toussaint F., C. Rabouille, C. Cathalot, B. Bombled, A. Abchiche, O. Aouji, G. Buchholtz, A. Clemencon, N. Geyskens, M. Repecaud, I. Pairaud, R. Verney and N. Tisnerat-Laborde. 2014. A new device to follow temporal variations of oxygen demand in deltaic sediments: the LSCE benthic station. *Limnology and Oceanography: Methods*. Accepted.
- Warner J., C.R. Sherwood, C.K. Harris and H. Arango. 2008. Development of a three-dimensional, regional, coupled wave, current, and sediment-transport model. *Comput. Geosci.* 34:1284-1306.

Yield strength determination from slump tests

Mosquera Rodrigo and Francisco Pedocchi

Facultad de Ingeniería, Universidad de la República, CP 11300, J. Herrera y Reissig 565,
Montevideo, Uruguay
E-mail: rmosquer@fing.edu.uy

In this work measurements of the final slump geometry are used to obtain accurate determinations of mud yield strength. The final profile of the mud deposit is captured using photography, and theoretical expressions are adjusted to the profile. Simultaneous measurements of mud yield strength using the proposed technique and a conventional vane rheometer showed very good agreement. Possible advantages of the proposed technique are presented and discussed.

Introduction

The slump test consists of filling a bottomless container resting on a horizontal plane, and lifting the container allowing the material to slump over the surface. The final shape of the deposit is then used to characterize certain rheological properties of the material. For example, the slump test is routinely done for fresh concrete quality control (ASTM, 2003); in this case, a standardized truncated cone without top or bottom is used. Similar tests are applied for quality control and sample comparison in the mining, food, and pharmaceutical industry.

The yield strength can be determined using conventional rheological equipment such as a cone or vane rheometer. However, these rheometers present limitations when used with highly heterogeneous materials (mixes of mud and gravel or shells, for example). Furthermore, rheometers are in general delicate pieces of equipment, which are not easy to carry into the field. The slump test based technique presented here may be useful for these particular conditions.

Theory

The material response to external forcing is determined by a constitutive equation that relates stresses with deformations and their rate. For example for a visco-elastic material, when a small shear stress τ is applied an elastic response of the material may be observed. However, when the shear stress overpasses a certain threshold, the material may respond as a viscous fluid. Similarly the material flow would stop if the shear stresses get below a certain threshold. Here these two thresholds are considered to be equal and are defined as the yield strength of the material (τ_y). When τ is equal to τ_y , the material is said to be on 'failure state'.

Murata (1984) proposed the use of the slump test to estimate τ_y . The comparison of slump results from different materials and moulds is not easy to achieve. Some researchers (Roussel and Coussot, 2005; Balmforth *et al.*, 2006; Dubash *et al.*, 2009;) studied the dynamics of the movement and determined correlations among the deposit final shape, the material density ρ , and the yield strength τ_y .

Near the end of the slump test, the accelerations of the material are very small and the quasi-equilibrium approximation may be applied. Assuming that the material is incompressible, that the solid plane over which the material flows is a slip plane, that a rotational symmetry solution exists, and that the material is at 'failure state' at every point, the shape of the deposit can be computed. Roussel and Coussot (2005) presented two asymptotic solutions, for when the slump height H is much larger/smaller than the slump radius R . On the other hand Dubash *et al.* (2009) used perturbation analysis to obtain an analytical expression for the final profile. The first order approximation of the profile is given by the following expression

$$h(r)^2 = \frac{2\tau_y}{\rho g}(R - r), \quad (1)$$

where h is the height of the profile, g is the acceleration of gravity, and r is a radial coordinate. The small quantities H/R and $\tau_y/\rho g H$ are assumed to be of the same order and are used as a single perturbation parameter in order to obtain higher order approximations to the solution.

Methodology and experiments

Restricting the analysis to zones where the final shape solution is applicable ($r \gg h$), and excluding problematic regions (the centre of the 'cake' and the nose of the profile), it is possible to fit the observed geometry with the proposed theoretical profile given by Equation (1). This fitting allows to determine the ratio between τ_y and ρ .

In order to obtain high resolution measurements of the final profile, the deposit was sliced over radials planes with a pre-wetted metallic plate, and the slump profile was captured using a 12.1 Megapixel digital camera (Panasonic Lumix DMC-ZR1). The images were rectified, and the profiles digitalized. A least squares fit of Equation (1) to the data was performed, determining τ_y/ρ , and once ρ was independently determined, τ_y was computed (Fig. 1). Several simultaneous yield strength measurements were performed using the proposed technique and a vane rheometer (Brookfield DV-III Ultra). Fig. 2 shows the obtained results for China clay.



Fig. 8. Photo of the slump test used to measure the final profile, original (left) and after rectification (right). On the far right a digitalized profile (o) and its least square fit (solid line) is shown over the selected zone (between the vertical dashed lines).

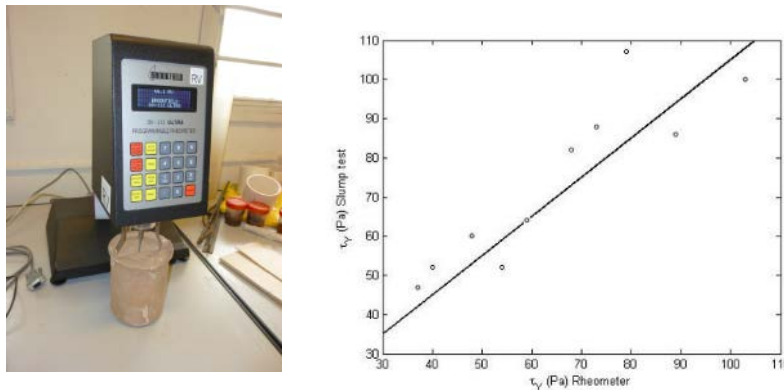


Fig. 9. On the left a photo of the rheometer is shown. On the right the comparison of both determinations of yield strength τ_y .

Conclusions

The proposed technique is simple and could be used in the field to determine the yield strength *in situ*. The technique can be applied to non-homogenous materials, where the analysis of a large sample is needed in order to obtain a global measurement. The yield strength values determined using the proposed technique compared very well with the ones determined using a vane rheometer. The use of the deposit profile, instead of global dimensions like the total slump and/or the maximum radius, gives more accurate results and it is not affected by the roughness of the slip plane.

References

- ASTM. 2003. WK27311 - New test method for measurement of cement paste consistency using a mini-slump cone. American Society for Testing and Materials, West Conshohocken, PA.
- Balmforth N.J., R.V. Craster, A.C. Rust and R. Sassi. 2006. Viscoplastic flow over an inclined surface. *Journal of Non-Newtonian Fluid Mechanics* 139:103-127.
- Dubash N., N.J. Balmforth, A.C. Slim and S. Cochard. 2009. What is the final shape of a viscoplastic slump. *Journal of Non-Newtonian Fluid Mechanics* 158:91-100.
- Murata J. 1984. Flow and deformation of fresh concrete. *Materials and Structures* 17:117-129.
- Roussel N. and P. Coussot. 2005. Fifty cent rheometer for yield stress measurements: From slump to spreading flow. *Journal of Rheology* 49:705.

Field measurement of fluid mud layer in dredged navigation channel at river mouth

Nakagawa Yasuyuki¹, Takumi Shinozawa², Yuji Matsumoto³ and Michiyuki Watanabe³

¹ Coastal and Estuarine Sediment Dynamics Research Group,
Port and Airport Research Institute, Nagase 3-1-1, Yokosuka, 239-0826, Japan
E-mail: y_nakagawa@ipc.pari.go.jp

² National Institute for Land and Infrastructure Management, Ministry of Land and Infrastructure,
Transport and Tourism, Nagase 3-1-1, Yokosuka, 239-0826, Japan

³ Niigata Port and Airport Office, Hokuriku Regional Development Bureau, Ministry of Land,
Infrastructure, Transport and Tourism, Irihune-cho 4-3778, Chuo-ku, Niigata, 951-8011, Japan

Introduction

Many ports and harbours in the world have been suffering from channel siltation which are crucial topics for the safety navigation of ships (e.g. PIANC, 2008). Mechanisms of the siltation depend on the sediment transport processes around navigation channels governed by several factors, such as sediment types, force conditions (waves and current) and sediment discharge through the river. A better understanding of the process is essential for selecting an effective countermeasure and minimizing siltation.

The aim of this study is to elucidate the siltation process in a navigation channel which is dredged in a river mouth area. This abstract describes results of field survey at a navigation channel under a flood condition with highly turbid water discharge and shows measured fluid mud layers in the dredged channel.

Study site and field measurements

The study site is in the Port of Niigata, which is one of the biggest ports located in the west coast of the Japanese main island (Fig. 1) and the port has been developed around the mouth of the Shinano river, which is the longest one with the total length of 367km in Japan. The channel of the port has been suffering from the siltation by the discharged sediment through the river and maintenance dredging is required around 800,000m³ annually to keep the depth of -5.5 to -11m in the navigation channel and harbour basin.

The field measurement was conducted along the channel, including acoustic sounding, *in-situ* mud density measurement with a tuning fork type densimeter and taking sediment core samples by Scuba-divers. The bathymetry of the site along the channel is shown in Fig. 2 with the data of multi frequency acoustic survey. The downstream area from the Stn.B are deepened by artificial dredging. The surveys were carried out in the summer of 2013 and the several data were taken just under a flood condition with relatively higher turbid water discharge from the upper tributary.

Results and discussions

Measured vertical profiles of salinity and SSC (calibrated from OBS measurements) at Stn.A and Stn.B are shown in Fig. 3. At the upstream points of Stn. A, only fresh water with high turbidity outflow was observed throughout the entire depth. In the dredged downstream area, clear interface can be seen around the depth of 3m from the water surface between the turbid fresh water in the upper and the less turbid sea water in the deeper layer. Another key point in the measured profile at Stn. B is the rapid increase of SSC near the bed. The concentration at the near bottom layer is extremely high such that the optical sensor is saturated. In this near bottom layer at Stn.B, high concentrated mud layer with the bulk density of around 1,200kg/m³ appears, according to *in-situ* density measurement as shown in Fig. 4. This high concentration layer does not appear consistently according to the previous field test during the normal discharge rate condition. It is conceivable that the near bed high concentrated layer could be formed by fluid mud transport from the upstream which is often observed on shelves off river delta (e.g. Fan *et al.*, 2004).

Conclusions

We conducted several field surveys in order to elucidate the siltation mechanism in the navigation channel located at the mouth of the Shinano River. The survey successfully captured the formation of high concentrated mud layer in the deeper dredged channel under the river flood condition with high turbid water discharge. We will also discuss, in the presentation, sediment properties such as particle size and water content obtained from analyses of sediment core samples comparing with the multi frequency soundings and the *in-situ* measured density data.

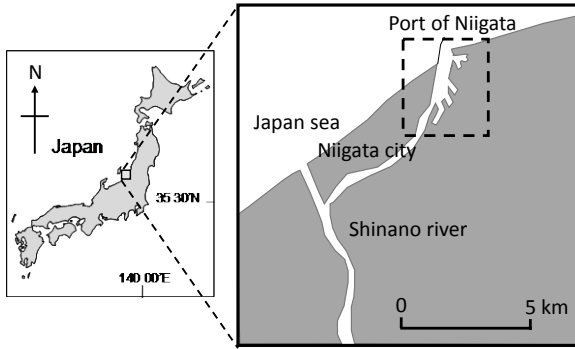


Fig. 1. The location of Port of Niigata (indicated in the dotted box).

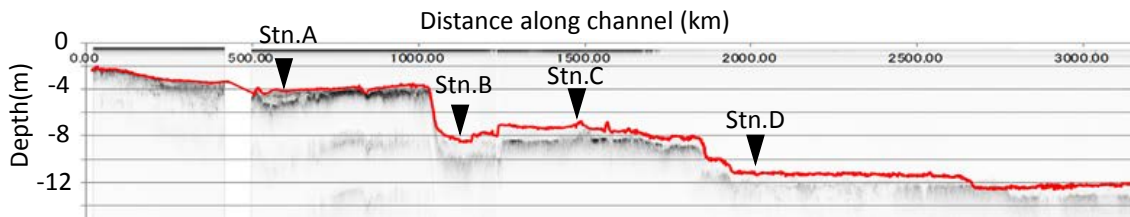


Fig. 2. Bathymetry and sub-bottom data along the channel. The triangles indicate the locations for *in-situ* measurements and core samplings.

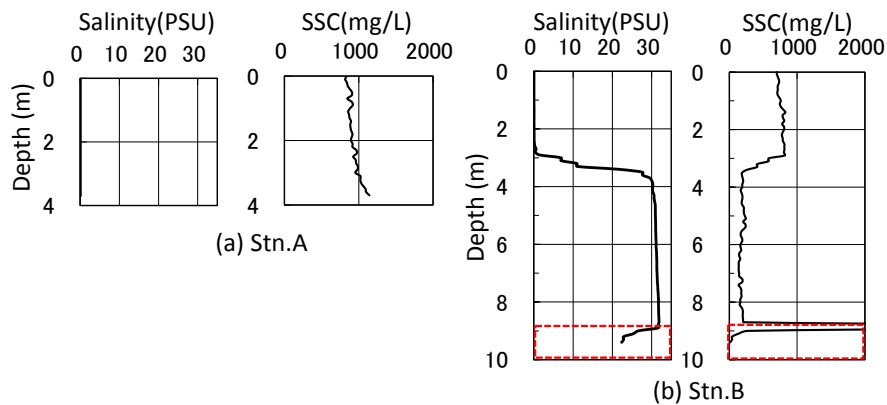


Fig. 3. Measured vertical profiles of Salinity and SSC at Stn.A and B. Salinity at Stn.A and near surface at Stn.B shows almost zero of fresh water. The rapid increase of SSC near the bed at Stn.B indicates saturation of optical turbidity sensor.

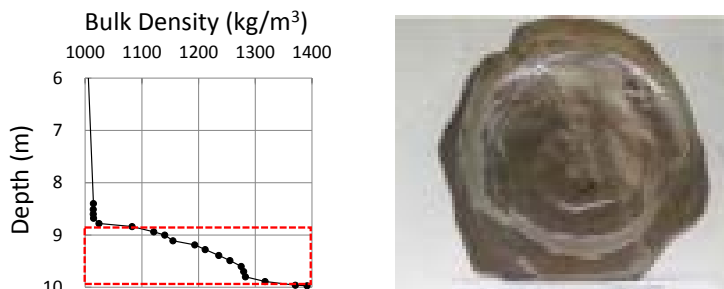


Fig. 4. Measured vertical profile of bulk density at Stn.B (left) and picture of bottom sediment sample taken from the station (right). The dotted line in the density data shows the same layer near the bottom as in Fig. 3 (b) indicating fluid mud layer with the density of around 1,200kg/m³.

References

- PIANC. 2008. Minimizing harbour siltation. The World Association for Waterborne Transport Infrastructures, Report 102. 75p.
- Fan S. *et al.* 2004. River flooding, storm resuspension, and event stratigraphy on the northern California shelf: observations compared with simulations. *Marine Geology* 201:17-41.

Combining turbulence and mud rheology in a numerical 3D-model of the Ems Estuary

Naulin Marie¹ and Andreas Malcherek²

¹ Federal Waterways Engineering and Research Institute
Wedeler Landstr. 157, 22559 Hamburg, Germany
E-mail: marie.naulin@baw.de

² Hydromechanics and Hydraulic Engineering, Institute of Hydro Sciences, University of the German Armed Forces, Munich, Werner-Heisenberg-Weg 39, 85577 Neubiberg, Germany

Introduction

The Ems Estuary is located at the North Sea between Germany and the Netherlands. In the upstream part of the estuary fluid mud layers of thicknesses of around 2m and suspended sediment concentrations of up to 300kg/m³ can be observed (Schrottke, 2006). As a consequence, there are deteriorating environmental conditions and high maintenance costs. Further knowledge of the system behaviour of the Ems Estuary is required in order to understand the increasing siltation and to analyse and develop possible counter measures.

The flow regime of muddy estuaries such as the Ems Estuary is dominated by cohesive sediment transport in transition of low concentrated suspension, high concentrated suspension and fluid mud layers (Fig. 1). The viscous behaviour of water (Newtonian fluid) can be described by turbulence models and the viscous behaviour of fluid mud (non-Newtonian fluid) can be described by rheological models. The rheological characteristics of fluid mud are dependent on the structural behaviour of the material, e.g. break-up and recovery of aggregates under the influence of shear impact (Toorman, 1997). In Knoch and Malcherek (2011) a numerical method was presented which enables the simulation of non-Newtonian flow behaviour in an isopycnal model (layers of constant density). However, in order to describe the dynamics of muddy estuaries a continuous transition from fluid mud to high concentrated suspension to low concentrated suspension with free turbulence is required.

Therefore, the continuous modelling concept (Le Hir *et al.*, 2001; Toorman, 2002; Roland *et al.*, 2012) combining turbulent viscosity and rheological viscosity will be applied. The methods and results of the modelling approach applied to a 3D model of the Ems Estuary will be presented and discussed at the conference.

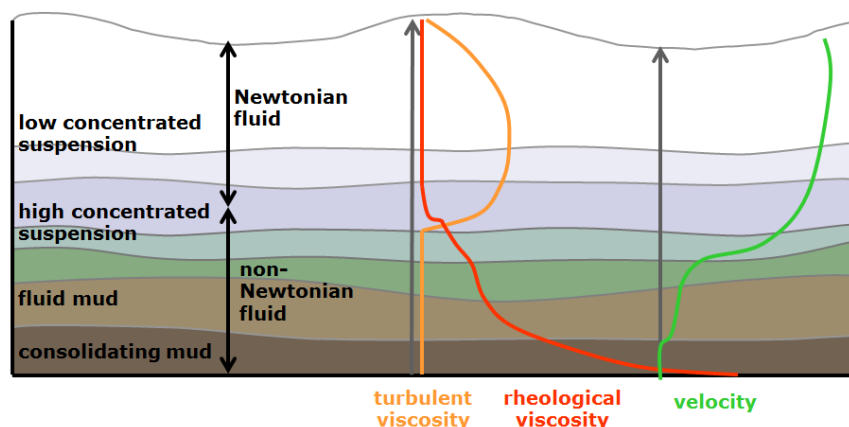


Fig. 1. Schematic diagram of turbulent viscosity and rheological viscosity depending on the sediment concentration (modified from Wehr, 2012).

Methods and Results

An established 3D hydrodynamic model including suspended sediment transport, salt transport and two-equation turbulence models with turbulence damping due to stratification (Casulli and Lang, 2002) will be extended by a rheological viscosity. Different expressions for the rheological viscosity can be applied in accordance with rheological constitutive laws, e.g. Worrall-Tuliani fluid. As a first step, the vertical viscosities are assumed to be the sum of rheological viscosity ν_r and turbulent viscosity ν_t :

$$\nu^v = \nu_t + \nu_r$$

This approach will be applied to the 3D model of the Ems Estuary (Fig. 2). The results will be compared to field measurements. Moreover, a comparison of the results with numerical simulations of different methods (classic Newtonian and isopycnal non-Newtonian) will be performed.



Fig. 2. Satellite image and model domain of the Ems Estuary.

References

- Casulli V. and G. Lang. 2002. Mathematical Model UnTRIM, Validation Document, Federal Waterways Engineering and Research Institute (BAW), Hamburg, <http://www.baw.de/vip/abteilungen/wbk/Methoden/hnm/untrim/PDF/vd-untrim-2004.pdf>
- Knoch D. and A. Malcherek. 2011. A numerical model for simulation of fluid mud with different rheological behaviors. *Ocean Dynamics* 61:245-256.
- Le Hir P., P. Bassoullet and H. Jestin. 2001. Application of the continuous modelling concept to simulate high-concentration suspended sediment in a macrotidal estuary. In: McAnally W.H. und A.J Mehta (Hg.): *Coastal and Estuarine Fine Sediment Processes*, 3: Elsevier Science (Proceedings in Marine Science), 229-247.
- Roland A., C. Ferrarin, D. Bellafiore, Y.J. Zhang, M.D. Sikric, U. Zanke and G. Umgiesser. 2012. Über Strömungsmodelle auf unstrukturierten Gitternetzen zur Simulation der Dynamik von Flüssigschlick. *Die Küste* 79.
- Schrottke K. 2006. Dynamik fluider Schlick im Weser und Ems Ästuar - Untersuchungen und Analysen zum Prozessverständnis. BAW/BfG-Kolloquium Nov.2006.
- Toorman E.A. 1997. Modelling the thixotropic behaviour of dense cohesive sediment suspensions. *Rheologica Acta* 36(1):56-65.
- Toorman E.A. 2002. Modelling of turbulent Flow with suspended cohesive Sediment. In: Winterwerp J.C. und C. Kranenburg (Hg.): *Sediment Dynamics in the Marine Environment*, 5. Amsterdam, the Netherlands: Elsevier Science (Proceedings in Marine Science), S. 155-169.
- Wehr D. 2012. An isopycnal numerical model for the simulation of fluid mud dynamics. Dissertation, Institut für Wasserwesen, Universität der Bundeswehr München, Mitteilungen, Heft 115.

Geomorphologic evolution of subtidal mud bank area through an estuary mouth. The case of Kaw mud bank (French Guiana)

Orseau Sylvain^{1,2}, Sandric Lesourd³, Nicolas Huybrechts⁴ and Antoine Gardel^{1,2}

¹ CNRS Guyane, USR 3456
PO Box 2, Cayenne 97300, French Guiana
E-mail: sylvain.orseau@cnrs.fr; antoine.gardel@cnrs.fr

² LOG, UMR 8187
Université du littoral Côte d'Opale, PO Box 32, Wimereux 69230, France

³ M2C, UMR 6143
Université de Caen Basse Normandie, PO Box 24, Caen 14000, France
E-mail: sandric.lesourd@unicaen.fr

⁴ Roberval Laboratory, LHN (joint research unit UTC-CEREMA)
Compiègne, France
E-mail: nicolas.huybrechts@cerema.fr

Introduction

Muddy shores located between the Amazon and the Orinoco deltas are subjected to a westward migration of huge mud banks (1.8-3km.yr⁻¹). Their migration is mainly generated by trade-wind waves and tidal currents. Located in shallow waters (5 to 20m), mud banks are derived from mud supplies of the Amazon sediment discharge (5 to 13x10⁸m³.yr⁻¹, Martinez *et al.*, 2009). Many studies have focused on processes driving mud banks migration (Augustinus, 2004; Gardel and Gratiot, 2005), on the impacts on shoreline dynamics and mangrove ecosystems (Allison and Lee, 2004; Anthony *et al.*, 2008; Gratiot *et al.*, 2008; Proisy *et al.*, 2009) and mud bank characteristics like topography, sediment concentrations or wave-mud interactions (Winterwerp and Van Kesteren, 2004; Winterwerp *et al.*, 2007). However, the dynamic of the mud bank subtidal area is poorly documented although it constitutes the major and the most dynamic area of a mud bank. The purpose of this study is to analyse the geomorphologic evolutions of the mud bank subtidal area and its effects on shoreline mobility in an estuary mouth.

Methods

In situ monitoring

To monitor geomorphologic evolutions of the subtidal area, bathymetric surveys are conducted annually with a single beam, bi-frequency (33-210kHz) echo sounder. Measurement area covers approximately 425km² off the estuary mouth. In the same area, 3 campaigns including 110 points each one are also performed to determine the in situ density of the bed sediment. To complete this dataset, acoustical measurements are conducted with a sub-bottom profiler (4-24KHz), well designed to work in shallow waters and to provide high-resolution imageries on cohesive sediments. It allows the estimation of the thickness and the volume of mud siltation layers with time. Acquisition of hydrological parameters (waves and tide) is also realized with pressure data loggers and tidal gauge.

Satellite imagery

Landsat (Land Satellite) and SPOT (Système Pour l'Observation de la Terre) images are used to extract shoreline with a semi-automatically process based on using of SAVI vegetation index to distinguish the limits of dense vegetation. In this way, mangrove forests are used as an indicator of shoreline mobility. Combined with bathymetric surveys, it will allow to estimate the interaction between the shoreline mobility and the subtidal area dynamic to determine the necessary time to swing in erosion to accretion regime.

Results

The analysis of bathymetric maps points out a strong variation of geomorphology with time. Since 2007, the east side of the navigation channel is enduring a severe settling reaching approximately 147.8x10⁶m³ and characterized by a high sediment deposition rate along the leading edge of mud bank (Fig. 1). As described on previous studies, intensive erosion induced by waves occurs in the trailing edge. Conversely, on the west side of the navigation channel, a strong wave damping induced by slight mud deposits has been noticed in front of the beaches.

Fig. 2 illustrates the density map obtained from the first survey at wet season. It underlines (i) a homogeneous leading edge mainly composed of fluid mud (1050-1250kg.m⁻³) particularly in

the navigation channel and the estuary mouth and (ii) a trailing edge characterized by higher-density areas ($> 1400 \text{ kg.m}^{-3}$) which are spatially heterogeneously distributed. It confirms a 'classic' migration behaviour with the erosion of the trailing edge by waves inducing a fluid mud displacement with alongshore currents toward the leading edge of mud bank.

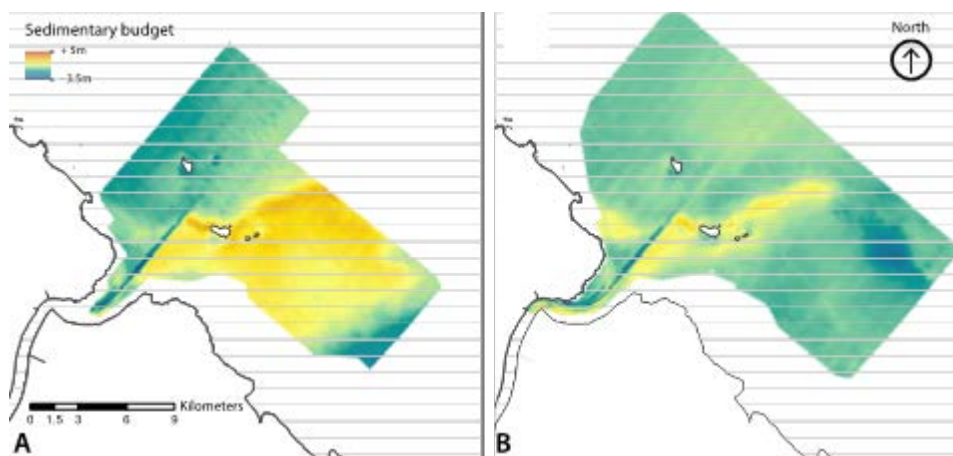


Fig. 1. Sedimentary budget (A) from 2007 to 2013 and (B) 2012 to 2013 off the Mahury mouth.

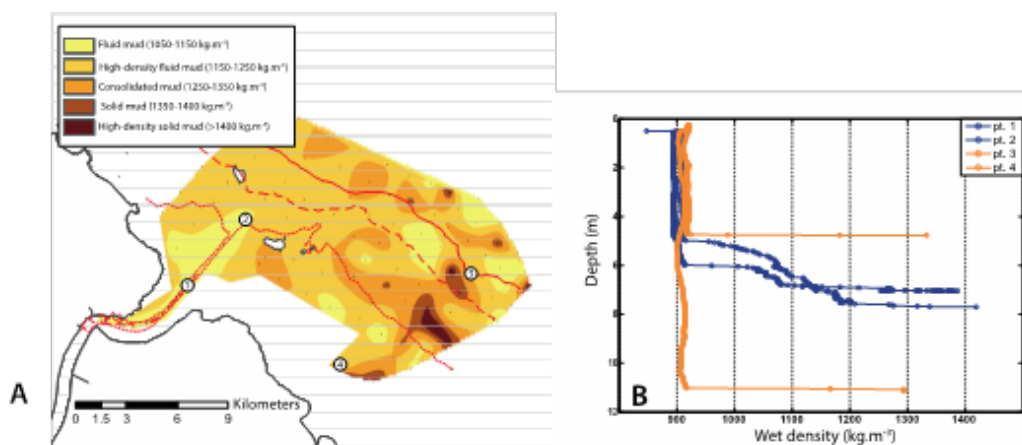


Fig. 2. (A) In situ density map of bottom sediments and (B) instantaneous density profiles over the water column for 4 measurement points.

Conclusion and perspectives

Preliminary results highlight a strong geomorphological changes over few years with contrasted areas of deposit and erosion for respectively, both leading and trailing edges. In this context, the navigation channel of the harbour seems to be a preferential area for fluid mud deposits requiring continuous dredging to ensure maritime traffic. These results will be used to set up a numerical model in order to understand more accurately the mud banks migration and its key role on mud deposits into an estuary.

References

- Allison M.A. and M.T. Lee. 2004. Sediment exchange between Amazon mudbanks and fringing mangroves in French Guiana. *Marine Geology* 208:169-190.
- Anthony E.J., F. Dolique, A. Gardel, N. Gratiot, C. Proisy and L. Polidori. 2008. Nearshore intertidal topography and topographic-forcing mechanisms of an Amazon-derived mud bank in French Guiana. *Continental Shelf Research* 28:813-822.
- Augustinus P.G.E.F. 2004. The influence of the trade winds on the coastal development of the Guianas at various scale levels: a synthesis. *Marine Geology* 208:141-151.

- Gardel A. and N. Gratiot. 2005. A satellite image-based method for estimating rates of mud bank migration, French Guiana, South America. *Journal of Coastal Research* 21(4):720-728.
- Gratiot N., E.J. Anthony, A. Gardel, C. Gaucherel, C. Proisy and J.T. Wells. 2008. Significant contribution of the 18.6 year tidal cycle to regional coastal changes. *Nature Geoscience* 1:169 - 172.
- Martinez J.M., J.L. Guyot, N. Filizola and F. Sondag. 2009. Increase in sediment discharge of the Amazon River assessed by monitoring network and satellite data. *Catena* 79:257- 264.
- Proisy C., N. Gratiot, E.J. Anthony, A. Gardel, F. Fromard and P. Heuret. 2009. Mud bank colonization by opportunistic mangroves : a case study from French Guiana using lidar data. *Continental Shelf Research* 29(3):632-641.
- Winterwerp J. and W. Van Kesteren. 2004. Introduction to the physics of cohesive sediment in the marine environment. Elsevier *Developments in Sedimentology* 56.
- Winterwerp J.C., R.F. de Graaff, J. Groeneweg and A.P. Luijendijka. 2007. Modelling of wave damping at Guyana mud coast. *Coastal Engineering* 54(3):249-261.

Deriving space-time information of the organic fraction of suspended particulate matter in a coastal environment

Riethmüller Rolf¹, Markus Schartau², Götz Flöser¹ and Wolfgang Schönfeld¹

¹ Institute of Coastal Research, Helmholtz-Zentrum Geesthacht
Max-Planck-Str.1, 21502 Geesthacht, Germany
E-mail: rolf.riethmueller@hzg.de

² GEOMAR Helmholtz Centre for Ocean Research Kiel
Düsternbrooker Weg 20, 24105 Kiel, Germany

This study introduces a method to estimate the temporal/spatial variability of total and organic suspended particulate matter (TSM, POM) in coastal seas based on a combination of water sampling analysis and satellite remote sensing products of surface concentrations of TSM (TSMC). Lab analysis of several thousand water samples indicates a general seasonally modulated link between TSMC and its organic fraction. This relationship can be well described by an analytical model. Applying this model to satellite TSM products yields images of the surface distributions of the suspended POM as a derived product. The model allows also for a separation between lithogenic and freshly produced pelagic components of the POM. The method was applied for the German Bight, North Sea, including its coastal fringe, the Wadden Sea, taking MERIS/ENVISAT products for case 2 coastal waters. The procedure resolves a transition zone between the Wadden Sea and the more open German Bight, where “fresh” and lithogenic organic material are of comparable magnitude. The transition zone is indicative of a belt of effective particle interaction where pelagic “fresh” POM is likely exported from the water column to the bed sediments.

Introduction

The exchange of particulate matter between the German Bight (North Sea) and its intertidal fringe, the Wadden Sea, is a critical and yet unresolved issue (Burchard *et al.*, 2008). The German Bight represents a coastal water mixing zone between riverine fresh water and oceanic waters of the shelf sea. It also corresponds to an environmental problem zone because of high nutrients and pollutants loading from land. At the same time, the Wadden Sea owes its high productivity the sustained import of POM from the German Bight (van Beusekom *et al.*, 2012). The mass flux estimations in coastal oceanography deal with variations in TSM, but their temporal/spatial patterns, and in particular the organic and inorganic components, are often insufficiently resolved. The study’s central idea is to look beyond the spatial/temporal variations of bulk TSMC derived from ocean colour satellite products. We take advantage of a large set of TSMC and Loss-on-Ignition (LoI) water sample data. These data are

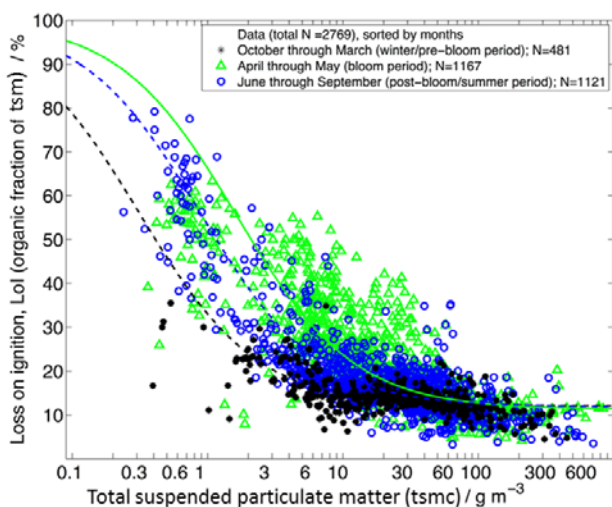


Fig. 1. Loss-on-Ignition versus TSMC. Symbols represent sample data, the lines the fitted functions due to eq. (1). The different colours indicate the seasons.

assimilated into a model that parameterises the separation between mineral and organic fractions of TSM after which it is combined with satellite products of surface TSMC.

Methods

Nearly three thousand water samples were collected between 2000 and 2013 in the framework of numerous field surveys in the German Wadden Sea and the German Bight. Filtration, weighing and combustion of the filtered material followed the same procedures each year. LoI was used as proxy for the fraction of organic matter in the filtered material.

Satellite products of surface TSMC for the German Bight and the Wadden Sea were taken from ENVISAT/MERIS ocean colour images applying the MERIS operational processor for case 2 coastal waters. The processor delivers the scattering length at 440nm (b_{440}) that was shown to be proportional to TSMC at concentrations typical for the North Sea (Doerffer and Schiller, 2007; Sørensen *et al.*, 2007). For the higher TSMC prevailing in the Wadden Sea ($>20\text{g m}^{-3}$) the relationship

between b_{440} and TSMC follows a power law with the exponent greater than one (Riethmüller *et al.*, in prep.).

Results

As Fig. 1 shows, Lol is decreasing with TSMC from about 70% at 0.6g m^{-3} to some 15% at 60g m^{-3} and then remaining constant at this value for higher TSMC. The data show a slight seasonal modulation with higher Lol during phytoplankton spring bloom and lower values in winter. This general behaviour can be well described by an analytical model that assumes that the organic fraction of TSM consists of living and non-living “fresh” particulate organic matter POM_f and POM chemically bound to the lithogenic part of the sediments (POM_s) in a fraction s_{POM} assumed to be constant over the whole range of TSMC. Hence $\text{POM} = \text{POM}_f + s_{\text{POM}} \cdot \text{SLM}$, SLM being the suspended lithogenic matter. Defining K_{POM} as the concentration of POM_f where the POM_f -to-SLM ratio becomes one, one can finally express Lol as a function of TSM and two free parameters s_{POM} and K_{POM}

$$\text{Lol} = \frac{\left(\frac{K_{\text{POM}}}{\text{TSM}}\right)}{\left(\frac{K_{\text{POM}}}{\text{TSM}} + 1\right) \cdot (s_{\text{POM}} + 1)} + \frac{s_{\text{POM}}}{(s_{\text{POM}} + 1)} \quad (1)$$

s_{POM} was found to be nearly constant (0.128 to 0.138), whereas K_{POM} varies by a factor of five (0.31 in winter, 1.63 in spring and 0.89 in summer). Knowing s_{POM} and K_{POM} also allows for the computation of POM_f and POM_s for any given TSMC.

If we apply the function (1) to the MERIS-TSM-products according to the respective season of observation, further satellite images of both the “fresh” and lithogenic component of POM may be generated. As an example the July 2010 result is shown in Fig. 2. One observes the typical situation of high TSMC in the Wadden Sea with a sharp decrease off the barrier islands (left panel). At the same time the percentage of POM increases (middle panel). Directly in front of the barrier islands a narrow band indicates a comparable magnitude of “fresh” and lithogenic POM resulting from resuspension and advection. These yellow areas mark regions where effective particle aggregation may enhance export of “fresh” material to the sediments. Their distances to the coast and spatial extensions vary with the season with the largest extension occurring during winter.

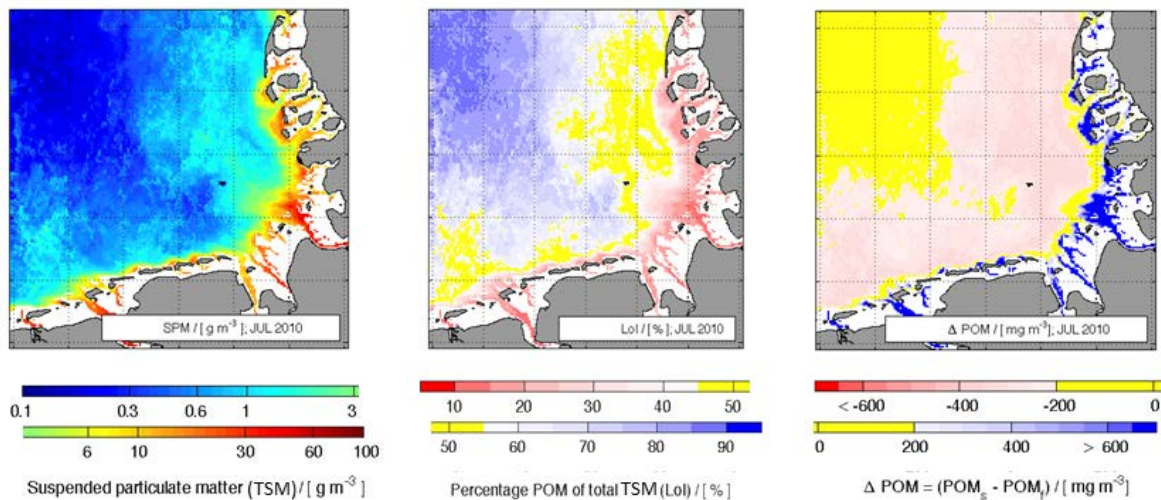


Fig. 2. July 2010 monthly averages for MERIS-TSM (left panel), Lol using eq. (1) (middle panel) and the difference between “fresh” POM_f and lithogenic POM_s (right panel).

References

- Van Beusekom J.E.E., C. Buschbaum and K. Reise. 2012. Wadden Sea tidal basins and the mediating role of the North Sea in ecological processes: scaling up of management? *Ocean & Coastal Management* 68:69-78.
- Burchard H., G. Flöser, J.V. Staneva, T.H. Badewien and R. Riethmüller. 2008. Impact of density gradients on Net Sediment Transport into the Wadden Sea. *J. Phys. Oceanogr.* 38:566-587.
- Doerffer R. and H. Schiller. 2007. The MERIS Case 2 water algorithm, *International Journal of Remote Sensing* 28(3-4):517-535.
- Riethmüller *et al.* 2015 (in preparation)
- Sørensen K., E. Aas and J. Høkedal. 2007. Validation of MERIS water products and bio-optical relationships in the Skagerrak, *International Journal of Remote Sensing* 28(3-4):555-568.

Attenuation of 'short waves' in the mudbank region off Alleppey, Kerala coast, India

Samiksha S.V., P. Vethamony, M.T. Babu and K. Sudheesh

CSIR, National Institute of Oceanography, Dona Paula, Goa - 403004, India
E-mail: vsamiksha@nio.org

Waves exert pressure on the seabed, and in the case of fluidized mud seafloor, the bed moves, resulting in damping of incoming waves by the fluid mud layer. One of the best examples for such a phenomenon are mudbanks (MB) off Kerala coast. MBs are reservoirs of fine suspended sediments occurring along the coast, which can dampen the waves resulting in clearly demarcated areas of calm water even during the roughest monsoon conditions. MBs off Kerala coast have been considered as unique formations as they occur in a non-estuarine region. Similar formations are reported off the Yellow River delta in the Bohai Sea of China, and near the Amazon River mouth along the northeast coast of Brazil and the Guianas; but these are permanent muddy-bottom, unlike Kerala MBs, which are proved to be dynamic, and shift their positions with time and most importantly occur far away from estuaries (Samiksha *et al.*, 2015). A clear-cut evidence to its formation is yet to be established, as various studies (Samiksha *et al.*, 2015) could not explain all the observed characteristics of the mud-banks and uniqueness of it. Mathew (1992) reported that MBs are typically 2 to 8km in length alongshore, 1 to 3km in the cross-shore direction and mud density in this region generally ranges between 1,080 and 1,300 kg/m³.

As a part of the Project on Alleppey Mudbank Process Studies (AMPS), we made an attempt to study mudbank-attenuated waves from the measured data. One wave rider buoy was deployed in the expected MB region off Alleppey, Kerala (Fig. 1) at 15m water depth ahead of the onset of the event (21 May - 31 July 2014) (B1), and another one at 7m water depth (26 June - 31 July 2014) (B2) after the formation of the MB. In this presentation, we would like to focus on the behaviour of wave energy spectra after the formation of MB. The highest significant wave height (H_s) observed at location B1 is 3.16m, with maximum wave height (H_{max}) of 5.31m for the whole measurement period. But, when we consider the common measurement period (including B2 location), H_s was 2.64m (H_{max} = 4.39m) at B1 and H_s was 2.03m and H_{max} = 2.12m at B2. Similarly, the mean period at both locations varied from 4 to 10s. Wave direction remained almost the same at both the locations, ranging between 200° and 280° (Fig. 2). H_s were also extracted from the ERA-Interim database (Dee *et al.*, 2011) for the study area in order to use it as reference data for no-MB condition. Comparison of measured H_s with the ERA-Interim H_s clearly indicates the arrival of MB at 15m water depth on 12 June 2014. We analysed the wave height data at both the locations to calculate the percentage of wave height attenuation at B2 location compared to B1 location (Fig. 3), and we found ≈ 50 - 60% attenuation at 7m water depth w.r.t 15m depth. It may kindly be noted that wave height attenuation percentage would be certainly much higher if we compare with H outside the periphery of MB. In our recent study (Samiksha *et al.*, 2015, communicated), we have used the latest version of WAVEWATCH III model with the two mud formulations, viz., Dalrymple and Liu (1978) and Ng (2000) to reproduce wave energy attenuation in the mudbank region, and the model results matched very well with measurements. We also proved the dynamic nature of the MB off Alleppey, which was otherwise only speculated.

In order to analyse wave energy attenuation in the frequency band, typical normalised wave spectra were extracted: (i) before the formation of MB at B1 i.e. on 6 June 2014 and (ii) after the formation of MB i.e. on 24 June and 4 July 2014. The low (long waves) and high (short waves) frequency bands are defined here as $f \leq 0.18\text{Hz}$ and $f > 0.18\text{Hz}$, respectively. We observe downshift of peak frequency as days progressed after the MB formation, with the attenuation of short waves (Fig. 4a). Similar features are observed for the spectra at B2 (Fig. 4b). The energy in the high frequency region of the spectra reduced considerably after the formation of MB at both the locations, but higher at B2. Sheremet *et al.*, (2005) suggested that the observed short-wave dissipation may be due to nonlinear energy transfer within the wave spectrum which further allows the coupling between the short- and long-wave spectral bands, allowing energy to flow toward long waves, where it can be efficiently dissipated via direct wave-bottom interaction. More detailed study is planned in order to study the attenuation of short waves by separating the wind, seas and swells, and also through numerical modelling. In our previous studies the dissipation source term will be analysed in order to account for the attenuation of short and long waves separately, and the results will be discussed during presentation. We acknowledge ECMWF for providing the ERA-Interim wave data.

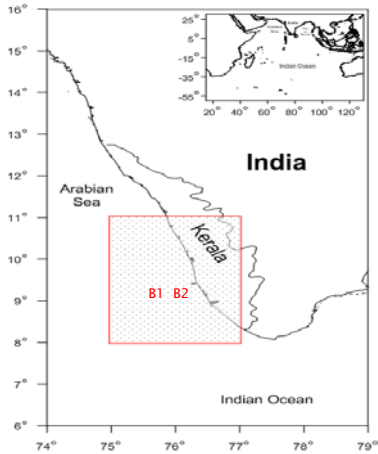


Fig. 1. Area of study and the locations of moored wave rider buoys (B1 and B2) at 15m and 7m water depths off Alleppey, Kerala, India.

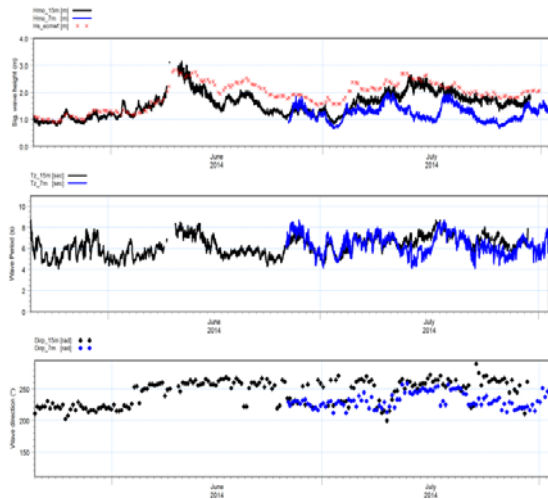


Fig. 2. Comparison of wave parameters (H_s , T_m and Dir) at 15m (B1) and 7m (B2) water depths. H_s obtained from ERA-Interim database is also plotted for reference of no-mud condition (Samiksha *et al.*, 2015).

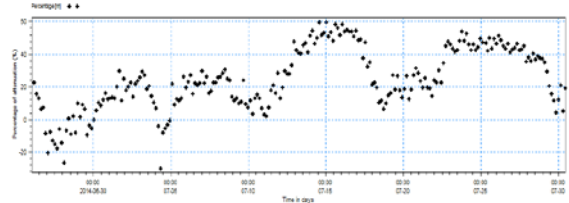


Fig. 3. Percentage of wave height attenuation at 7m water depth compared to 15m water depth.

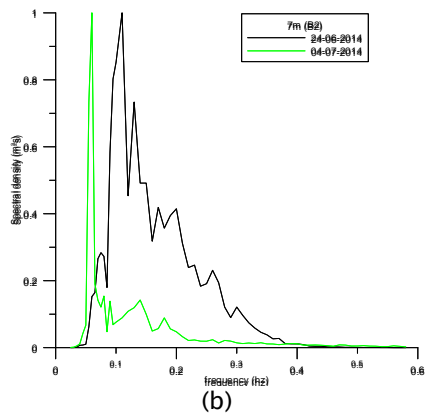
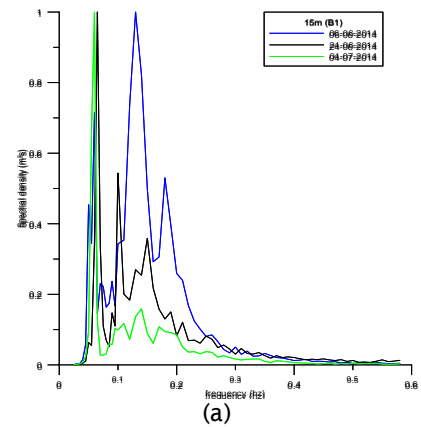


Fig. 4. Normalised wave energy spectra at (a) 15m depth and (b) 7m depth.

References

- Dalrymple R.A. and P.L.-F. Liu. 1978. Waves over soft muds: A two layer fluid model. *J. Phys. Oceanogr.* 8:1121-1131.
- Dee D.P. *et al.* 2011. The ERA-Interim reanalysis: configuration and performance of the data assimilation system, ECMWF, Reading, ERA report series 9. 71p.
- Mathew J. 1992. Wave-mud interaction in mudbanks. PhD Thesis.
- Mathew J. and M. Baba. 1995. Mudbanks of SW coast of India II: wave-mud interaction. *Journal of Coastal Research* 11:178-187.
- Ng C.-N. 2000. Water waves over a muddy bed: a two-layer Stokes boundary layer model. *Coastal Eng.* 40:221-242.

Multiscale modelling of dispersive plumes

Saremi Sina, Nils Drønen and Hans Jacob Vested

DHI, Agern Alle 5, 2970 Hørsholm, Denmark

E-mail: sis@dhigroup.com, nkd@dhigroup.com, hjv@dhigroup.com

The environmental impacts of the spill and deposition of fine dredged material or discharging sewage, thermal and mineral effluents into the marine waters, lakes or rivers have always been a matter of concern. The spatial and temporal extents of the impacts are dependent on the characteristics of the released material, the initial conditions at the point of release and the ambient conditions. Determining the initial (nearfield) behaviour of the released material and predicting the larger scale (farfield) dispersion of the resulting plumes require detailed modelling of both the small scale nearfield mixing and dilution processes and the larger scale farfield circulation and dispersion processes. A practical engineering solution is to combine different types of models each tailored and optimally focused on a certain scale ranges. Therefore coupling and correct interaction between the different models is an important factor to gain accurate results.

Regardless the type of the release (overflow spill, maintained jet, instantaneous puff, bulk deposition, etc.), the nearfield description of the flow requires detailed calculations of the entrainment, mixing and dilution processes. This can be done either by fully 3D CFD models, or by integrated models which are less computationally demanding. Traditionally the entrainment principle of Morton *et al.* (1956), which is based on averaged flow scales, is used to predict the nearfield mixing and dilution of the submerged effluents, which then acts as an input to the large scale circulation models based on shallow water equations. When coupling these two different scaled models, it is important to consider both the dynamic and kinematic interactions between the nearfield processes and the ambient environment in order to achieve an accurate solution.

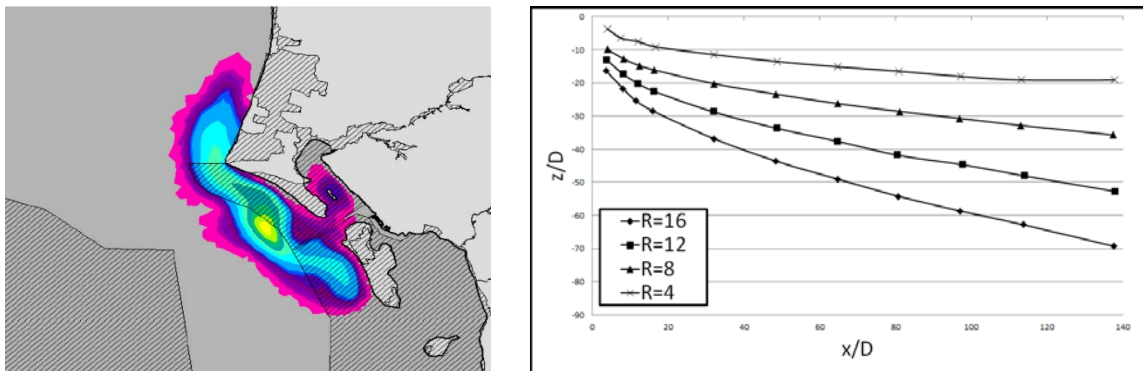


Fig. 1. Left: Example of far field dispersion model results (exceedance concentration around a sediment disposal site-MIKE3-FM); Right: Example of results (plume trajectories) from integrated nearfield model (R is the velocity ratio between intruding material from above and the horizontal cross flow, D is the diameter at the release point).

In the present work, the concept of multiscale solution is considered to model the release of material into marine environment. The idea is to solve the nearfield processes and determine the location and the characteristics of the released material at the point where they enter a passive state and can be introduced to the large scale model, as their dynamics are not governed by the small scale processes anymore. The choice of criteria deciding the point where the plume enters its passive state is a crucial factor in multiscale modelling. Different types and combinations of criteria (as function of plume's momentum, buoyancy, entrainment rate, etc.) have been tested and evaluated in terms of their effect on the far field behaviour of the plume. The farfield model used in this study is the MIKE3-FM hydrodynamic model. The coupling between the nearfield and the far field model is two-way, i.e. the computed far field ambient conditions are used for nearfield calculations, whereas the entrainment and dilution rates, and the local flow resistance computed by the nearfield model are feed backed to the farfield model. For the near field part of flow, two approaches are considered. In the first approach the nearfield calculations are based on the integrated solution developed by Jirka (2004), which predicts the trajectory, dilution and entrainment rates of jets and plumes in various ambient conditions. However, the model has limitations under certain conditions which result in invalid nearfield calculations. These conditions

are often due to the breakdown of the boundary layer nature of the flow which is the basis of calculations in the integrated model.

In order to further study the nearfield behaviour of the released material, and evaluating the performance of the integrated model under different conditions, a second approach is attempted where a 3D multiphase CFD model - developed and evaluated by Saremi (2014) - is used to supplement the simple model. The results from the CFD simulations will shed light on the role of important parameters driving the nearfield processes and the limitations of the integrated models. The choice of passive criteria which link the nearfield models to the farfield models will be studied and evaluated by using the CFD model to simulate the details of the plumes dynamics. The detailed results from the CFD model will be transformed into a parametric database with the possibility of replacing the integrated nearfield models in the multi-scale solutions, when they reach beyond their limits of validity.

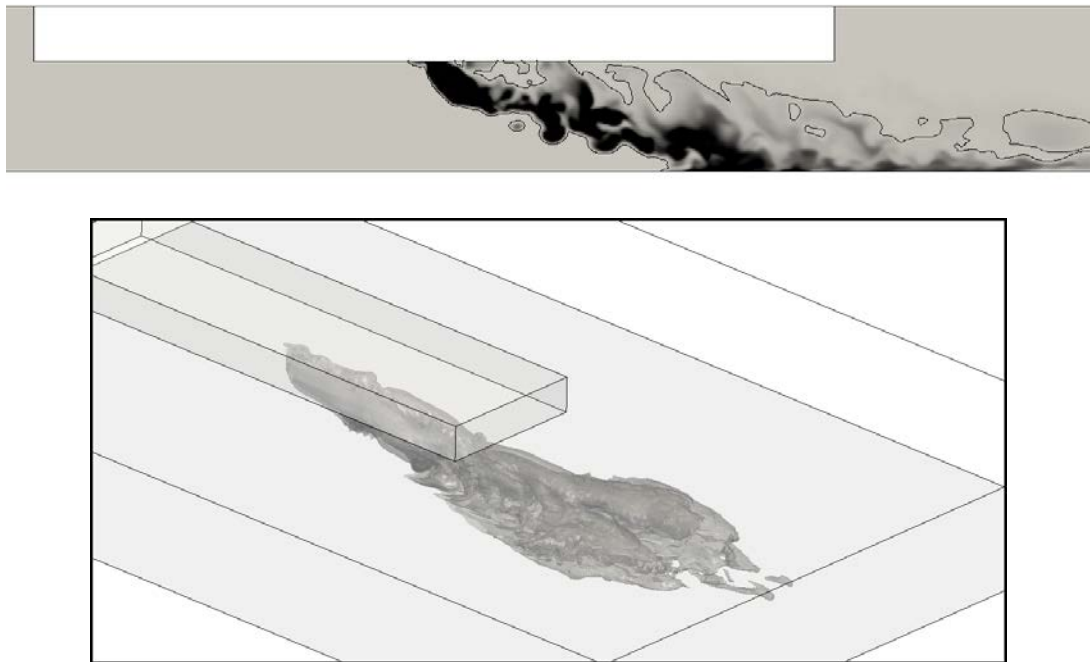


Fig. 2. Examples of CFD results (concentration contours) of simulating the overflow spill of fine dredged material from hoppers. Top: horizontal cross section view; Bottom: 3D view.

The aim of this study is to provide a robust and widely applicable multiscale model to calculate the nearfield behaviour of the released material and insert it into larger scale models, which their final accuracy in predicting the environmental impacts of the released material into the ambient environment relies strongly on the release conditions provided by the nearfield model. The CFD model can also be used as a useful tool in more complex engineering purposes, scientific and design applications.

References

- Jirka G.H. 2004. Integral model for turbulent buoyant jets in unbounded stratified flows. Part I: Single round jet. *Environmental Fluid Mechanics* 4(1):1-56.
- Morton B.R., G. Taylor and J.S. Turner 1956. Turbulent gravitational convection from maintained and instantaneous sources. *Proceedings of the Royal Society of London. Series A. Mathematical and Physical Sciences* 234(1196):1-23.
- Saremi S. 2014. Density driven currents and deposition of fine materials (Doctoral dissertation). Technical University of Denmark, Lyngby, Denmark.
- Winterwerp J. C. 2002. Near-field behaviour of dredging spill in shallow water. *Journal of Waterway, Port, Coastal, and Ocean Engineering* 128(2):96-98.

Erosion characteristics and horizontal variability for small erosion depths in the Sacramento – San Joaquin River Delta, California, USA

Schoellhamer David H.¹ and Andrew J. Manning^{2,3,4}

¹ United States Geological Survey, 2130 SW 5th Avenue, Portland, OR 97201, USA
E-mail: dschoell@usgs.gov

² HR Wallingford, Howbery Park, Wallingford, Oxfordshire, OX10 8BA, UK

³ Department of Geography, Environment and Earth Sciences, University of Hull, Kingston Upon Hull, Humberside, HU6 7RX, UK

⁴ School of Marine Science and Engineering, Plymouth University, Drake Circus, Plymouth, Devon, PL4 8AA, UK

Cohesive sediment transport in the Sacramento – San Joaquin River Delta landward from San Francisco Bay affects habitat for pelagic organisms, contaminant transport, and marsh accretion, restoration, and sustainability. Several numerical models of sediment transport are being developed and applied to address these issues. Erosion algorithms are determined by calibrating model output to measured suspended-sediment concentration (SSC). To better inform and constrain numerical model development, an erosion microcosm has been used to quantify erosion and develop a conceptual model of erosion in the Delta.

Field methods for applying the microcosm are similar to those described by Dickhudt *et al.* (2011). Two sediment cores are collected from a study site with a gravity Gomex (The use of firm, trade and brand names in this report is for identification purposes only and does not constitute endorsement by the U.S. Geological Survey.) corer lowered to the bed from a small boat. After raising the corer back onto the boat, a 10-cm-diameter tube is immediately pushed into the top of each core to collect a sample. Samples are disturbed as little as possible. The top 1cm is also sampled for grain size and water content. A piston inserted into the bottom of the tube is used to push the sediment surface up to 10cm from the top of the tube. The subsampled core is eroded using a dual core University of Maryland Center for Environmental Science - Gust Erosion Microcosm System. A disk rotates at the water surface at the top of the tube and water is pumped through the water column in the tube at predetermined rates that provide nearly uniform and known shear stresses at the sediment/water interface (Gust and Mueller, 1997). Turbidimeters continuously monitor the effluent. A 0.01 Pa shear stress is initially applied to flush and stabilize the system. Applied shear stress

about 3 hours. Water samples are collected during each step to calibrate turbidity to SSC. The time series of erosion rate (kg/m²/s) is calculated and the erosion model of Sanford and Maa (2001) is used to calculate erosion parameters. The erosion rate E for an experiment as a function of mass eroded (m) and time (t) is

$$E(m,t) = M(m) [\tau_b(t) - \tau_c(m)] \quad (1)$$

Critical shear stress τ_c is calculated at the end of each step and is assumed to increase with m which in turn increases with erosion depth. The erosion rate constant $M(m)$ is assumed to be a constant for each step.

A total of thirty cores from four sites in the Delta were analyzed from November 2011 to July 2014. Erosion parameters showed no seasonal signal. Erosion rate constant $M(m)$ generally increased with eroded mass or depth. The mass eroded where the bed critical shear stress equals 0.4 Pa and the mean value of $M(m)$ between the surface and where τ_c equals 0.4 Pa increased with water content.

Initial critical shear stress as a function of solids volume of the mud matrix concurs with other empirical data presented by Dickhudt *et al.* (2011). It is noteworthy that initial critical shear stress for one particular site in South San Francisco Bay was smaller than expected. SSC at this site (typically 100-200 mg/l) is 1-2 orders of magnitude greater than in the Delta, so it is possible that suspended sediment in the corer settles and creates a fluid mud or that the top 1cm sample is not representative of water content or grain size because a thin fluid mud actually exists.

During a tidal cycle, observed changes of SSC in the Delta indicate that about 0.05 to 0.20kg/m² are eroded from the bed. This corresponds to an erosion depth of about 30 to 150 microns if erosion is uniform horizontally, about the diameter of a typical suspended floc. We believe that these small erosion depths and visual observation of horizontally varying biota and texture at the surface of the

sediment cores indicate that a conceptual model of erosion depending on horizontally varying properties (van Prooijen and Winterwerp, 2010) may be more appropriate than assuming horizontally homogeneous erosive properties. In addition, observed erosion rate constant $M(m)$ increases with depth, contrary to expectations for a consolidating bed, possibly because the eroding surface area increases as applied shear stress increases.

To test this hypothesis, we collected five cores at Franks Tract in the Delta and measured the horizontal variability of shear strength within each core in the top 5.08cm with a shear vane. Small tubes built by a freshwater worm and macroalgae were observed on the surface of all cores. Measurements were made near the four corners and edge midpoints of the Gomex corer because the shear vane is too large to insert in the 10-cm-diameter subsampling tube. The shear vane was inserted into the sediment until the top of the vane was at the top of the sediment, torque was applied to the vane until the sediment failed and the vane rotated, and the corresponding dial reading in Nm was recorded. In a typical application, the vane is inserted further into the sediment and the dial reading is divided by a constant to get the vane shear strength in kPa. Here we assume that the dial reading is proportional to the surface strength. The midpoints had greater strength than the corners. Standard deviations were 35% and 26% of the mean for corner and midpoint readings respectively. Thus an approximation is that the horizontal standard deviation of the critical shear stress is 30% of the mean. The shear vane test provides some empirical evidence that surface strength of the bed does appreciably vary horizontally. A numerical experiment is conducted to determine the observed SSC for a sediment core in the erosion microcosm with horizontally varying erosion properties.

References

- Dickhudt P.J., C.T. Friedrichs and L.P. Sanford. 2011. Mud matrix solids fraction and bed erodibility in the York River estuary, USA, and other muddy environments. *Continental Shelf Research* 31:S3-S13.
- Gust G. and V. Mueller. 1997. Interfacial hydrodynamics and entrainment functions of currently used erosion devices. p.149-174. In: Burt N., R. Parker, J. Watts (Eds). *Cohesive sediments*. Wallingford, UK.
- Sanford L.P. and J.P.-Y. Maa. 2001. A unified erosion formulation for fine sediments. *Marine Geology* 179:9-23.
- van Prooijen B.C. and J.C. Winterwerp. 2010. A stochastic formulation for erosion of cohesive sediments: *Journal of Geophysical Research*, v. 115, C01005, doi:10.1029/2008JC005189.

A conceptual one-dimensional flocculation model for floc size distributions of suspended kaolinite in a cylindrical tank

Shen Xiaoteng and Jerome P.-Y. Maa

College of William and Mary, Department of Physical Sciences, Virginia Institute of Marine Science, Route 1208 Grete Road, Gloucester Point, VA 23062, USA

E-mail: xiaoteng@vims.edu

Introduction

Cohesive sediments transport is essential to managing coastal water quality and dredging operation, and to understanding coastal ecology, chemical fluxes and geological record. Nevertheless, the transport and fate of cohesive sediments are poorly predicted mainly due to the aggregation and breakage of fine, cohesive aggregates. A primary challenge to develop a flocculation model is that the time variation of Floc Size Distribution (FSD) is controlled by a partial differential equation that also contains the integration of the FSD itself. In this study, a conceptual one-dimensional flocculation model, i.e. the Population Balance Equation (PBE), is solved by using Quadrature Method Of Moments (QMOM). Model results of FSDs are verified by a laboratory experiment in a cylindrical tank placed at Virginia Institute of Marine Science (VIMS). The turbulence in the tank is generated by a marine bilge pump and measured by a 5MHz ADVOcean. The FSDs at selected places are statistically obtained by an underwater camera system and processed by using MATLAB® image processing toolbox. The results have shown that the FSDs can be efficiently and reasonably displayed by the quadrature nodes (i.e. the characteristic sizes) and corresponding weights (i.e. the characteristic number densities) in this PBE-QMOM flocculation model.

Flocculation model

The general transport equation (i.e. the PBE) that includes the kinetics of aggregation and breakage of flocs with size L is given in Eq.1 (Prat and Ducoste, 2006).

$$\begin{aligned} & \frac{\partial n(L;t)}{\partial t} + (U_s - W_{s,s}) \frac{\partial n(L;t)}{\partial s} - \frac{\partial}{\partial s} \left(\frac{\nu_t}{\sigma_t} \frac{\partial n(L;t)}{\partial s} \right) \\ &= \frac{L^2}{2} \int_0^L \left[\frac{\beta((L^3 - \lambda^3)^{1/3}, \lambda) \cdot \alpha((L^3 - \lambda^3)^{1/3}, \lambda)}{(L^3 - \lambda^3)^{2/3}} \cdot n((L^3 - \lambda^3)^{1/3}; t) \cdot n(\lambda; t) \right] d\lambda \\ & - n(L;t) \int_0^\infty \beta(L, \lambda) \alpha(L, \lambda) n(\lambda; t) d\lambda + \int_L^\infty a(\lambda) \cdot b(L | \lambda) \cdot n(\lambda; t) d\lambda - a(L) \cdot n(L; t) \end{aligned} \quad (1)$$

where $n(L; t)$ is the number density function defined on the basis of floc size L and time t , s denotes the direction along the streamline, U_s is the flow velocity along s , $W_{s,s}$ is projection of settling velocity in the direction of s , ν_t is eddy viscosity, σ_t is the turbulent Prandtl-Schmidt number, β is the collision frequency function, α is collision efficiency function, a is breakup frequency function, and b is fragmentation distribution function. The flocculation source and sink terms on the right hand side of Eq. 1 include: (1) the birth of flocs with size L due to aggregation of smaller particles, (2) the death of flocs with size L due to aggregation with other particles, (3) the birth of flocs with size L due to fragmentation of bigger particles, and (4) the death of flocs with size L due to breakup into smaller particles. The left hand side terms include, from left-to-right, an unsteady term, an advection and settling term, and a diffusion term, respectively. Among all the available methods for solving PBE, Shen and Maa (submitted) enhanced the classical QMOM approach (McGraw, 1997) to reasonably monitor the FSDs using a maximum of eight size classes in their flocculation box model. In this study, that box model is extended into a conceptual 1-D model to demonstrate the ability of simulating the time variation of FSDs in a tank.

Experimental setup

A kaolinite suspension in a cylindrical tank (diameter = 0.75m, height = 1.5m) is agitated with a 3700GPH submersible pump, mounted at the bottom with an upward outlet at the centre (Fig. 1). The submersible pump is started at a pre-determined power setting to mix the suspension during the first several minutes, obtaining a steady initial condition. Turbulence eddy diffusion coefficients and time-averaged current velocities are measured with a 5MHz SonTek ADVOcean, and the suspended sediment concentrations are measured by an OBS. These measured values are used as inputs for the flocculation model (i.e. Eq. 1). The evolution of kaolinite floc size will be observed by using an underwater camera system at selected locations. This camera system consists of a Sony Alpha NEX-7 camera, a Nikon Macro Lens, a Kenko extension tube, LED light sources, and a control circuit board assembled in a waterproof house. This combination has an image size of 23.5 x

15.6mm (6000 x 4000 pixels), and thus a native $3.9\mu\text{m}/\text{pixel}$. With a subject to image ratio 1:2 selected, an effective resolution of $1.9\mu\text{m}/\text{pixel}$ can be obtained for a sufficiently large subject window of 12 x 8mm. The images from the underwater camera system are analysed using MATLAB image processing toolbox. Several operations are applied to the raw images prior to statistical analysis, including contrast stretching, grayscale to binary conversion, background noise removing, dilation and erosion, and on-border incomplete objects removing. This underwater camera system, as well as the image processing program, is sufficient to find the time variation of FSDs with minimum particle size around $4\mu\text{m}$ (i.e. using 2 x 2 pixels).

Results and conclusions

This cylindrical tank experiment provides a valuable dataset dedicated to verify the One-Dimensional (1-D) Floc Size Distribution (FSD) under selected flow and sediment conditions. Although this is a conceptual 1-D model, i.e. along the streamline, it can be applied to the typical vertical 1-D simulation. The only difference is to couple with a vertical 1-D hydrodynamics model (also submitted to this conference in another abstract by Maa *et al.*) for flow field and turbulence information required in Eq. 1. While demonstrating the evolution of FSDs in a laboratory tank, this underwater camera system can also be utilized for in-situ measurements.

References

- McGraw R. 1997. Description of aerosol dynamics by the quadrature method of moments. *Aerosol Science and Technology* 27:255-265.
- Prat O.P. and J.J. Ducoste 2006. Modeling spatial distribution of floc size in turbulent processes using the quadrature method of moment and computational fluid dynamics. *Chemical Engineering Science* 61:75-86.
- Shen X. and J.P.Y. Maa Modeling floc size distribution of suspended cohesive sediment using quadrature method of moments: Comparison with available data. Submitted to *Marine Geology*.

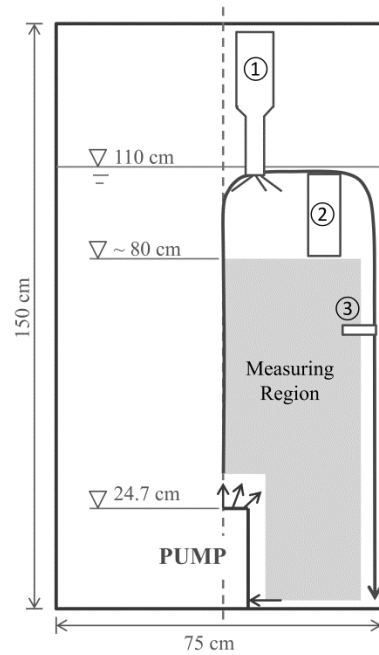


Fig. 1. Experimental setup (not to scale):

- ① ADV;
- ② Underwater Camera System;
- ③ OBS.

Modeling floc dynamics observed during the OASIS experiment

Sherwood Christopher R.¹, Alfredo Aretxabaleta¹, Romaric Verney², Emmanuel Boss³ and Peter Thorne⁴

¹ U.S. Geological Survey
384 Woods Hole Road, Woods Hole, Massachusetts 02543 USA
E-mail: csherwood@usgs.gov, aaretxabaleta@usgs.gov

² Laboratoire Dyneco/Physed, IFREMER
PO Box 70, 29280 Plouzané, France

³ Univeristy of Maine
Orono, Maine, USA

⁴ National Oceanography Centre
Liverpool, UK

The 2011 OASIS (Optics, Acoustics and Sediments In Situ) Experiment provided unique observations of particle distributions in the bottom boundary layer of the inner shelf. The observations were made at the Martha's Vineyard Coastal Observatory (Massachusetts, USA) at 12-m water depth with instruments mounted on a moving arm that obtained profiles of optical and acoustic measurements between about 0.5 and 2m above the sea floor (Sherwood *et al.*, 2012). The measurements reveal resuspension and settling of flocs and fine sand, and evolution of the particle field through floc dynamics (aggregation and disaggregation). We have simulated these processes using a coupled modelling system that links a wave model (SWAN) with a three-dimensional hydrodynamic model (ROMS) and with a mixed-sediment model that includes the floc-dynamics model FLOCMOD (Verney *et al.*, 2011). In addition, we have modelled the response of our sensors to the simulated particle field using optical response to particle areas and recently developed functions for acoustic response to floc volumes (Thorne *et al.*, 2014). Simulations with this modelling system reproduced the measured bottom stress and sand resuspension, and generated an evolving floc population that captured some of the features observed during the experiment. In particular, the model resuspended fine cohesive material and generated larger flocs during times of increased wave-current stresses, and the flocs settled rapidly during less energetic conditions. Shear-induced disaggregation was confined to the bottom-most layer of the model, also consistent with observations. However, the model did not reproduce features we attribute to lateral advection, or the low concentrations of large flocs observed during a period of low wave energy and neap tides. The model was sensitive to floc-model coefficients (for example, aggregation- and disaggregation-rate coefficients) and the sediment flux conditions imposed at the bottom boundary. The model results demonstrate the relative advantages of optical and acoustic sensors, and the need for both to measure concentrations of flocs and sand. The model also highlighted some of the difficulties in reproducing realistic floc conditions, including numerical challenges (computational cost and solution of stiff non-linear equations), uncertainty about floc behaviour during deposition and erosion, the role of biogenic contributions to the floc population, and the data requirements for setting initial and boundary conditions in a spatially explicit domain.

References

- Sherwood C.R., P.J. Dickhudt, M.A. Martini, E.T. Montgomery and E.S. Boss. 2012. Profile measurements and data from the 2011 Optics, Acoustics, and Stress In Situ (OASIS) project at the Martha's Vineyard Coastal Observatory: U.S. Geological Survey Open-File Report 2012-1178, at <http://pubs.usgs.gov/of/2012/1178/>.
- Thorne P.D., I.T. MacDonald and C.E. Vincent. 2014. Modelling acoustic scattering by suspended flocculating sediments. *Continental Shelf Research*, 88: 81-91. doi: 10.1016/j.csr.2014.07.003.
- Verney R., R. Lafite, J. Claude Brun-Cottan and P. Le Hir. 2011. Behaviour of a floc population during a tidal cycle: Laboratory experiments and numerical modelling. *Continental Shelf Research*, 31: S64-S83. doi: <http://dx.doi.org/10.1016/j.csr.2010.02.005>.

Erosion thresholds and rates for sand-mud mixtures

Smith S. Jarrell, David Perkey and Anthony Priestas

U.S. Army Engineer Research and Development Center
3909 Halls Ferry Road; Vicksburg, Mississippi, USA 39180
E-mail: Jarrell.Smith@usace.army.mil

Background

The differences in erosion behaviour of non-cohesive (sand, gravel) and cohesive sediments (mud) are widely recognized (Mehta, 1989; Mitchener and Torfs, 1996; Jacobs *et al.*, 2011). Erosion of non-cohesive sediments is dependent primarily upon the balance of weight, buoyancy, drag, and lift forces on the sediment grains, which in turn are associated with the size, density, and shape of the particles. Cohesive sediment erosion is largely influenced by electrochemical bonding between sediment particles. This cohesive bonding is influenced by clay mineralogy, pore water chemistry, organic content, biological cementation, and bed density (among others).

In many natural environments, sand and mud are not completely separated and occur as mixtures. Significantly less research has been conducted on the erosion behaviour of sand-mud mixtures compared to the separate treatment of sand erosion and mud erosion. Mitchener and Torfs (1996) found that adding sand to mud or mud to sand resulted in increased erosion resistance. Their study found that as little as 3-15 percent mud added to sand changed the erosion behaviour from non-cohesive to cohesive. The findings of van Ledden *et al.* (2004), Barry *et al.* (2006), and Jacobs *et al.* (2011) are similar to Mitchener and Torfs (1996); however each of these studies focus on the influence of mud fraction on the critical shear stress for initiation of erosion and very little on the effect of the mud fraction on the erosion rates. Additional research is required to define the effect of mud content on both the critical stress for erosion and erosion rate of mixed sediments (Jacobs *et al.*, 2011).

Erosion experiments were conducted on sand-mud mixtures with varying mud content to define the relationships between mud content, critical stress for erosion, and erosion rate. These experiments aim to improve the general understanding of erosion of sand-mud mixtures and to inform development of mixed sediment algorithms for sediment transport models.

Methods

Erosion experiments were conducted with Sedflume (McNeil *et al.* 1996) on a suite of mixed sediment beds prepared in the laboratory. Sedflume consists of a 100-cm long, 2 x 10cm cross-section rectangular duct with a test section milled into the bottom of the flume for inserting 10-cm diameter sediment cores. The mixed sediments for this study were prepared by mixing varying fractions of mud with well-sorted quartz sand ranging in size from 250 to 500 μ m. Sand-mud mixtures were prepared with three mud sources: 1) non-swelling clay (kaolinite), 2) swelling clay (kaolinite/bentonite), and 3) a natural mud collected from the lower Mississippi River. The mud fraction (by sediment mass) ranged from 0 - 100 percent according to the schedule presented in Table I. The mud was prepared as a 1.40g/l slurry, which was mixed with the corresponding proportions of sand and placed into the sediment cores to a depth of approximately 30cm. The sediment mixtures were fully saturated with fresh water and allowed to consolidate for 30 days prior to erosion with Sedflume. Five log-distributed shear stresses were applied to the surface of the core in a sequence that was repeated five times for each sample. A least-squares fit of $E = A\tau^n$ was performed for each sample (where E is erosion rate in cm/s, A and n are the fit parameters, and τ is applied shear stress in N/m² (Pa)). The critical shear stress is defined by the erosion rate of 10⁻⁴cm/s and was estimated for each sample from the least-squares fit.

Table I. Sand/mud mixtures for erosion experiments

	Weight % Mud														
Non-Swelling Clay	0	1	2	3	4	5	8	11	15	21	29	40	60	80	100
Swelling Clay	0	1	2	3	4	5	8	11	15	21	29	40	60	80	100
Natural Mud	0	1	2	3	4	5	8	11	15	21	29	40	60	80	100

Results

Similar to previous research of Mitchener and Torfs (1996) and Jacobs *et al.* (2011), the critical shear stress of the mixed sediments significantly departs from that of pure sand with mud fractions on the order of 2-10% (Fig. 1). The peak τ_{cr} for both mixtures occurs near 30% mud content, and the

kaolinite/bentonite mud achieves a ten-fold increase in τ_{cr} , whereas τ_{cr} for the kaolinite clay increases by a factor of five. At low mud content, erosion rates (Fig. 2) decrease by a factor of 10 to 100 with little change in the critical shear stress. Similar to the critical shear stress, minimum erosion corresponds to approximately 30% mud by mass. Erosion analysis for the natural mud mixture is in progress and will be available for presentation at the conference.

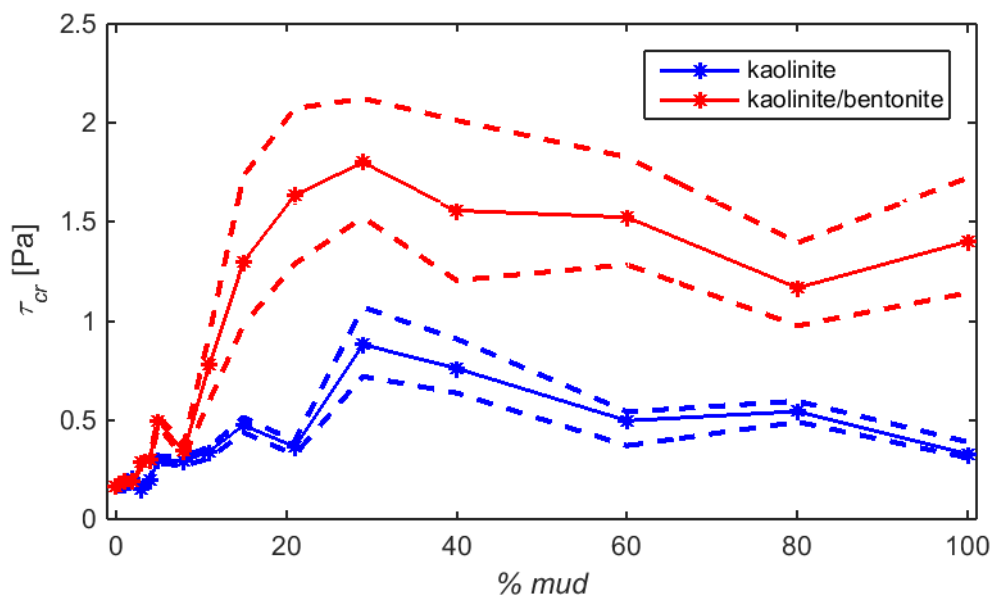


Fig. 1. Critical shear stress versus mud content for two (of three) mixed sediments. The solid lines and markers indicate the best estimate of τ_{cr} and the dashed lines indicate the 95% confidence interval.

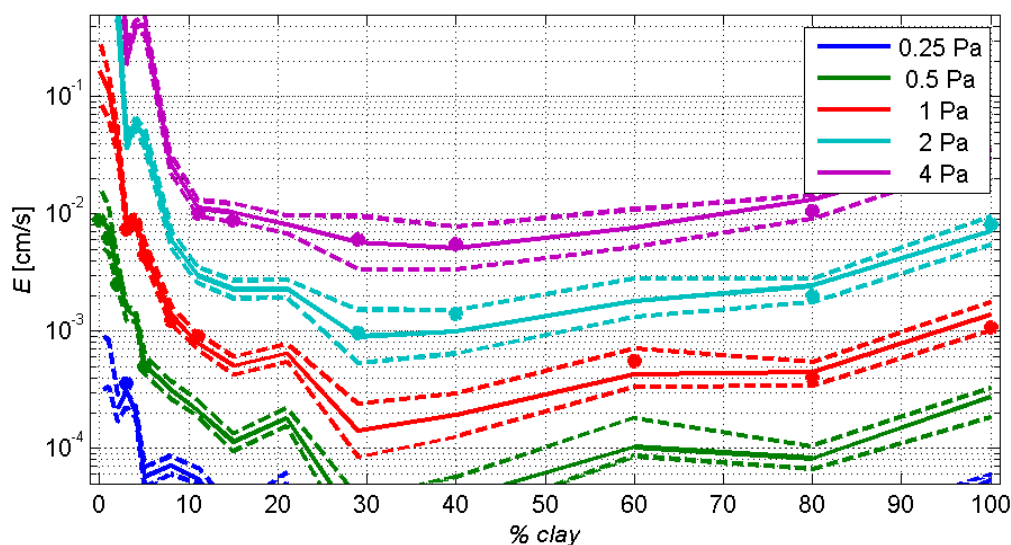


Fig. 2. Erosion rate versus mud content for the mixed sediment prepared with kaolinite. Markers indicate data from the experiments, solid lines are derived from the fit of $E = Ar^n$ to the data, and dashed lines indicate the 95% confidence interval on the estimates.

References

- Barry K.M., R.J. Thieke and A.J. Mehta. 2006. Quasi-hydrodynamic lubrication effect of clay particles on sand grain erosion. *Estuarine Coastal and Shelf Science* 67:161-169.
- Jacobs W., P. Le Hir, W. Van Kesteren and P. Cann. 2011. Erosion thresholds of sand-mud mixtures. *Continental Shelf Research* 31(10):S14-S25.
- McNeil J., C. Taylor and W. Lick. 1996. Measurements of erosion of undisturbed bottom sediments with depth. *Journal of Hydraulic Engineering* 122(6):316-324.
- Mehta A.J. 1989. On estuarine cohesive sediment suspension behaviour. *Journal of Geophysical Research* 94(C10):14303-14314.
- Mitchener H. and H. Torfs. 1996. Erosion of mud/sand mixtures. *Coastal Engineering* 29:1-25.
- Van Ledden M., G.G.M. van Kesteren and J.C. Winterwerp. 2004. A conceptual framework for the erosion behaviour of sand-mud mixtures. *Continental Shelf Research* 24:1-11.

Numerical modelling of wave and non-Newtonian mud interaction

Soltanpour Mohsen, Sami Saeideh and Hejazi Kourosh

Civil Engineering Department, K. N. Toosi University of Technology,
PO Box 15875-4416, Tehran, Iran
E-mail: soltanpour@kntu.ac.ir

Introduction

An extensive experiment and field measurements show surface waves attenuate significantly at muddy coasts and estuaries. Moreover, strong waves can force the mud particle movements resulting the mass transport of fluid mud layer. One noteworthy element in modelling these phenomena of wave-mud interaction is a description of the rheology of the mud. Owing to the geo-environmental conditions and diverse chemical/biological compositions, it is reasonable to expect that mud at different localities and in different periods of time may exhibit vastly different rheological behaviours. Different constitutive equations of viscoelastic (e.g. Kelvin-Voigt, Maxwell and Jeffreys), viscoplastic (e.g., Bingham, Casson and Herschel-Bulkley plastics) and visco-elastic-plastic models as well as site-specific empirical formulas have been widely used in the past to represent the rheological behaviour.

The objective of this study is to implement various viscoelastic and viscoplastic rheological models of the non-Newtonian fluid mud in numerical modelling of wave-mud interaction. The two-dimensional numerical model of Hejazi *et al.*, (2013), originally developed for two-layer of viscous mud-fluid system, is extended to both viscoelastic and viscoplastic non-Newtonian continua in order to simulate the wave and non-Newtonian mud interaction.

Numerical solution

The numerical model uses a structured non-orthogonal curvilinear staggered mesh and is capable of simulating non-homogeneous, stratified flow fields. The linearized equations of motion for a compressible viscoelastic medium, including both viscous and elastic responses, and FVM non-hydrostatic RANS equations of viscoplastic fluids are solved using the projection method.

The stress tensor in momentum equations of viscoplastic mud is related to the rate-of-distortion, $\dot{\gamma}$, and usually is expressed as follows:

$$\tau = \mu \dot{\gamma} \quad (1)$$

For a Newtonian fluid, μ presents a constant viscosity. However, a viscosity function for a general viscoplastic fluid is given by:

$$\mu = \mu(|\dot{\gamma}|) \quad (2)$$

where $|\dot{\gamma}| = \sqrt{0.5 \text{tr}(\dot{\gamma}^2)}$ is the second invariant of the rate of the deformation tensor. Then the constitutive equation for viscoplastic fluids may be written as follows:

$$\tau = \mu(|\dot{\gamma}|)\dot{\gamma} \quad (3)$$

where $\mu(|\dot{\gamma}|)$ is referred as the effective viscosity. Hence the viscosity varies in space and time according to the variation of the deformation-rate. Therefore in each time step, the second invariant of the deformation-rate tensor is calculated from the velocity field and then the corresponding viscosity of each cell is determined according to the rheological equation. The overall numerical solution for viscoplastic mud is obtained in two steps. In the first step the pressure gradient terms are omitted from the momentum equations, and the unsteady equations are advanced in time to obtain a provisional velocity field. The provisional velocity is corrected by accounting for the pressure gradient and the continuity equation in the second step. The water elevation is computed through the solution of the free surface equation obtained from the application of normal and tangential dynamic boundary conditions, and the integration of the continuity equation across the depth. The interface elevation is obtained by the application of the integration of continuity equation over mud depth and the kinematic boundary conditions at bed and the interface.

Results

To test the capability of the modified numerical model for simulating the relatively strong interaction between non-linear wave and uneven bottom, periodic wave propagation over a submerged bar was modelled first. The comparisons of the free-surface elevation simulations with the measured values of the experiments carried by Beji and Battijes (1994), at seven wave gauge locations, show good agreements. As an example of the model applications on interaction of wave and non-Newtonian fluid mud, the simulated results have been compared with the laboratory

measurements reported by Hsu *et al.*, (2013). The rheological experiments indicate that mud behaves as a non-Newtonian fluid, where the yield stress and the shear thinning effect depend on both shear rate and mud concentration. The suggested rheological model exhibits hybrid properties of a Bingham and pseudo-plastic fluid. Numerical prediction of surface wave elevation at three different wave gauges in comparison with measured data show good agreements (Fig. 1). Fig. 2 shows the surface wave height variation across the mud layer. The linear model of Dalrymple and Liu (1978) with an exponential wave height decay has also been plotted. Comparisons of the velocity profile in the water and mud layers for the predicted results of the model against experimental data and linear model have been presented in Fig. 3.

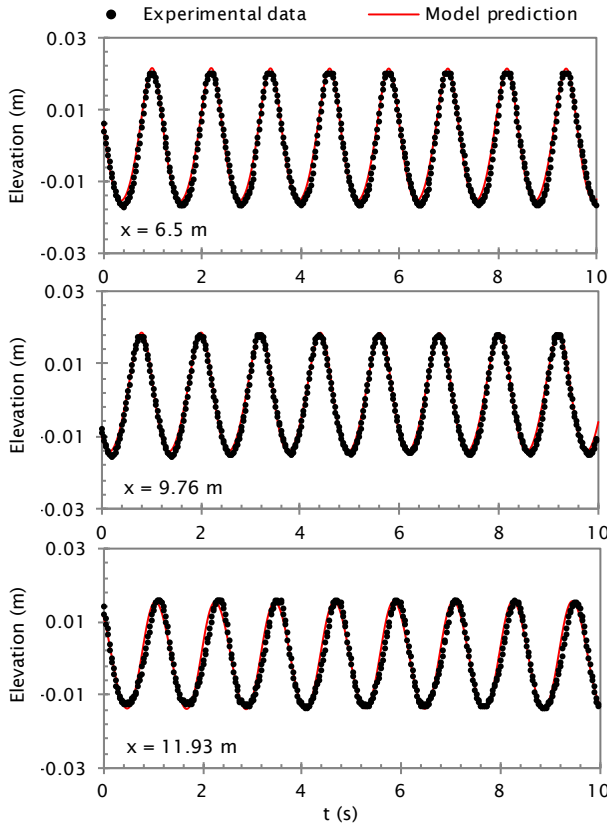


Fig. 1. Free-surface elevation at three wave gauge locations ($H_0 = 0.04\text{m}$, $T = 1.2\text{s}$, water depth = 0.24m , mud depth = 0.06m , mud density = 1420kg/m^3 , bulk density = 2500kg/m^3).

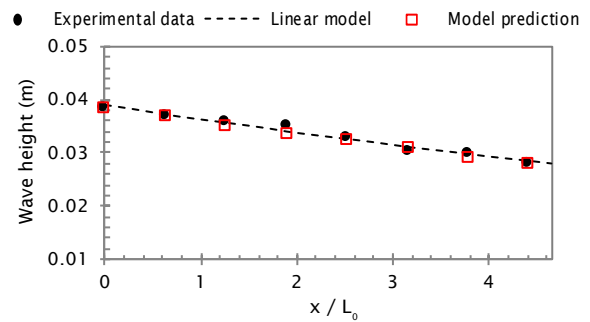


Fig. 2. Wave attenuation ($H_0 = 0.04\text{m}$, $T = 1.2\text{s}$, water depth = 0.24m , mud depth = 0.06m).

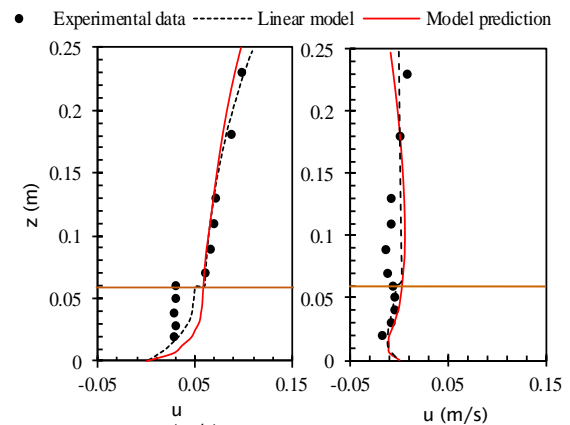


Fig. 3. Velocity profiles at wave crest and flow reversal ($H_0 = 0.04\text{m}$, $T = 0.9\text{s}$, water depth = 0.24m , mud depth = 0.06m).

Conclusions

A 2DV numerical model has been proposed for the simulations of a two-layer mud-fluid system, where the mud behaviour is considered like a non-Newtonian fluid. The decay rate and wave shape predicted by the numerical model are in agreement with the measured data. Above the water-mud interface, where the flow is not affected by the rheological stress, the linear model proposed by other researchers and the present model agree well with the measured velocity profiles. The velocity decreases significantly approaching the bottom mud layer with a clear boundary at the water-mud interface. The results also show that although the present model affords for the simulation of non-linear wave propagation, the linear model also provides satisfactory results.

References

- Beji S. and J.A. Battijes. 1994. Numerical simulation of non-linear waves propagation over a bar. *Coastal Engineering* 23:1-16.
- Dalrymple R.A. and P.L.-F. Liu. 1978. Waves over soft muds, a two-layer fluid model. *Journal of Physical Oceanography* 8:1121-1131.
- Hejazi K., M. Soltanpour and S. Sami. 2013. Numerical modelling of wave-mud interaction using projection method. *Ocean Dynamics* 63:1093-1111.
- Hsu W.Y., H.H. Hwung, T.J. Hsu, A. Torres-Freyermuth and R.Y. Yang. 2013. An experimental and numerical investigation on wave-mud interactions. *Journal of Geophysical Research: Oceans* 118:1126-1141.

Calibration of sediment parameterizations to simulate the turbidity maximum in a highly turbid estuary: integration of model, field and satellite data

Sottolichio Aldo, Isabel Jalon Rojas and Sabine Shmidt

EPOC Laboratory, University of Bordeaux, UMR CNRS 5805
F-33615 Pessac Cedex, France
E-mail: aldo.sottolichio@u-bordeaux.fr

Numerical modelling of turbidity maximum in macrotidal estuaries requires a robust hydrodynamical model coupled to a sediment transport model that accounts for the fundamental sediment processes. In theory, an exhaustive number of physical processes affecting cohesive sediment are needed. However, the deterministic simulation of turbidity patterns in large estuaries is often obtained through a limited number of simplified parameterization, which have been carefully calibrated.

The Gironde Estuary (Bay of Biscay, SW France) is a macrotidal estuary characterized by a high-concentrated turbidity maximum. A key issue during the last years was to grade the basic mechanisms inducing fine sediment trapping. This was achieved by a 3D numerical model which simulated turbidity in academic situations. In this work we apply the 3D model to reproduce realistic turbidity maximum and to explore sensitivity to sediment parameterization. Because of the lack of knowledge on physical properties of flocs in the Gironde, the parameterization of the settling velocity is based on comparisons with time series of surface suspended sediment concentration (SSC). A settling velocity ranging from 0.1 to 2mm.s⁻¹ is found to be the best adjustment to reproduce satisfactory the dynamics of measured turbidity, as well as to ensure the persistence of the turbidity maximum over time. The comparison with satellite imagery shows that the model reproduces well the geometry of the turbidity maximum at different seasons. In the lower estuary, the lateral suspended sediment flux from the main navigation channel to the eastern bank promotes the transfer of sediment towards the downstream part of the estuary and the escape of sediment through the mouth. One-year simulations allow the study of the mass budget in the estuary over seasonal cycles. These confirm the main role of tidal asymmetry on the turbidity maximum formation, and the secondary role of density gradients to maintain a stable mass of suspended sediment within the estuary. Moreover, the sensitivity of the turbidity maximum to sediment erodibility and to the process of consolidation is discussed.

Flocculation, self-similarity and the rheology of aqueous clay suspensions

Spearman Jez

HR Wallingford, Howbery Park, Wallingford, Oxon, OX8 10BA, UK

E-mail: j.spearman@hrwallingford.com

A dense cohesive sediment suspension, sometimes referred to as fluid mud, is a thixotropic fluid with a true yield stress. Its time-dependent rheological behaviour can be described by the structural kinetics theory, based on the Worrall-Tuliani (1964) approach, in which the fluid is described as a non-ideal Bingham fluid and the yield stress is taken as a measure for the structural parameter (Toorman, 1997). For a fluid in equilibrium (exposed to a constant shear rate for a sufficiently long time), the shear stress is given by,

$$\tau = \tau_0 + \mu_\infty \dot{\gamma} + \frac{c\dot{\gamma}}{1+\beta\dot{\gamma}} \quad (1)$$

where τ is the shear stress, τ_0 is the yield stress at equilibrium, $\dot{\gamma}$ is the shear rate, μ_∞ is the Newtonian viscosity of the suspension at high shear rate, $c = \mu_\infty - \mu_0$, μ_0 is the viscosity associated with low shear rate and β is a constant.

The Worrall-Tuliani approach requires 4 empirical values for $\tau_0, \mu_\infty, c, \beta$ (and 2 more empirical constants for identifying the transient behaviour). However, in a time varying cohesive sediment suspension these empirical values depend on the sediment concentration. This makes the Worrall-Tuliani approach unwieldy for use in sediment transport studies where sediment concentrations are constantly changing.

This paper is concerned with establishing a framework for establishing values for the constants, μ_∞ , c and β , which is valid for the whole range of sediment concentrations from the yield-point to Newtonian flow. The shear stress equation is re-constructed from first principles using an approach, based on floc fractal theory, put forward by Mills and Snabre (1988). This results in a Casson-like rheology equation which defines the value of μ_∞ in terms of the sediment concentration. Structural kinetics theory (Moore, 1959) is then added to this equation, giving an equation similar to Equation (1). The form of c and β are derived by comparison of the resulting equation with the results of Coussot (1995). Application of the self-similar relationships found by Coussot indicates that $c \sim c(\tau_0, \mu_\infty)$ while β remains an empirical constant. The resulting rheological equation for equilibrium conditions is as follows

$$\tau^{1/2} = \tau_0^{1/2} + \left(1 + \frac{\alpha(\tau_0/\mu_\infty)^m}{1+\beta\dot{\gamma}^m}\right)^{1/2} (\mu_\infty \dot{\gamma})^{1/2} \quad (2)$$

where α and m are empirical constants. This equation contains the same number of empirical unknowns (τ_0, α, β, m) as Equation 1 but of these only τ_0 is a function of the sediment concentration.

An example of the comparison of Equation 2 against data derived by Coussot (1995) for kaolinite in freshwater is shown in Fig. 1. Additional comparisons with other data sets are presented in the paper.

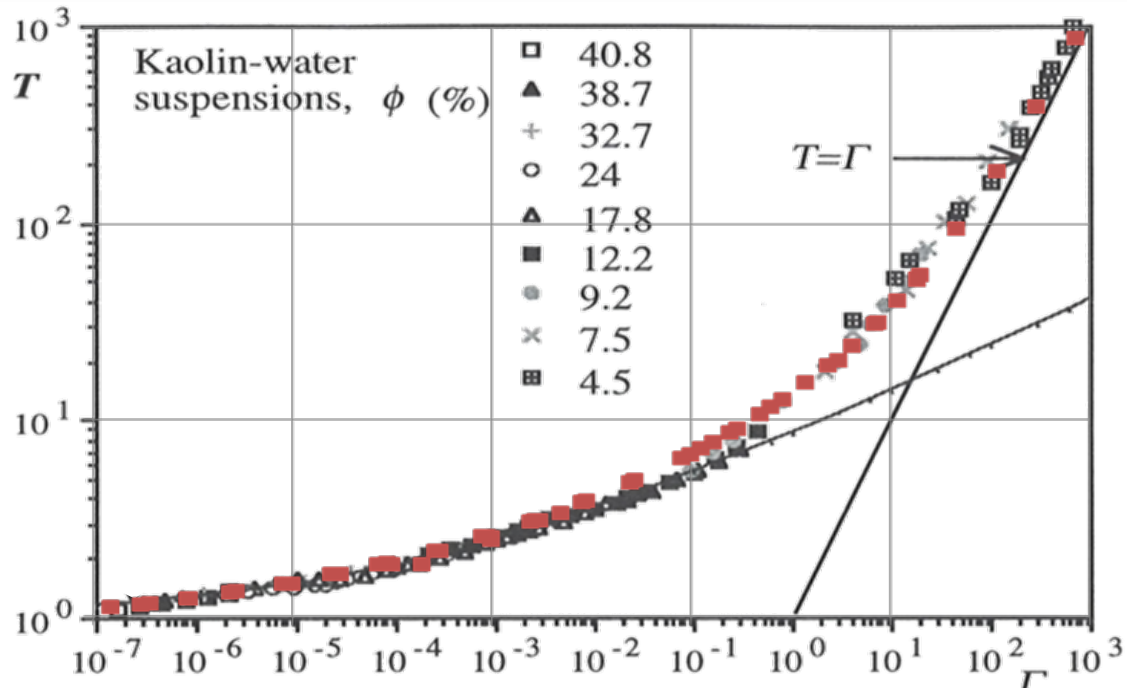


Fig. 1. Comparison of Equation 2 with data from Coussot (1995). The values of T and Γ on the axes are given by $T = \left(\frac{\tau}{\tau_0}\right)$. $\Gamma = \left(\frac{\dot{\gamma}\mu_{\infty}}{\tau_0}\right)$.

References

- Coussot P. 1995. Structural similarity and transition from Newtonian to non-Newtonian behaviour for clay-water suspensions. *Physical Review Letters* 74(20):3971-3974.
- Mills P. and P. Snabre. 1988. The fractal concept in the rheology of concentrated suspensions. p.105-108. In: *Progress and Trends in Rheology II*. Giesekus H. *et al.*, (Eds). Springer-Verlag, Berlin, Heidelberg.
- Moore F. 1959. The rheology of ceramic slips and bodies. *Trans. Brit. Ceramic Soc* 58:470-494.
- Toorman E. 1997. Modelling the thixotropic behaviour of dense cohesive sediment suspensions. *Rheol. Acta* 36:56-65.
- Worrall W.E. and S. Tuliani. 1964. Viscosity changes during the ageing of clay-water suspensions. *Trans. Brit. Ceram. Soc.* 63:167-185.

Rheology and local study of a transparent model cohesive sediment

Tarhini Zaynab, Sébastien Jarny and Alain Texier

Pprime Institute, UPR 3346 CNRS, University of Poitiers, SAE ENSMA, PO Box 30179, 86962
Futuroscope Chasseneuil Cedex, France
E-mail: zaynab.tarhini@univ-poitiers.fr

A transparent model sediment with the same rheological properties than a natural one is used to study erosion in a narrow channel or a flume. Optical measurements allow accessing to local velocity fields within water and transparent sediment simultaneously.

Introduction

A cohesive sediment is a complex material of inorganic mineral, organic material and biological functions lead to viscoplastic and thixotropic characteristics (Toorman, 1997). To characterize their erosion two parameters are to be identified: bed shear stress from hydrodynamic forces and erosion rate from suspended sediment concentration. In a macroscopic framework, previous experimental studies on erosion have already defined different thresholds sediment behaviour (Van Rijn, 1993; Jacobs *et al.*, 2011). This study is based on the development of transparent model cohesive sediment to allow optical measurements and lead to local kinematic information during erosion tests. First, the transparent cohesive sediment is elaborated with similar rheological properties than a natural one (Pouv *et al.*, 2014). Secondly, erosion tests are carried out of the flume using particle image velocimetry (PIV) both to lead to, in the same time, the water velocity field and the displacements of the transparent sediment.

Material development

The transparent model cohesive sediment is prepared with classical modifier agent of viscosity: synthetic clay, laponite RD (Rockwood), and polymer, carboxymethylcellulose (Prolabo). Laponite leads to thixotropic properties and carboxymethylcellulose (CMC) enhances viscoplastic effects of the mixture.

CMC solution is prepared first with powder sprinkle in deionized water in 0.5% mass concentration. The solution is stirred at 600rpm with a magnetic agitator for 1 hour. In the same time, Laponite suspension with 1% mass concentration is prepared sprinkling laponite powder in deionized water. The suspension is then mixed during 15 minutes at 11000rpm with a homogenizer Ultraturax T25 (IKA). Finally the laponite suspension is added to the CMC solution for 1 hour mixing at 1100rpm with the magnetic agitator. The transparent sediment has a density close to $1\text{kg}\cdot\text{m}^{-3}$.

Rheological measurements

The rheological characterisation of the transparent sediment is carried out with a HR-2 rheometer (TA Instruments) using plate-plate geometry of 4cm diameter. Both surfaces are covered with sand paper with a mean roughness of $58.5\mu\text{m}$ to prevent slippage effects. Each measurement is realised for a $300\mu\text{m}$ gap. Before flow curve measurements and to ensure a reproducible proceeding a pre-shear is applied with a shear rate of 10s^{-1} during 120s following by a 600s rest period. Then shear rate steps ranging from 10^{-3} to 10^3s^{-1} are applied in a logarithmic repartition to obtain up and down curves. Each curve is corrected using Rabinowicz formula to minimize existing error on the estimation of shear rate by using plate-plate geometry.

Rheological properties of the transparent sediment evolve with time but reach to a stable state after 20 days. It has been confirmed by following rheological properties of the sediment throughout 35 days.

To study the relation between rheological properties and concentration, a range up from 20% to 70% (mass concentration) was done from the transparent sediment which has a solid fraction of 10g/l. Hereafter solid part is representing by CMC and laponite particles.

The down curves of each obtained rheogram follow a Herschel-Bulkley model:

$$\begin{cases} \tau = \tau_s + k\dot{\gamma}^n & \text{for } \tau \geq \tau_s \\ \dot{\gamma} = 0 & \text{for } \tau < \tau_s \end{cases} \quad (1)$$

Where τ is the shear stress, $\dot{\gamma}$ the shear rate, τ_s the yield stress, k the consistency and n the viscosity index.

Flow curves are well classified as a function of the concentration (Fig. 1a): lowest concentration leads to a small yield stress, weak consistency and viscosity index tending to 1. Evolution of the yield stress as a function of solid fraction can be fitted with a power law model (Migniot, 1989; Berlamont *et al.*, 1993) (Fig. 1b).

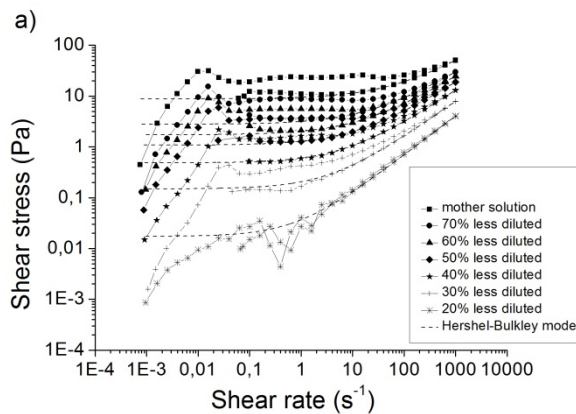


Fig. 1a. Rheogram of transparent sediment and their diluted concentrations fitted with Herschel-Bulkley model.

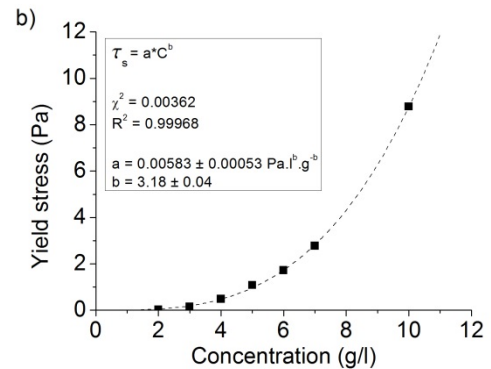


Fig. 1b. Yield stress from Herschel-Bulkley model as a function of concentration.

Flume measurements

Experiments are realised in a transparent PMMA flume with a square section (160mmx160mm). The channel is close to obtain bounded flow which is easier to control and prevent from the gravity effect. Hydraulic pumps allow to apply an average velocity up to 5cm.s⁻¹. Particle image velocimetry (PIV) measurements are obtained from a Yag laser and CCD cameras devices. Two different lighting seeds are used in order to distinguish water velocity fields (standard seeds) and transparent sediment (fluorescent seeds).

First, channel measurements are realised only with water to obtain hydrodynamic conditions in the reference simplest case (no sediment). Then, the visualized channel background is replaced with the transparent sediment which has almost the same refractive index than the water. Comparisons between flow fields obtained with these two configurations can be conducted.

Conclusion

A transparent model sediment with the same rheological properties as a natural one is used to study erosion in a flume. Optical measurements allow to access to local velocity fields within water and transparent sediment simultaneously. The kinematic evolutions of the two fluids are distinguished using two different lighting seeds. This work is the first step of a kinematic and dynamic study to understand local phenomena operating during erosion processes. A next step will be to add concentration measurements in the same time as PIV. Combined with the rheological data, the final goal of this new study is to rebuild the local shear stress field during erosion experiments.

References

- Berlamont J., M. Ockenden, E.A. Toorman and J. Winterwerp. 1993. The characterization of cohesive sediment properties. *Coastal Engineering* 21:105-128.
- Jacobs W., P. Le Hir, W. Van Kesteren and P. Cann. 2011. Erosion threshold of sand-mud mixtures. *Continental Shelf Research* 31:14-25.
- Migniot C. 1989. Tassement et rhéologie des vases. Deuxième partie. *La houille blanche* 2 :95-111.

- Pouv K.S., A. Besq, S. Guillou and E.A. Toorman. 2014. On cohesive sediment erosion: A first experimental study of the local processes using transparent model material. *Advances in Water Resources* 72:71-83.
- Toorman E.A. 1997. Modelling the thixotropic behaviour of dense cohesive sediment suspensions. *Rheologica Acta* 36:56-65.
- Van Rijn L. 1993. Principles of sediment transport in rivers, estuaries and coastal seas. Aqua Publications: Amsterdam. ISBN 90-800356-2-9. vi, 715p.

Examining flocculation processes using multi-frequency acoustics

Thorne Peter D.¹, Iain T. MacDonald² and Christopher E. Vincent³

¹ National Oceanography Centre, Joseph Proudman Building, 6 Brownlow Street, Liverpool, L3 5DA, United Kingdom
E-mail: pd@noc.ac.uk

² National Institute of Water and Atmospheric Research, Hamilton, Waikato, 3216, New Zealand

³ School of Environmental Sciences, University of East Anglia, Norwich, NR4 7TJ, United Kingdom

The modelling of sediment transport is still a developing area and this is particularly true in environments where the process of flocculation occurs. In such environments modelling is underpinned by observations and the use of acoustic profiling systems to investigate water column hydrodynamics and suspended sediments is commonly employed (Sherwood *et al.*, 2011). In general to extract the suspended sediment concentration from the acoustic measurements, physical samples of the water column are collected and used to calibrate the acoustic system. This is a regular practice when ADCP backscattered signal levels are utilised to monitor suspended load. Problems arise in the interpretation of the suspended load from the backscattered signal in fine sedimentary environments if flocculation takes place. This occurs because the interpretation of the acoustic signals backscattered from the flocculating sediments is problematic due to a lack of understanding of the interaction of sound with flocs. This deficiency has impeded sound being used to extract quantitative suspended sediment parameters in suspensions containing flocs.



Fig. 1. A view over the mixed sediment River Dee estuary, UK, at sunset.

As a step towards practically solving acoustic scattering by flocculating suspensions, a relatively simple heuristic approach has been adopted. A model is presented for the interpretation of acoustic scattering from a suspension of fine sediments as they transition from primary particles, through an intermediate regime, to the case where low density flocs dominate the acoustic scattering. The approach is based on spherical elastic solid and elastic fluid scatterers and a combination of both (Thorne *et al.*, 2014). To evaluate the model the variation of density and compressional velocity within the flocs as they form and grow in size is required. The density can be estimated from previous studies; however, the velocity is unknown and is formulated here using a fluid mixture approach.

To assess the proposed model, predictions are compared with recently published laboratory observations of acoustic scattering by flocculating cohesive suspensions (MacDonald *et al.*, 2013). The results from this study and its application to using multi-frequency acoustic systems to investigate flocculation processes in an estuarine environment will be examined. The extension of the application of acoustics measurements to suspensions of sand-mud mixtures will also be explored. These developments will improve measurement techniques in flocculating environment,

which, in turn, will contribute to improving our modelling capability in mixed sediment environments (Amoudry and Souza, 2011).

References

- Amoudry L.O. and A.J. Souza. 2011. Deterministic coastal morphological and sediment transport modelling: A review and discussion. *Rev. Geophys.* 49. RG2002, doi:10.1029/2010RG000341.
- MacDonald I.T., C.E. Vincent, P.D. Thorne and P.D. Moate. 2013. Acoustic scattering from a suspension of flocculated sediments. *J. Geophysical Research: Oceans* 118:1-14. doi:10.1002/jgrc.20197, 2013.
- Sherwood C.R., P.J. Dickhudt, M.A. Martini, E.T. Montgomery and E.S. Boss. 2012. Profile measurements and data from the 2011 Optics, Acoustics, and Stress In Situ (OASIS) project at the Martha's Vineyard Coastal Observatory: US Geological Survey Open-File Report 2012-1178, at <http://pubs.usgs.gov/of/2012/1178/>.
- Thorne P.D., I.T. MacDonald and C.E. Vincent. 2014. Modelling acoustic scattering by suspended flocculating sediments. *Continental Shelf Research*, 88: 81-91. doi: 10.1016/j.csr.2014.07.003.

Interaction of suspended sediment and salt wedge in a river estuary

Tokuzo Hosoyamada¹, Ayurzana Badarch² and Takeshi Ohtake²

¹ Department of Civil and Environmental Engineering
Nagaoka University of Technology, 1603-1, Kamitomioka Nagaoka Niigata Japan, 940-2188
E-mail: rng@nagaoka.ut.ac.jp

² Graduate School of Energy and Environmental Eng., Nagaoka University of Technology,
1603-1, Kamitomioka, Nagaoka, Niigata, Japan, 940-2188

³ Graduate School of Civil Engineering, Nagaoka University of Technology,
1603-1, Kamitomioka, Nagaoka, Niigata, Japan, 940-2188

Estuarine turbidity maximums (ETM) are observed at the frontal zone between the fresh and saline waters in macrotidal estuary. Strong mixing process and interaction of sediment and salt wedge intrusion are supposed to make an influence on resuspension of sediment and turbidity transport. To understand the phenomena, the paper studies dynamics of the gravity head of salt wedge and its effects to sediment transport by means of numerical simulation based on Navier Stokes equation directly. Settling and resuspending flux at the riverbed is estimated by an empirical formulation. Effects of the gravity head reveal themselves remarkably in temporal development of velocity vectors, transport of suspended sediment, density deviation. Numerical results for total amount of sediment and vertical flux for resuspension and sedimentation are discussed.

Introduction

Estuaries act in a sense as a link between the limnetic and marine environments. One typical and very important region in estuary is the frontal zone between the fresh and saline water. In many estuaries, the front is characterized by salt wedge moving almost horizontally on a riverbed. The fluctuating flow fields caused by density difference may trigger resuspension of sediment and a peak of sediment concentration (estuarine turbidity maximum, ETM) on salt wedge (Burchard and Baumert, 1998).

The mechanics of density driven currents has been studied for a long time (Simpson and Britter, 1979). The research field is extending to so many fields such as volcanic dynamics, atmospheric dynamics for a macroscopic point of view, and chemical engineering for a microscopic point of view. Sediment and turbidity transport are studied in the field of river and coastal engineering. It is well known that the dynamics in estuary is characterized by a variety of complicated processes. Transport of suspended sediment or various elements of chemical substances in river flow are supposed to be influenced by salt wedge.

To understand such complicated processes (sediment and density transport together) by numerical simulation, the numerical scheme should be directory based on Navier-Stokes equation (NS eq.), which is essential of fluid dynamics. In this study, numerical results of density and sediment distribution and characteristics of fluid motion will be discussed.

Numerical methods

Governing equations for the unknown variables (velocities, pressure, sediments transport and density fluctuation) are incompressible continuity equation, NS eqs. and advection diffusion equations, which are shown in eq.(1),eq.(2), eq.(3) and eq.(4),respectively.

$$\frac{\partial u_i}{\partial x_i} = 0 \quad (1)$$

$$\frac{\partial u_i}{\partial t} + u_m \frac{\partial u_i}{\partial x_m} = -(1 + \frac{\Delta \rho}{\rho}) g \delta_{i2} - \frac{1}{\rho} \frac{\partial p}{\partial x_i} + \gamma_t \nabla^2 u_i \quad i = 1,2 \quad (2)$$

$$\frac{\partial \Delta \rho}{\partial t} + u_m \frac{\partial \Delta \rho}{\partial x_m} = D \nabla^2 \Delta \rho \quad (3)$$

$$\frac{\partial c}{\partial t} + u_1 \frac{\partial c}{\partial x_1} + (u_2 - w_s) \frac{\partial c}{\partial x_2} = D \nabla^2 c \quad (4)$$

Here, $i, u_i, t, x_i, g, \rho, \Delta \rho, p, t, c, w_s$ are suffix for vector components, $i (=1,2)$ component of velocity vectors, time, spatial coordinate for i direction, gravity acceleration, average density, density deviation, pressure, effective viscosity (turbulent and molecular), sediment concentration and sediment settling velocity. Temporal development of velocity vectors is calculated by integration of NS equation directly. To satisfy incompressible continuity condition, pressure-velocity simultaneous relaxation scheme, which is referred as SOLA method (Hirt, 1975) is used. Large eddy simulation

with Smagorinsky eddy viscosity model is used. Erosion flux and sedimentation flux through the riverbed are estimated as function of the bottom shear stress, critical shear stress and total amount of material for sediment.

Numerical results

Fig. 1. shows typical distribution of sediment, density, vorticity and vertical velocity. Sediment distribution has very high values at the top of the salt wedge, which is caused by high upper ward vertical velocity shown in Fig. 1 (vertical velocity). Interface between salt water and river water has wavy pattern. In pure water (upper part), horizontal velocity is higher than salt wedge and opposite direction to salt wedge (lower). In the interface of such region, the Kelvin-Helmholtz type instability occurs and vortex train is formed. In the paper, interaction of sediment and salt wedge, effects of surface water elevation to salt wedge will be discussed.

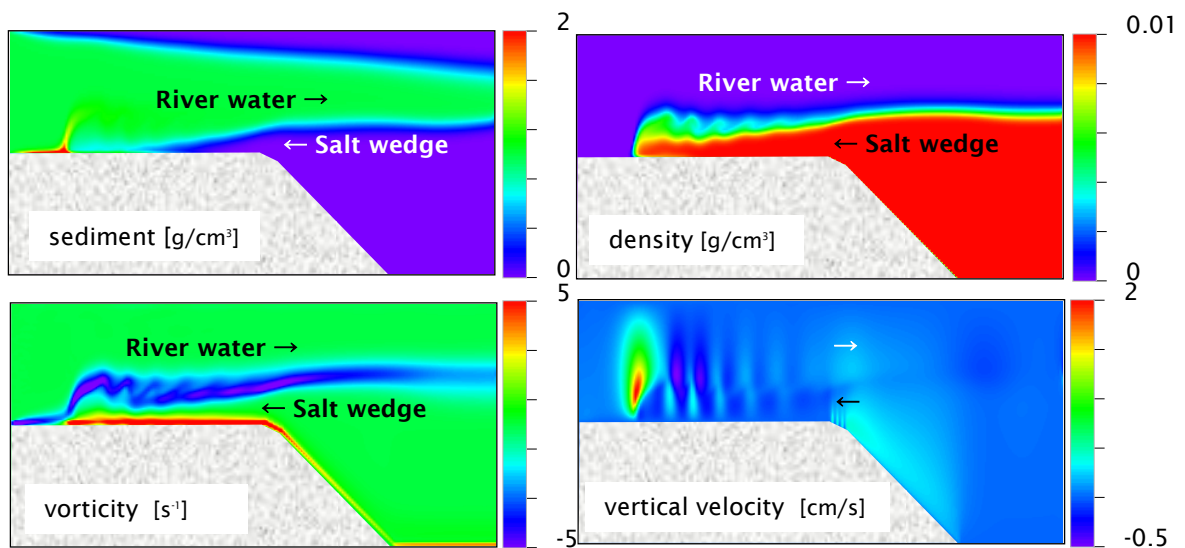


Fig. 1. Typical distribution of sediment, density, vorticity and vertical velocity

References

- Burchard H. and H. Baumert. 1998. The formation of estuarine turbidity maximum due to density effects in the salt wedge. A Hydraulic Process Study. *Journal of Physical Oceanography* 28:309-321.
- Simpson J.E. and R.E. Britter. 1979. The dynamics of the head of a gravity current advancing over a horizontal surface. *Journal of Fluid Mechanics* 94(3):477-495.

Drag on an object towed through a fluid mud layer: CFD versus experiment

Toorman E.A.¹, I. Vandebek¹, M. Liste-Muñoz^{1,6}, M. Heredia², I. Rocabado², J. Vanlede³, G. Delefortrie³, M. Vantorre⁴ and Y. Meersschaut⁵

¹ Hydraulics Laboratory, Department of Civil Engineering, KU Leuven, Kasteelpark Arenberg 40, B-3001 Leuven, Belgium
E-mail: erik.toorman@bwk.kuleuven.be

² Antea Group, Buchtenstraat 9, B-9051 Gent, Belgium

³ Flanders Hydraulics Research, Ministry of Mobility and Public Works, Berchemlei 115, B-2140 Antwerpen, Belgium

⁴ Department of Civil Engineering, Gent University, Technologiepark Zwijnaarde 904, B-9052 Zwijnaarde, Belgium

⁵ Maritime Access Department, Ministry of Mobility and Public Works, Antwerp, Belgium

⁶ present address: US Geological Survey, 384 Woods Hole Road, Woods Hole, MA 02543, USA

Introduction

The managing authorities of harbours and navigation ways are under increasing pressure to reduce the costs for maintenance dredging. Therefore, the Flemish Government has been investing in a unique and ambitious research programme to study the so-called *nautical bottom* problem, i.e. the search for a universal definition and a practical *in-situ* measurement technique for a (set of) parameter(s) which allows decision makers to accurately know when the passage of a ship over a mud bottom is without danger.

The traditional criterion for the nautical bottom is based on bulk density of the mud layer, because density is a characteristic which can be determined in a relatively easy way *in situ*. The typical critical value in many harbours is 1.2T/m^3 , but may vary in other places. However, this criterion implicitly assumes a unique and monotonous relationship between bulk density and bulk viscosity. Rheological measurements on fluid mud have indicated that it can be characterized as a yield stress fluid, with typical visco-elastic behaviour below yield and visco-plastic behaviour above yield. However, the parameters that describe this behaviour are found to change with time. To be more precise, due to the fact that fluid mud is a gel-forming water-cohesive sediment mixture (a weak, continuous 3D network of aggregated flocs), the bonds of the floc structures may break or reform depending on the deformation history. This is called thixotropy. Consequently, there is no unique relationship between nautical resistance and bulk density.

Research

Since the actual resistance experienced by a ship manoeuvring closely above or even in contact with a fluid mud layer depends on the kinematic history the ship and deformation history of the fluid mud layer, Flanders Hydraulics Research (FHR) has decided to start a research project to investigate the ability of CFD to simulate such manoeuvres. In the present first phase, the aim is to investigate whether it is possible to simulate with a numerical model a simple experiment where an object is towed through a fluid mud layer. The water layer is omitted at this stage in order to avoid the added complexity of the problem generated by the occurrence of multi-scale turbulence phenomena in this layer, which then need to be simulated as well.

The rheological model implemented in the CFD code is a corrected version of the structural kinetics model proposed by Toorman (1997) (Toorman *et al.*, 2014; Toorman, in prep.).

For this reason a towing test facility has been designed and built at FHR, where the drag force is continuously measured on an object towed at a controlled speed (Fig. 1). These data are used to validate a numerical simulation of the experiment, fed with rheological parameters determined by a specially designed protocol, partially based on Toorman (1994), applied to samples of the fluid mud tested in a Paar-Fysica 300C rheometer (Claeys *et al.*, 2015).

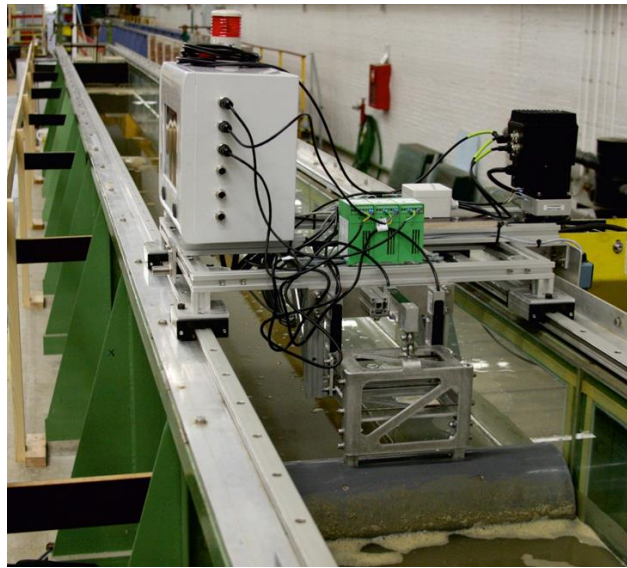


Fig. 1. Test section at Flanders Hydraulics Research showing a 0.2m diameter cylinder at rest in the test section. The cylinder can be towed at controlled speed, and horizontal and vertical forces are recorded.

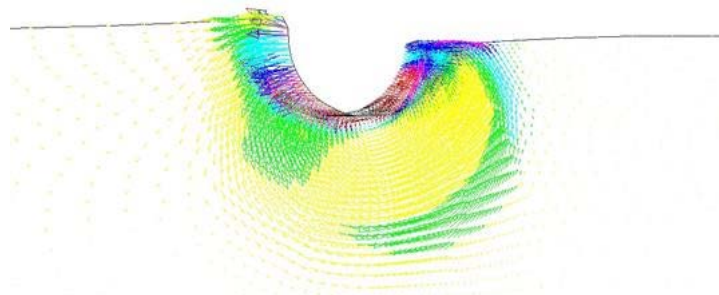


Fig. 2. Predicted flow field and free surface deformation around a 0.2m diameter cylinder, towed at a speed of 0.05m/s (to the left) through a fluid mud layer with a bulk density of 1.17T/m³ (colours represent variation in degree of structural break-down).

Results and discussion

The first towed object is a 0.2m diameter cylinder, submerged for 50%, spanning the full width of the channel (Fig. 1). This object allows a reduced 2DV model. The problem has been simulated first with the finite element FENST-2D research code from KU Leuven (Fig. 2). Since the flow field cannot be measured in the experiment, validation of the model is carried out by comparison of the drag force evolution and the deformation of the mud surface.

Subsequently, the open source OpenFOAM software will be adapted to allow full 3D simulation of the experiments. This 3D model will be used to test more complex object shapes.

Comparison of model results with experimental data will be presented at the conference.

References

- Claeys S., P. Staelens, J. Vanlede, M. Heredia, T. Van Hoestenbergh, T. Van Oyen and E. Toorman. 2015. A rheological lab measurement protocol for cohesive sediment. INTERCOH2015. Book of Abstracts. (this volume).
- Toorman E.A. 1994. An analytical solution for the velocity and shear rate distribution of non-ideal Bingham fluids in a concentric cylinder viscometer. *Rheologica Acta* 33:193-202.
- Toorman E.A. 1997. Modelling the thixotropic behaviour of dense cohesive sediment suspensions. *Rheologica Acta* 36(1):56-65.
- Toorman E.A., M. Liste, M. Heredia, I. Rocabado, J. Vanlede, G. Delefortrie, T. Verwaest and F. Mostaert. 2014. CFD Nautical Bottom. Subreport WP1 - Rheology of fluid mud and its modelling. WL Report 00_0048. Flanders Hydraulics Research, KU Leuven Hydraulics Laboratory & Antea Group, Antwerp, Belgium.

Validation of modelled bottom shear stress under the influence of currents and waves, using long-term measurements

Van den Eynde Dries, Matthias Baeye, Michael Fettweis, Frederic Francken and Vera Van Lancker

Suspended Matter and Seabed Monitoring and Modelling Group
Operational Directorate Natural Environment (OD Nature)
Royal Belgian Institute for Natural Sciences
Gulledelle 100, B-1200 Brussels, Belgium
E-mail: D.VandenEynde@mumm.ac.be

More than 2800 days of currents measurements with a benthic tripod and almost 400 days with a bottom mounted ADCP have been collected in the Belgian part of the North Sea during the period 2005-2013. These data have been used to derive the bottom shear stress from the current profile and the high frequency currents and have been used to validate the modelled bottom stresses. The validated model allows to get insight in the spatial and temporal variability of the bottom roughness.

Introduction

Bottom shear stress links the sea floor to the water column, and is a prime factor for the calculation of sediment transport, including erosion, resuspension and deposition, and bottom morphology. Bottom shear stress is influenced by a large number of factors, including the surface sediment texture, micro-bathymetry, benthic organisms, all influencing the bottom roughness.

In literature, many different methods are available for the calculation of the bottom shear stress, ranging from simple models, using a constant drag coefficient and depth-averaged currents, to complicated ones that take the different bottom boundary layers and the instantaneous bottom shear stresses in a wave cycle into account.

Comparison of the model results with measurements is not only important for validation of the model, but also to gain more insight in the variability of the bottom roughness, both in space and time. However, measuring bottom stresses is difficult and the (lack of) qualitative bottom stress measurements may hamper a sound validation of the model results.

Bottom shear stress measurements

Since 2005 more than 70 deployments have been carried out using benthic tripods. The frame was equipped with (1) a SonTek ADV Ocean point current sensor and a downward looking SonTek 3MHz ADP current profiler for currents; (2) a Sequoia LISST-100X Laser In-Situ Scattering & Transmissometer for particle size distribution and the volumetric concentration of the material in suspension; (3) a Sea-Bird SBE37 thermosalinograph for temperature and salinity; (4) optical backscatter sensors for turbidity in the water column. Furthermore RDI bottom mounted Acoustic Doppler Current Profilers, type Sentinel 1200 kHz Workhorse, were deployed to measure the complete current profile.

Over the period 2005-2013 more than 2100 days of current measurements are available from the tripods and about 400 days from the ADCPs. Most of the data (68%) were collected in the nearshore in the vicinity of the port of Zeebrugge (MOW1) (see Fig. 1.), but also at some more offshore stations current data were collected.

The bottom shear stress was derived from the current measurements using three methods. The first one calculates the bottom shear stress and bottom roughness, and their associated error ranges, from a least-square regression of the current profile for the lower part of the water column using the data from the ADP and ADCP (Wilkinson, 1983). In the second method, the bottom shear stress is calculated from the high frequency ADV current measurements using the second moment (turbulent) statistics (Andersen *et al.*, 2007). Since the bottom shear stress is assumed to be linearly related to the turbulent kinetic energy, it can be calculated from the variance of the current fluctuations (Stapleton and Huntley, 1995). Finally, the inertial dissipation method was applied, including a correction for the advection of waves (Trowbridge and Elgar, 2001; Sherwood *et al.*, 2006). In this method, the bottom shear stress is calculated as a function of the turbulent dissipation, derived from the energy spectrum of the currents.

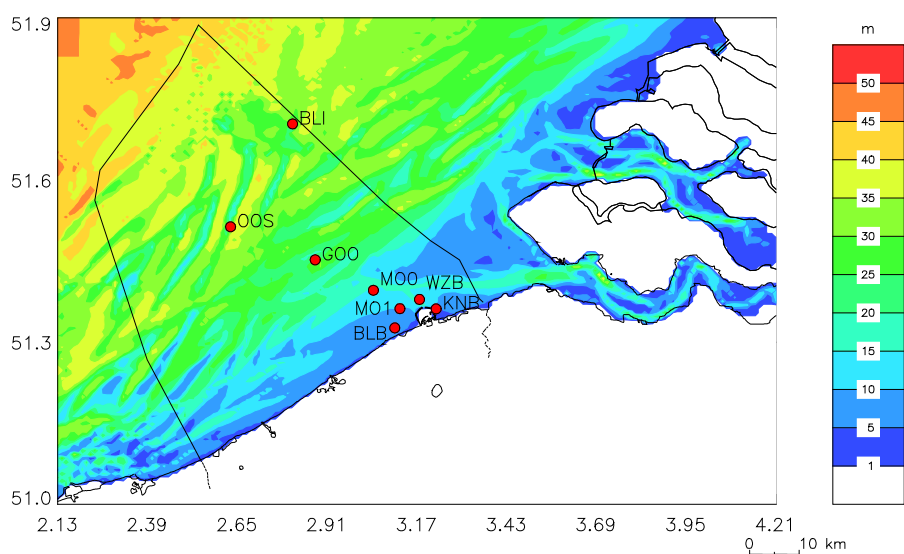


Fig. 1. Position of the measuring stations: OOS: Oosthinder, BLI: Bligh Bank, GOO: Gootebank, MOO: MOW0, BLB: Blankenberge, MO1: MOW1, WZB: WZ-Boei, KNE: Knokkebank.

Bottom shear stress calculations using a numerical model

The modules of Soulsby and Clarke (2005) and Malarkey and Davies (2012) have been used to calculate the bottom shear stress. Both modules parameterise the complex model results in an efficient way, so that they can be included in larger scale sediment transport models. Currents were calculated using a three-dimensional hydrodynamic model, based on the COHERENS software (Luyten, 2014), waves were calculated using an implementation of the WAM model (WAMDIG, 1988).

Acknowledgements

Data were acquired in several monitoring programmes [MOMO and MOZ4 (Flemish Government); ZAGRI and WinMON (private revenues)]. RV Belgica shiptime was provided by RBINS, OD Nature and Belgian Science Policy Office. The commander and crew of the RV Belgica, and the Measuring Service Ostend (RBINS, OD Nature) are acknowledged for logistical support.

References

- Andersen T.J., J. Fredsoe and M. Pejrup. 2007. *In situ* estimation of erosion and deposition thresholds by Acoustic Doppler Velocimeter (ADV). *Estuarine Coastal and Shelf Science* 75:327-336.
- Luyten P. (Ed.). 2014. COHERENS – A Coupled Hydrodynamical-Ecological Model for Regional and Shelf Seas: User Documentation. Version 2.6. RBINS Report, Operational Directorate Natural Environment, Royal Belgian Institute of Natural Sciences, Brussels, Belgium. 1554p.
- Malarkey J. and A.G. Davies. 2012. A simple procedure for calculating the mean and maximum bed stress under wave and current conditions for rough turbulent flow based on Soulsby and Clarke's (2005) method. *Computers & Geosciences* 43:101-107.
- Sherwood C.R., J.R. Lacy and G. Voulgaris. 2006. Shear velocity estimates on the inner shelf off Grays Harbor, Washington, USA. *Continental Shelf Research* 26:1995-2018.
- Soulsby R.L. and S. Clarke. 2005. Bed shear-stresses under combined waves and currents on smooth and rough beds. Report TR 137. HR Wallingford, Wallingford, United Kingdom. 42p.
- Stapleton K.R. and D.A. Huntley. 1995. Seabed stress determinations using the inertial dissipation method and the turbulent kinetic energy method. *Earth Surface Processes and Landforms* 20:807-815.
- Trowbridge J. and S. Elgar. 2001. Turbulence measurements in the surf zone. *Journal of Physical Oceanography* 31:2403-2417.
- WAMDIG: The WAM Development and Implementation Group. 1988. The WAM model: a third generation ocean wave prediction model. *Journal of Physical Oceanography* 18:1775-1810.
- Wilkinson R.H. 1983. A method for evaluating statistical errors associated with logarithmic velocity profiles. *Geo-Marine Letters* 3:49-52.

The impact of sea level rise on tidal mudflats: modelling decadal time scale mudflat morphodynamics in South San Francisco Bay

van der Wegen Mick^{1,2}, Bruce Jaffe³, Amy Foxgrover³, Edwin Elias⁴ and Dano Roelvink^{1,2,5}

¹ UNESCO-IHE, PO Box 3015, 2601 DA, Delft, the Netherlands
E-mail: m.vanderwegen@unesco-ihe.org

² Deltares, PO Box 177, 2601 DA, Delft, the Netherlands

³ Pacific Coastal and Marine Science Center, USGS, 400 Natural Bridges Drive, Santa Cruz, CA 95060, USA

⁴ Deltares USA, 8070 Georgia Ave, Silver Spring, MD 20910, USA

⁵ CITG TU Delft, PO Box 5048, 2600 GA, Delft, the Netherlands

Introduction

Estuarine tidal flats are rich habitats that change at seasonal and decadal time scales. Their shape and width is determined by the interplay of wind waves, tides, sediment availability and biotic dynamics (Friedrichs, 2012). Variable forcing conditions shape the profile (Bearman *et al.*, 2010) but changing forcing conditions will disturb possible equilibrium conditions.

It is important to gain understanding in the morphodynamic adaptation rates of mudflats as the result of decadal and centennial forcing variations in order to assess the conditions of mudflats and associated ecological parameters due to sea level rise.

Earlier mudflat modelling studies focussed on sediment transport dynamics on a fixed bed (e.g. Van Maren and Winterwerp, 2013), equilibrium profiles by development towards shear stress conditions below a critical erosion threshold (e.g. Roberts *et al.*, 2000; Pritchard *et al.*, 2002) or the effect of sediment grain sorting [e.g. Zhou *et al.*, (in prep.)].

Objective

The objective of this work is to explore the processes governing tidal mud flat evolution of tidal flat channel system at Dumbarton Bridge in South San Francisco Bay and the impact of sea level rise. This study will improve assessment of possible impacts of restoration and sea level rise on tidal flats and their ecosystems.

Methodology

We use a combination of observations and 1D process based modelling (Delft3D). A series of bathymetric surveys collected approximately every 30 years from 1858 to 2005 shows that the average tidal flat height varied from -2 to 0 MSL. Width is correlated with net deposition/erosion patterns in the entire South Bay. Tidal flats widen during periods of net sediment import and narrow during net sediment export from South Bay.

The 1D model describes a 800m long and 100m wide mudflat stretch bordered by a closed boundary at the landward side and a channel at the seaward side. Mud transport is modelled by the well-known Krone-Parteniades formulation (Ariathurai, 1974). First aim of this model is to reproduce the current mudflat profile. In order to understand the governing factors that shaped the profile we subsequently conducted extensive sensitivity analysis on model input parameters related to sediment characteristics, wind wave forcing and tidal dynamics. Finally, we assessed the impact of sea level rise on profile development.

Model results

Model runs with constant sediment supply and wave and tide forcing show slow development from a flat bed towards the current profile within 50 years (see Fig. 1). This profile consists of similar erosion and deposition rates, maintaining locally high sediment concentrations above the tidal flat. Still, small developments continue and suggest that the profile will further steepen under current conditions. This behaviour is qualitatively independent of reasonable variations in sediment characteristics and forcing conditions. However, adaptation time scales may differ considerably (10-80 years). For example, low sediment concentrations at the boundary show slower adaptation rates but will eventually lead to the same profile. Calculations reflecting sea level rise impact are currently running.

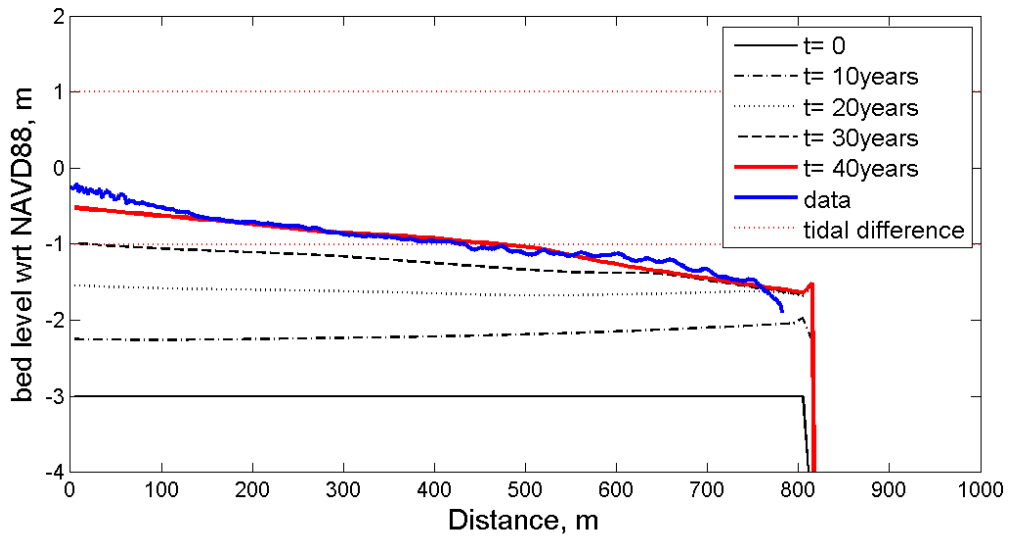


Fig. 10. Profile development towards measured bathymetry of Dumbarton mudflat.

Conclusions

Measured mudflat profiles over the past 150 years on Dumbarton mudflat show that considerable profile development occurred as the result of changing sediment supply. Our modelling effort reproduces the current mudflat profile, but also suggests that development continues over coming decades. Model results are sensitive to uncertain model parameters only in a quantitative manner. Formal equilibrium is not present due to prevailing high sediment concentrations above the mudflat, both in our model as well as reflected by measurements. We can assess the impact of sea level rise on mudflat dynamics.

References

- Ariathurai C.R. 1974. A finite element model for sediment transport in estuaries, Ph.D. thesis. Univ. of Calif. Davis, Davis.
- Bearman J.A., C.T. Friedrichs, B.E. Jaffe and A.C. Foxgrover. 2010. Spatial trends in tidal flat shape and associated environmental parameters in South San Francisco Bay. *Journal of Coastal Research* 26(2):342-349.
- Friedrichs C.T. 2012. Tidal flat morphodynamics: a synthesis. p.137-170. In: *Treatise on Estuarine and Coastal Science, Vol. 3, Estuarine and Coastal Geology and Geomorphology*. Hansom J.D. and B.W. Flemming (Eds).
- Pritchard D., A.J. Hogg and W. Roberts. 2002. Morphological modelling of intertidal mudflats: the role of cross-shore tidal currents. *Continental Shelf Research* 22:1887-1895.
- Roberts W., P. Le Hir and R.J.S. Whitehouse. 2000. Investigation using simple mathematical models of the effect of tidal currents and waves on the profile shape of intertidal mudflats. *Continental Shelf Research* 20:1079-1097.
- Van Maren D.S. and J.C. Winterwerp. 2013. The role of flow asymmetry and mud properties on tidal flat sedimentation. *Continental Shelf Research* 60S:S71-S84.

Sediment management in the Seascheldt - risk of hyper turbidity

van Holland Gijsbert¹, Davy Depreiter¹, Han Winterwerp² and Michael De Beukelaer-Dossche³

¹ International Marine & Dredging Consultants
Coveliersstraat 15, B-2600 Berchem (Antwerp), Belgium
E-mail: gijsbert.van.holland@imdc.be

² Faculty of Civil Engineering and Geosciences, Delft University of Technology
PO Box 5048, 2600 GA Delft, the Netherlands

³ Seascheldt division, Waterwegen & Zeekanaal NV
Lange Kievitstraat 111-113, 2018 Antwerp, Belgium

Recent studies (Winterwerp, 2013ab) have indicated the risk of regime shifts in small, narrow and converging estuaries. Large scale engineering works including deepening, embankments and straightening works have led to tidal amplifications. As a result the sediment (sand and mud) dynamics in the estuary have changed, leading to changes in maintenance dredging volumes. Similar changes in other estuaries have led to increased suspended sediment concentrations and even regime shifts to hyper-turbid conditions.

The Upper-Seascheldt is a navigable (class IV) tidal river in the region of Flanders (Belgium). The connection is identified as a major European bottleneck for inland navigation on the Mediterranean – North Sea corridor. Within the framework of the project “Integrated plan Upper-Seascheldt” commissioned by the Seascheldt division of the Waterwegen & Zeekanaal NV, alternatives to improve navigation (to class Va) are investigated. It is the goal of this integrated study to look for synergy in order to mitigate negative impacts of the proposed measures or even to improve the functioning of the system. This study investigates whether solutions (e.g de-poldering) or strategies can be identified that may reduce the risk of a change towards hyper-turbid conditions.

This paper will illustrate and discuss the relation between observed changes in sediment concentrations, the evolution in maintenance dredging volumes and bathymetric adaptations. By means of a combination of the theoretical framework developed by Winterwerp (2013a) and numerical simulations that are envisaged within this project it will be demonstrated how the proposed alternatives will affect the risk of hyper-turbidity.

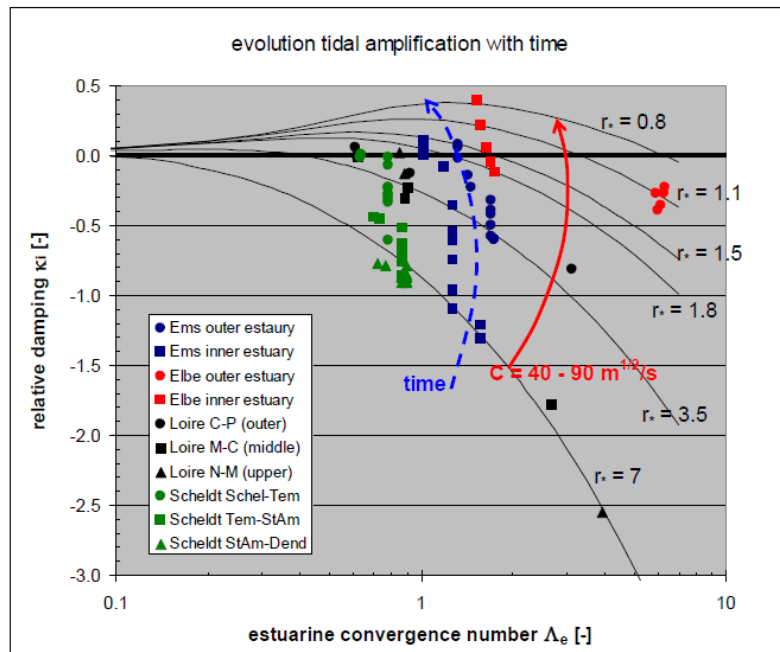


Fig. 1. Comparison of tidal evolution in four European rivers, a shift of position indicates an increased risk on hyper-turbidity (from Winterwerp, 2013b).

In Fig. 1 (taken from Winterwerp, 2013b) the black lines indicate different states (for different values of hydraulic drag) of the estuary in function of the estuarine convergence number and the relative damping, based on the theoretical framework of Winterwerp. The dots represent (historical) states of various European estuaries. For some estuaries the shift over time is indicated towards a state where damping is small (or absent) and the system is insensitive to further changes. The reduced drag indicates a state of strong mud depositions or high near-bed concentrations. The dots are based on field observations and historical bathymetric surveys. By using numerical simulations the application of this graph will be extended to include future states of the Seascheldt Estuary. Based on the outcome of these simulations and (the shift of) position of the dots in the graph the impact of the proposed measures to improve navigation on the risk of regime-changes toward hyper-turbid conditions is estimated.

References

- Winterwerp J.C. and Z.-B. Wang. 2013a. Man-induced regime shifts in small estuaries. I. Theory. *Ocean Dynamics*. DOI 10.1007/s10236-013-0662-9.
- Winterwerp J.C., Z.-B. Wang, A. Van Brackel, G. Van Holland and F. Kösters. 2013b. Man-induced regime shifts in small estuaries. II. A comparison of rivers. *Ocean Dynamics*. DOI 10.1007/s10236-013-0663-8.

On the impact of human activities on the SPM dynamics of the Dutch Wadden Sea

van Kessel Thijs, Katherine Cronin and Luca van Duren

Deltares, PO Box 177, 2600 MH Delft, the Netherlands
E-mail: thijs.vankessel@deltares.nl

The Wadden Sea is one of the large intertidal systems in the world. Although it has been designated as a UNESCO world heritage site and is protected under the EU water framework directive, human activities continue to play a role. However, it remains quite unclear what the impact of these activities are, for example on the dynamics of Suspended Particulate Matter (SPM), steering important ecological indicators such as light, climate, bed composition and deposition rate. This presentation aims at providing some science-based quantitative input to the debate on the human impact on the SPM dynamics in relation with the natural variability. A calibrated process-based numerical model describing the SPM dynamics of the Wadden Sea is used in which human interventions are switched on and off. From the difference between both cases conclusions are drawn on the human impact, of course in the context of the assumptions and limitations of the model.

Methods

The research is based on a combination of field observations and a process-based numerical SPM model using Delft3D (Sassi *et al.*, 2014; Duran-Matute *et al.*, 2014). Although short-term, local impacts can be identified from the available field observations in the Dutch Wadden Sea, they are insufficient to quantify the large-scale and long-term impact of human interventions such as harbour and fairway maintenance (including disposal of dredged material) or fisheries. However, such effects can well be quantified with numerical models, if such models would represent reality in sufficient detail. In this approach, field observations are not directly used to quantify impacts, but to validate the numerical model and to identify its strengths and weaknesses.

Results

In essence, the results will consist of maps of the SPM distribution (e.g. Fig. 1.) and graphs of the SPM variability in time (e.g. Fig. 2.) with and without harbour and fairway maintenance or with and without fisheries. Although these maps are highly relevant for the managers and stakeholders of the Wadden Sea, the scientific interest is in the way these maps and graphs may be interpreted and how confident one can be about the results. Next to the results as such, this will be the main focus of the presentation.

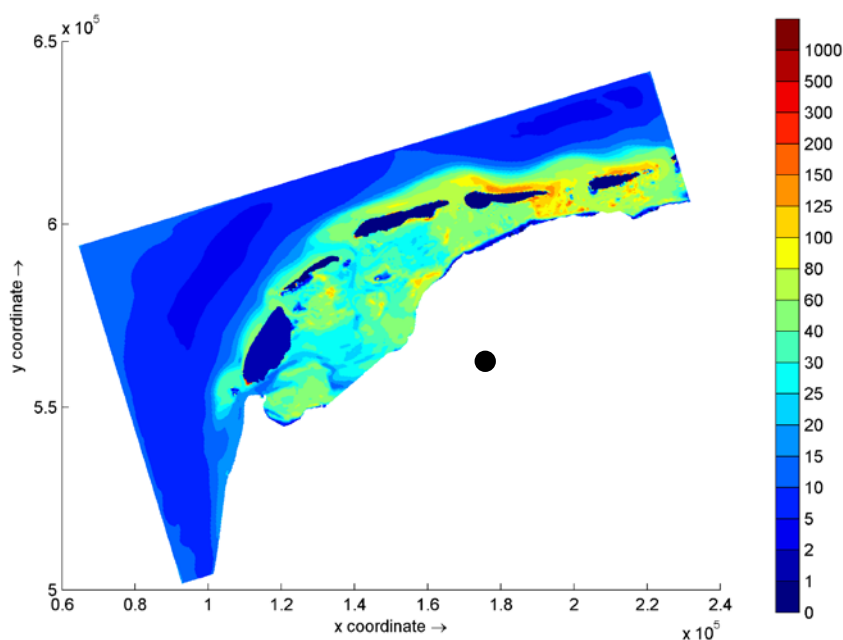


Fig. 1. Computed time-average near-surface SPM concentration (mg/l) in March, 2009.

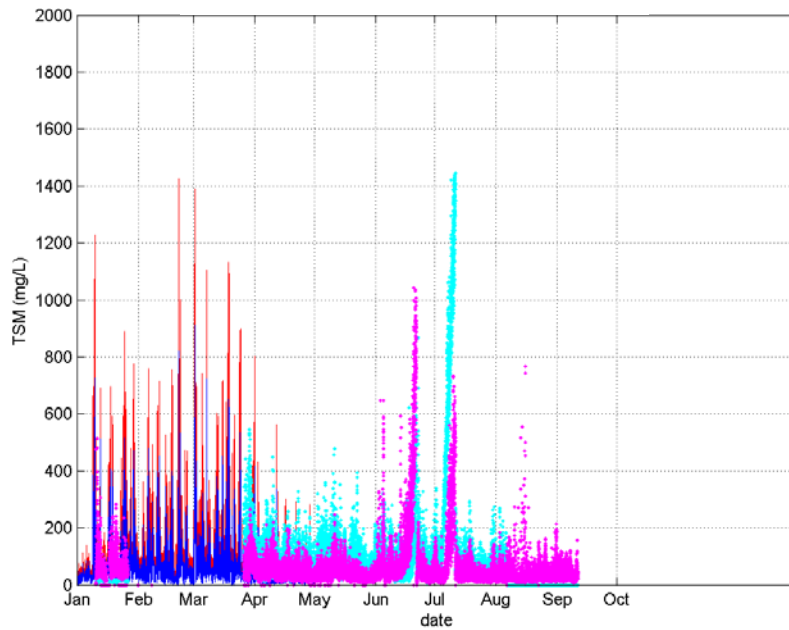


Fig. 2. Computed (lines) and observed (dots) near-bottom SPM concentration (mg/l) at two levels above the bed at station Boontjes Noord (indicated in Fig. 1. with a black dot).

References

- Duran-Matute M., T. Gerkema, G.J. de Boer, J.J. Nauw and U. Gräwe. 2014. Residual circulation and freshwater transport in the Dutch Wadden Sea: a numerical modelling study. *Ocean Sci.* 10:611-632.
- Sassi M.G., M. Duran-Matute, T. Gerkema, T. van Kessel, U. Gräwe, G.J. de Boer and K. Cronin. 2014. Subtidal variability of suspended sediment transport in a multiple tidal-inlet system: a modelling study. *Proc. 17th Physics of Estuaries and Coastal Seas (PECS) conference*, Porto de Galinhas, Pernambuco, Brazil, 19–24 October 2014.

The impact of channel deepening and dredging on the sediment concentration of the Ems Estuary

van Maren Bas, T. van Kessel, K. Cronin and L. Sittoni

Coastal and Marine department, Deltares, Boussinesqweg 1, 2629 HV Delft, the Netherlands
E-mail: bas.vanmaren@deltares.nl

Introduction

The tidal channels of many estuaries worldwide have been deepened in the past decades to centuries, in order to reclaim land and to allow ever larger ship access to inland waterways. The response of estuarine suspended sediment concentrations to anthropogenic influences is still poorly known, mostly because of lack of data and the complex estuarine sediment transport processes. These deeper channels influence the hydrodynamics (tidal propagation and estuarine circulation), and thereby the sediment concentration. Sedimentation in the ports and access channels requires regular maintenance dredging and disposal. On the short term, maintenance dredging leads to increasing concentration levels in the direct vicinity of the dredging vessel, but long-term effects of dredging on SSC is more difficult to quantify. In this paper, we systematically investigate the individual contributions of deepening and dredging by setting up and apply a numerical sediment transport model in an estuary in which a reasonably large amount of data (recent and historical) exists: the Ems Estuary.

The Ems Estuary

The Ems estuary has undergone large anthropogenic changes in the past decades to centuries, but human interferences have accelerated in the past 50 years. Three ports and a large shipyard exist in the estuary, requiring regular deepening and permanent maintenance dredging of the access channel. In the lower Ems River (draining into the Ems Estuary), the channel depth increased approximately a factor two, transforming it from a normal tidal river into a hyperconcentrated system. Channel deepening was comparatively smaller (channels already over 10m deep were deepened with one to several meters) in the outer estuary. Since the 1960's the dredging activities in the Ems Estuary have increased significantly – at present about 10 million m³/year is annually dredged. Until 1994, a large amount (5 million m³/year) of the dredged sediment was not disposed in the estuary, but brought on land.

Model setup

In order to quantify the individual impacts of dredging and deepening on the suspended sediment dynamics, a 3D numerical model was set up using 8 vertical layers with hydrodynamic forcing by wind, waves, tides and salinity-driven density flows. The hydrodynamic model is calibrated against a range of water level observations stations and flow velocity observations at two locations. A sediment transport model has been set up incorporating the effect of the buffering of fine sediments in the seabed and accounting for deposition in, and dredging and dispersal of sediments from, the three ports that exist in the estuary. The model predicts an up-estuary increase in the surface sediment concentration (and seasonal variation thereof), corresponding to observations. The calibrated model is subsequently applied to investigate various scenarios related to dredging, bathymetry, and hydrodynamic processes.

These scenarios suggest that the effect of dredging on absolute concentration levels is limited. Compared to an estuary without ports, the sediment concentration is larger near the disposal grounds. However, elsewhere in the estuary the concentration levels decrease, because the port also acts as a sink of sediment. The effect of ports and their associated dredging and disposal mostly leads to a redistribution of sediment. More important is the effect of deepening, despite the fairly low increase of typically 10-12 to 12-14m. Deepening of the estuary increased the up-estuary sediment transport, resulting in much larger sediment concentrations at the head of the estuary. The tide-averaged flow velocity profile has a much more pronounced up-estuary component near the bed using the 2005 bathymetry compared to the 1985 bathymetry (Fig. 1). This change can probably be attributed to changes in estuarine circulation, which has been analysed by running the model in barotropic and baroclinic mode. Without salinity effects, there is no up-estuary flow near the bed (Fig. 1) and as a result the estuarine suspended sediment concentrations are much lower.

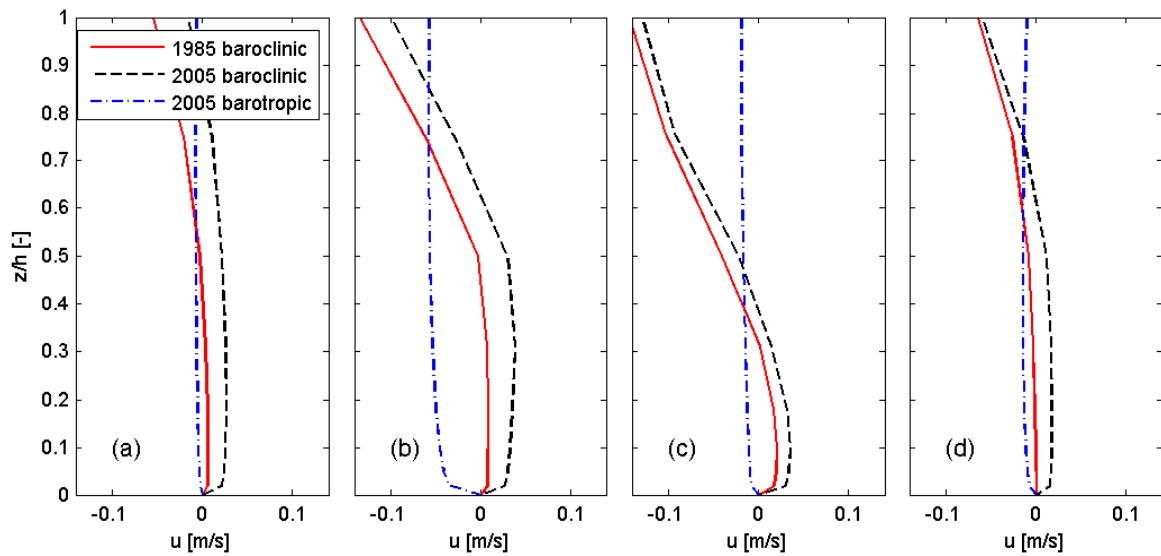


Fig. 1. Residual flow velocity profiles, with positive values directed up-estuary, computed at 4 locations in the estuary, for 1985 and 2005 (baroclinic mode) and 2005 (barotropic mode, i.e. no density effects).

Conclusions

Our model suggests that baroclinic processes strongly influence the suspended sediment dynamics in the Ems Estuary, and that the magnitude of estuarine circulation increased as a result of channel deepening. As a result, the modelled response to channel deepening is an up-estuary increase in the suspended sediment concentration. The effect of dredging and subsequent sediment dispersal is low when compared to natural conditions, but large compared to periods in which sediment depositing in the ports was extracted from the system.

Horizontal coherent structures between channel and mudflat

van Prooijen Bram C.¹ and Qin Zhu²

¹ Department of Hydraulic Engineering, TU Delft, 2628 CN Delft, the Netherlands
E-mail: B.C.vanProoijen@TUDelft.nl

² State Key Laboratory of Estuarine and Coastal Research
East China Normal University, Shanghai 200062, P.R. China

Introduction

At various aerial pictures of estuaries, large scale eddies are visualized by a distinct difference in sediment concentration. Fig. 1 shows such a picture, where horizontal eddies or horizontal coherent structures are found at the interface between tidal flats and a channel. They are characterized by horizontal length scales that are an order of magnitude larger than the water depth. In general, these coherent structures are instabilities that grow due to an inflection point in the transverse profile of the streamwise velocity. As already shown in the areal picture, these coherent structures result in an exchange of sediment between the mudflat and the channel. It is however unknown what their contribution is to the net exchange.

In this study we explore the occurrence and development of coherent structures in tidal flow. Furthermore, we aim to determine the effect of these coherent structures on exchange of sediment between channel and tidal flat.

A field campaign was therefore set up to measure the horizontal coherent structures. High resolution flow measurements were carried out with velocimeters (ADV and ADCP), path lines were tracked by means of GPS-drifters and the footprint of the coherent structures was visualized with an Unmanned Automatic Vehicle (UAV or drone).

Study area and experimental setup

The field campaign was set up at the Kapellebank, a semi-enclosed flat bordering the outer bend of one of the channels of the Westerschelde (the Netherlands), see Fig. 1. At this location, the coherent structures were most clear on various areal pictures. Three methods have been used to determine the hydrodynamic processes at the interface between tidal flat and channel. First, *in-situ* measurements by flow instruments were installed. Upward looking ADCPs (Nortek Aquadopp) were buried in the bed and used in high frequency mode. A frame with an ADV (Nortek Vector) and a downward looking ADCP (Nortek Aquadopp) were employed. Second, path lines were tracked by means of GPS drifters. The drifters were employed for 3 hours during the ebb phase. Third, areal pictures were taken by a UAV. The coherent structures are visualized by the differences in sediment concentration. Dye release was tested, but turned out to be unsuccessful in the turbid water. Sediment concentrations were measured with 2 OBS's and a LISST (see also contributions of Zhu *et al.*, and of Guo *et al.*).

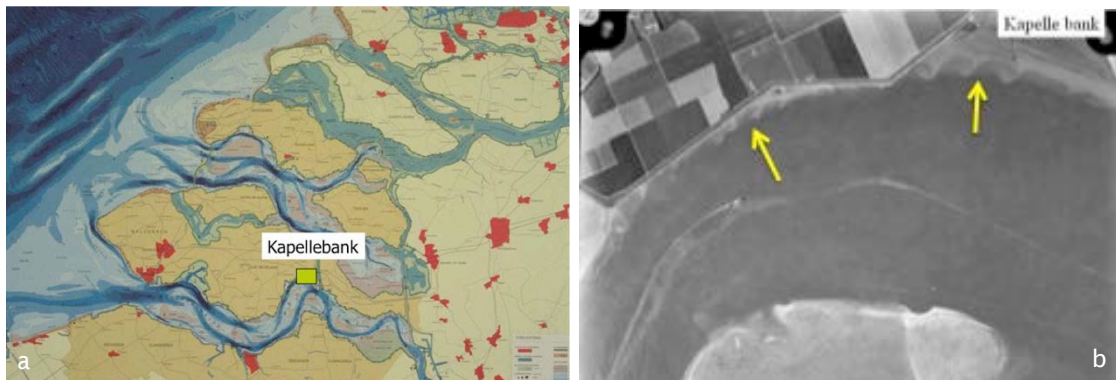


Fig. 1: (a) Map of the south-western part of the Netherlands with the Westerschelde (lower estuary) and the location of areal picture. (b) Areal picture with the Kapellebank at the upper right corner. The arrows indicate the horizontal coherent structures as visualized by the sharp sediment concentration gradients.

Results and conclusions

Fig. 2a shows a typical picture made by the UAV, one hour before low water. It shows sharp gradients in sediment concentration, visualizing the coherent structures. Low concentrations are found in the channel. Relatively small waves stir up the sediment at the shallow water part along the waterline, resulting in high concentrations. The coherent structures result in sediment transport from the tidal flat into the channel. The typical size of the coherent structures is 100m-300m. Such dimensions are also found from the path lines of the GPS drifters, Fig. 2b. These path lines show typical turn over time scales of 20 minutes. From the drifter measurements, almost no translation of the coherent structure was found. For over one hour, the coherent structures stayed in place. The along shore flow at the water line was even opposite of the along shore ebb flow in the channel. This was also observed in the ADV and ADCP data. Fig. 2c shows the velocity (ADV) and water level variation for 4 typical tidal periods at the interface between channel and flat. Where a consistent flow pattern is found for the flood phase, significant differences in velocities are found in the ebb phase, just before falling dry. Especially in the third cycle, a significant along shore flow is found in eastern direction. This implies that the flow is opposite of the ebb flow in the channel.

It is concluded that horizontal coherent structures could be detected by various instruments at the interface between channel and tidal flat. The results from the UAV, velocimeters and GPS-drifters show a consistent pattern. The coherent structures were found during the ebb period, just before falling dry. In this period, the conditions seem to be most favourable with shallow water and sufficient lateral shear. From the GPS-drifter data followed that the coherent structures rotate slowly, taking about 20 minutes to make a full rotation. The drifter data also show that the coherent structures only show weak translations. Further analysis will be carried out on the effect of the coherent structures on net sediment transport between channel and tidal flat.

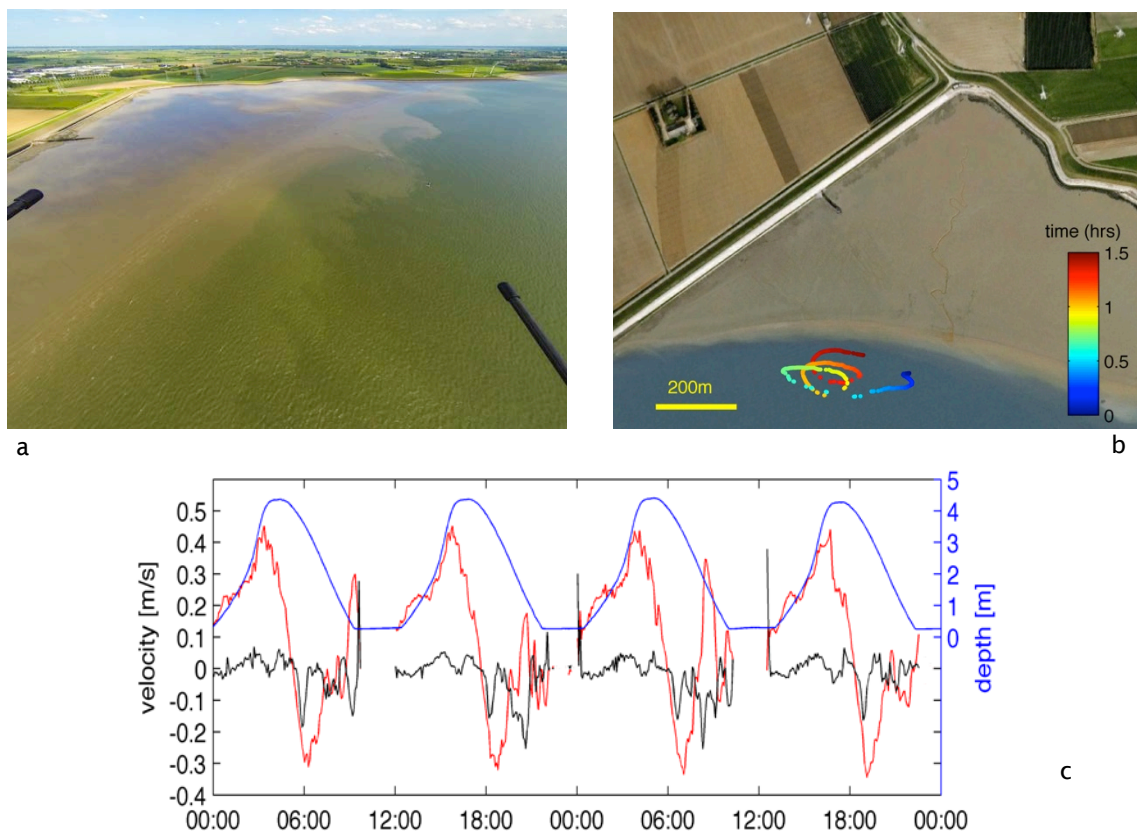


Fig. 2. (a) Areal picture of the Kapellebank, made with the UAV. (b) Path line of GPS-drifter. The colours indicate the time in hours. (c) Time series of the water depth (blue), along shore velocity (red) and cross shore velocity (black). Positive along shore velocities indicate flow to the East (landward), and positive cross shore velocities indicate flow to the North (onto the flat). Velocities are measured at 15cm above the bed.

Evaluating turbidity maximum patterns and their variability in the Seine Estuary from metrics: associating observations and model results

Verney Romaric¹, Florent Grasso¹, Virginie Lafon², Emmanuelle Mulamba-Guilhemat², David Doxaran³, Flavie Druine⁴, Julien Deloffre⁴, Jean Philippe Lemoine⁵ and Pierre Le Hir¹

¹ Laboratoire DYNECO/PHYSED, IFREMER, PO Box 70, 29280 Plouzané, France
E-mail: romaric.verney@ifremer.fr

² Geotransfer, UMR 5805 EPOC, Université de Bordeaux I, Bâtiment B18, Allée Geoffroy St Hilaire, 33615 Pessac Cedex, France

³ Observatoire Océanologique, Laboratoire d'Océanographie de Villefranche, UMR 7093 – CNRS/UPMC, 181 Chemin du Lazaret, 06230 Villefranche sur Mer, France

⁴ UMR CNRS 6143 Morphodynamique Continentale et Côtière, Batiment IRESE A, Université de Rouen, 76821 Mont Saint Aignan Cedex, France

⁵ GIP Seine Aval, Pole Régional de Savoirs, 115 Boulevard de l'Europe, 76100 Rouen, France

Context

Turbidity Maximum (TM) zones represent key sedimentary features in estuaries, whose dynamics are driven by small-scale processes (i.e. turbulence, flocculation, erosion), circulation patterns (tidal range, density stratification, flood/ebb dominance) and modulated by seasonal and inter-annual hydrological forcing. The HYMOSED project is aimed to investigate the TM dynamics in the Seine Estuary, from the tidal scale to pluri-annual and (ultimately) decadal scale, combining complementary sources of information: remote sensing ocean colour data, pluri-annual *in situ* measurements and numerical model results. The objectives are first to validate these tools, next to build simple metrics and finally to investigate their variability at various time scales.

Methods

NASA MODIS AQUA observations constitute the longest archive of ocean colour data (from 2002 to now), mainly used in the open ocean or coastal seas. Using MODIS FR observations (250m) in estuaries is a challenging issue, as suspended solid concentration (SSC) gradients are strong and usual 'generic' algorithms can generate large uncertainties. Based on similar experience in the Gironde Estuary, a dedicated field campaign was conducted in September 2014 to collect joint suspended sediment samples and radiances measurements at multiple wave lengths, in order to build a site-specific algorithm and evaluate uncertainties associated to ocean colour derived SSC.

These synoptic / surface / low frequency observations are complemented by the SYNAPSES monitoring network, providing time series of turbidity in 5 stations (surface or bottom/surface in the TM) along the different compartments of the estuary, operated since 2011. These measurements are not yet calibrated in SSC but field surveys are being conducted in 2015 for this purpose. A careful attention will be paid to the analysis of SSC from this network prior to 2015.

The MARS3D hydrodynamics and sediment transport numerical model was implemented in the Seine Estuary, using a specific curvilinear grid more suitable for estuarine geomorphologies (resolution down to 50mx200m within the TM zone). This model reproduces the estuarine circulation and the main sediment processes using the MIXSED module (Le Hir *et al.*, 2011) with 5 sediment classes (1 gravel, 3 sands, 2 muds). It is forced by daily river discharge measurements, METEOFRACTANCE ARPEGE model wind results and WAVEWATCHIII wave fields simulated on this typical configuration.

Results and conclusions

The TM is a full 4D structure, developing both spatially and temporally and driven by tidal, meteorological and hydrological forcings. Therefore, only numerical model can provide representative metrics (mass in suspension, position, extension and displacement of the TM)... However, models always simplify the complex dynamics of estuaries, and must be validated. In our study, we decided to build and evaluate metrics derived from times series of ocean colour and *in situ* measurements. In the mouth and the adjacent Seine Bay, we quantified the spatial extension, the central position and shape of the surface TM around low tide, tracking the pixels above SSC thresholds estimated from three percentiles of the SSC at the mouth. The same metrics are evaluated within the estuary, with a discussion on the reliability of satellite observations in sections

of 1 km width. From the monitoring network were estimated the percentiles (10, 50 and 90) of SSC during the 4 phases of the tidal cycles over several years, and the duration of period when SSC exceed key concentration levels (bottom and surface), i.e. 0.1 g.l⁻¹, 0.5 g.l⁻¹ and 1 g.l⁻¹. All these metrics were analysed together with the main forcings, i.e. wind, waves (direction and height), river discharge, tidal range, and confronted to similar metrics estimated from the model. From the model itself are estimated the mass in suspension in the TM and its distribution within the water column.

These metrics are built to evaluate the TM and evaluate its variability. They are also useful to compare estuarine systems.

References

Le Hir P., F. Cayocca and B. Waeles. 2011. Dynamics of sand and mud mixtures: A multiprocess-based modelling strategy. *Continental Shelf Research* 31(10):S135-S149.
doi:10.1016/j.csr.2010.12.009.

Evaluation of the effect of climate change on the muddy deposits in the flood plain of the Loire Estuary and on the turbidity maximum (C3E2 Project- French research program)

Walther Régis¹, Pierre Lehir² and Florence Cayocca²

¹ Artelia, 6 rue de Lorraine, 38120 Echirolles, France
E-mail: regis.walther@arteliagroup.com

² Ifremer, Centre Bretagne, ZI de la Pointe du Diable, CS 10070, 29280 Plouzané, France

The project C3E2 (Consequences of Climate Change on Estuarine Ecogeomorphology – French research program: ‘Gestion et Impacts du Changement Climatique’ driven by MEDDE) proposes to contribute to the evaluation of the effect of climate change on the evolution of the morphology of estuaries. Two approaches are implemented, both based on numerical modelling coupling the morphodynamic aspects:

- One studies the morpho-sedimentary response of schematic estuaries, defined from different geometrical characteristics and environmental conditions representative of French estuaries.
- The second is applied to the estuary of the Loire, where the existence of long time series allow for validation of the 3D model hydro-sedimentary (mud sediment) already operational; secondly, this estuary has the distinction of having preserved natural areas on which the interactions between vegetation and physical processes can be studied. The importance of a high bank between main channel and floodplain is here to overcome, particularly in view of a change in frequency of flooding.

This is the second part of the applied to the Loire estuary project that is developed in this paper with the assessment of the impact of climate change on the mud dynamic and particularly on deposits in the floodplains.

Description of the 3D model hydro-sedimentary

The model is based on the Telemac-3D system. The simulated area is about 90km inland and 40km offshore. The model is forced with the daily discharge of the Loire river, the astronomical tide level, variation of mean sea level due to meteorological conditions, waves and wind conditions. This operational 3D model is calibrated and validated in the inner estuary: sea levels, currents, salinity, sedimentology including turbidity of mud transport and bed level evolutions in mud (Walther *et al.*, 2012).

The model proved to be able to reproduce a full annual cycle of the dynamics of the maximum turbidity in the Loire Estuary without any assumption regarding the bathymetric state of the estuary. The model has been adapted and refined on submersible areas to accommodate drainage channels, with a minimum mesh size of 10m on the northern mudflats of the estuary of the Loire.

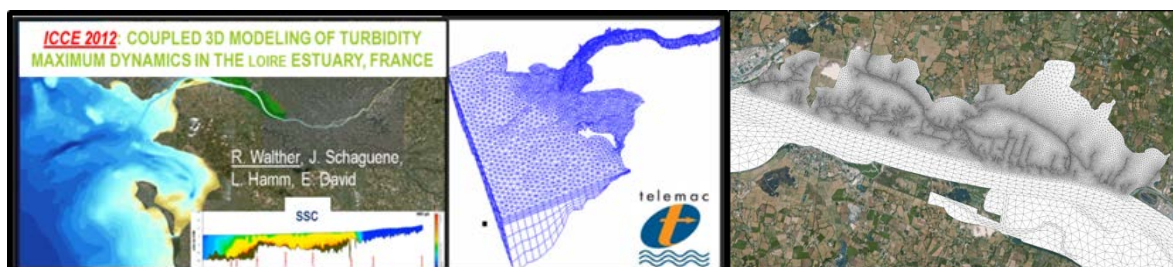


Fig. 1. View of the 3D hydro-sedimentary model and refinement northern mudflats of the Loire Estuary.

Validation of the 3D hydro-sedimentary model in the submersible area

An important, measurement campaign on a submersible area was effected in 2012 with spring tide conditions in water level, salinity, SSC and mud deposit. The model was compared to these measurements to calibrate and validate the exchanges between Loire and submersible area. It appears that the model was able to reproduce the short-term dynamics and long-term dynamics in the floodplains (deposits) (partially presented in Intercoch (Lehir *et al.*, 2013).

Analysis of the model results provided a better understanding of the dynamic in these areas.

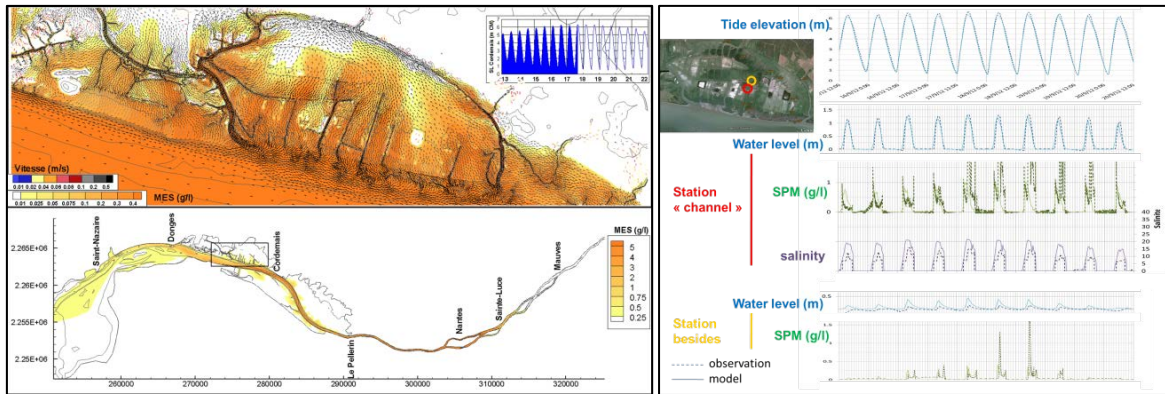


Fig. 2. Suspended sediment concentration during spring tide and submersion of mudflats and grasslands.

Evaluation of the morphodynamic submersible area during the period 2010-2040

Since the computation time, a modelling methodology was developed to simulate the changes of submersible areas until about 2040. The 3D hydro-sedimentary model simulates a year in real time every 5 years, with a morphological factor in the area of deposit for consolidated sediment. At each iteration, the Loire bathymetry is updated from the riverbed evolutions pre-calculated by a sand model.

Four scenarios of climate change were established and used in simulations. Evolution of submersible areas and new dynamics in maximum turbidity are analysed for each scenario.

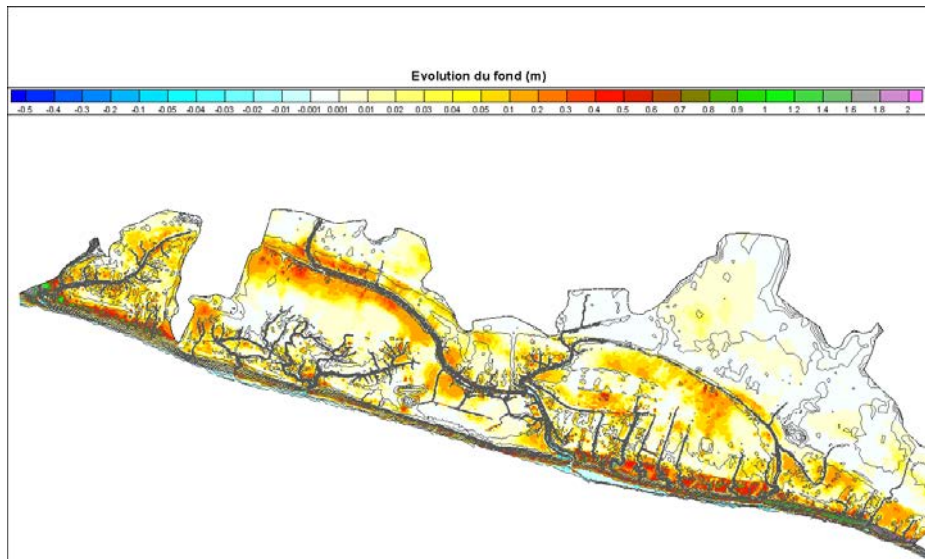


Fig. 3. Example of calculated evolution of the bed on mudflats and grasslands between 2010 and 2040 for one climate change scenario.

References

- Lehir P., R. Walther, F. Cayocca, P. Bassoullet, H. Jestin and R. Verney. 2013. C3E2: Consequences of climate change on estuarine ecogeomorphology. IntercoH 2013 Conference, Gainesville (FL), 21-24 Oct.
- Walther R., J. Schaguene, L. Hamm and E. David. 2012. Coupled 3D modelling of turbidity maximum dynamics in the Loire Estuary. Coastal Engineering Proceedings 1(33).

Modeling of seasonal variations of fine-grained suspended sediment dynamics in the Yangtze Estuary

Wan Yuanyang^{1,2}, Dano Roelvink² and Fengfeng Gu¹

¹ Shanghai Estuarine and Coastal Science Research Center, Shanghai 201201, P.R. China
E-mail: sway110@qq.com

² Institute for Water Education, UNESCO-IHE, 2601 DA Delft, the Netherlands

When the median grain size (D_{50}) of natural sediment is finer than $62\mu\text{m}$ (Mehta and McAnally, 2008), the sediment composition and cohesive content of fine-grained sediment changes the degree of cohesion, introducing significant flow-sediment interaction and furthering impact macro-scale behaviour of sediment transport and hydrodynamics. Firstly, spatial and temporal measurement data characterizing dry-wet seasonal variations of velocity, salinity and suspended sediment concentration (SSC) in the North Passage Deepwater Navigational Channel (DNC) of the Yangtze Estuary, China are presented. Subsequently, using a Delft3D-based 3D model, the seasonal variations of fine-grained suspended sediment dynamics in the Yangtze Estuary are simulated. A series of numerical experiments as related to various effects from riverine inflow, seasonal wind and sediment-current interactions are carried out to identify the primary mechanism describing the complexity of water circulation and sediment dynamics in the complex estuarine system. The modelling results highlight: (1) Saltwater intrusion controls vertical structure of currents near the estuarine turbidity maximum (ETM) area, especially during lower current speed time, when baroclinic pressure gradient forcing could significantly reshape local vertical velocity profile; (2) the transport of residuals generated by internal tidal asymmetry plays a dominant role in sediment trapping and maintaining ETM dynamics; (3) SSC-varied settling velocity and turbulence damping effects are of critical importance to reproduce the density stratification.

Fine sediment properties: determination, interpretation and use

Winterwerp Johan C.^{1,2}, Claire Chassagne², Maria Ibanez², Miguel de Lucas Pardo¹, Thijs van Kessel¹, Walther van Kesteren¹ and Bram van Prooijen²

¹ Marine and Coastal Management, Deltares, PO Box 177, 2600 MH, Delft, the Netherlands
E-mail: han.winterwerp@deltares.nl

² Section of Fluid Mechanics, Civil Engineering and Geosciences, Delft University of Technology, PO Box 5048, 2600 GA, Delft, the Netherlands

This paper describes the methods and protocols developed over the last decades at Deltares and Delft University of Technology to determine the chemo-physical properties of fine sediments, the interpretation of the results, and their application in research, consultancy studies and numerical models.

Our methods are based on laboratory analyses of grab samples collected from the sediment bed. These samples may have been disturbed/moulded. However, it is crucial that the water content of these samples is not altered, i.e. we require the in-situ bulk density of the samples. The first series of analyses comprise determination of the sample's dry density, and the organic and carbonate content, and the salinity of the pore water. Generally, we use Dutch standard protocols, or differently when requested by our client.

One of the key parameters for fine sediment characterization is the particle size distribution. A crucial step in this determination is sample preparation. For use in empirical soil mechanical formulations, samples are depleted of organic components and carbonates, dried, and ground again in a mortar. Assessment of the unflocculated particle size distribution requires removal of organics and carbonates (using H₂O₂ and HCl), whereas these components should be maintained if the distribution of the flocculated sediment is required. It is widely known that different instruments can yield very different particle size distributions, for the same material. Infamous are the differences between optical methods (Malvern) and methods based on Stokes' law, such as Sedigraph, Hydrograph, sedimentation balance and Pipette method. We show that by a proper separation of the samples in sub-samples (through sieving and sedimentation), these instruments however do yield almost identical results (Chassagne, in prep.). By plotting the results in a triangular diagram (sand-silt-clay) we get a first impression on whether the sediments at the study site are of one origin only, or whether sources containing sediment with different composition/properties play a role.

Next, we determine the Atterberg Limits determining Plastic Limit (PL), Liquid Limit (LL) and Plasticity Index (PI). From the Plasticity Chart (PI vs LL) we get a first idea on the relevant clay minerals (by comparing with literature values for individual clay minerals), and whether the Atterberg Limits have been measured properly. From the Activity Chart (PI vs clay content) we establish whether the bed from which the sample was taken depicts cohesive or non-cohesive behaviour.

More insight into the sediment properties and clay minerals is obtained from determining the zeta potential, for which we remove the organic fraction and carbonates. We always measure the zeta-potential at a variety of pH-values (by adding HCl), and sometimes also the salinity is varied (mono- and divalent salts, Chassagne *et al.*, 2009, Tsujimoto *et al.*, 2013; Ibanez *et al.*, 2014). By comparing with literature values for individual clay minerals, we get more information on the mixture of minerals in the sample. Moreover, these analyses yield qualitative information on flocculation behaviour of the sediments, and the size and strength of the flocs to be expected in the water column, of course assuming that sediments in the bed and in the water column are of the same origin.

The undrained strength of the sediment, as a function of its dry density (water content) is determined with undrained vane measurements. Done properly, the peak and undrained strength of these measurements should not differ too much (~10%), and both values can be used in further interpretation. We assume self-similar properties of the sediment, which implies power-law behaviour. When plotted against the content of fines (<64µm), we obtain the fractal dimension of the soil, which is a measure for its structure.

Small-scale consolidation experiments are done with the CST-instrument (Capillary Suction Time). Diluted and pre-consolidated sub-samples are put in a small container (few cm³) upon which the CST

is measured. These analyses provide parameters describing the permeability and effective stress of the soil as a function of bulk density. Again assuming self-similar behaviour, we obtain a second value for the fractal dimension, which in general proves to be identical to the one obtained from the vane tests.

We also carry out meso-scale consolidation experiments in settling columns of 0.5 – 1 m height. We prepare three mixtures at concentrations below the gelling concentration, and follow the interface over time. Ideally we measure the vertical dry density distribution in the consolidated bed at equilibrium. From analysis of the hindered settling phase, we obtain the undisturbed settling velocity of the sediment and its gelling concentration. From the consolidation phase, we obtain again the parameters for permeability and effective stress, again assuming self-similar behaviour (Merckelbach and Kranenburg, 2004; Winterwerp and van Kesteren, 2004).

When all these analyses have been performed properly, we obtain identical/similar values for the various parameters. As some of these analyses are more laborious than others (in particular zeta-potential, vane test and CST-measurements are fast and very cheap), we set up a hierarchy in these experiments, which allows for a space covering picture of the open water body to be studied at relatively small costs. This picture adds to our system understanding of a specific site, helping to set up numerical models for assessing fine sediment dynamics. Moreover, the information on the fractal dimension yields the ratio between mass and volume concentration of the soil, an indispensable parameter when assessing maintenance dredging needs.

Also we deploy the Gust micro-cosm for erosion experiments on undisturbed cores from the field to compare with erosion parameters obtained from the soil mechanical analyses. As this instrument is accurate up to stresses of about 0.8Pa only, the micro-cosm is applicable for soft soils only. Finally, we developed an in-situ floc camera obtaining direct information on floc size and settling velocity.

The parameters obtained give us direct information on the erodibility of the soil, as described in previous publications of the authors (Winterwerp *et al.*, 2012).

Finally, in our full paper we will show some application of the method through elaboration of two case studies in which our method provided valuable data for setting up our numerical models. In fact, without these analyses, we would not have been able to obtain any credible model result at all.

References

- Chassagne C., F. Mietta and J.C. Winterwerp. 2009. Electrokinetic study of kaolinite suspensions. *J Colloid Int. Sci.* 336(1):352-9.
- Ibanez M., A. Wijdeveld and C. Chassagne. 2014. Role of mono- and divalent ions on the stability of kaolinite suspensions and fine tailings. accepted in *Clays and Clay minerals* (2014)
- Merckelbach L.M. and C. Kranenburg. 2004. Constitutive equations for soft mud determined from simple laboratory experiments. *Géotechnique* 54(4):235-24.
- Tsujimoto Y., C. Chassagne and Y. Adachi. 2013. Comparison between the electrokinetic properties of kaolinite and montmorillonite suspensions. *Colloid Int. Sci.* 407:109-115.
- Winterwerp J.C. and W.G.M. van Kesteren. 2004. Introduction to the physics of cohesive sediments in the marine environment. Elsevier, *Developments in Sedimentology* 56.
- Winterwerp J.C., W.G.M. Van Kesteren, B.C. Van Prooijen and W. Jacobs 2012. A conceptual framework for shear-flow induced erosion of cohesive sediment beds. *AGU, Journal of Geophysical Research* 117:C10020, doi:10/0129/2012JC008072.

Mud flocculation model considering the effects of distribution of fractal dimensions and yield strength

Xu Chunyang and Ping Dong

University of Dundee, Dundee, DD1 4HN, UK
E-mail: c.y.xu@dundee.ac.uk

Introduction

Flocculation of cohesive sediment particles has a strong influence on settling, deposition and other sediment transport processes. The aggregation and disaggregation rates of flocs depend on many factors including the fluid shear, turbulence and the properties of flocs such as primary particle size, floc size, density and shape (fractal dimension) not all of which are independent.

Based on the constant fractal dimension assumption Winterwerp (1998) developed a flocculation model by linearly combining aggregation and break-up processes. This assumption was challenged by Martinis and Risovic (1998) who proposed that the value of fractal dimension decreases from 3 to 1.2 as the floc size increases. The values of the fractal dimension are also affected by variable flow conditions and aggregation mechanisms (Dyer and Manning, 1999; Khelifa and Hill, 2006; Maggi *et al.*, 2007; Vahedi and Gorczyca, 2011). Son and Hsu (2009) improved the existing flocculation model by taking into account the variable fractal dimension suggested by Khelifa and Hill (2006) and also considering variable yield strength of flocs.

In many field measurements a range of settling velocities are measured for one floc size. This has led Vahedi and Gorczyca (2012) to propose a normal distribution of fractal dimensions and as a consequence a floc of given size can also have a probability distribution of yield strength. The purpose of this study is to improve the flocculation model by taking into consideration the distributions of both fractal dimensions and yield strength.

The formulation

Normal distribution of fractal dimensions and yield stress

Here we follow the study by Vahedi and Gorczyca (2012) and the normal distribution of fractal dimensions for one floc size is given as:

$$P(nf)_D = \frac{1}{\sqrt{2\pi}\sigma_D} \exp\left(-\frac{(nf - \mu_D)^2}{2\sigma_D^2}\right) \quad (1)$$

where nf is the fractal dimension, D is the floc size, μ_D and σ_D are the mean and standard deviation of fractal dimensions for floc with size D respectively. For a normal distribution the probability $P(\mu - 4\sigma < x < \mu + 4\sigma)$ is much more than 99.9% thus for simplicity we assume all the fractal dimensions of one fixed floc size fall within the interval $[\mu - 4\sigma, \mu + 4\sigma]$.

The yield stress of floc is the function of fractal dimension. According to Son and Hsu (2009) it can be estimated based on the number of primary particles in the plane crossing the centre of a floc as:

$$\tau_y = B_1 \left(\frac{D}{d}\right)^{2nf/3} D^{-2} \quad (2)$$

where $B_1 = (\pi/6)^{-2/3} F_{c,p}$ and $F_{c,p}$ is the cohesive force of primary particles.

The complete model

Both flocculation models of Son and Hsu (2009) and Winterwerp (1998) assume that the break-up rate of flocs is proportional to the number (n) of flocs suspended in the water. But in reality only those flocs with yield stress smaller than the turbulent shear stress contribute to the break-up rate. In this study n is replaced as $n_e = nP(D)$, $P(D)$ is the probability of yield strength smaller than turbulent shear with floc size of D . $P(D)$ is calculated using equation (3):

$$P(D) = \int_{\mu_D - 4\sigma_D}^{nf_{\max}(D)} \frac{1}{\sqrt{2\pi}\sigma_D} \exp\left(-\frac{(\mu_D - \sigma_D)^2}{2\sigma_D^2}\right) \quad (3)$$

where $nf_{\max}(D)$ is the maximum fractal dimension allowing yield stress smaller than turbulent shear stress for a floc with size D .

The flocculation model by Son and Hsu (2009) can thus be modified as:

$$\frac{dD}{dt} = \frac{Gd^\beta}{\beta \ln(D/d) + 1} \left[\frac{k'_A c}{3 \rho_s} d^{nf-3} D^{-nf+4-\beta} - \frac{k'_B P(D)}{3} \left(\frac{\mu G}{B_1} \right)^q d^{-p+(2q/3)nf} D^{1-\beta+(2q/3)(3-nf)} (D-d)^p \right] \quad (4)$$

where $k'_A = (3e_c \pi e_d) / 2f_s$ and $k'_B = ae_b$. This model is denoted as Model A, model originally proposed by Son and Hsu (2009) is denoted as Model B.

Model results

The typical model results are shown in Fig. 1 and 2.

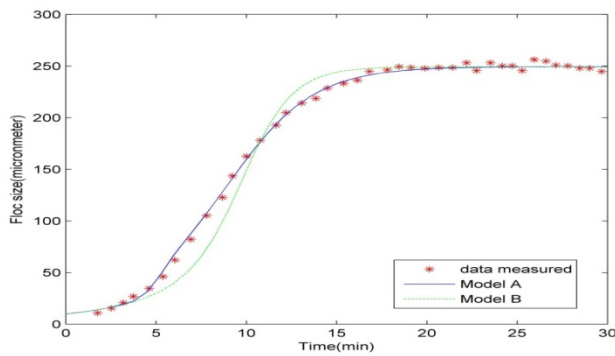


Fig. 1. Experimental data of Spicer (1998) and simulation results of flocculation models.

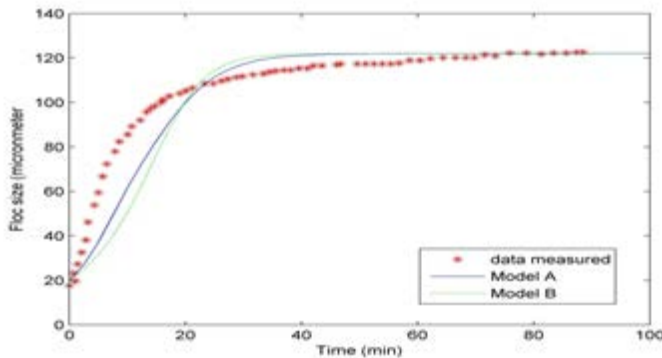


Fig. 2. Experimental results of Biggs and Lant (2000) and simulation results of flocculation models.

Conclusions

It can be concluded that the results obtained by considering variable yield stress and variable fractal dimensions in the flocculation model are encouraging. In both simulations (Fig. 1 and 2), model A shows much improved predictions.

References

- Dyer K.R. and A.J. Manning. 1999. Observation of the size, settling velocity and effective density of flocs, and their fractal dimensions. *Journal of Sea Research* 41:87-95.
- Khelifa A. and P.S. Hill. 2006. Models for effective density and settling velocity of flocs. *Journal of Hydraulic Research* 44:390-401.
- Maggi F., F. Mietta and J.C. Winterwerp. 2007. Effect of variable fractal dimension on the floc size distribution of suspended cohesive sediment. *Journal of Hydrology* 343:43-55.

- Martinis M. and D. Risovic. 1998. Fractal analysis of suspended particles in seawater. FIZIKA B-ZAGREB- 7:65-72.
- Son M. and T.J. Hsu. 2009. The effect of variable yield strength and variable fractal dimension on flocculation of cohesive sediment. Water Res. 43:3582-92.
- Vahedi A. and B. Gorczyca. 2011. Application of fractal dimensions to study the structure of flocs formed in lime softening process. Water Res. 45:545-56.
- Vahedi A. and B. Gorczyca. 2012. Predicting the settling velocity of flocs formed in water treatment using multiple fractal dimensions. Water Res. 46:4188-94.
- Winterwerp J.C. 1998. A simple model for turbulence induced flocculation of cohesive sediment. Journal of Hydraulic Research 36:309-326.

POSTER PRESENTATIONS

Modelling estuarine sediment budget impacts: anthropogenic or natural?

Achete Fernanda¹, Mick van der Wegen^{1,2}, Dano Roelvink^{1,2} and Bruce Jaffe³

¹ Department of Coastal Engineering and Port Development, UNESCO-IHE
PO Box 2601 DA, Delft, the Netherlands
E-mail: f.achete@unesco-ihe.org

² Deltares, Boussinesqweg 1, 2629 HV Delft, PO Box 177, the Netherlands

³ US Geological Survey Center
400 Natural Bridges Drive, Santa Cruz, CA 95060 United States of America

As is the case with many estuaries worldwide, the San Francisco Bay-Delta Estuary is heavily impacted by human activities. Human activities that change hydrodynamics including river damming and industrial and agricultural uses of water alter the sediment budget of the entire system. In addition, the hydrodynamics and sediment budget of the San Francisco Bay-Delta Estuary will be affected by climate change resulting in the acceleration sea level rise and there is the possibility of levee failures due to earthquakes. Applying a previously calibrated process based model (Dflow-FM), it is possible to quantify the contribution of anthropogenic activities and natural changes to the total sediment budget of the system, as well as assess changes in sediment dynamics within the rivers and creeks that composes the Delta system.

Introduction

Estuaries host industries, ports and endemic species and are the source of fresh water and sediment that prevent coastal erosion and maintain habitat conditions. The many stakeholders of the system have different water and/or space demands and often modify the estuary in many ways including building of dams, breakwaters, altering the geometry of river branches, and pumping water. In addition, estuaries are affected by sea level rise and earthquakes that damage levees.

Located landward of San Francisco Bay, the Delta is an inland channel network formed by the junction of the Sacramento and San Joaquin Rivers (Fig. 1a). The Delta collects more than 40% of the total fresh water from the entire state of California forming the largest estuary in the west coast of the United States (Kimmerer, 2004). Currently, fresh water is exported in a major pumping effort from the southern Delta to supply cities and agriculture to the south with fresh water (about 200 m³/s). Hydraulic mining in the mid-19th century supplied vast amounts of sediments to the Bay-Delta system. In the 20th century, reservoir construction in the watershed decreased sediment loads drastically. Water diversion works constructed in the 20th century in the Delta (such as gates and pumping stations) and a (possible) future extension of the pumping facilities further alter the flow regime, leading to significant impact in morphology (Jaffe *et al.*, 2007). Another important forcing for changes in sediment budget in estuaries is the increase of accommodation space by natural forcing like sea level rise. For the San Francisco Estuary, levee failure due to earthquakes would also drastically change the system. Ganju and Schoellhamer (2009) discuss how intertidal flats and wetlands may not be able to keep pace with sea level rise. The objective of this paper is to quantify changes in sediment dynamics and budget in the Delta system due to anthropogenic (dam construction, pumping) and natural (sea level rise and earthquake) changes.

Methodology

In order to meet the study objectives we applied a process-based numerical model, DFlow FM (finite volume model) covering the entire Bay-Delta System. The model domain is 150 by 180km and has a network of 80.000 node flexible mesh with spatial resolution varying from 10m to 400m. Since salinity does not enter the Delta we applied the 2D version. We calibrated the model using an extensive data set available for the Bay-Delta system to match observed water discharge, water level and suspended sediment concentration (SSC).

The anthropogenic impacts are assessed based on a multiple scenario analysis of reservoir construction and water diversion works. The natural impacts are based on 3 sea levels rise scenarios and island levee failure due to an earthquake. Covering the required range of spatial scales and time frames with a process-based approach is a unique and challenging aspect of this study.

Conclusions

This paper identifies flow pattern and sediment budget changes in the Delta caused by human intervention and natural variability. The model results are described in terms of sediment fluxes, such as the ones already determined for the existing system (Fig. 1), throughout the Delta and the spatial distribution of deposition and erosion from convergences and divergences in sediment

fluxes. Changes in sediment flux and budget for each stressor allow us to define the most and the least important of them to the San Francisco delta system. Insight is gained on past, as well as possible, future change to prepare and prevent major damage.

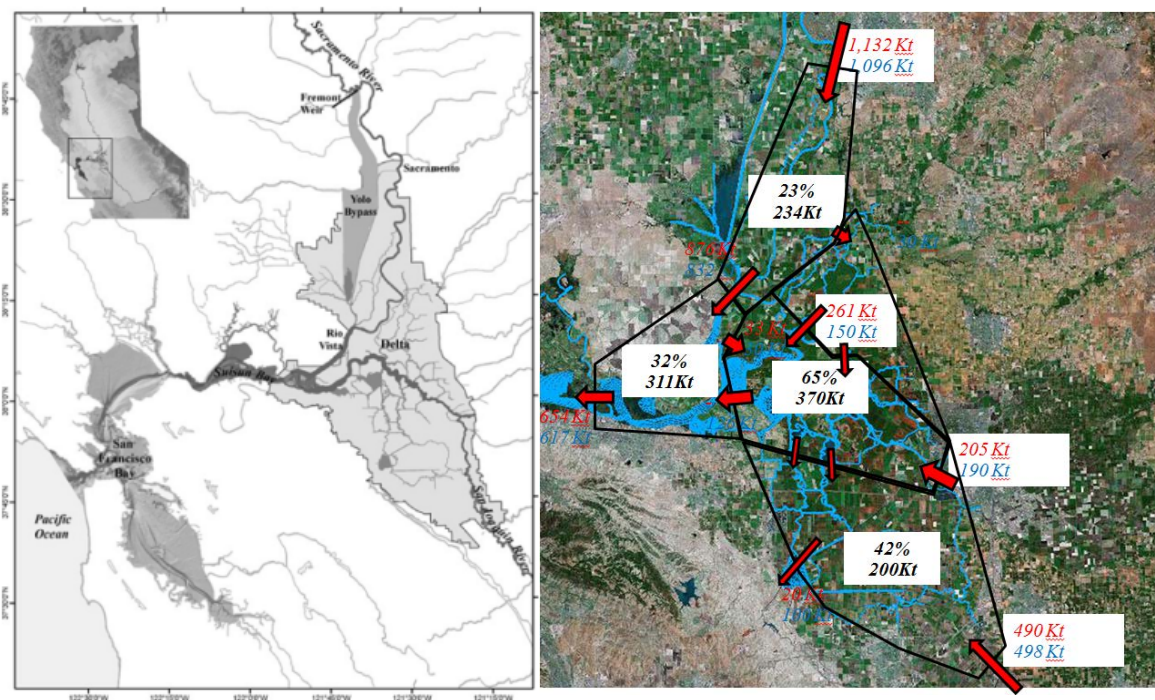


Fig. 1. a) Bay-Delta system map and location. b) Delta Sediment Budget for the year 2011. The arrows indicate the sediment flux direction and magnitude, which is also given by the numbers. The top (red) number is the data flux estimation and the bottom (blue) the model. The areas represent the net deposited sediment. In the background is the Delta unstructured mesh.

References

- Ganju N.K. and D.H. Schoellhamer. 2009. Decadal-timescale estuarine geomorphic change under future scenarios of climate and sediment supply. *Estuaries and Coasts* 33(1):15-29.
- Jaffe B.E., R.E. Smith and A.C. Foxgrover. 2007. Anthropogenic influence on sedimentation and intertidal mudflat change in San Pablo Bay, California: 1856-1983. *Estuarine, Coastal and Shelf Science* 73(1-2):175-187.
- Kimmerer W. 2004. Open water processes of the San Francisco Estuary: from physical forcing to biological responses. *San Francisco Estuary and Watershed Science* 2(1).

Physical and biogenic influences on sediment dynamics in a mixed sediment intertidal environment

Bass S.J.¹, J. Hope², A.J. Manning^{1,5,7}, R.J. Aspden², T. Downs¹, H.S. Eccles¹, P.L. Forsberg¹, I.D. Lichtman^{3,4}, R.J. Schindler¹, P.D. Thorne³, J.H. Baas⁴, A.G. Davies⁴, J. Malarkey⁴, D.R. Parsons⁵, D.M. Paterson², J. Peakall⁶ and L. Ye⁵

¹ School of Marine Science & Engineering, Plymouth University, Drake Circus, Plymouth, PL4 8AA, UK
E-mail: sbass@plymouth.ac.uk

² Sediment Ecology Research Group, Scottish Oceans Institute, School of Biology, University of St Andrews, East Sands, St Andrews, KY16 8LB, Scotland, UK

³ National Oceanography Centre, Joseph Proudman Building, 6 Brownlow Street, Liverpool L3 5DA, UK

⁴ School of Ocean Sciences, Bangor University, Menai Bridge, Anglesey, LL59 5AB, UK

⁵ Department of Geography, Environment and Earth Sciences, University of Hull, Cottingham Road, Hull, HU6 7RX, UK

⁶ School of Earth and Environment, The University of Leeds, Leeds, LS2 9JT, UK

⁷ HR Wallingford, OX10 8BA, UK

Introduction

In mixed sediment environments, clay and silt particle content, together with organic compounds, can play a key role in suspended sediment flocculation dynamics. Benthic and pelagic bacteria and algae secrete extracellular polymeric substances (EPS) that significantly increase the cohesion of muddy sediments (e.g. de Brouwer *et al.*, 2005) acting to enhance both flocculation and bed stability. Similarly, epipsammic diatoms, cyanobacteria and other microphytobenthos have the potential to bind together sand size particles (e.g. Harper and Harper, 1967). While these biogenic processes are recognized to be important in mixed sediment flocculation dynamics (Manning *et al.*, 2013), prediction of their contribution remains elusive and detailed field measurements are vital for extending the parameter range of existing data sets, validating and improving the calibration of numerical mixed sediment transport models (e.g. Spearman *et al.*, 2011).

Flocculation critically influences the flux of sediment to the bed and alters transport potential of deposited sediment. This plays a role in the development of bedforms, which in turn effect turbulent flow fields and thus interact through a range of sedimentary processes. To date there are few published comprehensive field data sets of both bed and floc dynamics in sediments containing a mixture of both mud and sand (Manning *et al.*, 2010, 2013). The work presented herein (which is part of the UK NERC-funded COHBED project) concerns the influence of biological and sediment cohesion on bedform dynamics and thus evolve a process-based knowledge of the sediment suspension mechanisms that feed and respond to bed evolution. Here we examine a comprehensive set of floc, suspension, biochemical, hydrodynamic and bedform data in an intertidal mixed sediment estuarine environment. The evolution of the suspension concentrations, floc and primary particle size distributions and hydrodynamics are analysed over a tidal inundation together with the organic content in the water column. These changes over the flood tide are discussed in relation to the bed composition and the net change in bedform features over a single tide.

Methodology

Fieldwork was conducted in the intertidal region of the Dee Estuary situated in North-West England. The Dee estuary is a macrotidal, funnel-shaped estuary, with a tidal range between 5.33m and 9.72m (Potter Huckle and Marrs, 2004). A variety of measurements were undertaken from the 21st of May to the 1st of June 2013 (as part of the wider COHBED project) and the results presented here represent time series over two single inundation events that were collected from sites with different bedform features and varying bed composition, with site B being notably muddier than site A.

At both sites data were collected during inundation via an instrument rig and also from a moored boat in close proximity to the instrument rig. Bed samples were collected prior to and after inundation and analysed for particle size distribution and organic content. Three-dimensional point clouds derived from Terrestrial Laser Scanning (TLS), taken at low water on either side of the inundation event, were used to provide information on bedform characteristics and scales. Amongst the equipment positioned on the rig were two Optical Backscatter Systems (for estimating suspended sediment concentrations), two water sampling tubes leading to ISCO water sampler carousels on the nearby research vessel, two Acoustic Doppler Velocimeters and a Pressure

Transducer. To obtain measurements of floc size (D) and settling velocity (W_s) distributions a water sample was collected using a 2.2L Van Dorn horizontal water sampler every fifteen minutes during the flood and ebb. Sub-samples from the Van Dorn sampler were extracted via a modified pipette and transferred separately to a low intrusion, video-based laboratory spectral flocculation characteristics (LabSFLOC) instrument (Manning, 2006) for instant data analysis. Indications of individual floc effective density (ρ_{eff}) and floc mass were determined.

The two ISCO water samplers, containing 24 bottles each, were automated to collect three 500ml replicates of water every ten minutes over both the flood and ebb tide. Samples were collected for suspended mass concentration, EPS content (spectrophotometric methods), and for laser particle sizing. Representative floc populations were carefully extracted from the Van Dorn using a modified pipette and then transferred to the LabSFLOC settling column, whereby settling flocs were viewed by a high resolution digital video camera, (resolution $\sim 10\mu\text{m}$) from which size and settling velocity distributions were estimated.

Results

Peak current speeds reached a nominal value of 0.6m/s during the flood at both site A and site B. The ambient flow produced maximum near bed turbulent shear stresses of $\sim 0.25\text{Pa}$. However, the point clouds data from the TLS taken at both sites indicates that bedforms at site B are both smaller in scale and underwent less net change over a single tide than those at site A. Despite similar hydrodynamic conditions and primary particle size at the two sites, suspended sediment concentrations (SSC) from the muddier site indicate higher near bed concentrations (SSCs of 118-466mg/l on 25th May 2013 compared to 56-215mg/l on 20th May 2013 during floc sampling at sites A and B, respectively) and greater suspended sediment stratification. A total of 67 LabSFLOC-2 populations were collected. Tables I and II summarise key parameterized floc properties for run and sub-run timescales at Sites A and B. While mean floc properties varied little at both sites, slightly higher mean floc size and a higher percentage of macroflocs ($D > 160\mu\text{m}$) were observed alongside the higher sediment concentrations at the muddier site (site B).

Initial biochemical results suggest that over the period of tidal inundation there was relatively little temporal variation of organic matter, while primary particle size analysis indicates that the relative proportions of silt to sand increased over the slack high water period as expected with the concomitant decrease in turbulent shear. Further biochemical analyses of the bed composition and suspension will be used to compare the temporal evolution of bed and suspension characteristics before, during and after inundation and mechanisms contributing to these characteristics will be discussed in relation to the two different sites.

Table I. Floc property ranges and average Macrofloc content for Site A (25th May 2013) and Site B (29th May 2013)

	D (μm)	w_s (mm/s)	ρ_{eff} (kg/m^3)	Macroflocs (%)
Site A	127-251	4-11	263-839	61.5
Site B	147-254	4-13	312-704	86.7

Table II. Total run and sub-run average floc properties for Site A (25th May 2013) and Site B (29th May 2013)

		D (μm)	w_s (mm/s)	ρ_{eff} (kg/m^3)
Site A	Entire tidal cycle	175.2	6.9	552.0
	Flood	142.9	6.4	655.4
	Ebb	195.4	7.3	487.4
Site B	Entire tidal cycle	189.7	7.9	548.6
	Flood	202.9	8.1	532.2
	Ebb	150.7	6.8	448.1

References

De Brouwer J.F.C., K. Wolfstein, G.K. Ruddy, T.E.R. Jones and L.J. Stal. 2005. Biogenic stabilization of intertidal sediments: the importance of extracellular polymeric substances produced by benthic diatoms. *Microbial Ecology* 49(4):501-512.

- Harper M.A. and J.F. Harper. 1967. Measurements of diatom adhesion and their relationship with movement. *British Phycological Bulletin* 3:195-207.
- Manning A.J. 2006. Labsfloc - a laboratory system to determine the spectral characteristics of flocculation cohesive sediments. Report TR 156. Release 1.0. HR Wallingford. p.1-13.
- Manning A.J., J.V. Baugh, J.R. Spearman and R.J. Whitehouse. 2010. Flocculation settling characteristics of mud: sand mixtures. *Ocean dynamics* 60(2):237-253.
- Manning A.J., J.R. Spearman, R.J.S. Whitehouse, E.L. Pidduck, J.V. Baugh and K.L. Spencer. 2013. Laboratory assessments of the flocculation dynamics of mixed mud: sand Suspensions. p.119-164, Chapter 6. In: *Sediment Transport Processes and their Modelling Applications*. Manning A.J. (Ed.). InTech, Rijeka, Croatia, ISBN: 978-953-51-1039-2. DOI: org/10.5772/3401.
- Potter Huckle and Marrs. 2004. Spatial and temporal changes in salt marsh distribution in the Dee Estuary, NW England, determined from aerial photographs. *Wetlands Ecology and Management*. p.483-498.
- Spearman J.R., A.J. Manning and R.J.S. Whitehouse. 2011. The settling dynamics of flocculating mud: sand mixtures: Part 2 - Numerical modelling. *Ocean Dynamics* 61:351-370. DOI: 10.1007/s10236-011-0385-8.

Local mechanisms of cohesive soil erosion

Brunier-Coulin Florian, Pablo Cuellar and Pierre Philippe

French Research Institute of Science and Technology for Environment and Agriculture, OHAX Research Unit, IRSTEA, 3275 route de Cézanne, 13100 Aix-en-Provence, France
E-mail: florian.brunier@irstea.fr; pablo.cuellar@irstea.fr; pierre.philippe@irstea.fr

Introduction

Soil erosion concerns several domains of agriculture, ecology and engineering. According to Girard *et al.* (2005) there are 25 billion of tons of annual sediment losses due to water erosion worldwide, while Syvitski *et al.* (2005) identified 20 billion of tons of the same sediments delivered annually by rivers into the oceans. For civil engineering, erosion is a central problem for many infrastructures located next to erodible areas or which are themselves directly erodible. According to Foster *et al.* (2000), 90% of embankment failures are caused by erosion. Furthermore, the International Commission Of Large Dams (ICOLD) estimates that 75% of dams are built in sand, clay or muddy sediments and are consequently subject to erosion.

Surface erosion

For the general case of a soil exposed to the flow of water, the surface erosion takes place at the solid-liquid interface. The solid phase (the soil) is generally a cohesive material where internal forces are primarily due to Van der Waals attractive forces and electrostatic forces in balance with repulsive forces (Lick *et al.*, 2004). The water flowing on the surface constitutes the liquid phase and is the eroding agent. In terms of quantification, the most common erosion model is probably the linear threshold model firstly proposed by Partheniades (1965) and Ariathurai and Arulanandan (1978). According to this law, if the average stress τ due to turbulent flow surpasses a certain critical stress τ_c , it can cause erosion. Beyond this threshold, the rate of removed material, which can be defined either in terms of eroded mass or volume, is proportional to the distance to the threshold through an erosion coefficient k . These two parameters can be used to calculate the erosion rate depending on an average hydrodynamic stress. However, in practice the average magnitude of the stress is often insufficient for a precise quantification, since the fluctuating flow creates instantaneous local peak stresses which can significantly exceed the average stress and result in particles dislodgment (see e.g. Diplas *et al.* (2008) for the case of non-cohesive grains). For cohesive material, the fluctuations have a similar role but the mechanism of material removal is different from the non-cohesive case. Winterwerp and Van Kesteren (2004) distinguish four modes of cohesive particles dislodgment: entrainment (fluidization), floc erosion (disruption and break up of flocs), surface erosion (drained process where eroded particles were replaced by water) and mass erosion (undrained process, local failure within the bed).

To evaluate the soil's resistance to erosion, several erosion tests have been developed. The Jet Erosion Test (JET) is a circular impinging vertical turbulent jet introduced by Moore and Mash (1962) and later used e.g. by Hanson and Cook (2004), who measured the deepening of a soil scour hole as a function of time. The Hole Erosion Test (HET), firstly introduced by Lefebvre *et al.* (1985) and further developed by Bonelli *et al.* (2006), is used to modelling piping erosion by measuring variation of the radius of an initial pipe, eroded by a permanent flow. The Erosion Function Apparatus proposed by Briaud *et al.* (1999) consists in measuring the velocity by which a 1mm thick circular section of soil sample (76.2mm diameter) is completely eroded when it is placed inside a flow field in a pipe with rectangular cross-section. Another apparatus developed by Le Hir *et al.* (2008) consists in a sample of sediment placed inside a pipe with rectangular cross-section where the erosion rate is estimated by measuring sand accumulation in a sand trap and by measuring turbidity.

Present contribution

Our contribution will focus on the elementary mechanisms involved during the surface erosion of a cohesive soil by a fluid flow in order to improve the local modelling of erosion. An experimental approach enables us to develop model materials, which then can be subjected to given hydrodynamic stresses and controlled mechanic stresses. Preliminary results will be presented on the following points. Firstly, the development of materials for which it is possible to adjust specifically and continuously certain characteristics of the soil and then to identify the soil properties having a strong incidence on the resistance to erosion. Secondly, the local analysis of erosion mechanisms by using transparent medium and adapted optical equipment. This makes the time-space monitoring during erosion possible and allows to see the mechanisms by which a fluid flow leads to the removing of elementary particles in cohesive material. The two optical techniques, which are the refractive index matching between the matrix and the grains and the planar laser-

induced fluorescence already used by Philippe and Badiane (2013), made possible to model a cohesive medium with transparent cohesive medium.

References

- Ariathurai R. and K. Arulanandan. 1978. Erosion rates of cohesive soils. ASCE 104(2):279-283.
- Bonelli S., O. Brivois, R. Borghi and N. Benahmed. 2006. On the modelling of piping erosion. *Comptes Rendus de Mécanique* 334:555-559.
- Briaud J.L., F.C.K. Ting, H.C. Chen, Y. Cao, W. Han and K.W. Kwak. 2001. Erosion function apparatus for scour rate predictions. *J. Geotach. Geoenviron. Eng.* 127(2):105-113.
- Diplas P., C.L. Dancey, A.O. Celik, M. Valyrakis, K. Greer and T. Akar. 2008. The Role of impulse on the initiation of particle movement under turbulent flow conditions. *Science* 332:717-720.
- Foster M., R. Fell and M. Spannagle. 2000. The statistics of embankment dam failures and accidents. *Can. Geotech. J.* 37:1000-1024.
- Girard M.C., C. Walter, J.C. Rémy, J. Berthelin and J.L. Morel. 2005. *Sols et environnement*. Dunod Publishing, Paris. 816p.
- Hanson G.J. and K.R. Cook. 2004. Apparatus, test procedures, and analytical methods to measure soil erodibility *in situ*. *Applied Engineering in Agriculture* 20(4):455-462.
- ICOLD: International Commission Of Large Dams, Technology of Dams, online, http://www.icold-cigb.org/GB/Dams/technology_of_dams.asp (Page visited on 25 November 2014).
- Le Hir P., P. Cann, B. Waeles, H. Jestin and P. Bassoullet. 2008. Erodibility of natural sediments: experiments on sand/mud mixtures from laboratory and field erosion tests. *Proceedings in Marine Science*, Elsevier publishing, Volume 9:137-153.
- Lefebvre G., K. Rohan and S. Douville. 1985. Erosivity of natural intact structured clay: evaluation. *Can. Geotech. J.* 22:508-517.
- Lick W., L. Jin and J. Gailani. 2004. Initiation of movement of quartz particles. ASCE 130(8):755-761.
- Moore W.L. and F.D. Masch. 1962. Experiments on the scour resistance of cohesive sediments. *J. Geophys. Res.* 67(4):1437-1446.
- Partheniades E. 1965. Erosion and deposition of cohesive soils. ASCE 91(HY1):105-139.
- Philippe P. and M. Badiane. 2013. Localized fluidization in a granular medium. *Phys. Rev. E* 87, 042206.
- Syvitski J.P.M., C.J. Vörösmarty, A.J. Kettner and P. Green. 2005. Impact of humans on the flux of terrestrial sediment to the global coastal ocean. *Science* 308:376-380.
- Winterwerp J.C. and W.G.M. Van Kesteren. 2004. *Introduction to the physics of cohesive sediment in the marine environment*. Elsevier publishing, Eastbourne. 576p.

Online monitoring, conceptual model of sediment dynamics and numerical modelling of non-tidal lagoon system

Bundgaard Klavs, Ulrik Lumborg and Pernille Forsberg

DHI, Agern Allé 5, DK-2970 Horsholm, Denmark.
E-mail: klb@dhigroup.com

Rødsand Lagoon is a non-tidal lagoon located in the south of Denmark approximately 10km east of the proposed immersed tunnel over the Fehmarnbelt between Denmark and Germany. The lagoon is a Natura 2000 area and home to a variety of birds, seals and other animals. It is protected by a 20-km long barrier which, under normal conditions, shelters the lagoon from incoming waves. The lagoon system is of great interest for the EIA for the Fehmarnbelt connection since spilled material from the dredging works may enter the lagoon.



Fig. 1. Overview of the Rødsand Lagoon and the measuring stations (the NS stations).

DHI, Femern A/S and University of Copenhagen have joined together to setup a field laboratory in the Rødsand Lagoon. The idea is to create an area in which data and models are abundant and where students and scientists can test ideas and developments. The first step was to set up a field test programme. DHI and Femern A/S deployed four fixed stations in the lagoon in the spring 2014. The stations measure NTU, waves, currents, wind, water levels, salinity, temperature, light, grain size distributions, and fluorescence (chlorophyll-a). Three of the stations are equipped with automatic water samplers. All stations are online which allows for monitoring of data streams and for extraction of water samples at specified times without having to be physically present. The monitoring system is scheduled to run to spring 2015. As part of the programme, DHI and University of Copenhagen also plan to hold a PhD course in the area in 2015.

As part of the monitoring campaign DHI has developed new methods for measuring light and shallow water waves using available sensors from other fields. The new sensors are smaller and cheaper than those available commercially. So far they have proved to provide similar results compared to commercially available products.

Based on the field survey programme DHI has developed a conceptual model of the area. The conceptual model describes and explains various processes governing the flushing and sediment dynamics in the area. Among the many findings are:

- that the inflow of sediment to the system happens on rising water when waves are present at the entrances;
- that local reorganisation of sediment happens during periods with small water level variations and strong winds;
- that several populations of sediment exist depending on the level of waves. This is due to floc breakup, import of external sediment and the presence of fine sand. Grain sizes are determined directly by laser diffraction technology and indirectly using water samples;

- that light attenuation is correlated to the sediment concentration;
- that calibration of NTU to SSC is very difficult due to changing grain sizes in time;
- new simpler measuring devices perform similarly to existing commercial products.

Based on the findings from the stations it has become clear that non-tidal coastal lagoons can be very complex with respect to sediment dynamics. The presented monitoring setup in combination with a 3D numerical model is a strong tool to understand the system. This is of large value with respect to general research of sediment dynamics as well as for assessing direct and indirect effects of the dredging activities in connection with nearby dredging works.

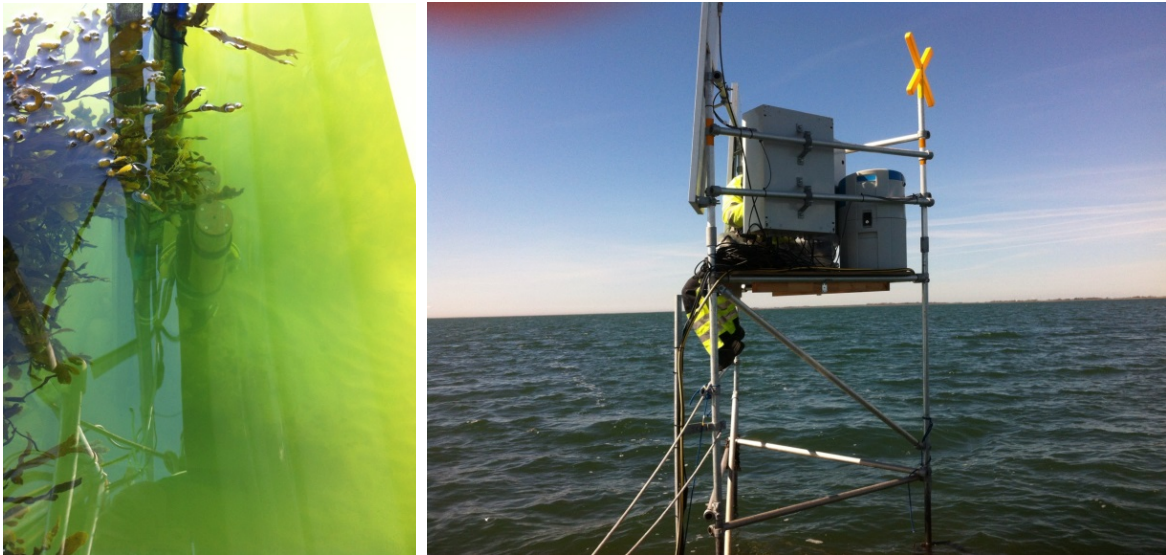


Fig. 2. NTU mounted at NS04A (left), platform station (right).

DHI will present the ideas, the findings and the challenges from measuring and modelling at the field laboratory in Rødsand.

Flocculation characteristics on a muddy tidal flat

Chao Guo¹, He Qing¹, Bram van Prooijen² and Wang Xianye¹

¹ State Key Laboratory of Estuarine and Coastal Research, East China Normal University, P.R. China
E-mail: chaoguo@ecnu.cn

² Department of Hydraulic Engineering, Faculty of Civil Engineering and Geosciences, Delft University of Technology, Delft, the Netherlands

Introduction

In the estuarine intertidal flats, the fate of suspended matter highly depends on flocculation processes. The relationship between floc size, settling velocity and the turbulent shearing and suspended sediment concentration (SSC) has been discussed in various estuaries (e.g. Manning, 2004; Pejrup and Mikkelsen, 2010). Despite this progress, there are still many issues unresolved. To gain more insight in the flocculation characteristics and their significance for the deposition of suspended sediment on the mud tidal flat, a field survey was carried out on a muddy tidal flat of the Westerschelde (the Netherlands). The prime objective was to evaluate the short-term variations of flocculation and de-flocculation over a full spring-neap cycle as well as the potential settling flux of suspended sediment.

Methods

The field observation was done on the muddy Kapellebank tidal flat in Westerschelde, the Netherlands (Fig. 1) for one month, from 28 April 2014 to 28 May 2014. The landform of this flat is simple with a small slope from the bank to channel. Tidal currents generate peak velocities of 0.45m/s and 0.35m/s during flood and ebb, respectively, with a maximum tidal range of 290cm during spring tide. Increased wind speeds were found over a period of 6 days, while the remaining period could be classified as calm.

A LISST-100C was used together with an ADV (Nortek 6.0MHz Vector), two OBS-3+ at 15 and 30cm above the bed, and a downward looking ADCP (Nortek 2.0MHz HR-Profiler). All the instruments were moored on the tidal flat to get synchronous information of hydrodynamics and sediment flocs. The sensor of the LISST was 15cm above the bed, and it was used to get *in situ* particle size distributions and the mean effective density and settling speed of flocs. The calculated floc effective density through the results of LISST and SSC include the effects of porosity and shape, however, their influences on settling velocity of flocs were only minor factors according to Lick and Huang (1993). Therefore we consider the settling velocity of floc through effective density by Stokes law as reasonable.



Fig. 1. Location of the measurement site.

Results

Fig. 2 shows a subset of the measurements during spring tide. A consistent variation of the floc size is found over a tidal cycle. The largest flocs were over $200\mu\text{m}$ and occurred at low turbulent shear stress at the turning of the tidal velocity from flood to ebb. The smallest flocs of around $60\text{-}70\mu\text{m}$ were found at maximum ebb velocity. Just before falling dry, a peak in southern velocity is found (most clear in the second and third tide). This peak can be attributed to large scale turbulent eddies at the interface between channel and flat. These velocities result in a local minimum in floc diameter. The flocculation and floc break-up were asymmetric in a tidal cycle. During the spring tides (Fig. 2), the fragile macroflocs break up to the stronger $60\text{-}70\mu\text{m}$ microflocs soon after the low turbulent shear. However, the time it took to form the macroflocs was twice or triple. The pattern was quite different during the neap tide, the time of floc break up was a little longer than sediment flocculation. The turbidity shows a close correlation with the shear stress due to tidal flow. For shallow water, waves will play a role as well.

Conclusion and outlook

A comprehensive data set was obtained recently at a muddy tidal flat in the Westerschelde, containing high-resolution hydrodynamic results and sediment characteristics. The patterns show a very consistent pattern for the different tides. Furthermore, clear correlations are found between hydrodynamic data and sediment data. A full interpretation of the data set is in progress and will be discussed in the full paper.

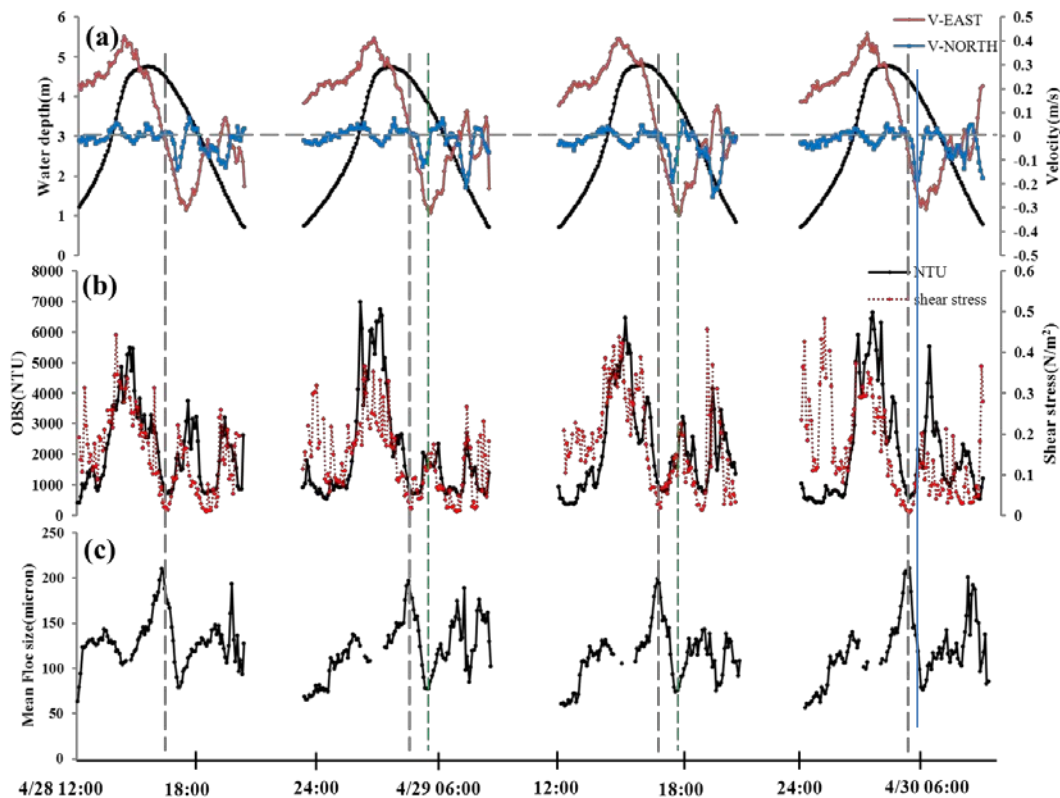


Fig. 2. Results during spring tides. (a) Depth (black line) and current speed of two directions (east and north), (b) NTU from OBS-3+ sensor (black line) and turbulent shear stress (red dotted line) and (c) mean floc size.

References

- Lick W. and H. Huang. 1993. Flocculation and the physical properties of flocs. Nearshore and estuarine cohesive sediment transport 21-39.
- Manning A.J. 2004. Observations of the properties of flocculated cohesive sediment in three western European estuaries. *Journal of Coastal Research* 41:70-81.
- Pejrup M. and O.A. Mikkelsen. 2010. Factors controlling the field settling velocity of cohesive sediment in estuaries. *Estuarine, Coastal and Shelf Science* 87(2):177-185.

Zeta potential: a new tool for assessing the properties of clays?

Chassagne Claire and Maria E. Ibanez

Section of Environmental Fluid Mechanics, Civil Engineering and Geosciences, Delft University of Technology, PO Box 5048, 2600 GA, Delft, the Netherlands
E-mail: C.Chassagne@tudelft.nl

Important properties of cohesive clays, like flocculation ability, Cation Exchange Capacity (CEC), sedimentation and compaction behaviour are linked to the interfacial properties of the constitutive clay particles. One of the most important properties is surface charge, responsible for clay-clay and clay-(poly)ions interactions. A measure of this surface charge is the zeta potential.

The zeta potential is a parameter that can be obtained from electrokinetic experiments, i.e. measuring the response of a sample to the application of an electric field. One of the most popular electrokinetic techniques for assessing the zeta potential of particles suspended in a liquid is electrophoresis, where the zeta potential is extracted from the velocity at which the particles travel under influence of the electric field.

The link between surface charge and zeta potential has long been established (Sposito, 1984), as is the relation between surface charge and flocculation (Overbeek, 1952). These relations between surface charge - zeta potential - flocculation are however extremely complex, as they are challenging from a theoretical point of view and because some parameters required in the theory, like ionic interactions close to the particle's surface, are very difficult to assess experimentally. Progresses have been made in the recent years, both experimentally and theoretically. Many different clayey systems have been investigated in detail experimentally, and the relations between zeta potential, suspending medium properties and flocculation or settling behaviour have been established (Yukselen and Kaya, 2002; Mpofu *et al.*, 2003; Chassagne, 2009; Lee *et al.*, 2012; Ibanez *et al.*, 2014).

A major shortcoming of the theoretical models linking electrophoresis and zeta potential is that these models are only applicable to spherical particles.

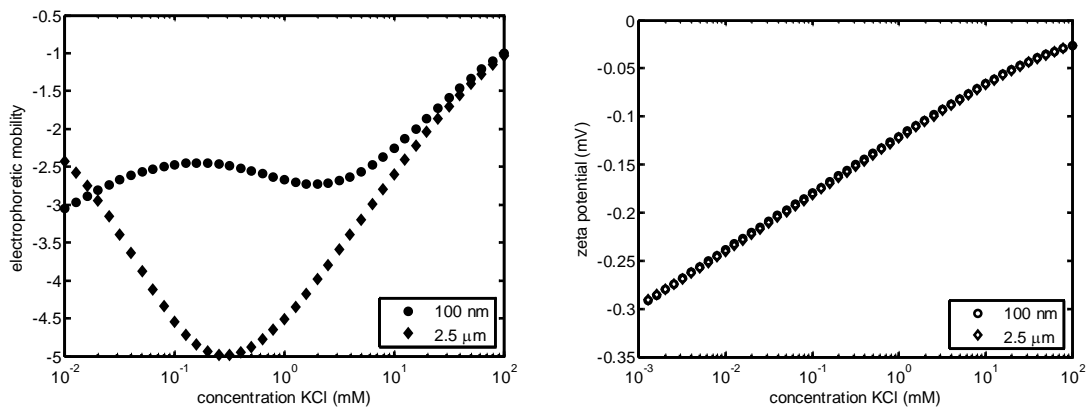


Fig. 1. Left: theoretical velocity (electrophoretic mobility) of two spherical particles, of different sizes but same surface charge density, as a function of added KCl salt concentration. Right: their corresponding zeta potential.

Recent studies have demonstrated the importance of non-sphericity in both the qualitative behaviour and quantitative values of the zeta potential upon changes in salinity in particular (Chassagne and Bedeaux, 2008; Chassagne *et al.*, 2009; Chassagne, 2013; Tsujimoto *et al.*, 2013). From an engineering point of view, the zeta potential ought to be a quantity that is easily accessible and provide sufficient information with a limited amount of data processing and in a reasonable amount of time.

In this study, we will demonstrate that electrophoretic studies can indeed be used to provide useful information about the clay surface properties, when performing a specific set of experiments, and being aware of general rules. These rules are derived from the systematic investigations undertaken in our group on various clayey suspensions, in combination with our theoretical models.

References

- Chassagne C. and D. Bedeaux. 2008. The dielectric response of a colloidal spheroid. *J. Coll. Int. Sci.* 326(1):240-253.
- Chassagne C., F. Mietta and J.C. Winterwerp. 2009. Electrokinetic study of kaolinite suspensions. *J. Colloid Int. Sci.* 336(1):352-9.
- Chassagne C. 2013. Dielectric response of a charged prolate spheroid in an electrolyte solution. *Int. J. of Thermodynamics* 34(7):1239-1254.
- Ibanez M.E., C. Chassagne and A. Wijdeveld. 2014. Role of mono- and divalent ions on the stability of kaolinite suspensions and fine tailings. (submitted *Clay and Clays Minerals*)
- Lee B.J., M.A. Shlautman, E. Toorman and M. Fettweis. 2012. Competition between kaolinite flocculation and stabilization in divalent cation solutions dosed with anionic polyacrylamides. *Water Res.* 46(17):5696-5706.
- Mpofu P., J. Addai-Mensah and J. Ralston. 2003. Influence of hydrolyzable metal ions on the interfacial chemistry, particle interactions, and dewatering behaviour of kaolinite dispersions. *J. Colloid Int. Sci.* 261(2):349-359.
- Overbeek J.T.G. 1952. Kinetics of flocculation. p.278-300. In: *Colloid Science*. Kruyt H.R. (Ed.). Elsevier Publishing Company.
- Sposito G. 1984. *The surface chemistry of soils*. Oxford University Press, New York
- Tsujimoto Y., C. Chassagne and Y. Adachi. 2013. Comparison between the electrokinetic properties of kaolinite and montmorillonite suspensions. *J. Colloid Int. Sci.* 407:109-115.
- Yukselen Y. and A. Kaya. 2002. Zeta potential of kaolinite in the presence of alkali, alkaline earth and hydrolysable metal ions. *Water, Air, and Soil Pollution* 145:155-168.

The relationship between waves, mud deposition and meteorological events in the Rio Grande do Sul state coastal area (Brazil)

Cuchiara Debora¹, Gustavo Cuchiara², José Francisco de Souza¹ and Elisa Fernandes¹

¹ Fundação Universidade Federal do Rio Grande, CP 474, CEP: 96201-900, Rio Grande, Brazil
E-mail: debora.cuchiara@furg.br, jfas.ee.furg@gmail.com, dfsehf@furg.br,

² Department of Earth and Atmospheric Sciences, University of Houston, TX77004, USA
E-mail: gustavo.cuchiara@gmail.com

Introduction

Fluid mud deposits have been found in many coasts, rivers, and estuaries around the world, especially where one or more rivers lead significant amounts of fine sediment in suspension in the sea (Perillo & Kjerfve, 2003). In addition to the availability of continental sediments, the processes of transport and deposition of mud on the inner shelf is a consequence of the interaction between coastal currents generated by winds, associated with the passage of frontal systems, and low tidal range (Drake, 1976).

Resulting from the action of winds on ocean surface, the gravity waves are closely related to atmospheric variations and have high spatial and temporal variability playing an important role in the formation of coastal features. The wind blowing over the water surface induces shear stresses and pressure variations which result in waves that grow in the direction of the wind until a balance arises between the energy input and the dissipation in the wave field (Kinsman, 1965). The properties of the wind field (i.e. speed, direction, and duration) and the geometry of the water body where the waves are being generated (i.e. fetch, bottom type and water depth) determine the wave height, period, and direction. Waves generated by open sea will ultimately reach shallow water, where depth-limited wave breaking occurs and the wave energy is mainly dissipated, resulting in a gradually decay of wave height. When ocean waves approach intermediate and shallow waters, seabed fluid-mud interacts with the waves propagating over it. This interaction exerts influence on both waves and fluid-mud, the seabed fluid-mud produces a gradual dissipation of the wave energy, which promotes the attenuation of the wave heights. On the other hand, the pressure exerted on seabed by waves is the main cause of mud suspension and transportation. Both effects are important, and the interaction between them has long been attracting attention of researches due to the great importance of accurately estimating the sea state conditions for coastal engineering purposes (Holland *et al.*, 2003).

The coast of Rio Grande do Sul state presents a Northeast-Southwest orientation, and is characterized by open sandy beaches exposed to wave action. The coastal topography is complex and influences the physical processes determining the waves and the sediment transport at the coast. Over the whole 640km that separates Torres headland in the north (29.5°S) and the Chui Estuary in the south (33.8°S), the only significant interruption occurs at the entrance of the Patos Lagoon (32°S).

The Cassino Beach, located in the southernmost part of Rio Grande do Sul state, is characterized by extensive offshore mud deposition. Previous studies show that the source of the mud deposited offshore and on the shoreface of Cassino Beach is the Patos Lagoon (Martins, 1972; Martins *et al.*, 1979). The fine sediments are carried out from the rivers located at the north of the lagoon and transported towards the ocean by the wave action and wind driven circulation (Calliari *et al.*, 2007). These sediments are periodically suspended, transported and deposited on shore and on the surf zone, exerting important effects on the short and long features observed at the bottom, and bringing negative ecological and economical consequences for the area. Although the dynamics of the fluid mud deposition is still not fully understood, it seems that during stormy conditions, which are generally associated with the periodic passage of cold fronts over the area, the deposit can be reworked and mud is transported to the surf-zone and foreshore of Cassino Beach (Calliari *et al.*, 2007).

The main objective of this work is to investigate the relationship between meteorological events, the behaviour of waves and the mud deposition in the Rio Grande do Sul state coastal area. This work aims to understand the processes that control the dynamics, sediment transport and periodic remobilization of mud banks present in this region. This information is essential to evaluate the influence of waves in various coastal processes (estuarine hydrodynamics, sediment dynamics, occurrence of fluid mud, etc.) and their implications on nautical, maritime and sports activities in this region.

Methodology

A case study is presented for the Cassino Beach, based on a combination of preterits data and field experiments with numerical modelling. For this work were used wave models that include the formulation of damping effect of the wave due to the presence of mud banks. The use of nesting technique between both models with different scales, the WAVEWATCH III (global and regional) and the SWAN (local), will allow the generation and propagation of waves from offshore oceanic regions (offshore) up near the coast regions. The study will be conducted on the records of occurrences of mud banks on Cassino Beach in the period between 1998 and 2014.

The SWAN model (Simulating WAVes Nearshore) is a third-generation wave model for obtaining realistic estimates of wave parameters in coastal areas, lakes and estuaries from given wind, bottom and current conditions. However, SWAN can be used on any scale relevant for wind-generated surface gravity waves. The model is based on the wave action balance equation with sources and sinks. The current version of SWAN (41.01) is a modified version of the model, which considers the mud effects formulated by Winterwerp *et al.*, (2007), which derived the physical and mathematical formulations of Gade (1958) and implemented their two-layer model in the standard SWAN model.

The WAVEWATCH III® (Tolman, 2014) is a third generation wave model developed at NOAA/NCEP in the spirit of the WAM model (WAMDI G., 1988; Komen *et al.*, 1994). This model, however, differs from its predecessors in many important points such as the governing equations, the model structure, the numerical methods and the physical parameterizations. The WAVEWATCH III® solves the random phase spectral action density balance equation for wavenumber-direction spectra. The governing equations of WAVEWATCH III® include refraction and straining of the wave field due to temporal and spatial variations of the mean water depth and of the mean current (tides, surges etc.), when applicable.

References

- Calliari L.J., K.T. Holland, P.S. Pereira, R.M.C. Guedes and R.E. Santo. 2007. The influence of mud on the inner shelf, shoreface, beach and surf zone morphodynamics - Cassino, southern Brazil. In: Proceedings, Coastal Sediments '07.
- Drake D.E. 1976. Suspended matter on continental shelves. p.127-158. In: Stanley D.J. & D.J.P. Swift (Eds). Marine Sediment Transport and Environmental Management, New York.
- Gade H.G. 1958. Effects of a non-rigid, impermeable bottom on plane surface waves in shallow water. *Journal of Marine Research* 16(2):61-82.
- Holland K.T., T. Keen and J.M. Kaihatu. 2003. Understanding coastal dynamics in heterogeneous sedimentary environments, Coastal Sediments '03, Clearwater Beach, FL.
- Kinsman B. 1965. Wind waves. Prentice Hall, Englewood Cliffs, New Jersey. 676p.
- Komen G.J., L. Cavalieri, M. Donelan, K. Hasselmann, S. Hasselmann and P.A.E.M. Janssen. 1994. Dynamics and modelling of ocean waves. Cambridge University Press, Cambridge.
- Martins L.R. 1972. Distribuição faciológica dos sedimentos da margem continental Sul-Riograndense, trecho Rio Grande Torres. p.210-211. In: Resumos dos Anais do XXVII Congresso Brasileiro de Geologia (CBG).
- Martins L.R., I.R. Martins, J.A. Villwock and L.J. Calliari. 1979. Ocorrência de Lama na praia do Cassino. *Anais Hidrográficos*. Rio de Janeiro. p.3-20.
- Perillo G.M.E. and B. Kjerfve. 2003. Mechanisms of sediment retention in estuaries. *Land-Ocean Interactions in the Coastal Zone (LOICZ)*. Newsletter 29:5-6.
- Tolman H.L. 2014. User manual and system documentation of WAVEWATCH-III version 1.18. NOAA/NCEP Tech. Note 166. 110p.
- WAMDI Group 1988. The WAM model-A third generation ocean wave prediction model. *Journal of Physical Oceanography* 18:1775-1810.
- Winterwerp J.C., R.F. de Graff, J. Groeneweg and A.P. Luijendijk. 2007. Modelling of wave damping at Guyana mud coast. *Coastal Engineering* 54:249-261.

Creating wetlands with cohesive sediment

Dankers Petra

Rivers Deltas and Coasts, Royal HaskoningDHV, PO Box 151, 6500 AD Nijmegen, the Netherlands
E-mail: petra.dankers@rhdhv.com

The case Lake Marken

Lake Marken is a fresh water lake in the centre of the Netherlands, separated by a dike from Lake IJssel. The latter was created by closing off an estuary in the 1930's. From then onwards, the water changed from salt and brackish to fresh. In the 1970's a dike was constructed in Lake IJssel and Lake Marken was born. Since that time, the ecosystem in Lake Marken has strongly declined. Nowadays, the lake has a high turbidity. Water plants and bivalves have difficulties to survive or have disappeared and what should be a birds paradise has a low biodiversity.

In 2010 Royal HaskoningDHV was granted a 6 year research programme by the Department of Waterways and Public works of the Dutch Ministry of Infrastructure and the Environment. The goal of this programme was to find out which measures would be most suitable and fruitful to improve the biodiversity and resilience of the ecosystem. One of the measures to be examined was a large scale wetland. However, the wetland needed to be constructed with local materials, in this case cohesive sediments from the bed of the lake. A pilot project was set up to examine the possibilities of building with cohesive sediment. The pilot project consists of the creation of a lagoon with different depth regions and wetlands of different altitudes. The construction phase started in 2013 and an extensive monitoring programme started at the same time. At the end of 2015, the research programme and the monitoring will end. By that time the project is expected to have given much insight in the behaviour of cohesive sediment when used as building material and the possibilities for flora and fauna when developing such an island.

Design of the island

The pilot island was constructed for the sole reason of gathering scientific knowledge on constructing such an island. The results can be used at a later stage for designing and constructing a large scale wetland. The island as constructed at the moment can therefore be seen as a laboratory in the field. Fig. 1 shows a photograph of the island just after finalising the construction. The island consists of two compartments and 8 small test fields. One of the compartments is in open contact with the water of lake Marken while the other compartment is closed off from the lake. At the start of the experiment, bed levels in the open compartment lie between just above the water level to 80cm below water level. In the closed compartment bed levels vary from 1m above water level to 20cm below water level. Furthermore the sediment in the closed compartment is constructed with a slope (from the top left corner to the right low corner in the photograph). All material in the compartments and test fields consists of cohesive sediment. The boundaries of the island consist of geo containers and geo tubes that are filled with cohesive sediment.



Fig. 1. Aerial photograph of the pilot island.

Monitoring programme

There are several research questions to be answered by the pilot project. Most important are the questions relating to the behaviour of the cohesive sediment, such as consolidation velocity and soil formation. Other important questions relate to morphology and ecology, e.g. sustainability of the island and morphological and ecological development. In order to answer these questions we set up an extensive monitoring programme. We use settlement rods, water pressure meters and sediment samples for consolidation monitoring. Morphological monitoring is performed by using flow meters, wave rods, settlement rods, visual observations, echo sounder measurements and OBS measurements for turbidity. Finally, the ecological development is monitored, thereby focussing on specific species of fish, birds and fauna.

Preliminary results

The first results already give some insight in the suitability of using the soft, cohesive material as building material. From the construction phase it became clear that the material is not suitable for creating slopes of more than 1:100 and that landscaping, i.e. creating differences in height, is difficult. Differences in height however do develop due to different consolidation velocities at different parts of the island. Furthermore, it was striking that after a few months the top layer at some locations already developed a crust which was strong enough to carry a person. More results, especially on consolidation velocity and morphological development will be available in 2015.

Acknowledgements

This research project is performed in close cooperation with the Department of Waterways and Public works of the Dutch Ministry of Infrastructure and the Environment and contractor Gebr. Van der Lee Dredging.

Monitoring sludge spill of the AMORAS underwater cell

De Maerschallck Bart¹, Maarten Van Esbroeck², Stefaan Ides³ and Yves Plancke^{1,3}

¹ Flanders Hydraulics Research, Berchemlei 115, 2140 Antwerp, Belgium
E-mail: bart.demaerschallck@mow.vlaanderen.be

² department of Maritime Access, Flemish Ministry of Mobility and Public Works, Poldervlietweg, 2140 Antwerp, Belgium

³ Port of Antwerp, Entrepotkaai 1, 2000 Antwerp, Belgium

Introduction

In 2006 the Flemish authorities in association with the Antwerp port authority launched the AMORAS project as a sustainable solution for maintenance dredging material from the port of Antwerp. AMORAS stands for Antwerp Mechanical Dewatering (Ontwatering), Recycling and Application of Sludge. The building of the site started in October 2008. End of 2011 the installation became operational.



Fig. 1. AMORAS production sites: 1. underwater cell, 2. Sand separation, 3. Piping, 4. Consolidation ponds, 5. Dewatering installation, 6. Water treatment, 7. Storage.

After separating the sand from the dredged material, the remaining sediment is mechanically dewatered and stored, see Fig. 1. The ambition is to finally recycle the dewatered sediment for other beneficial uses, e.g. in construction materials.

AMORAS underwater cell

Dredged material is temporarily stored in the AMORAS underwater cell (underwater cell), step 1 in Fig. 1. An electrically powered cutter suction dredger picks up the sediments from the underwater cell and pumps it to the sand separation: step 2 in Fig. 1. The underwater cell is a local deepening, up to 16m depth (-12mTAW) in the shelter dock. The underwater cell is separated from the navigation channel by an underwater steel dam reaching up to 9m below the surface (-5mTAW), see Fig. 2.

Problem statement

In 2013 it was noticed that from all the dredged material dumped into the underwater cell only 70% was recovered again by the cutter suction dredger and send to the sand separator. Since summer 2013 both de dredging activities inside the port and the production rate of the cutter dredger and the AMORAS dewatering site have been increased. Since that time no more that 50% of the delivered material could be removed from underwater cell by the cutter dredger. At the same time the Antwerp port authorities noticed an increasing mud layer in the neighbouring navigation channel. One could assume that the underwater cell is saturated and overflowing. The operator of the AMORAS site and the cutter suction dredger, however, claims that the cutter is still operating on

more than 12m depth (-8mTAW) in order to pump sludge with a preferable density of 1.12ton/m³ while the delivered sediment typically has a density between 1.15 and 1.2ton/m³.



Fig. 2. Location of the underwater cell.

Methodology

For both the operator of the AMORAS site and the authorities it was necessary to get a clear view on the spill of sludge at the underwater cell. Therefore different analyses have been performed. Densities and shear resistance inside the underwater cell and the neighbouring navigation channel have been monitored by means of two Graviprobe® survey campaigns in 2012 and 2014. The fast response of the mud levels inside the underwater cell have been monitored intensively by means of regular single beam echo sounding surveys during a normal tree-week working regime. Sediment losses during dumping of the material in the underwater cell have been measured by optical backscatter. Historical multi- and single beam echo soundings of the underwater cell and navigation channel since the underwater cell came into operation have been analysed. Finally consolidation processes of the delivered sediment have been analysed under laboratory conditions by means of consolidation columns.

Results of these analyses and recommendations to the operators and authorities will be discussed in the proposed paper.

Contribution of waves and currents to observed suspended sediment distribution patterns in a macro-tidal beach

Delgado Rosalia¹, Anne-Lise Montreuil^{1,2}, Sebastian Dan¹ and Margaret Chen²

¹ Flanders Hydraulics Research, Berchemlei 115, 2140 Antwerpen, Belgium
E-mail: rosalia.delgado@mow.vlaanderen.be

² Hydrology and Hydraulic Engineering, Vrije Universiteit Brussel (VUB), 2 Pleinlaan, 1050 Brussels, Belgium

Introduction

Near-bed sediment and turbulence interaction is one of the challenging issues in understanding sediment transport dynamics. The objective of this paper is to present our findings about the relative contribution of waves and currents to the distribution of suspended sediment based on field measurements obtained under both wave and (tidal) current dominated conditions. Near-bed single point measurements of 3D flow velocities and velocity profiles were obtained simultaneously with suspended sediment concentration and free surface elevation. Based on these data, shear stress and turbulent kinetic energy (TKE) are calculated for two different periods of 35h during spring tide: one characterized by significant wave heights exceeding 2m (Nov. 14-15, 2013), and a second period, during which mild waves not exceeding 0.5m height were measured (Nov. 16-18, 2013). Based on these measurements, we examined wave and current contribution to shear-stresses and TKE magnitudes and established relations with sediment (re)suspension patterns. Results suggest the presence of a specific mechanism responsible for reducing the efficiency of the flow in bringing and keeping sediment in suspension under energetic wave and current conditions.

Field measurements

The study area, located at the Southern North Sea in Mariakerke (Oostende, Belgium), is a rectilinear beach presenting a fairly constant slope and exposed to spring tides exceeding 5m and waves mostly from West-Northwest. Littoral drift coincides with flood direction going from Southwest to Northeast. Sediment is considered as fine sand with a high content in finer material.

Field data was collected in the framework of the ARGONAUTS project financed by the Flemish government. The deployment consisted on an up-looking AWAC at 1.7m above the bottom measuring waves at 2Hz and 5 minutes time-averaged current profiles, a down-looking ADCP measuring velocity profiles at the lowest 1.5m of the water column, an ADV measuring at 16Hz at 0.3m above the bed and a vertical array of three OBS measuring suspended sediment at 4Hz at nominal heights of 0.3, 0.5 and 0.8m above the bottom. 10 to 20 minutes of simultaneous time-series were collected every two hours during six weeks in November and December 2013. In this paper results based on a small part of this dataset are presented.

Effect of wave energy and turbulence on SSC

Results for the two different periods during which spring tide is combined with energetic and mild wave condition are examined. Fig. 1 shows time series of water levels, wave heights, depth averaged velocities for the lowest 1.5m of the water column, the three spatial components of ADV near-bed velocities and OBS signal for suspended sediment concentration (SSC) at 0.5 and 0.8m above the bed. (The interpretation of the OBS data will be limited to qualitative aspects. Calibration will be completed end 2014). The figure shows, for spring tide with high waves, the dominant influence of waves on the range of near-bed and depth averaged velocities measured. High suspended sediment concentrations are found during the first half of the flood period also under high waves. However, it is under moderate wave conditions and not under the most energetic waves when the highest concentrations are observed. Highest shear stresses (not in figure) are found to be maximum during low water, before and after the most energetic conditions occur. This could be explained by the fact that the transfer of energy from waves to the bed is most limited by the water depth during high water. However, suspended sediment concentrations become persistently low during most of the two tidal cycles during which more energetic conditions and this suggests the possibility of a mechanism preventing the sediment to be brought in suspension higher in the water column.

Under mild waves, (right side of Fig. 1), flow velocity variations are clearly influenced by tidal periodicity. Maximum SSC signals are detected again mostly during the first half of flood but also at the end of the ebb phase of the tide. This is not the case under the presence of energetic waves, where no high concentrations are observed during the ebb period in the presence of high waves.

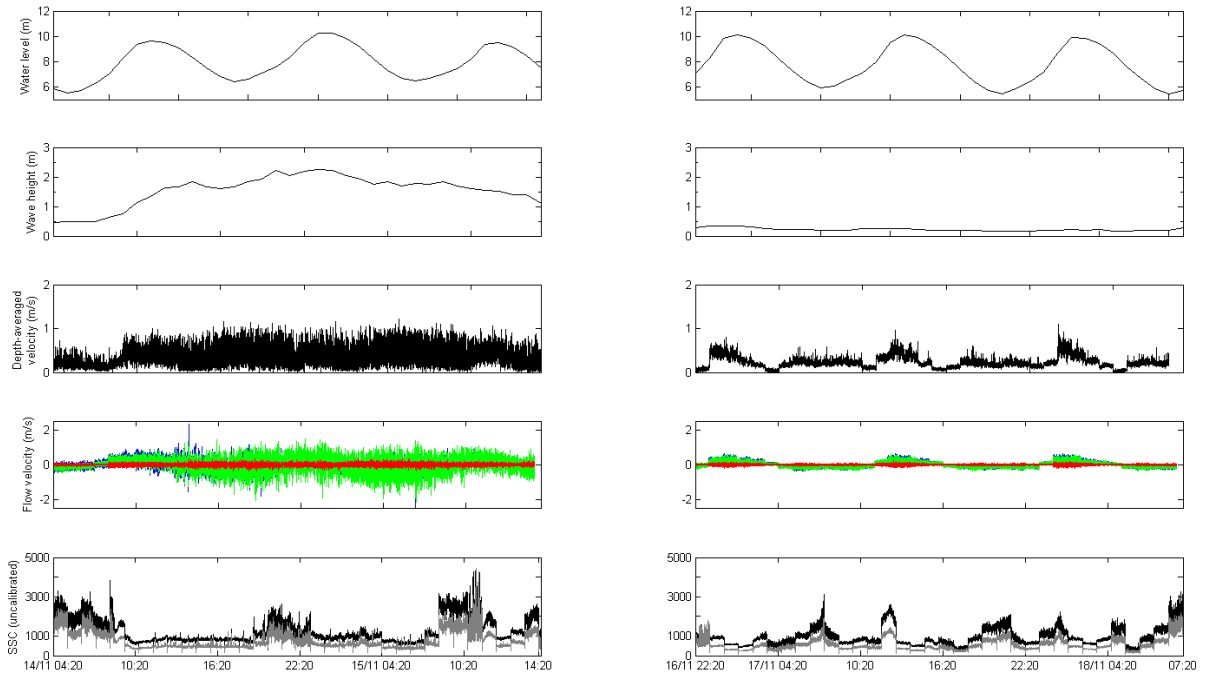


Fig. 1. Time series of a spring tide with energetic waves (left), and with mild waves (right). From top to bottom: water level, wave height, depth-averaged velocity, near-bed flow velocity u (blue), v (green) and w (red) and, signal for SSC in Volts at 0.5m (black) and 0.8m (grey) above the bed.

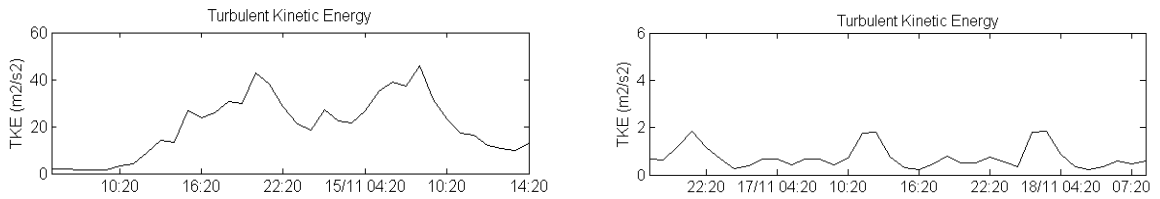


Fig. 2. TKE under energetic wave conditions (left) and under mild wave conditions (right).

Fig. 2 shows ten minutes averaged time series of TKE for the two cases. TKE is obtained by extracting turbulent normal stresses of the 3D near-bed velocities and applying the expression:

$$TKE = \frac{1}{2} \left(\overline{u'^2} + \overline{v'^2} + \overline{w'^2} \right) \quad (1)$$

Under mild waves, maximum TKE is found during high water. Maximal re-suspension occurs however during low water and in some cases during slack water. For high waves, TKE results are one order of magnitude larger than for the case with mild waves suggesting the relevance of the contribution of the oscillatory flow to producing near-bed turbulence. However, the time variation of TKE is not consistent with the variation of SSC as observed in the mild waves case where in addition much less turbulent energy seems to be more efficient in triggering (re)suspension events. With energetic wave conditions a reduction of TKE takes place under high water together with a persistently low SSC signal until close to slack water, when SSC maxima are observed. At this point, current velocities are minimal and waves dominate the generation of near-bed turbulence. During ebb and the following low water however, wave generated turbulence seems to be much less efficient in bringing and keeping sediment up in the water column.

Conclusions

Results suggest that a specific mechanism limiting the efficiency of the flow in suspending sediment is triggered under certain energetic wave-current conditions. This makes it necessary to investigate alternative models to understand and define the relationships between turbulence generation and re-suspension of sediment under the combined action of currents and waves.

Suspended solid concentration in the Seine Estuary based on the SYNAPSES turbidity monitoring network: quantification and variability

Druine Flavie¹, Robert Lafite¹, Julien Deloffre¹, Romaric Verney² and Jean-Philippe Lemoine³

¹ UMR CNRS 6143 Morphodynamique Continentale et Côtière, Batiment IRESE A, Université de Rouen, 76821 Mont Saint Aignan Cedex, France
E-mail: flavie.druine@etu.univ-rouen.fr

² Laboratoire DYNECO/PHYSED, IFREMER, PO Box 70, 29280 Plouzané, France

³ GIP Seine Aval, Pole Régional de Savoirs, 115 Boulevard de l'Europe, 76100 Rouen, France

Estuaries are 'critical' interfaces between continental systems and coastal seas and concentrate environmental, economic, societal and scientific issues. A particularly challenging issue concerns the evaluation of fine sediment fluxes in estuaries, as they drive the morphological evolution of estuaries, habitat modification, siltation in waterways and estuarine water quality. Quantifying suspended solid fluxes requires to quantify suspended particulate matter (SPM) concentrations in key compartments within the estuary, fast enough to capture the tidal scale, and over long periods to evaluate the inter-annual variability. A main difficulty is related to the SPM behaviour in estuaries: SPM form aggregates, whose size, shape and density are strongly variable and controlled by flocculation processes. Meantime, SSC are usually measured indirectly from optical and acoustic sensors. These methods are based on the backscattering properties of the particles in suspension, and hence are strongly controlled by the floc features. This project aims to first examine and optimize methodologies applied to quantify SPM concentrations and next to investigate SPM concentration variability, from the tidal scale to inter-annual scale.

Since 2012, the Rouen Port Authorities and GIP Seine-Aval coordinate the SYNAPSES automated monitoring network measuring physico-chemical parameters at 6 key stations from the fluvial compartment to the estuary mouth, including the turbidity maximum zone (Fig. 1). In 2014, each station is equipped with an YSI multi-parameter probe, measuring pH, conductivity, salinity, temperature, dissolved oxygen, fluorescence and turbidity in sub surface and also close to the bed for the three downstream stations. In 2015, over the full year, monthly field campaigns will be conducted to calibrate the optical sensors in mass concentration, regarding associated SPM features measured from LISST and collected water samples (measuring total suspended solid concentration, organic matter content, chlorophyll a concentration, EPS/TEP concentrations, microfloc/primary particle size distribution). The preliminary results of this study will be examined, and especially the evolution of calibration relationships at various time scales: the tidal scale, the fortnightly cycle, and the seasonal scale. These results will be used to quantify and discuss measurement uncertainties based on different possible scenarios of optical sensor calibration usually applied in such environments.

The following phase of the project will be dedicated to the evaluation of sediment fluxes from these local measurements, and evaluate their fluctuations, associating ADCP measurements and model results. ation network SYNAPSES stations.

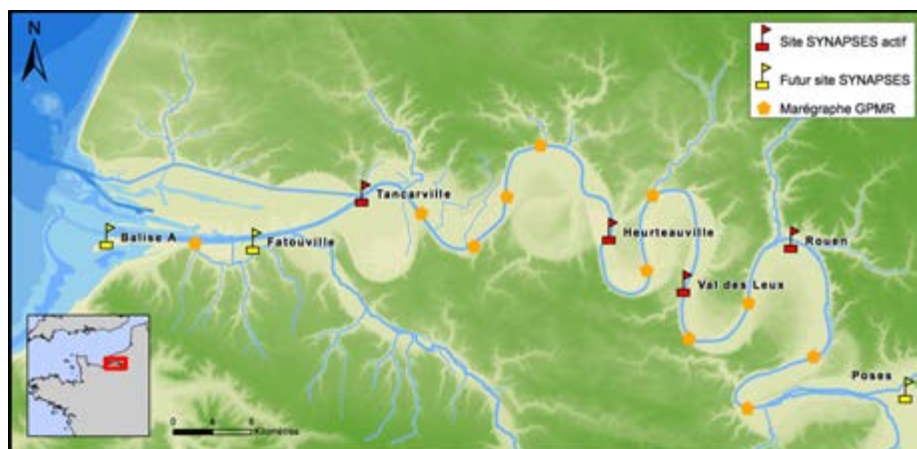


Fig. 1. Location network SYNAPSES stations.

In situ measurements of SPM concentration to evaluate the impact of the disposal of fine grained sediments from maintenance dredging

Fettweis Michael¹, Matthias Baeye¹, Thomas Van Hoesteberghe², Luc Van Poucke², Arvid Dujardin^{2,3} and Chantal Martens⁴

¹ Operational Directorate Natural Environment, Royal Belgian Institute of Natural Sciences, Gulledele 100, B-1200 Brussels, Belgium
E-mail: m.fettweis@mumm.ac.be

² Antea Group, Buchtenstraat 9, B-9051 Gent, Belgium

³ Flanders Hydraulics Research, Department of Mobility and Public Works, Flemish Government, Berchemlei 115, B-2140 Antwerp, Belgium

⁴ Maritime Access Division, Department of Mobility and Public Works, Flemish Government, Tavernierkaai 3, B-2000 Antwerp, Belgium

The aim of this study is to present and discuss the impact of disposal of fine-grained sediments on the SPM concentration and on the fluid mud dynamics in the turbid Belgian nearshore area (southern North Sea). Measurements show that the SPM concentration reaches more than 3g/l near the bed and up to 0.3g/l at the surface; lower values (<0.01g/l) occur more offshore (Fettweis *et al.*, 2010). The high SPM concentration results in high deposition of cohesive sediments that accumulate in man-made areas such as the ports and navigation channels. About 5 million tons (dry matter) per year of mainly fine-grained sediments is dredged in the port of Zeebrugge and is disposed on a nearby disposal site (Lauwaert *et al.*, 2008). The disposed sediments are quickly resuspended and transported away from the site. The results of a numerical study showed that a significant part recirculates back to the dredging places and that a relocation of the disposal site to another location at equal distance to the dredging area reduces this recirculation (Van den Eynde and Fettweis, 2014). In order to validate the model results a one year field study was set up in 2013-2014. During one month the dredged material was disposed at a new site and the efficiency of the new location was evaluated. Measurements inside and outside the port of Zeebrugge of various oceanographic and sediment parameters (SPM concentration, current velocity, waves, salinity, temperature, tides, wind, bathymetry, density of mud layers) were conducted during the experiment.

The measurements inside the port are presented in Dujardin *et al.* (this volume). The monitoring outside the port was carried out at two locations near the entrance of the port using instrumented tripods. Variations in SPM concentration were related to tides, storms, seasonal changes and human impacts. In order to evaluate the impact of the relocation of the disposal operations a statistical approach was used (Baeye *et al.*, 2011; Fettweis *et al.*, 2011). The measured SPM concentration time series during the relocation experiment were statistically compared against the population data. Both experiment samples and population are characterized by statistical properties, such as median, geometrical mean, standard deviation and probability density distribution. The analysis method is based on the concept of statistical populations and provides a tool to account for the complexities associated with natural dynamics and the need to evaluate quantitatively human impact. SPM concentration can be used as an indicator of environmental changes if sufficiently long time series are available that are representative of the natural variability.

References

- Baeye M., M. Fettweis, G. Voulgaris and V. Van Lancker. 2011. Sediment mobility in response to tidal and wind-driven flows along the Belgian inner shelf, southern North Sea. *Ocean Dynamics* 61:611-622.
- Dujardin A., J. Vanlede, T. Van Hoestenbergh, L. Van Poucke, M. Fettweis, C. Cardoso, C. Velez and C. Martens. 2015. Factors influencing top sediment layer and SPM concentration in the Zeebrugge harbor. *Proc. IntercoH 2015*. (this issue)
- Fettweis M., F. Francken, D. Van den Eynde, T. Verwaest, J. Janssens and V. Van Lancker. 2010. Storm influence on SPM concentrations in a coastal turbidity maximum area (southern North Sea) with high anthropogenic impact. *Continental Shelf Research* 30:1417-1427.
- Fettweis M., M. Baeye, F. Francken, B. Lauwaert, D. Van den Eynde, V. Van Lancker, C. Martens and T. Michielsen. 2011. Monitoring the effects of disposal of fine sediments from maintenance dredging on suspended particulate matter concentration in the Belgian nearshore area (southern North Sea). *Marine Pollution Bulletin* 62:258-269.

- Lauwaert B., K. Bekaert, M. Berteloot, D. De Brauer, M. Fettweis, H. Hillewaert, S. Hoffman, K. Hostens, K. Mergaert, I. Moulaert, K. Parmentier, G. Vanhoey and J. Verstraeten. 2008. Synthesis report on the effects of dredged material disposal on the marine environment (licensing period 2006-'08). MUMM, ILVO Fisheries, Maritime Access Division, and Coast Division. Ostend, Belgium. 128p.
- Van den Eynde D. and M. Fettweis. 2014. Towards the application of an operational sediment transport model for the optimisation of dredging works in the Belgian coastal zone (southern North Sea). p.250-257. In: Dahlin H., N.C. Flemming, S.E. Petersson (Eds). Sustainable Operational Oceanography.

Self-weight consolidation tests of the Río de la Plata sediments

Fossati Mónica, Rodrigo Mosquera, Francisco Pedocchi and Ismael Piedra-Cueva

Instituto de Mecánica de los Fluidos e Ingeniería Ambiental (IMFIA), Uruguay
 E-mail: mfossati@fing.edu.uy

Introduction

As it is described in Been and Sills (1981) sediment particles and flocs suspended in the water column settle down as the flow velocity reduces. As material accumulates on the bottom, the pore space between the particles decreases and the water is expelled. This process is known as self-weight consolidation of the deposit. As the consolidation progresses, the sediment particles stop to behave as isolated particles in a suspension and start to behave as a soil where particle-particle interactions are relevant. Due to the large vertical deformations observed during the consolidation process, a simple laboratory 1D vertical test is usually used to analyse consolidation characteristics under motionless conditions (Migniot, 1989; Been and Sills, 1981; Samadi-Boroujeni *et al.*, 2005). In this article we describe the sedimentation and self-weight consolidation tests carried on cohesive sediments extracted from five different locations in the Río de la Plata river-estuarine system (Fig. 1 left panel). The tests focused on the influence of mud composition, initial concentration and salinity on the self-weight consolidation process.

Methodology

Three 2m height and 0.088m diameter Plexiglas columns with measuring tapes were placed at our Laboratory (Fig. 1 right panel). At the beginning of each test the column was filled with a mixture of cohesive sediment and water. During the sedimentation-consolidation experiment the clear-muddy water interface and the bed-muddy water interface positions were registered over an extended time period.

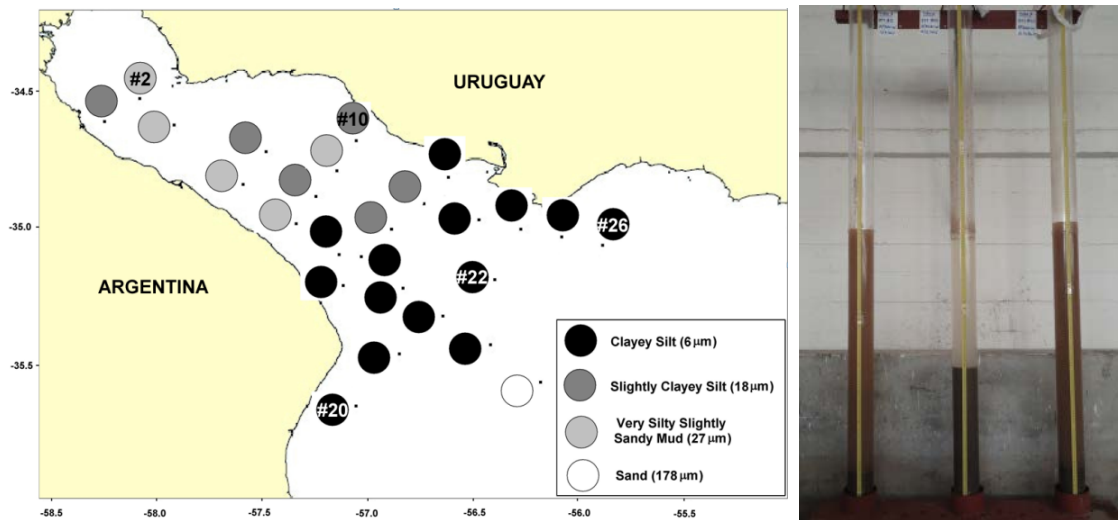


Fig. 1. Left panel: The Río de la Plata and sediment samples classification, numbers indicate the samples selected for this study. Right panel: A view of the consolidation columns at IMFIA.

Table I. Test main characteristics

Test name	Initial concentration C0 [g/l]	Initial column height [m]	Experiment duration [days]	Mud sample	Mud composition				Salinity [g/l]
					% sand	% silt	% clay	R= %clay / %silt	
e1t1	98	1.011	23	#22	1	68	31	0.45	0
e1t2	91	0.944	21	#22	1	68	31	0.45	0
e1t3	62	0.933	22	#22	1	68	31	0.45	0
e2t1	100	1.003	162	#2	19	71	9	0.13	0
e2t2	100	0.973	162	#26	0	66	33	0.50	0
e2t3	100	1.032	162	#10	1	86	14	0.16	0
e3t1	100	0.957	65	#20	0	56	44	0.77	0
e3t2	100	0.966	53	#20	0	56	44	0.77	18
e3t3	100	0.962	51	#22	1	68	31	0.45	18

The main parameters of the experiments are presented on Table 1. Nine experiments were performed with the same initial suspension height (approximately 1m). Experiments e1t1, e1t2 and e1t3 were performed with the same mud sample (#22) but different initial suspension concentration. Experiments e2t1, e2t2, e2t3 and e3t1 were performed using different mud samples (#2, #10, #20, #26) but with the same initial concentration. Finally, experiments e3t2 and e3t3 repeated the conditions of experiments e3t1 and e1t1 but with a 18 g_{NaCl}/l salinity.

Results

The bed-muddy water interface position for some of the tests is presented in Fig. 2. The right panel of Fig. 2 shows that the consolidation process depends on sediment composition, particularly on the fine fraction. For silty samples (more than 70% silt/clay, e2t1 and e2t3) the interface moved down very fast and the obtained curves show a clearly distinct behaviour when they are compared with the ones obtained for finer samples (e1t1, e2t2, e3t1). Finer samples present a slowly initial sedimentation stage followed by a long consolidation stage, extends for several days, with a decreasing rate (e2t2, e3t1). Comparing these last two tests we can see that the initial sedimentation stage is essentially the same, while the second stage shows a higher consolidation rate for the sample with a higher clay content. The third stage shows the same consolidation rate for both sediments with a longer extension for the finer sample. The e3t1 test did not reach the fourth stage.

Finally, the role of salinity on the sedimentation and consolidation process of two different samples (e3t2, e3t3) was studied. The results are shown on the left panel of Fig. 2, floc formation was visually observed during these tests. The results show that the salinity modifies the extension of the first stage maintaining the rate during the second and third stages. Nevertheless, the deposit height at the end of these two tests is greater than the one obtained in the test without salinity, showing a clear influence of floc properties on these last stages. Regarding tests with different initial concentrations (not presented here) the results showed the decrease of the initial concentration produced an increment of the sedimentation front velocity during the initial stage and essentially the same overall characteristic during the other stages.

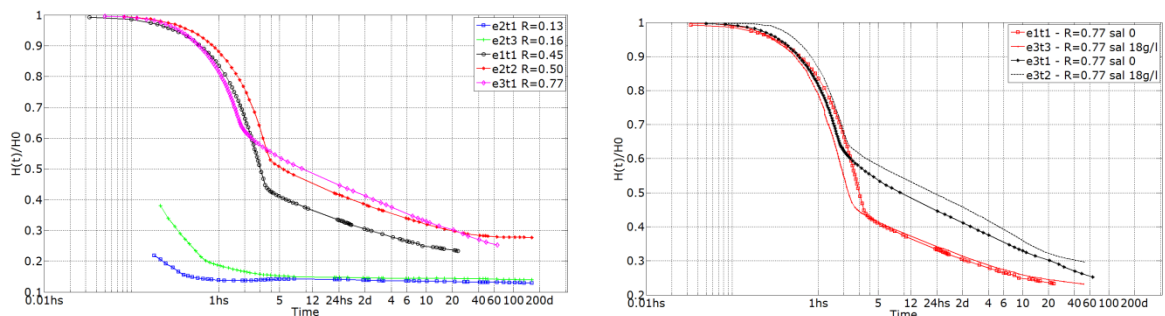


Fig. 2. Temporal variation of front position, during the sedimentation test.

Conclusions

We presented several self-weight consolidation tests performed with Río de la Plata sediments. The main results are in good agreement with exiting results available in the bibliography (Migniot, 1989; Samadi-Boroujeni, 2005). Samples with higher silt/clay proportion showed faster settling and consolidation stages with a stable height during the first day of the experiment. A different behaviour is observed for cohesive sediment with a balanced proportion between silt and clay, here a slow initial settling stage and a continuous consolidation process during several days with a decreasing rate. The data collected during these tests allowed for a better understanding of the consolidation process for the different regions of the Río de la Plata, and the future incorporation of the consolidation process into existing numerical models.

References

- Been K. and G. Sills. 1981. Self-weight consolidation of soft soils: an experimental and theoretical study. *Geotechnique* 31(4):519-535.
- Migniot C. 1989. Tassement et rhéologie des vases. Première partie. Deuxième partie. *La Houille Blanche* (1-2):11-28 ;95-111.
- Samadi-Boroujeni H., M. Fathi-Moghaddam, M. Shafae-Bajestan and H. Mohammad Vali-Samani. 2005. Modelling of sedimentation and self-weight consolidation of cohesive sediments. Chapter 13. In: *Sediment and Ecohydraulics: INTERCOH 2005*.

Controls on bed erodibility in a muddy, partially-mixed estuary: York River, Virginia, USA

Friedrichs Carl T.¹, Grace M. Cartwright¹, Patrick J. Dickhudt², Kelsey A. Fall¹ and Lindsey M. Kraatz³

¹ Virginia Institute of Marine Science, Gloucester Point, VA, USA
E-mail: carl.friedrichs@vims.edu, gracec@vims.edu, kafall@vims.edu

² US Geological Survey, Woods Hole, MA, USA
E-mail: pdickhudt@usgs.gov

³ National Oceanic & Atmospheric Admin., Washington, DC, USA
E-mail: lmkraatz@gmail.com

Introduction and methods

Appropriate parameterization of time-dependent erodibility of muddy seabeds is a significant barrier to improved understanding and accurate modelling of sediment dynamics in estuaries and other coastal regions. In an effort to better understand controls on muddy seabed erodibility, bed erodibility and associated bed sediment properties have been measured by our group on cores collected on dozens of cruises over the last decade in the York Estuary (e.g., Dickhudt *et al.*, 2009, 2011; Kraatz, 2013). We have also inferred time-varying erodibility indirectly in the York Estuary over several years by vertically integrating observations of tidally-varying suspended sediment concentration (e.g. Friedrichs *et al.*, 2008; Cartwright *et al.*, 2009; Fall, 2012). This paper synthesizes the results of these long-term observations in this partially-mixed estuary, whose seabed is similar to that of many other moderately energetic, muddy tidal estuaries.

Seabed erodibility was measured directly on bed samples from the York Estuary utilizing a dual core Gust erosion microcosm. This device uses a rotating disc with central suction to impose a nearly uniform shear stress on the surface of 10cm diameter sediment cores. After collection of box cores in the York River Estuary, sub-cores for use in the microcosm were carefully transported to the Virginia Institute of Marine Science (VIMS) located nearby on the banks of the York. To minimize consolidation effects, erodibility measurements were generally underway in our sediment lab within about 2h of core collection. Erodibility measurements consisted of a sequence of seven steps of approximately 20-min duration, each with a consecutively increasing shear stress (0.01, 0.05, 0.1, 0.2, 0.3, 0.45 and 0.6Pa) applied to the sediment surface. Bed erodibility was also measured indirectly in the York Estuary utilizing Acoustic Doppler Velocimeters (ADV). Although an ADV cannot control shear stress, a bottom-mounted ADV still documents time-varying bed stress by measuring near-bed turbulent velocity, and ADV backscatter can be calibrated for suspended sediment concentration. Estimating the vertical integral of suspended sediment concentration then gives an estimate of eroded mass as a continuous function of stress, analogous to the data provided by a Gust microcosm.

Results

Digital X-radiographs of cores from the muddy middle section of the York Estuary have seasonally revealed (i) thick sequences (10–20cm) of laminated sediments at the surface coincident with periods of highest erodibility and (ii) more biologically reworked sediment during the rest of the year. These results suggest that a dominant control on erodibility in this type of estuary is occasional rapid deposition introducing new sediment that is seasonally easy to erode. Rapid seasonal deposition and associated high erodibility in the York occurs in response to a seasonal secondary turbidity maximum. The secondary turbidity maximum occurs in a stratification-induced mid-estuary trapping zone that, in turn, is triggered by the winter/spring freshet. The freshly deposited material quickly disperses once the freshet is over, and the salinity-induced trapping zone dissipates, which returns the bed to a more commonly observed state of lower erodibility (Fig. 1).

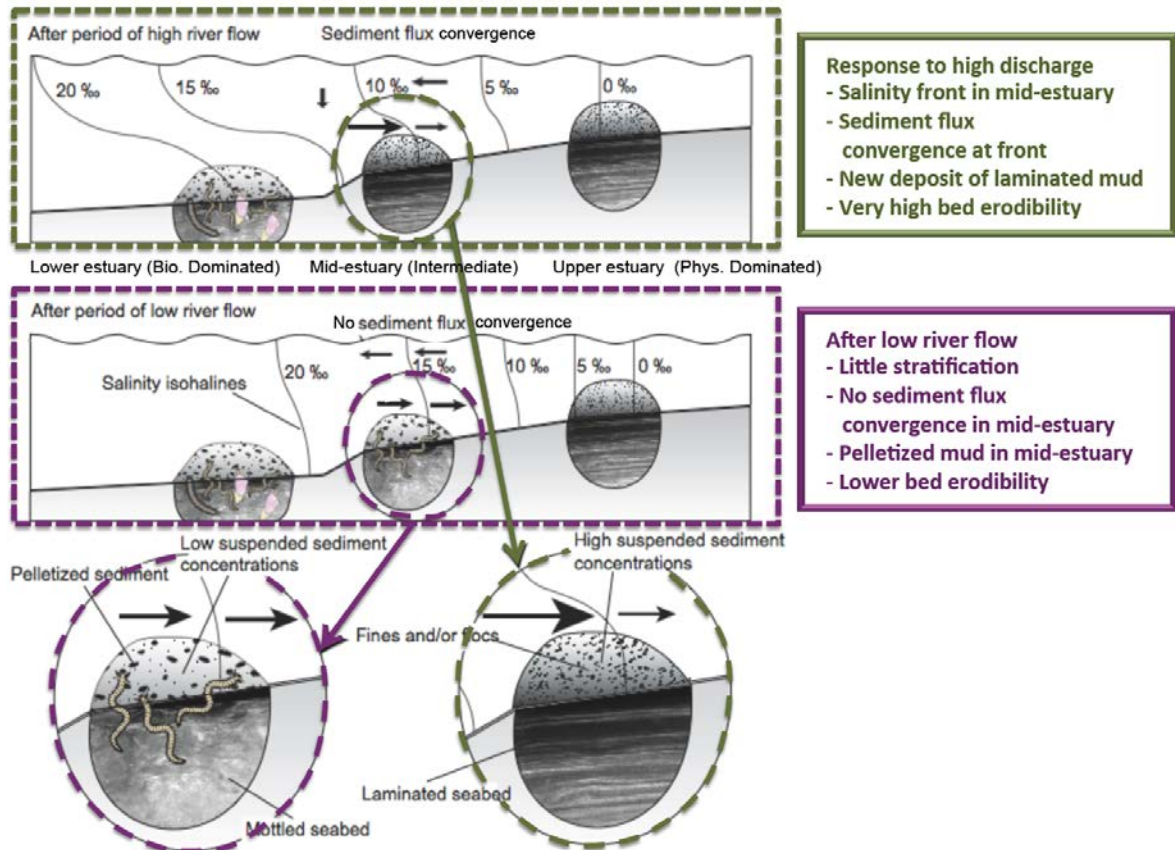


Fig. 1: Conceptual model for York Estuary dynamics (modified from Dickhudt *et al.*, 2009).

The more commonly observed 'low' erodibility state represents a more biologically influenced, pelletized bed with ongoing competition between the effects of physical resuspension and consolidation versus biological reworking and repackaging. For example, observations over several consecutive weeks starting about one month after the end of the winter/spring freshet have demonstrated a tendency for the erodibility of biologically reworked sediment to slowly decrease, consistent with both dewatering and a progressive winnowing of the most easily suspended material from the uppermost centimetre. As time passed, the percentage of resilient muddy pellets, median pellet size, content of fine sand, and median sand size were all observed to increase at the surface, while the percent water, organics, silt, and ²¹⁰Be activity decreased. Consistent with recent advances in cohesive bed modelling, results suggest that cohesive-like consolidation and non-cohesive-like bed armouring occur simultaneously in pelletized muddy beds.

Along with a tendency for erodibility to increase following deposition events and decrease with dewatering and bed armouring, this study also identified a superimposed temporal oscillation in erodibility correlated to tidal range. A larger tidal range drives stronger tidal currents that then disturb the bed, partly counteracting the temporal effects of armouring/consolidation. It was found that the correlation between eroded mass and low-passed tidal range peaked when tidal range was averaged over 11 semi-diurnal tidal cycles immediately preceding core collection. This suggests a characteristic bed consolidation time scale of about 5 to 6 days under conditions of ongoing, moderate disturbance. Consolidation over a several-day time-scale, 'reset' by intermittent resuspension events, is also qualitatively consistent with recently developed models for time-dependent cohesive seabed erodibility.

References

- Cartwright G.M., C.T. Friedrichs, P.J. Dickhudt, T. Gass and F.H. Farmer. 2009. Using the acoustic Doppler velocimeter (ADV) in the MUDBED real-time observing system. p.1428-1436. In: OCEANS 2009, Institute of Electrical and Electronics Engineers, ISBN: 978-1-4244-4960-6.
- Dickhudt P.J., C.T. Friedrichs, L.C. Schaffner and L.P. Sanford. 2009. Spatial and temporal variation in cohesive sediment erodibility in the York River Estuary: a biologically-influenced equilibrium modified by seasonal deposition. *Marine Geology* 267:128-140.

- Dickhudt P.J., C.T. Friedrichs and L.P. Sanford. 2011. Mud matrix solids fraction and bed erodibility in the York River and other muddy environments. *Continental Shelf Research* 31(10S):S3-S13.
- Fall K.A. 2012. Relationships among fine sediment settling and suspension, bed erodibility, and particle type in the York River Estuary Virginia. MS Thesis. College of William & Mary. 144p.
- Friedrichs C.T., G.M. Cartwright and P.J. Dickhudt. 2008. Quantifying benthic exchange of fine sediment via continuous, non-invasive measurements of settling velocity and bed erodibility. *Oceanography* 21(4):168-172.
- Kraatz L.M. 2013. Acoustic and sedimentological investigations of seabed conditions and related bio-physio-geological parameters in a tidally energetic, fine-grained environment: York River Estuary, Virginia. PhD Dissertation. College of William & Mary. 199p.

Pre- and post-processing unstructured grids for estuary and coastal sea models with the PUG Matlab toolbox

Gourgue Olivier^{1,2}, Joris Vanlede² and Margaret Chen¹

¹ Department of Hydrology and Hydraulic Engineering, Vrije Universiteit Brussel, Pleinlaan 2, 1050 Brussels, Belgium
E-mail: ogourgue@gmail.com

² Flanders Hydraulics Research, Flemish Government, Berchemlei 115, 2140 Antwerp, Belgium

Introduction

Sediment transport in coastal and estuarine environments is a complex and dynamic process. Modelling approaches need to describe both hydrodynamics and sediment dynamics, as well as their interactions. This includes processes like tidal and wind wave propagation, turbulence, advection-diffusion and erosion-deposition of sediments, particle-fluid interactions, etc. As these processes may occur at very different time and space scales, there is a growing interest for using unstructured grid models to simulate them using one only multiscale model.

There are many software solutions to generate unstructured grids, but none offer satisfactory built-in functionalities to define the contour of a real domain, which can be painful to obtain. Another issue is the lack of a standard file format to save unstructured grids or model outputs. As a result, many different file formats coexist, and the choice of a specific mesh generation programme is often driven by its possible output file formats rather than its mesh generation capabilities. The PUG Matlab toolbox is developed with the aim to offer a solution to those problems encountered by many unstructured grid model users. Indeed, it gathers several functionalities to define domain contours in an integrated framework, and it can write unstructured grid files into different formats. As an example, it can be used to generate TELEMAC input files from Gmsh grids.

The objective of this paper is to present an original open source procedure to define domain contours and design unstructured grids for any unstructured grid model. This work is part of a broader research programme whose objective is to develop a multiscale mixed sediment transport model that uses TELEMAC to simulate sediment concentration, tidal and fluvial processes and wind waves in the Scheldt Estuary and Belgian coastal area.

Domain contour definition using PUG and Inkscape

PUG uses the GSHHG database to define most of the domain shorelines (Fig. 1). However, it may lack important details in some areas. PUG offers two alternatives to overcome this problem. If the area to correct is not too large, a new coastline may be defined by creating a path in Google Earth, and pointing and clicking along the land boundary to recreate its shape. If the path is exported into a KML file, PUG is able to read it and adds it to the domain contour (Fig. 2). If the area to correct is too large, and if a large data point cloud is available (e.g. bathymetry data) there, PUG computes the alpha shape of the data point cloud and adds it to the domain contour (Fig. 3).

Besides the definition of the land boundaries, it is necessary to define an open boundary offshore as well, for example at the shelf break. PUG makes use of the bathymetry data set ETOPO1 to extract coordinates along the shelf break and add a closure to the domain contour (Fig. 4).

A few manipulations are always necessary before considering mesh generation. For example: remove entire or part of lines, remove individual points, join lines, etc. This is done using the open source computer-aided design programme Inkscape, with whom PUG can interact.

Grid design using Gmsh

Gmsh is widely used in many branches of engineering, but it remains poorly known within the TELEMAC user community, probably because it does not support grid exportation to TELEMAC input files. This should not be a problem anymore, since one of the functionality of PUG is to write TELEMAC input files from Gmsh grid files.

As an example, the mesh density of the grid designed for the model of the Scheldt Estuary and the Belgian coastal area with Gmsh varies as a function of the distance to the coastlines and the distance to the area of interest (Fig. 5), and also as a function of the bathymetry and its gradient in the Scheldt Estuary (Fig. 6).

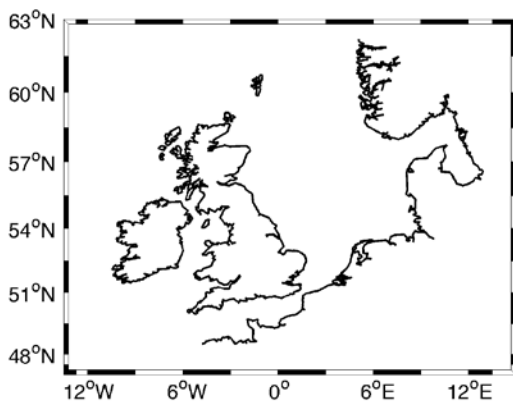


Fig. 1. Contour data from GSHHG describing the coastlines of North-Western Europe.

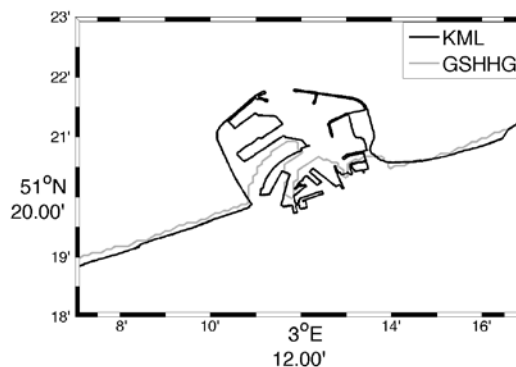


Fig. 2. Contour data from a KML file representing the port of Zeebrugge, Belgium.

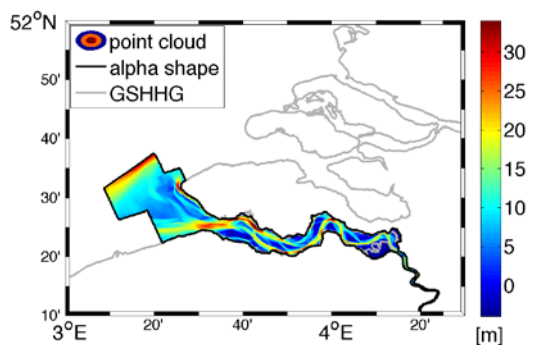


Fig. 3. Alpha shape computed from a bathymetry point cloud of the Scheldt basin.

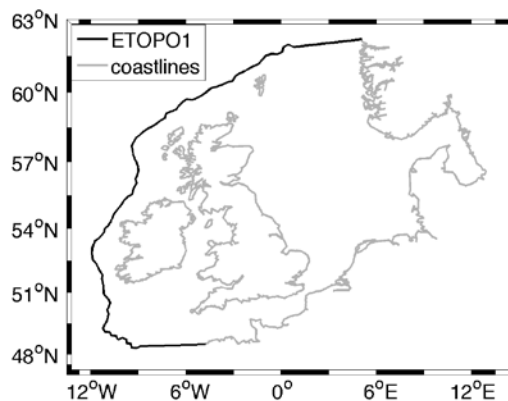


Fig. 4. Contour line 200m below the mean sea level, extracted from ETOPO1 and representing the shelf break

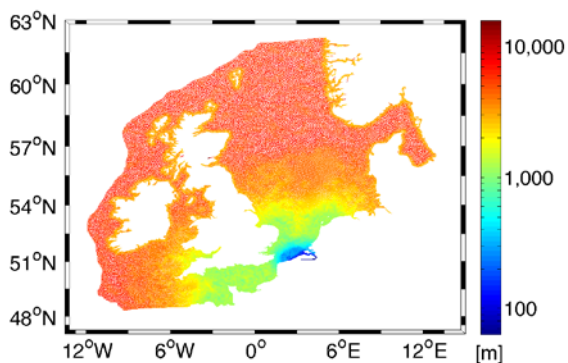


Fig. 5. Unstructured grid generated by Gmsh (261926 triangles); the colour scale gives the circumradius of the triangles.

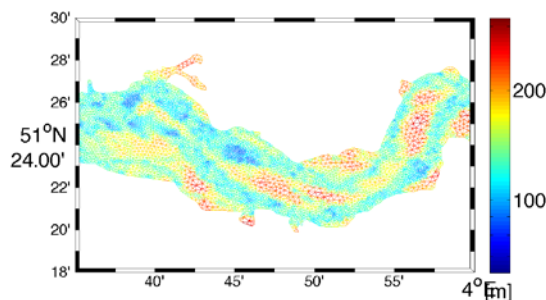


Fig. 6. Zoom on the grid of Fig. 5. to focus on the Western Scheldt, where the mesh density is a function of the bathymetry and its gradient.

Conclusion and perspectives

The development of the PUG Matlab toolbox offers an almost complete open source strategy to design unstructured grids, when used together with Inkscape and Gmsh. One can think of two reasons to believe that PUG could become very popular in the future. Firstly, the integration of different open source tools to define domain contours is unique and can be useful for any unstructured grid model user. Secondly, it provides a link between Gmsh and TELEMAC, which are very powerful and complementary pieces of software, but very little used together so far.

Estimations of settling speed using remotely sensed suspended material concentrations

Griffiths Joshua¹, David Bowers¹, Francis Gohin², Romaric Verney², Timothy Clarke³ and Carole Nahum⁴

¹ School of Ocean Sciences, Bangor University, Menai Bridge. Anglesey, LL59 5AB, UK
E-mail: osu868@bangor.ac.uk

² Ifremer, F-29280 Plouzané, Brittany, France

³ DSTL, Porton Down, Salisbury, Wiltshire, SP4 0JQ, UK

⁴ DGA, Rue des Mathurins, F-92220 Bagneux, Paris, France

Suspended material variation is driven by both seasonal changes in the magnitude of wind/waves and particle flocculation, with the addition of semi-diurnal and spring-neap variation due to the tides. We report satellite observations of spring-neap cycles of suspended material, which show a seasonal modulation in their amplitude. In January, when wind/wave activity is high and flocculation is low, the spring-neap variation in suspended load is lower than that observed in June, when wind/wave activity is lower and flocculation is higher. The phenomenon is reproduced using a simple numerical model including the effects of tides, waves and a seasonally varying settling speed. Through comparing the model output with the remotely sensed observations of suspended material, it is possible to estimate the seasonal and spatial variation of the energy efficiency of sediment re-suspension. From this efficiency, it is then possible to infer an estimate of the settling speed of particles.

Study of spectral wave transformation over muddy beds

Haghshenas S. Abbas¹ and Mohsen Soltanpour²

¹ Institute of Geophysics, University of Tehran
North Kargar Ave., Tehran PC 1439951113, Iran
E-mail: sahaghshenas@ut.ac.ir

² Faculty of Civil Engineering, K. N. Toosi University of Technology
No. 1346, Vali-Asr St., Tehran PC 1996715433, Iran

Introduction

A prerequisite for the reliable estimation of waves on maritime structures is a detailed understanding of how waves transform during their propagation (Goda, 2000). Considerable decay of wave energy along the wave trajectory over muddy beds makes a different wave transformation in comparison to sandy environments. The role of soft mud to dissipative waves has been investigated through modelling and laboratory experiments by many researchers (e.g., Sakakiyama and Bijker, 1989; Ross and Mehta, 1990; and de Boer *et al.*, 2009). The present study offers two sets of data for interacting waves with soft muddy beds; one is a large set of wave basin experiments on a general three-dimensional bathymetry under both regular and irregular waves, and the other one is a one-month period of field measurements at two stations in Hendijan mud coast on the Iranian coastline of the Persian Gulf. They have been utilizing a two-dimensional numerical model for better understanding of the complex spectral wave transformation on conditions where the combined effects of shoaling, refraction and diffraction as well as the wave energy dissipations due to mud bed existence and wave breaking exist.

Laboratory experiments

Wave basin experiments were carried out at the hydraulic laboratory of Yokohama National University. The basin was measured 10.5m in length by 9.0m wide with a bottom slope of 1:30. Commercial kaolinite was used to prepare the fluid mud bed. A mud sample was put in a box in the middle of the basin measured 2.7m in both directions and 10cm in height. Regular and irregular waves were generated by the wave paddles at the edge of the basin. The mud bed was subjected to wave action for the duration of 300s. The characteristics of incident wave approaching the mud section and the waves at five points over the mud box were recorded.

Field measurements

The north-west part of the Persian Gulf is covered with mud originating mainly from Arvand River. Mud deposits up to 20 metres thickness are observed at the very shallow coast of Hendijan Fishery Port. A set of field measurements was performed at the field site. Directional wave spectra and vertical current velocity profiles were simultaneously recorded at two stations. Mud samples from the top 1-metre layer were also collected to define mud characteristics. Fig. 1 shows the wave energy spectra in two stations during an extreme storm event.

Numerical model

The REF/DIF S wave model is employed in the present study to simulate spectral wave propagation over the physical model domain and also Hendijan muddy coast. A multi layered fluid system is employed to simulate the wave attenuation rate. The calculated values of the energy dissipation rates in the area covered by fluid mud are finally introduced to REF/DIF S wave transformation model to simulate wave propagation over the muddy beds.

Results and discussion

Introducing incident wave spectrum to the numerical model, Fig. 1 illustrates an example of the measured and simulated irregular wave spectra at one of the six stations in the wave basin as well as measured wave spectra in both stations at Hendijan mud coast together with the simulated wave spectrum in the nearshore station through REF/DIF S modified model. Comparisons between the measured and simulated wave spectra presented in Fig. 1 show fair agreements.

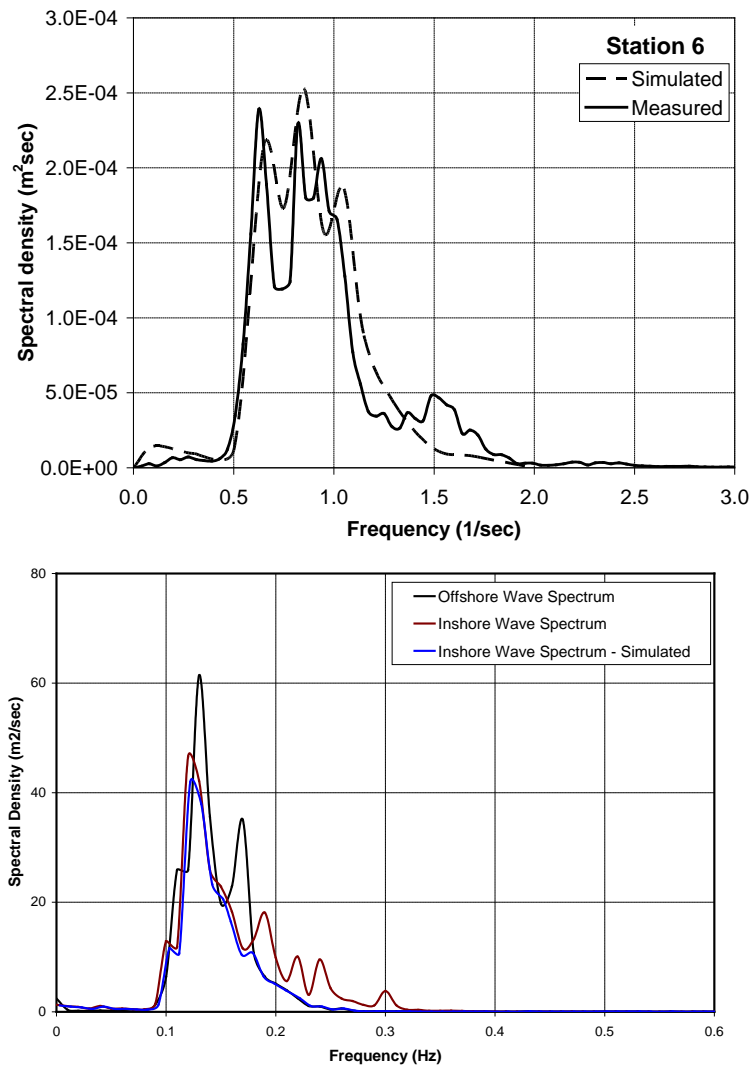


Fig. 1. Measured and simulated wave spectra, wave basin data (top) and Hendijan mud coast field data (bottom).

References

de Boer G.J., J.C. Winterwerp and Ap. van Dongeren. 2009. Flume experiments of wave damping by fluid mud. Proc. of INTERCOH 2009, Brazil.

Goda Y. 2000. Random seas and design of maritime structures. World Scientific Publishing Co.. 443p.

Ross M.A. and A.J. Mehta. 1990. Fluidization of soft estuarine mud by waves. p.185-191. In: The Microstructure of Fine Grained Sediments: From Mud to Shale. Bennett R.H. (Ed.). Springer-Verlag, New York.

Sakakiyama T. and E.W. Bijker. 1989. Mass transport velocity in mud layer due to progressive waves. Journal of Waterway, Port, Coastal and Ocean Engineering. ASCE 115(5):614-633.

Linking sediment transport and geochemical processes in a numerical model with application offshore of the Mississippi River

Harris Courtney K.¹, Justin J. Birchler^{1,2}, Tara Kniskern¹ and D. Reide Corbett³

¹ College of William & Mary, Virginia Institute of Marine Science
PO Box 1346, Gloucester Point, Virginia 23062, USA
E-mail: kharris@vims.edu; knista@vims.edu

² Now at Cherokee Nation Technology Solutions, St. Petersburg, FL, USA
E-mail: jbirchler@usgs.gov

³ UNC Coastal Studies Institute, East Carolina University
Wanchese, North Carolina, USA
E-mail: corbettd@ecu.edu

Sediment transport models that represent flood and storm sedimentation for coastal areas typically estimate grain size patterns and deposit thicknesses and are therefore disconnected from field data that rely on short-lived radioisotopic tracers to describe event bed character. Interpreting field data based on radioisotopes presents challenges that stem from the tracers' source terms, as well as confounding processes, including suspended transport and physical and biological mixing. We use a numerical sediment transport model capable of representing ⁷Be and ²³⁴Th profiles in the seabed to develop a quantitative tool that can be used to reconcile model estimates with observational studies, and better interpret field studies. The numerical model, built within the Community Sediment Transport Modeling System (CSTMS, see Warner *et al.*, 2008), accounts for multiple sediment types, suspended sediment transport, and erosion and deposition. It has recently been modified to also include cohesive sediment processes, and biodiffusion (Sherwood *et al.*, in prep.). To this framework, we have added a capability to represent particle – reactive tracers and used this to quantify radioisotopic activity for short-lived tracers within the seabed (Birchler, 2014).

A one-dimensional (vertical) model that includes two sediment classes and reactive tracers ⁷Be and ²³⁴Th was configured to represent a 50-m deep site offshore of the Mississippi River delta in the northern Gulf of Mexico, US, the “proximal” site previously studied by Corbett *et al.*, (2004). Though one-dimensional models typically neglect flux convergence and divergence, ours was configured to have sediment source and sink terms at the top of the model grid to produce deposition and erosion. The modelled sediment bed could then be subjected to deposition of riverine sediments and storm resuspension, with the input forcing based on time-series data of local wave conditions and Mississippi River discharge from the study period. The model estimates of radioisotopic penetration depth and activity matched field observations from the northern Gulf of Mexico made in April and October 2000 (Corbett *et al.*, 2004). These study periods differed in that the earlier time (prior to April, 2000) had higher wave energy than the later time period (prior to October, 2000).

Modelled radioisotopic profiles were similar to field observations, but the simulated profiles of ⁷Be and ²³⁴Th could be directly related to the flood and storm sequences used as model input to evaluate how the sediment bed tracers responded to individual discharge pulses and wave resuspension events. The model-estimated profiles were sensitive to the timing of ⁷Be input, phasing of wave and current energy, and the intensity of biodiffusion. Deposition of riverine sediment, and seabed resuspension both typically produced fining upwards layers of grain size. Deposition of riverine – derived sediment increased the activities and inventories of both radioisotopes, while resuspension increased the activity and inventory of ²³⁴Th only. Erosion events removed radioisotopes from the bed surface, reducing their total inventory, and winnowed the more easily suspended fine sediment from the bed.

References

- Birchler J.J. 2014. Sediment deposition and reworking: A modelling study using isotopically tagged sediment classes. Master's Thesis. School of Marine Science, College of William & Mary, Gloucester Point, VA, USA. 164p.
- Corbett D.R., B.A. McKee and D. Duncan. 2004. An evaluation of mobile mud dynamics in the Mississippi River deltaic region. *Marine Geology* 209:91-112.
- Sherwood C.R., A. Aretxabaleta, C.K. Harris, J.P. Rinehimer, B. Ferré and R. Verney. (in prep.). Cohesive and mixed sediment model: extension of the community sediment transport modeling system. In prep. for *Ocean Dynamics*.
- Warner J.C., C.R. Sherwood, R.P. Signell, C.K. Harris and H. Arango. 2008. Development of a three-dimensional, regional, coupled wave-, current-, and sediment-transport model. *Computers and Geosciences* 34:1284-1306. doi: 10.1016/j.cageo.2008.02.012.

Estimating the amount of erodible contaminated sediments within the groyne fields of the Elbe River

Hillebrand G., P. Heininger, T. Krämer, C. Möhlenkamp, J. Pelzer, D. Schwandt and E. Claus

Federal Institute of Hydrology (BfG), Am Mainzer Tor 1
56068 Koblenz, Germany
E-mail: hillebrand@bafg.de

The International Commission for the Protection of the Elbe River (ICPER) aims at establishing a sediment management concept both in terms of quantity and quality. To this aim, key processes of sediment transport and budget had to be defined under regular and under extreme conditions. Sediment budgets in regulated rivers are strongly influenced by lateral exchange processes. This study focused on the function of groyne fields acting as source and sink for cohesive sediments and particle-bound contaminants along the Elbe River. One specific aim was to assess the amount of erodible contaminated sediments within the groyne fields as basis for establishing a sediment management plan.

The contamination level of fine sediments within the Elbe catchment is generally high and following a precautionary principle, all fine-grained material in the Elbe groyne fields should be considered potentially contaminated, even though there are known local hot spots, and patterns of contaminants differ regionally resulting from tributaries and smaller sub-basins.

The German inland Elbe River has about 6600 groyne fields. In order to assess the number of groyne fields with deposits of fine sediments, about 270 groyne fields were probed in several field campaigns in 2010 and 2011 by sounding rods, push core samplers and Van Veen grabs along a river reach of about 450 kilometres. The bed sediments of the groyne fields were subjectively classified on site as 'gravel', 'sand' or 'mud'. The total amount of mud per investigated groyne field was categorized as 'high', 'low' or 'none'. Mud content of 73 groyne fields was considered high, low in 59, no mud was found in 128 groyne fields.

To enable extrapolation of these classifications, a number of variables, deemed to influence fine sediment deposition in groyne fields, were determined for all groyne fields following a literature research. These variables included parameters describing groyne field geometry, river alignment, grain size distribution of the main channel and other characteristics of the near and far field of the groyne fields. For all Elbe groyne fields, the values of these variables were determined. Using uni- and multivariate statistics, they were checked for correlation to observed mud contents. As an example, strong interdependency was found for groyne fields with high mud content between conventional groyne structures when they were connected to backwaters and exhibited longitudinal ridges within the groyne field (cf. Fig. 1). Observed mud contents were best reproduced (correct prediction of 2 out of 3 groyne fields in the categories 'high', 'low' and 'no' mud content) using a multinomial logistic regression with the following variables: river kilometre index, alignment of the groyne field (interior/exterior bank), aspect ratio, wetted area at low water, connection to backwater areas, existence of ridges within the groyne field or existence of incised groynes.

The multinomial logistic regression model was then used to extrapolate mud content to all groyne fields. 10% of all groyne fields were classified by the statistical model as having a high mud content, 4% as low mud content and 83% were classified as mud-free. 3% could not be classified due to missing values. From the results of the field campaigns and additional investigations of sedimentological and chemical properties of the sediments in muddy groyne fields, we estimate that the depth of fine sediments which are regularly mobilized and reworked is of the order of 0.5m. Using two thirds of the wetted area during low water conditions as an estimate for the size of the groyne fields and the area on which fine sediments may be found, the overall amount of fine sediments in the groyne fields of the River Elbe is of the order of 1 million m³.

In order to prioritize potential remediation measures, groups of contaminated groyne fields in close proximity to each other have to be determined, as remediation of single groyne fields is not feasible. From the extrapolated classification, it was estimated that 10 groups of 20 or more such groyne fields in close proximity can be identified along the whole river reach. Remediation of those groyne fields is estimated to remove about 30% of the total volume of erodible contaminated sediments within the groyne fields of the Elbe.

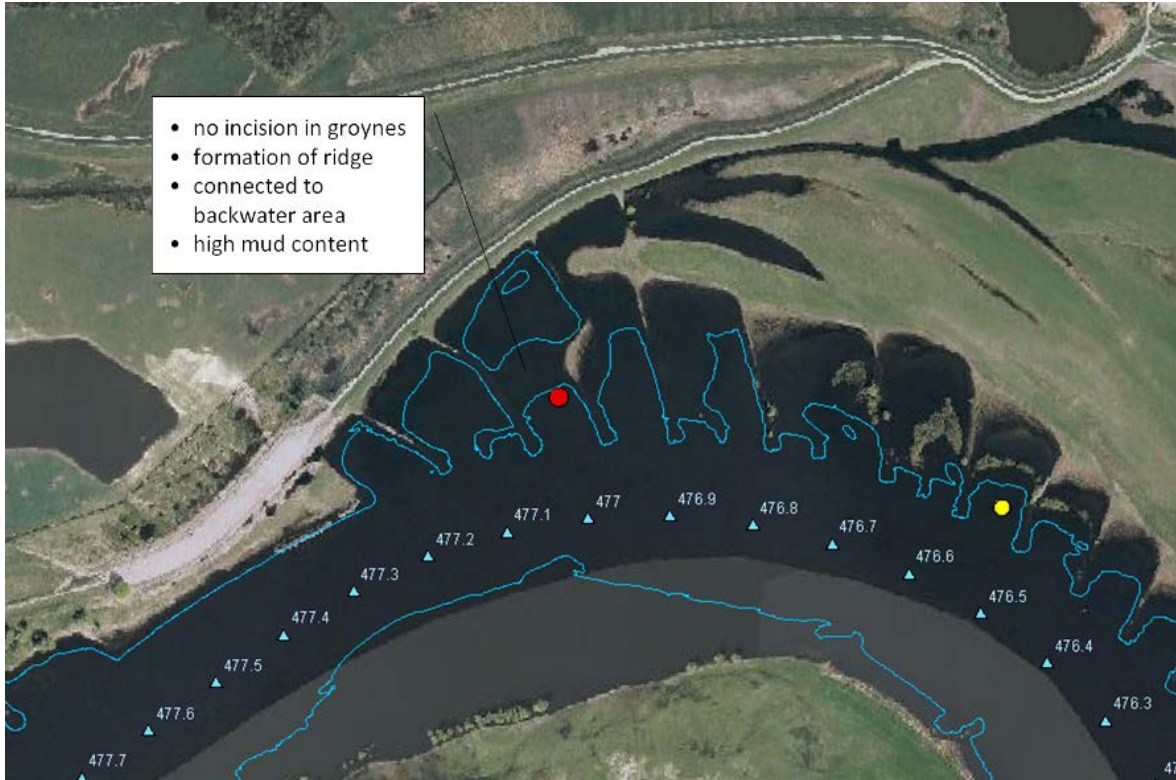


Fig. 1. Illustrative example of groyne field with high mud content (groyne field at km 477.0). The light-coloured dot within the groyne field at km 476.55 indicates a groyne field with low observed mud content. The wetted area during low water conditions is depicted by the light-coloured line.

Assessment of flocculation, settling and consolidation of cohesive sediments using the zeta potential

Ibanez Maria¹, Claire Chassagne^{1,2} and Johan C. Winterwerp^{1,2}

¹ Section of Environmental Fluid Mechanics, Civil Engineering and Geosciences, Delft University of Technology, PO Box 5048, 2600 GA, Delft, the Netherlands
Email: M.E.IbanezSanz-16@tudelft.nl

² Marine and Coastal Management, Deltares, PO Box 177, 2600 MH, Delft, the Netherlands

The aim of this paper is to link the flocculation, settling and consolidation of cohesive sediments through the colloidal properties of clays. Flocs are formed by the aggregation of clays and polymers depending on the presence of ions (Mietta *et al.*, 2009). Due to electrostatic interactions (Coulomb, van der Waals, ...) bridging between polymer and particles occurs. Cationic, anionic and uncharged polymers will be used in this study, to demonstrate the role of surface charge in the binding to the clay.

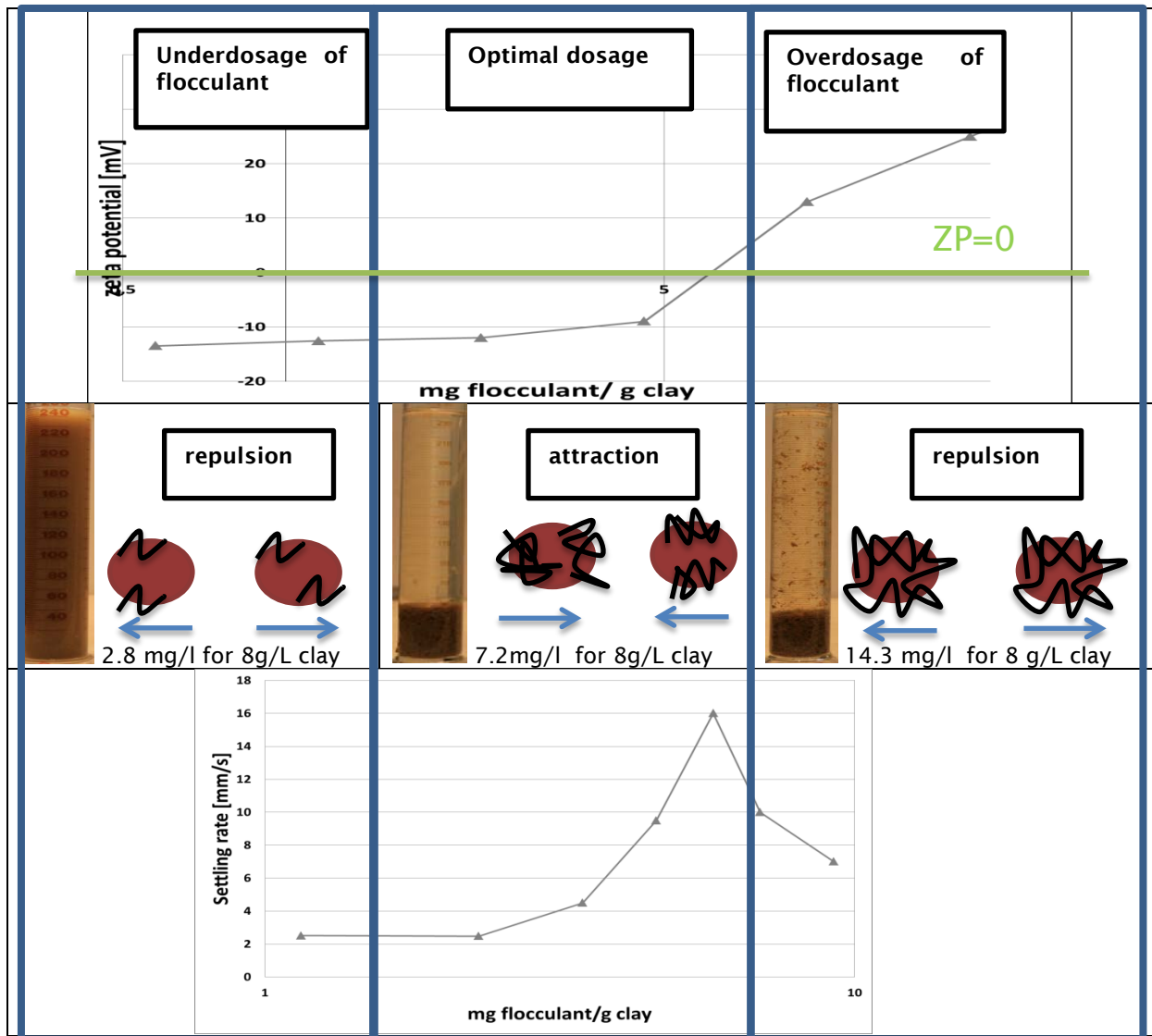
The bridging of polymers to clay particles is evaluated through the study of the interfacial properties of the clay-polymer system by electrophoretic mobility measurements. From these measurements, an estimation for the surface charge of the clay is obtained in terms of the zeta potential.

The zeta potential has proven to be a good indicator for predicting the changes (changes in particle size, density and floc strength) of clayey materials as a function of the fluid properties (changes in salinity, pH, shear stresses) (Chassagne *et al.*, 2009; Mietta *et al.*, 2009; Ibanez *et al.*, 2014).

These changes can in turn be related to changes in settling and consolidation behaviour (Merckelbach *et al.*, 2002; Winterwerp, 2002; Merckelbach and Kranenburg, 2004).

The figure below illustrates the results obtained when studying settling velocity and flocculation as function of the amount of added cationic polymer. Three regions can be defined:

1. Underdosage of flocculant: for lower dose, the repulsive forces between particles (negatively charged in the absence or low amount of cationic polymers) do not allow flocculation, and hence settling does not occur.
2. Optimal dosage: cationic polymers attach to the negatively charged particles, neutralizing their electrokinetic charge and making aggregation possible. At neutral zeta potential, flocculation is optimal and the supernatant is clear, indicating that we have reached the optimal polymer coverage and the settling velocity is the highest in this moment.
3. Overdosage of flocculant: when the optimum dose is exceeded, flocculation still occurs, but at a lower rate. This is caused by the "excess" of positive charges at the clay surface, which increase the time for positive particles to encounter a negatively charged zone. The resulting flocs are large because of their high polymers content (particles bind not with each other, but with many polymers in between). When the flocculant dose is further increased, all particles become too positively charged, resulting in mutual steric repulsion, and a decrease in the settling velocity.



References

- Chassagne C., F. Mietta and J.C. Winterwerp. 2009. Electrokinetic study of kaolinite suspensions. *Journal of Colloid and Interface Science* 336:352-359.
- Ibanez M., A. Wijdeveld and C. Chassagne. 2014. Role of mono- and divalent ions on the stability of kaolinite suspensions and fine tailings (under review).
- Ibanez Sanz M.E., C. Chassagne, L. van Passen and J.C. Winterwerp. 2014. Effect of polyelectrolytes on surface charge and flocculation of cohesive sediments (under review).
- Merckelbach L.M., C. Kranenburg and J.C. Winterwerp. 2002. Strength modelling of consolidating mud beds. *Proceedings in Marine Science* 5:359-373.
- Merckelbach L.M. and C. Kranenburg. 2004. Equations for effective stress and permeability of soft mud-sand mixtures. *Géotechnique* 54(4):235-243.
- Merckelbach L.M. and C. Kranenburg. 2004. Determining effective stress and permeability equations for soft mud from simple laboratory experiments. *Géotechnique* 54(9):581-591.
- Merckelbach L.M. and J.C. Winterwerp. 2007. A parameterised consolidation model for cohesive sediments. *Proceedings in Marine Science* 8:243-262.
- Mietta F., C. Chassagne and J.C. Winterwerp 2009. Shear-induced flocculation of a suspension of kaolinite as function of pH and salt concentration. *Journal of Colloid and Interface Science* 336:134-141.
- Mietta F., C. Chassagne, A.J. Manning and J.C. Winterwerp. 2009. Influence of shear rate, organic matter content, pH and salinity on mud flocculation. *Ocean Dynamics* 59:751-763.
- Winterwerp J. C. 2002. On the flocculation and settling velocity of estuarine mud. *Continental Shelf Research* 22(9):1339-1360.

Effect of discharge on hydrodynamics and sediment transport by the operation of tidal power plant

Jong-Wook Kim, Ha Ho Kyung and Woo Seung-Buhm

Department of Ocean Sciences, College of Natural Sciences
Inha University, Incheon 402-751, South Korea
E-mail: kaonesis@gmail.com

Shihwa Lake was located in the southern part of Gyeonggi Bay in South Korea, which has been formed by seawall of Shihwa. After the construction of seawall leading to the restriction of free exchange between freshwater discharge and seawater, the sedimentation and water pollution in Shihwa Lake became worse by continuous inflow of point and non-point source from the living, agriculture and industrial water. To solve this problem, desalination of Shihwa Lake was abandoned by decision of government in December 2000 and the Shihwa Tidal Power Plant (STPP) was constructed in middle of seawall for energy generation and water quality improvement in August 2011. The STPP has been operating for power generation during flood periods and the repetition of strong inflow and artificial discharge over tidal cycles caused rapid changes in hydrodynamics and sediment dynamics in the vicinity of STPP (Ra *et al.*, 2011; Won *et al.*, 2012). The study focused on the spatial and temporal variability of hydrodynamics and suspended sediment concentration (SSC) which had been investigated using the long-term moorings in the vicinity of STPP (Fig. 1).

The mean water depth was measured about 23, 8, 20m at the ST1, ST2 and ST3, respectively. The mean tidal range measured at Songdo tidal station was about 5.5m and the mean ranges for spring and neap tides were approximately 7.7 and 3.3m, respectively. The freshwater input was low in spring, fall and winter (0.16 to $0.47 \times 10^3 \text{m}^3 \text{s}^{-1}$) and high in summer (0.87 to $2.31 \times 10^3 \text{m}^3 \text{s}^{-1}$) by the discharge of Han River. Therefore, the freshwater was only affected to the vicinity of STPP in summer. The predominant wind was the northwest wind in winter and became weaker southerly wind in summer. Episodically, an extreme tropical storm passed in summer monsoon season.

The moorings were configured with a surface float. Each buoy was equipped with 600-kHz Acoustic Doppler current profiler (ADCP) and Conductivity-Temperature-Depth (CTD), which were used to measure current profile, temperature, and salinity. The ADCP was located 0.5m under the surface to obtain the profiles of velocity and echo intensity backscattered by suspended sediments. The bin size was set at 0.5m and blanking distance was set to 0.8m. Two CTDs were located at 0.5m below the surface and 1.5m above bottom. The measurements were conducted every 10 minutes for approximately 37 days at ST1, ST2 (from March 9 to April 15, 2013) and ST3 (from June 9 to July 16, 2013). The profiles of SSC were obtained from calibrated acoustic backscatter data using an optical backscatter sensor (OBS) and bottle samples. Additional physical data including sea level, wind, and freshwater discharge were integrated to evaluate the function of external forcing conditions.

The hydrodynamics and SSC were greatly affected by the presence or absence of artificial discharge at the STPP. In the short-term (spring and neap) scale, the current speed increased ($>1.0 \text{ms}^{-1}$) and vertically sheared by high artificial discharge. The depth-averaged SSC increased, because of greater resuspension of bottom sediment by high artificial discharge at ST1, ST2 and ST3. In contrast, the current speed decreased ($< 0.5 \text{ms}^{-1}$) and vertically sheared two-layer flow persists and the depth-averaged SSC decreased by the low artificial discharge. In the long-term (seasonal) scale, effects of freshwater and artificial discharge were comparatively strong because of large rainfall in summer compared with winter. In summer, the current speed increased at surface layer by powerful artificial discharge and shear was stronger than in winter. But the depth-averaged SSC was low, despite powerful artificial discharge, because of the strong stratification formed by freshwater ($\Delta S > 7 \text{psu}$).

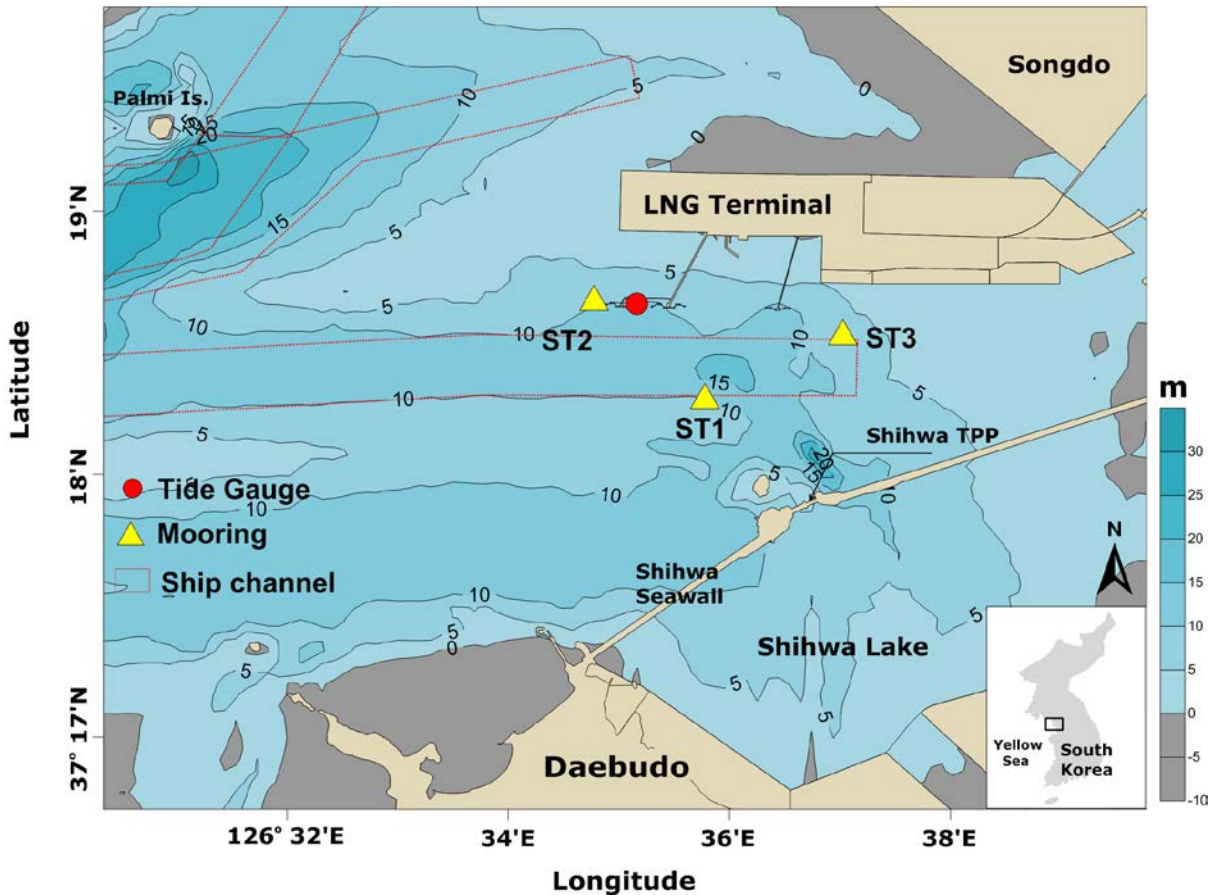


Fig. 2. Map of the Shihwa Estuary and the adjacent region, South Korea. The tidal level and wind data were obtained from Songdo tidal station (red circle). Current and backscatter data were collected from three mooring sites (yellow triangles, ST1 to ST3). The red dotted lines indicate ship channels and grey area represents the intertidal zone.

References

- Ra K.T., J.H. Bang, J.M. Lee and K.T. Kim. 2011. The extent and historical trend of metal pollution recorded in core sediments from the artificial Lake Shihwa, Korea. *Marine Pollution Bulletin* 62:1814-1821.
- Won E.J., S.J. Hong, K.T. Kim and K.H. Shin. 2012. Evaluation of the potential impact of polluted sediments using Manila clam *Ruditapes philippinarum*: bioaccumulation and biomarker responses. *Environmental Science and Pollution Research* 19:2570-2580.

The influence of clay mineralogy on the erosion thresholds of estuarine cohesive sediments

Kilkie Paul, Heidi Burgess, Callum Firth and Phillip Teasdale

School of the Environment and Technology, University of Brighton,
Lewes Road, Brighton BN2 4GJ, UK
E-mail: p.kilkie2@brighton.ac.uk

Advances in understanding sediment stability within estuarine systems are inhibited by the complexity of the physicochemical properties of the cohesive sediment and their interactions within these chemically and biologically diverse and dynamic environments (Whitehouse *et al.*, 2000; Grabowski *et al.*, 2011). Of the key properties of cohesive sediments the geochemical characteristics have received the least attention, with little investigation into their influence on erosion within estuarine systems. The electrochemical nature of the sediments that control cohesion are subject to various geochemical influences within these environments, consequently having implications for sediment stability (Ravisangar *et al.*, 2001; Grabowski *et al.*, 2011).

A fundamental geochemical property of cohesive sediments is the clay mineralogy. The variance in characteristic properties between the different clay mineral groups is recognised as a significant factor in erosion resistance in terrestrial sediment studies (Igwe *et al.*, 1999; Wakindiki and Ben-Hur, 2002; Kasanin-Grubin, 2013). This knowledge has yet to be applied to the sediment stability within the contrasting geochemical environments of estuaries (Allen, 2000; Zhu *et al.*, 2008; Grabowski *et al.*, 2011).

Through a series of laboratory and field studies this research aims to establish how variance in clay mineral composition of estuarine sediments influences erosion. This poster summarises the results of the study, identifying distinct differences in erosion thresholds between sediments with contrasting clay mineralogies. Furthermore, changes to erosion resistance of the clay mineral groups are observed between marine and freshwater eroding fluids during shear strength testing, identifying the influence of water chemistry on the stability of the different clay mineral suites.

References

- Allen J.R.L. 2000. Morphodynamics of Holocene salt marshes: a review sketch from the Atlantic and Southern North Sea coasts of Europe. *Quaternary Science Reviews* 19(12):1155-1231.
- Grabowski R. *et al.* 2011. Erodibility of cohesive sediment: The importance of sediment properties. *Earth science reviews* 105(3-4):101-120.
- Igwe C. *et al.* 1999. Chemical and Mineralogical properties of soils in south eastern Nigeria in relation to aggregate stability. *Geoderma* 92(1-2):111-123.
- Kasanin-Grubin M. 2013. Clay mineralogy as a crucial factor in badland hillslope processes. *Catena* 106:54-67.
- Ravisangar V. *et al.* 2001. Effect of sediment pH on resuspension of Kaolinite. *Journal of Environmental Engineering* 127(6): 531-538.
- Wakindiki I. and M. Ben-Hur. 2002. Soil mineralogy and texture effects on crustal micromorphology, infiltration and erosion. *Soil Science Society of America Journal* 6(3):897-905 (Cited in Lado and Ben-Hur 2004).
- Whitehouse R. *et al.* 2000. *Dynamics of estuarine muds*. Thomas Telford Publishing, London.
- Zhu Y. *et al.* 2008. Research on cohesive sediment erosion by flow: An overview. *Science in China series E: Technological Sciences* 51(11):2001-2012.

An effect of pore water flow on the re-suspension of cohesive sea bottom sediment

Kyunghoi Kim¹, Lee In-Cheol¹ and Hibino Tadashi²

¹ College of Environmental and Marine Sciences and Technology, Department of Ocean Engineering, Pukyong National University, 45, Yongso-ro, Nam-Gu, Busan, 608-737, Korea
E-mail: hoikim@pknu.ac.kr

² Graduate School of Engineering, Hiroshima University, 1-4-1 Kagamiyama, Higashi Hiroshima, 739-8527, Japan

In order to clarify an effect of pore water flow on the re-suspension of cohesive sea bottom sediment, water content variation experiments and re-suspension experiments of the cohesive sea bottom sediment in pore water flow field were carried out. By the pore water flow, water content of cohesive sea bottom sediment was increased and it depends on the amount of organic matter and C/N ratio. Water content influenced on the re-suspension of the cohesive sea bottom sediment. And it is experimentally clarified that the re-suspension of cohesive sea bottom sediment occurred at the current velocity of 4cm/s, which is observed in Hiroshima Bay, due to a decrease of critical erosion threshold in the pore water flow field.

Introduction

Hiroshima Bay, a semi-closed bay located in western Japan, is connected with Seto Inland Sea. Cohesive sea bottom sediment have been excessively deposited around the river mouth due to inflow of domestic wastewater and aquaculture, especially from 1950s to 1970s, the period of high economic growth in Japan. Several articles have reported that re-suspension of cohesive sea bottom sediment plays an important role in the functionality and health of coastal area (Lee and Hoshika, 2000; Ali and Lemckert, 2009). Therefore, analysing the mechanism of cohesive sea bottom sediment re-suspension is an important component in the assessment of the health of aquatic environments.

Most papers concerning re-suspension of the cohesive sea bottom sediment approached from bottom shear stress. However, behaviours of cohesive sea bottom sediment is characterized by plasticity, consolidation pressure, pore water quality and eroding fluid (Kamphuis, 1987). And our previous study has proven that pore water flow is one of the main factors that influences the re-suspension of cohesive sea bottom sediment in Hiroshima Bay (Imagawa *et al.*, 2007). The objective of this paper is to investigate the changes in water content and critical shear stress of the cohesive sea bottom sediment by the pore water flow.

Materials and methods

Changes in water content of the cohesive sea bottom sediment by the pore water flow was investigated by experiments using parted water tank shown in Fig. 1. And experiments for the analysis of critical shear stress of the cohesive sea bottom sediment in the pore water flow field were carried out using unidirectional flow channel (Fig. 2).

Cohesive sediments sampled in several areas of Hiroshima Bay were used for in-door experiment. IL and C/N of the sampled sediments ranged 11.9 – 17.0% and 10.8 – 14.0, respectively.

Results and discussion

Fig. 3 shows the results of the water content variations by the pore water flow. Water content of the cohesive sea bottom sediment in the condition without pore water flow ($dh=0$) ranged 270 - 420%, while it increased to 470 - 710% in the pore water flow condition ($dh=1$). From these, it can be said that the pore water flow increase water content of the cohesive sea bottom sediment. And water content tended to increase with IL and to decrease with C/N ratio.

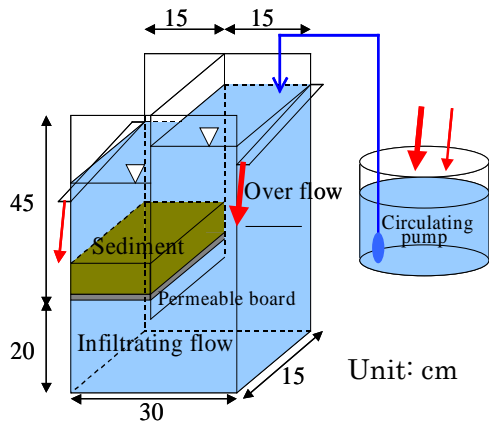


Fig. 1. Parted water tank.

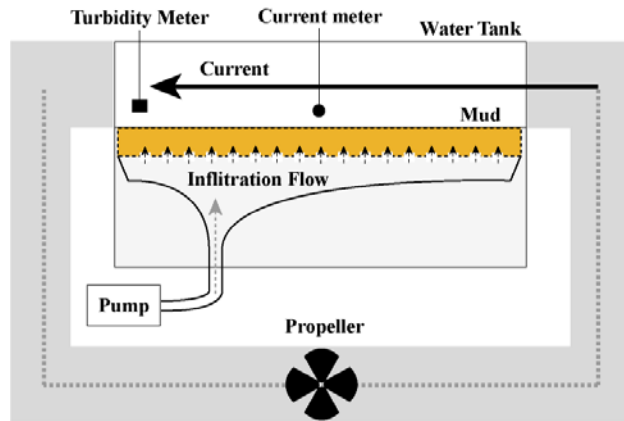


Fig. 2. Unidirectional channel.

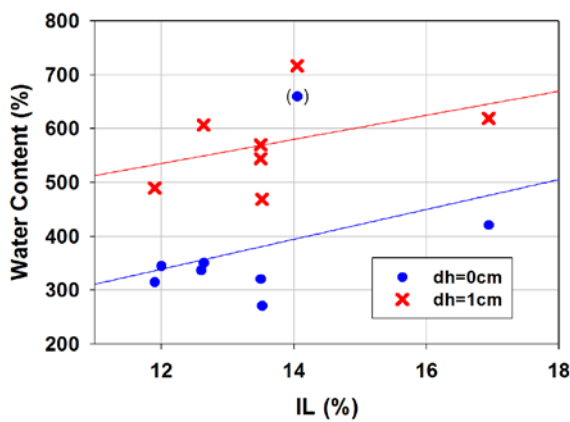


Fig. 3. Relationship between IL and water content.

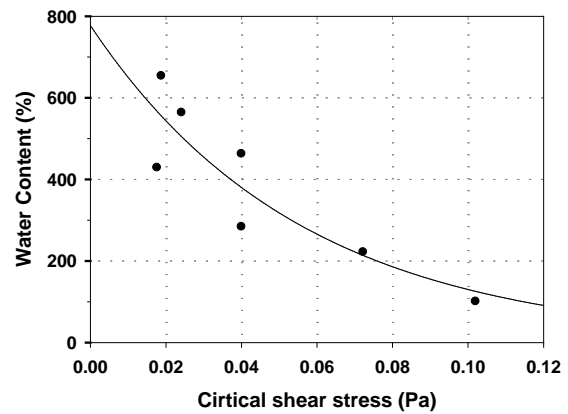


Fig. 4. Relationship between critical shear stress and water content.

Fig. 4 shows the relationship between critical shear stress and water content. The cohesive sea bottom sediment with over 400% of water content started to re-suspend at the critical shear stress of 0.02 - 0.04 Pa (current velocity of 4 - 8cm/s) and this may be contributed by the pore water flow. From the results obtained above, it is concluded that the re-suspension of cohesive sea bottom sediment is enhanced due to both expansion of the sediment (increase of water content) and lifting force on the sediment particle accompanied by the pore water flow. And it is experimentally clarified that the re-suspension of cohesive sea bottom sediment occurred under current velocity of 4cm/s, which is observed in Hiroshima Bay, due to decrease of critical erosion threshold in the pore water field.

References

- Ali A. and C. Lemckert 2009. A traversing system to measure bottom boundary layer hydraulic properties. *Estuarine, Coastal and Shelf Science* 83:425-433.
- Imagawa M., T. Hibino, K. Komai and Y. Matsunaga. 2007. Study on upwelling of organic mud in pore water infiltration field. *Proceedings of Coastal Engineering, JSPS* 54:1011-1015 (in Japanese with English abstract).
- Kamphuis J.W. 1987. Recession rate of glacial till bluffs. *Journal of Waterway, Pore, Coastal and Ocean Engineering, ASCE* 113:60-73.
- Lee I.C. and A. Hoshika 2000. Prediction of oyster culture and water quality change in Hiroshima Bay - development of water-sediment ecosystem model. *Report of Chugoku National Industrial Research Institute* 54: 33-41 (in Japanese with English abstract).

Experimental investigation of the variability of the peak shear stress within consolidating cohesive sediment

Landuyt Sydney¹, Stijn Claeys¹, Thomas Van Hoestenbergh², Meshkati Shahmirzadi^{1,2}, Peter Staelens³ and Tomas Van Oyen^{1,4}

¹ Flanders Hydraulics Research, Berchemlei 115, Antwerp, Belgium

E-mail: tomas.vanoyen@mow.vlaanderen.be

² Antea Group, Roderveldlaan 1, Berchem, Belgium

³ Dotocean, Pathoekeweg 9b, 8000 Brugge, Belgium

⁴ Department of Civil Engineering, Ghent University, Ghent, Belgium

An experimental analysis of the variation of the peak shear stress within consolidating cohesive sediment is presented. To this end, the occurring peak shear stress of the cohesive sediment is analysed with a rotating vane based rheometer. By measuring the peak shear stress within samples with an identical initial condition at different time intervals, the temporal evolution of the peak shear stress is acquired. In addition, the influence of the considered deformation rate is examined by applying 10 different rotation speeds of the vane. The variability of the peak shear stress in function of the deformation rate and consolidation time is examined and mathematical formulations describing the dependence of the peak shear stress on both will be introduced.

Introduction

Many harbours and ports suffer from a net import of sediment, affecting the navigability and manoeuvrability of vessels entering. In order to guarantee safe access, commonly, the sediment is periodically dredged and disposed. When the sediment imported into the harbours chiefly consists of cohesive sediment, the efficient organization of maintenance dredging programs, however, is not straightforward. In particular, the rheology of consolidating cohesive sediment is known to be time dependent (e.g. Nichols, 1984; Kessel and Blom, 1998) and can strongly vary between different locations and with different local conditions (Claeys *et al.*, 2012). As such, a precise parameter which can be used as an indicator of the necessity to dredge is currently still under debate.

In the present study, we investigate the variation of the peak shear stress, i.e. the shear stress necessary to break the structure within the sediment build up during consolidation, with respect to consolidation time and deformation rate. The latter parameter is evaluated as it can be considered as a mimic of the speed of a vessel; while the first provides insight in the temporal evolution of the peak shear stress.

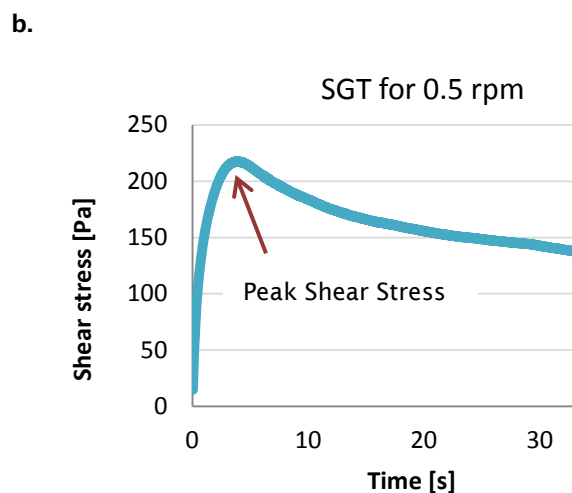


Fig. 1a. Picture illustrating the sample cups filled with cohesive sediment dredged in the harbour of Zeebrugge. Initially, the sediment has a density of 1.229g/cm^3 .

Fig. 1b. Typical SGT result obtained with a rheometer and considering a constant rotation speed of 0.5 rotations per minute.

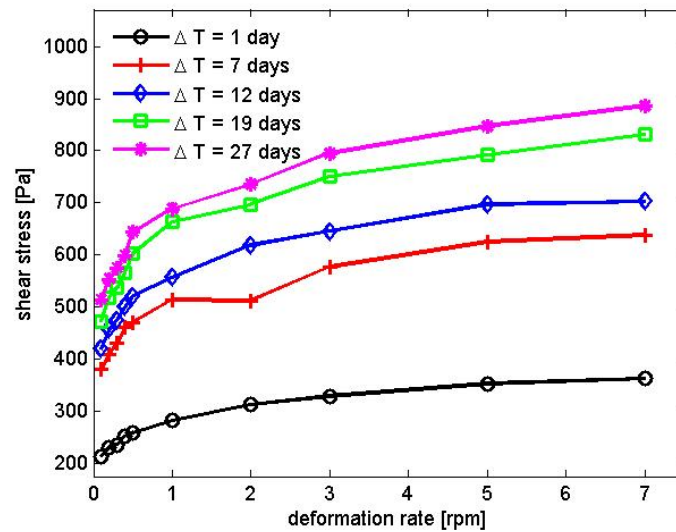


Fig. 2. The peak shear stress [Pa] (obtained by the instrument) plotted as function of the deformation rate (vane rotations per minute [rpm]) for five different consolidation times (ΔT).

Methods and materials

Within this study, we analyse the rheological characteristics of cohesive sediment dredged from the harbour of Zeebrugge. The sediment is homogenized, manipulated to a starting density of 1.229g/cm^3 and divided over 180 sample cups, see Fig. 1a. The variability of the peak shear stress is evaluated by applying a stress growth test (“SGT”) on each (undisturbed) sample using a vane spindle (model: ST22-4V-40-SN11294) (Instruments, n.d.). This means that we monitor the shear stress needed to maintain a constant shear rate (\sim constant revolution rate of the vane). In Fig. 1b, a typical SGT result is plotted illustrating the occurrence of a peak in the shear stress.

To investigate the influence of the deformation rate θ , 10 different rotation speeds are considered; while stress growth tests are performed on undisturbed samples at five different time intervals (ΔT).

Results

Fig. 2 illustrates the variation of the peak shear stress as function of the deformation rate after various consolidation times. In this study different deformation rates are obtained by varying the vane rotation rate. The figure indicates that different deformation rate significantly affects the required shear stress necessary to break up the sediment structure. On the other hand, Fig. 2 indicates that the increase in peak shear stress is smaller for high deformation rates than for lower values of θ , suggesting a logarithmic interdependence. Similarly, it is found that the time interval the sediment has consolidated can appreciably impact the peak shear stress.

Conclusions and outlook

The variability of the peak shear stress within consolidating cohesive sediments is analysed experimentally. It is found that both deformation rate as consolidation time significantly affect the occurring peak shear stress. In particular, the obtained data suggests that the peak shear stress increases logarithmically with deformation rate, while also ΔT is found to have a significant influence. Currently, laboratory experiments are ongoing in order to extend the dataset on the peak shear stress as function of consolidation time and deformation rate such that mathematical formulations can be confidently fitted to the data. Moreover, additional tests are presently performed to evaluate also the impact of the starting density.

References

- Claeys S., B. Dierikx, P. Simon and J. van Reenen. 2012. Fluid mud density determination in navigational channels. *Hydro12 - Taking Care of the Sea*. Rotterdam. Instruments, Malvern. (n.d.). *Understanding Yield Stress Measurements*.
 Kessel v.T. and C. Blom. 1998. Rheology of cohesive sediments: comparison between a natural and an artificial mud. *J. Hydraulic Research* 36(4):591-602.
 Nichols M.M. 1984. Fluid mud accumulation processes in an estuary. *Geo-Marine Letters* 4:171-176.

Two-class flocculation kinetic model: development and application to large-scale, multi-dimensional cohesive sediment transport

Lee Byung Joon¹, Qilong Bi², Erik Toorman², Michael Fettweis³ and Holger Weilbeer⁴

¹ School of Construction and Environmental Engineering, Kyungpook National University
2559 Gyeongsang-daero, Sangju, Gyeongbuk, 742-711, South Korea
E-mail: bjlee@knu.ac.kr

² Hydraulic Laboratory, Civil Engineering Department, KU Leuven
Kasteelpark Arenberg 40, Heverlee, 3001, Belgium

³ OD Natural Environment, Royal Belgian Institute of Natural Sciences
Gulledelle 100, 1200 Brussels, Belgium

⁴ Federal Waterways Engineering and Research Institute (BAW)
Wedeler Landstr. 157, 22559 Hamburg, Germany

Introduction

Fluid mud layer, composed of cohesive sediments, has been a serious problem in many waterways, docks and harbours. For example, Zeebrugge Harbour in Belgium has been reported to build up one- or two-meter thick fluid mud layer. Flocculation is known to be a key process for developing such fluid mud layers. Flocculation is a combined process of (1) aggregation of small mud particles to large flocs and (2) breakage of large flocs, depending on a turbulent shear condition. Cohesive sediments remain small in an open water (e.g. river or ocean), due to breakage under high turbulent shear. When entering/traveling into a closed water (e.g. harbour or dock), cohesive sediments aggregate to large, settleable flocs under low turbulent shear and finally settle/deposit on the bottom.

Most of flocculation models assume an equilibrium (or pseudo-equilibrium) condition and a single floc size, thus disregarding the two important aspects, (1) flocculation kinetics in a time and space and (2) bimodal (or multimodal) floc size distributions of cohesive sediments. Flocculation is a relatively slow process, taking several to ten hours to reach an equilibrium condition in a river, estuarine or coastal environment. Therefore, an empirical, equilibrium flocculation model may cause errors, when involving a time or spatial transition. For example, the Deurganckdok study (WL | Delft Hydraulics, 2006) reported that an equilibrium flocculation model resulted in under- (or over-) estimation of flocculation and sedimentation in a dock next to a turbulent river (i.e. at a transition). Also, flocculation often develops bimodal floc size distributions. This bimodal behaviour cannot be simulated with a conventional single-size flocculation model.

To minimize such errors, we developed a new flocculation kinetic model, based on Two-Class Population Balance Equation (TCPBE) (Eqn. (1)) (Lee *et al.*, 2011). The two discrete size groups of flocculi and flocs, as building blocks and aggregates, were found to approximate a bimodal floc size distribution of cohesive sediments (Lee *et al.*, 2012, 2014). This observation led us to develop a new two class population balance equation (TCPBE), which can track the concentration of size-fixed flocculi and the size and concentration of size-varying flocs as an approximation of a multimodal PSD.

$$\begin{aligned}
 & \left[\frac{\partial N_i}{\partial t} \right] + \left[\frac{\partial u_x N_i}{\partial x} + \frac{\partial u_y N_i}{\partial y} + \frac{\partial u_z N_i}{\partial z} \right] - \left[\frac{\partial}{\partial x} \left(\frac{0.09 \rho_w k_e^2}{S_c \varepsilon} \frac{\partial N_i}{\partial x} \right) + \frac{\partial}{\partial y} \left(\frac{0.09 \rho_w k_e^2}{S_c \varepsilon} \frac{\partial N_i}{\partial y} \right) + \frac{\partial}{\partial z} \left(\frac{0.09 \rho_w k_e^2}{S_c \varepsilon} \frac{\partial N_i}{\partial z} \right) \right] = \pm (\text{agg} / \text{break})_i - w_{s,i} \frac{\partial N_i}{\partial z} \\
 & (\text{agg} / \text{break})_{N_p} = \frac{\partial N_p}{\partial t} = -\frac{1}{2} \alpha_{pp} \beta_{pp} N_p N_p \left(\frac{N_c}{N_c - 1} \right) - \alpha_{pf} \beta_{pf} N_p N_f + f N_c \alpha_f N_f \\
 & (\text{agg} / \text{break})_{N_f} = \frac{\partial N_f}{\partial t} = +\frac{1}{2} \alpha_{pp} \beta_{pp} N_p N_p \left(\frac{1}{N_c - 1} \right) - \frac{1}{2} \alpha_{ff} \beta_{ff} N_f N_f + \alpha_f N_f \\
 & (\text{agg} / \text{break})_{M_f} = \frac{\partial M_f}{\partial t} = +\frac{1}{2} \alpha_{pp} \beta_{pp} N_p N_p \left(\frac{N_c}{N_c - 1} \right) + \alpha_{pf} \beta_{pf} N_p N_f - f N_c \alpha_f N_f \\
 & w_{s,i} = \Phi_{HS} \left(\frac{1}{18} \frac{(\rho_s - \rho_w) g}{\mu} D_p^{3-n_f} \frac{D_f^{n_f-1}}{1+0.15 Re_i^{0.687}} \right) \\
 & \Phi_{HS} = (1-\phi)^a
 \end{aligned}
 \tag{1}$$

(Nomenclature)

$N_i = N_p, N_f, \text{ or } M_f$

$N_c = \text{Number of Flocculi in a Floc}$

$M_f = N_f \times N_c$

$f = \text{Flocculi Fraction Generated by Breakage}$

$w_{s,i} = \text{Floc Settling Velocity } D_p, D_f = \text{Diameter of Flocculi and Floc}$

$n_f = \text{Fractal Dimension}$

$\Phi_{HS} = \text{Factor for Hindered Settling}$

$\Phi = \text{Factor for Hindered Settling}$

Model development and application: large-scale, multi-dimensional TCPBE-TELEMAT model.

For application to large-scale cohesive sediment transport, TCPBE is implemented to an open-source hydrodynamic and sediment transport model (TELEMAT in this study). We modify the original code of TELEMAT, adopting shear rate ($G = (\mathcal{E}/\nu)^{0.5}$) and settling velocity (w_s) as two key factors for controlling flocculation kinetics and sediment transport. At each time step in computation, TELEMAT calculates shear rates (G), which then control flocculation kinetics of TCPBE. On the other hand, TCPBE calculates flocculation settling velocities (w_s), which then determine flocculation sedimentation/deposition (i.e. sink) rates.

The combined TCPBE-TELEMAT model is applied to simulate cohesive sediment transport in Belgian near-shore area and Elbe Estuary in Germany. The results show that the TCPBE-TELEMAT model can more realistically simulate cohesive sediment processes (i.e. flocculation, advection, dispersion, sedimentation and deposition) than the equilibrium flocculation model. For example, the TCPBE-TELEMAT model can simulate a lag phase of flocculation at a time and spatial transition (e.g. from slack to peak flow; from an open ocean to a harbour), because it takes into account "kinetics". The conventional equilibrium flocculation model however does not consider kinetics nor the lag phase, so that it often develops steep gradient (or discontinuity) of flocculation at a time and spatial transition. In addition, because the TCPBE-TELEMAT model takes into account the bimodality with the two groups of flocculi and flocs, it can simulate background turbidity floating around in the water column. The single-class equilibrium flocculation model often develops zero turbidity, which is not real, because it does not differentiate turbidity-causing flocculi from flocs.

Further remarks: biologically-mediated TCPBE

The TCPBE model is theoretical but not empirical. This implies that the TCPBE model can easily add on other physical, chemical and biological processes without breaking the physics of flocculation. Thus, in future studies, the TCPBE model will be used as a generic model to adopt biologically-mediated flocculation. Especially, Extracellular Polymeric Substances (EPS) are known to scavenge and assemble biomass and sediment particles into large flocs (Engel *et al.*, 2004). Thus, the biologically-mediated TCPBE will include: (1) EPS formation kinetics controlled by microbial population dynamics and (2) particle aggregation and breakage kinetics between different particles species (i.e. EPS, biomass and minerals) (Fig. 1).

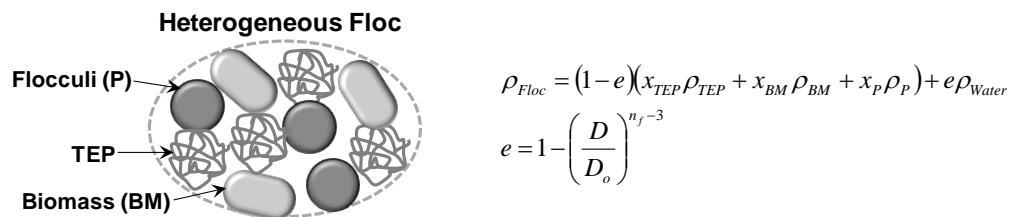


Fig. 1. A schematic diagram of a biomass-sediment floc with heterogeneous composition and mathematical formula for calculating the density of a heterogeneous floc. x is the volume fraction of TEP, biomass or flocculi in a floc, e is the void fraction, D is the size of a floc and D_o is the size of a primary particle.

Acknowledgement

This research was supported by Basic Science Research Program through the National Research Foundation of Korea (NRF) funded by the Ministry of Education (No: 2014R1A1A2055622).

References

- Engel A., S. Thoms, U. Riebesell, E. Rochelle-Newall and I. Zondervan. 2004. Polysaccharide aggregation as a potential sink of marine dissolved organic carbon. *Nature* 428:929-932.
- Lee B.J., E. Toorman and M. Fettweis. 2014. Multimodal particle size distributions of fine-grained sediments: mathematical modeling and field investigation. *Ocean Dynamics* 64(3):429-441.
- Lee B.J., M. Fettweis, E. Toorman and F. Molz. 2012. Multimodality of a particle size distribution of cohesive suspended particulate matters in a coastal zone. *Journal of Geophysical Research* 117. C03014.
- Lee B.J., E. Toorman, F.J. Molz and J. Wang. 2011. A two-class population balance equation yielding bimodal flocculation of marine or estuarine sediments. *Water Research* 45(5):2131-2145.
- WL | Delft Hydraulics. 2006. 3D sliibtransport model Zeeschelde - Scenario 4: effect CDW op sedimentatie Deurganckdok, nieuw instrumentarium.

Bedform dynamics in mixed sand-clay-EPS substrates

Leiping Ye¹, D.R. Parsons¹, R.J. Schindler^{1,2}, A.J. Manning^{1,2,3} and COHBED Project Team⁴

¹ Department of Geography, Environment and Earth Science, University of Hull, Hull, UK
E-mail: L.Ye@2012.hull.ac.uk

² School of Marine Science & Engineering, University of Plymouth, Plymouth, UK

³ HR Wallingford, Howbery Park, Wallingford, Oxfordshire, UK

⁴ J. Baas, J. Malarkey and A. Davies (Bangor University); J. Peakall (University of Leeds); P. Thorne (NOC Liverpool); S. Bass (University of Plymouth); D. Paterson, J. Hope, R. Aspden (University of St Andrews); S. Simmons (University of Hull)

Introduction

Understanding and quantifying sediment dynamics in coastal and estuarine environments remains challenging. This is particularly the case when including and considering the complexities of sediment mixtures, such as sand and clay and their biological mediation. Quantifying such mediation is key to parameterizing physical processes at the flow bed interface, which ultimately controls morphodynamics at local and regional scales (French, 2010). Moreover, understanding sediment movement is also vital for monitoring water quality, fate of pollutants, and the success of coastal dredging operations (Rao *et al.*, 2011). Fine sediments, which commonly exist in natural estuarine flow systems and are composed of fine silts and clays, with biological agents that have cohesive properties that modulate the complex interactions between flow, sediment transport and morphological evolution (Baas and Best, 2008). In morphodynamic investigations, the properties and influence of the substrate has largely been ignored, but can significantly impinge on the behaviour and dynamics of sediment transport, which ultimately influences and interacts with the form and the size of bedforms. Our existing flow and transport predictions for these environments are seriously impeded by an almost complete lack of process based knowledge of sediment behaviour consisting of complex mixture of cohesionless sand and biologically active cohesive muds. The work presented here forms a part of the UK NERC "COHBED" project which mainly aims to fill this gap in knowledge. Herein results from a set of controlled laboratory experiments, conducted using mixed cohesive and noncohesive sediment and Xanthan gum (as a proxy for the biological stickiness of Extracellular Polymeric Substances (EPS)), are presented and discussed.

Experiment design

Experiments were undertaken at the University of Hull's Total Environment Simulator flume/wave tank facility [Fig. 1 (www.hull.ac.uk/tes)]. The tank was sectioned into a 10 x 2m flume channel and filled with varying ratios of fine sand and kaolin clay, varying ratios of fine sand and EPS (Xanthan gum, a natural biopolymer) and varying ratios of sand, clay and EPS (Table I).



Fig. 1. Flume lab set-up at the University of Hull's Total Environment Simulator flume/wave tank facility.

Saline water (at 15 PSU) was used throughout the experimental set and was pumped to produce a constant unidirectional current with a depth-averaged flow velocity and depth in the test section that occupied the known dune regime for noncohesive sands. A total of 16 individual runs were

conducted lasting 10.5 hours for each, with continuous acoustic monitoring of the flow current and bed topography via automated traverse and profilers, with water and bed samples also taken every 30 minutes during the run.

Table I. Clay content of start, end, loss percentages in substrates of 16 runs

Run	Clay % at start	Clay % at end	Clay Loss by % of total mass	Clay loss by % of clay mass
1	18.15	16.8	1.35	7.4
2	14.11	12.09	2.02	14.3
3	12.67	11.26	1.41	11.1
4	11.92	7.56	4.36	36.6
5	9.77	9.53	0.24	2.5
6	8.87	8.21	0.66	7.4
7	4.74	1.85	2.89	61.0
8	1.93	1.25	0.68	35.2
9	20.86	17.70	3.16	15.15
10	17.70	17.39	0.31	1.75
11	17.39	15.09	2.30	13.23
12	12.02	10.51	1.51	12.56
13	9.89	9.19	0.70	7.08
14	6.77	6.15	0.62	9.16
15	4.83	4.08	0.75	15.53
16	4.65	3.35	1.30	27.96

Methods and results

Suspended sediments were measured using a LISST100X (Laser In Situ Scattering and Transmissometry) using physical water samples. Grain size and concentration data has been analyzed using Matlab R2012b software creating a database from each of the 16 runs. Additionally, selected water samples were analysed using the LabSFLOC - Laboratory Spectral Flocculation Characteristics - instrument (e.g. Manning *et al.*, 2007), facilitating the measurement of the floc sizes and settling velocities using high resolution video technology (see Manning and Dyer, 2002), and thus enabling the determination of the densities of suspended particulates and flocs across each of the substrate mixtures. Thus the effects of varying suspended sands, clays and EPS within the substrate mixture on flocculation processes and suspended sediment dynamics were monitored throughout each of the runs.

Additionally, flow and turbulence structure were sampled at-a-point through a stacked profile of 5 ADVs, which sampled velocity at 25Hz. The bedform development was monitored throughout the experiments through side and plan view wide angle video and through ultrasonic ranging transducers spanning a 4.5 x 0.5m working section swath. The paper will present and discuss the detailed results, highlighting the influence of substrate characteristics on sediment transport, flocculation and bedform dynamics.

References

- Baas J.H. and J.L. Best. 2008. The dynamics of turbulent, transitional and laminar clay-laden flow over a fixed current ripple. *Sedimentology* 55:635-666.
- French J.R. 2010. Critical perspectives on the evaluation and optimization of complex numerical models of estuary hydrodynamics and sediment dynamics. *Earth Surface Processes and Landforms* 35(2):174-189.
- Manning A.J. and K.R. Dyer. 2002. The use of optics for the in-situ determination of flocculated mud characteristics. *J. Optics A: Pure and Applied Optics*, Institute of Physics Publishing 4:S71-S81.
- Manning A.J., P.L. Friend, N. Prowse and C.L. Amos. 2007. Preliminary findings from a study of Medway Estuary (UK). Natural mud floc properties using a laboratory mini-flume and the LabSFLOC system. *Continental Shelf Research*, doi:10.1016/j.csr.2006.04.011.
- Rao V.P., R. Shynu, P.M. Kessarkar, D. Sundar, G.S. Michael, T. Narvekar, V. Blossom and P. Mehra. 2011. Suspended sediment dynamics on a seasonal scale in the Mandovi and Zuari estuaries, Central west coast of India. *Estuarine, Coastal and Shelf Science* 91:78-86.

Analysis on variations of water/sediment and morphodynamics response in Hangzhou Bay in recent 50 years

Lu Hai-yan^{1,2}, He Qing¹, Pan Cun-hong² and Cao Ying²

¹ State Key of Estuarine and Coastal Research, East China Normal University, Shanghai 200062, P.R. China
E-mail: luhy@zjwater.gov.cn

² Zhejiang Institute of Hydraulics and Estuary, Hangzhou 310020, P.R. China

Hangzhou Bay is located on the eastern coast of China, the south of the Yangtze River Delta. The total length of the bay from the head named Ganpu to the mouth named Luchaogang is about 85km. Hangzhou Bay with the strong tide and the swift current, is the waterfront section of the Qiantang River Estuary, abuts on the estuarine section of the Qiantang River and the Yangtze River, where water and sediment exchange closely. Under such complex dynamic conditions and high intensity development activities by human impacts, the bathymetry, the hydrograph and sediment field in Hangzhou Bay have been changed significantly in the past 50 years. In order to further understand the dynamic mechanism of the erosion/deposition pattern and the sediment transport in the Hangzhou Bay, the measured bathymetry data combined with DEM (digital elevation model) is used to analyse the changes of the major geomorphic units in Hangzhou Bay. Based on the calibration and verification of the model parameters of the hydrology and sediment, a two-dimensional numerical model is employed to reproduce the current and suspended sediment field before and after the large-scale reclamation project in the adjacent waters.

The results show that the tidal influx volume and the sediment load from JinShan to Ganpu area in the Hangzhou Bay reduced by 10% to 40%, 17% to 28% respectively. It is mainly owing to the large-scale reclamation of tidal flat in Qiantang River Estuary since 1960s, which reduce the storage capacity for tidal water. The net accretion in the Hangzhou Bay is up to 4 billion m³ in recent 50 years, though the sediment discharge from the Yangtze River is decreasing. The transport rate of suspended sediment is asymmetric with the suspended sediment concentration of flood tide higher than that of ebb tide, which results in a net onshore transport during the tidal cycle.

However, the spatial distribution of erosion/deposition are different between the north channel, the middle channel and the south channel in Hangzhou Bay. The sea bed near the north channel is eroded, with the sediment scour amount of 340 million m³, and the average scour depth amount of 0.21m. The bed of the middle channel is relatively stable, with the average accretion depth about 0.06cm, and the sediment siltation amount of 80 million m³. Substantial siltation occurs in the south channel, the total sediment storage amounts to 4.2 billion m³, even more than the total net sediment storage in the Hangzhou Bay. The sharp decline of sediment discharge from the Yangtze River Basin, the large-scale reclamation of the Nanhui tidal flat, and the north extension of the Andong tidal flat, is the main cause of the scour in the north shore of Hangzhou Bay (zhapu ~ Luchaogang coast).

Keywords

Hangzhou Bay; Sediment transport; Human reclamation; Morphodynamics changes.



Fig. 1. Location of Hangzhou Bay.

References

- Ding P.X., K.L. Hu and Y.Z. Kong *et al.* 2003. Numerical simulation of total sediment under waves and currents in the Changjiang Estuary. *Acta Oceanologica Sinica* 25(5):113-124. (in Chinese).
- Du Panjun, Ding Pingxing and Hu Kelin. 2010. Simulation of three-dimensional cohesive sediment transport in Hangzhou Bay, China. *Acta Oceanologica Sinica* 29(2):98-106.
- Grant W.D. and O.S. Madsen. 1979. Combined wave and current interaction with a rough bottom. *Journal of Geophysical Research* 84(C4):1797-1808.
- Hu K.L., P.X. Ding and S.X. Zhu *et al.* 2000. 2-D current field numerical simulation integrating Yangtze Estuary with Hangzhou bay. *China Ocean Engineering* 14(1):89-102. (in Chinese).
- Huo Miao, Fan Dai-du, Lu Qi and Liu A-cheng. 2010. Decadal variations in the erosion/deposition pattern of Nanhui muddy bank and their mechanism in the Changjiang Delta.[J].*China Acta Oceanologica Sinica* 32(5):41-51.
- Yang Z., H. Wang, Y. Saito *et al.* 2006. Dam impacts on the Changjiang (Yang tze) River sediment discharge to the sea: the past 55 years and after the Three Gorges Dam [J].*Water Resources Research* 42:w04407. doi :10.1029/ 2005W R003970.
- Zhu S.X., P.X. Ding and F.Y. Shi. 2000. The simulation studies on the residual currents in the Hangzhou Bay and the Changjiang Estuary and their role in material transport. *Acta Oceanologica Sinica* 22(6):1-12.

The effect of different physico-chemical parameters on the rheological behavior of consolidating mud

Meshkati Shahmirzadi M.E.^{1,3}, S. Claeys³, T. Van Hoestenberghé¹, P. Staelens², T. Van Oyen^{3,4}, J. Vanlede³ and R. De Sutter¹

¹ Antea Group, Roderveldlaan 1, Berchem, Belgium
E-mail: Meshkati.Shahmirzadi@anteagroup.com

² Dotocean, Pathoekeweg 9b, 8000 Brugge, Belgium

³ Flanders Hydraulics Research, Berchemlei 115, Antwerp, Belgium

⁴ Department of Civil Engineering, Ghent University, Ghent, Belgium

Studying the characteristics of consolidating fluid mud is of vital importance, as it may provide insight into the navigability of ships in the harbours. In this study, the evolution of rheological and physical properties of mud during the consolidation process is experimentally investigated. The main objective of this study is to verify the parameters that influence the rheological behaviour of fluid mud by comparing mud from different origins.

The strength of mud plays an important role in consolidation and erosion processes of mud (Gularte *et al.*, 1979). Measuring the strength of mud *in situ*, however, is a challenging task and not yet solved in the literature (Berlamont *et al.*, 1993; Huang and Huhe, 2009). This is why researchers attempt to explore relationships between the strength of mud and more tangible physical parameters such as density. In the present study, we investigate the rheological behaviour of consolidating mud through examining the effect of parameters such as yield stress, density distribution, grain size composition, organic matter content and mineral compositions on this behaviour. To increase the practical use of the results, mud from five different origins are studied; namely mud from the harbours of Zeebrugge (ZB) and Deurganckdok (DG) in Belgium, the harbours of Rotterdam (RO) and IJmuiden (IJ) in the Netherlands and the Emden (EM) harbour in Germany.

A unique experimental setup for consolidation tests is constructed at Flanders Hydraulic Research laboratory, Belgium. Using this facility, for each mud type 5 consolidation columns (57mm inner diameter and 3 meter high) are filled by the corresponding mud with the initial density of 1.1g/cm³. These consolidation columns were kept undisturbed during the consolidation process. At different time points during the experimental period (i.e. 1, 7, 14, 28 and 56 days after initiation of the experiments), these consolidation columns are gradually sub-sampled. The mud sub-samples are analyzed to obtain the physical and rheological properties of mud. For this purpose, an Anton Paar MCR 301 Rheometer is used to determine the rheological properties of each sub-sample. The sub-samples are examined with 9 different rotation rates, from 112 to 56, 28, 14, 7, 4, 2, 0.5 and 0.2 rpm, and the corresponding torque is measured. The density, grain size and organic matter content the sub-samples were measured by using an Anton Paar DMA 38 density meter, a Mastersizer 2000 grain size analyzer and a PrepAsh thermogravimetric analyzer, respectively.

The temporal variation of density along the depth of consolidation column is examined. Fig. 1a illustrates the vertical distribution of density of mud from the harbour of Zeebrugge at different time points. As for the other mud types, it is found for the Zeebrugge mud that the density of the top sub-samples is significantly lower than that of the deeper sub-samples within a column for all mud types. The difference in density of top samples from the rest is particularly pronounced at Day 1 and Day 7. It is also found that the consolidation speed is significantly different for the different mud types, as the mud types cover a different range of densities at the end of the experimental period. For Zeebrugge, density cover a wide range of densities from less than 1.1 up to 1.25g/cm³ by the end of the experiments. The differences in temporal evolution of density for the different harbours will be discussed in the full paper.

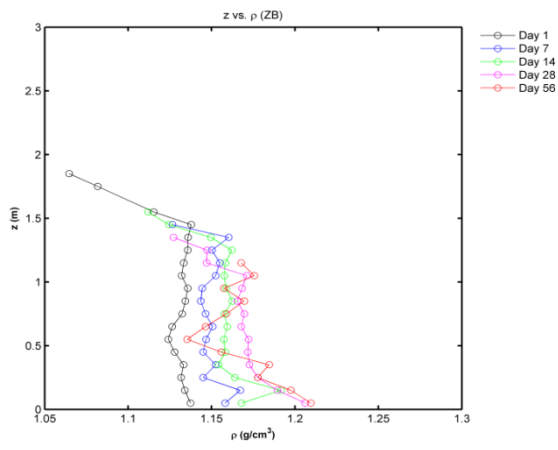


Fig. 3a. The temporal evolution of density along the depth in the Zeebrugge consolidation column.

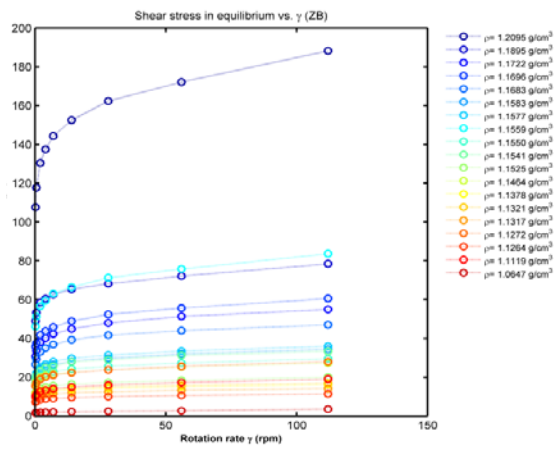


Fig. 1b. Equilibrium flow (EF) curves for Zeebrugge.

Equilibrium flow (EF) curves are obtained with Rheometer tests using a vane. In Fig. 1b the EFC for different densities are shown for Zeebrugge. It is found that the general pattern of EF curves is independent of density and follows a similar trend for all the studied mud types. All studied mud types showed a non-Newtonian shear thinning behaviour. A typical upward shift is recognized in EF curves as density rises. The upward shift between EF curves in respect to the rise in density is more or less equal till a certain level of density. Beyond this level, a big jump in EF values is observed. For Zeebrugge a density level higher than 1.20g/cm³ demonstrates a sharp increase in the EF values (Fig. 1b). A further descriptions of the EF curves of different studied mud types will be presented in the full paper.

A comparison of the temporal evolution of grain size distribution and organic matter content of different studied mud types will be presented. The study on the grain size distribution includes a detailed examination of the fractions of clay, silt and sand in each mud type as well as the span (width of the cumulative grain size distribution curve), the surface mean and the volume mean of grains.

The results of clay mineralogy tests will be analyzed to investigate whether the mineralogical characteristics of mud affect the rheological behaviour of fluid mud. The mineralogical study includes the determination of the following parameters: CaCo₃, clay minerals (XRD-analysis), CEC and pH.

Acknowledgments

This project is funded by the department Maritime Access from the Flemish Government. Both first authors have evenly contributed to the results of this project.

References

Berlamont J., M. Ockenden, Erik. A Toorman and J. Winterwerp. 1993. The characterization of cohesive sediment properties. The characterization of cohesive sediment properties. Coast. Eng. 21:105-128.

Gularte R.C., W.E. Kelly and V.A. Nacci. 1979. Rheological methods for predicting cohesive erosion. p.251-258. In: Proc. 15th Annual Conf. of the Marine Technology Soc., New Orleans, LA.

Huang Z. and A. Huhe. 2009. A laboratory study of rheological properties of mudflows in Hangzhou Bay, China. International Journal of Sediment Research 24:409-423.

Factors affecting the rheological characteristics of mud

Pang Qixiu and Ruibo Zhang

Tianjin Research Institute for Water Transport Engineering, Key Laboratory of Engineering sediment of Ministry of Transport, Tianjin 300456, P.R. China
E-mail: panqixiu@163.com

Introduction

The results of rheological tests from different researchers are quite different. The factors affecting the rheological characteristics include the density, particle size, and temperature, salinity. Moreover, the methods of test and analysis are also important factors to the difference, for example, the shear mode, the waiting time after the sample being inputted the rheometer, and rheological model as well. It is difficult to analyse the true reasons of the difference, and therefore, it is necessary to conduct rheological tests with the same methods and conditions on sediment samples collected from different ports.

Methodology

Equipment

Tests were conducted in laboratory using a rheometer with type of R/S-cc manufactured by Brookfield Company in America.

Sediment sample

Sediment was collected from different ports in China, including Tianjin south port, Lianyun channel and Xuwei channel of Lianyungang port, Yangtze Estuary channel in dry season and flooding season, Dachan Bay port area of Shenzhen port, Nansha port area of Guangzhou port, Zhuhai Power Plant port, Taishan Power Plant port. The average particle sizes of the sediment (D50) are smaller than 0.01mm, and the clay contents are larger than 30%, except for the sediment from Yangtze Estuary in dry season which average particle size is about 0.03mm.

Tests for the effect of temperature

In the tests for the effect of temperature, the sediment collected from Lianyun channel of Lianyungang port was prepared to be different density sample. The temperature of the samples in tests are controlled constantly with 2, 10, 20 and 30 °C.

Rheological model

Bingham rheological model is selected to represent the rheological characteristics, and the formula is as followed:

$$\tau = \tau_B + \mu\dot{\gamma} \quad \tau > \tau_B \quad (1)$$

where, τ_B is the Bingham stress, and μ is the viscous parameter, and $\dot{\gamma}$ is the shear rate.

Results and conclusions

The Bingham model can be employed to represent the rheological characteristics of mud in most muddy ports of China. Fig. 1 is the relation of shear stresses and shear rates with different densities of mud, showing that the shear stress increases with the shear rate. And in range of high shear stress rates, namely larger than $10s^{-1}$, the Bingham mode is properly satisfied for the data.

The density of mud is the main factor affecting the Bingham stress. Fig. 2 shows the Bingham stresses of different densities of mud sample collected from different ports. The curves of Bingham stresses are not overlapping well, meaning that the differences of rheological characteristics are large for mud from different ports. The differences of particle size and the content of clay are the main reasons.

The effect of temperature on the rheological characteristics is not too significant, as illustrated in Fig. 3, while it is a little different in the range of high shear rates with different temperature.

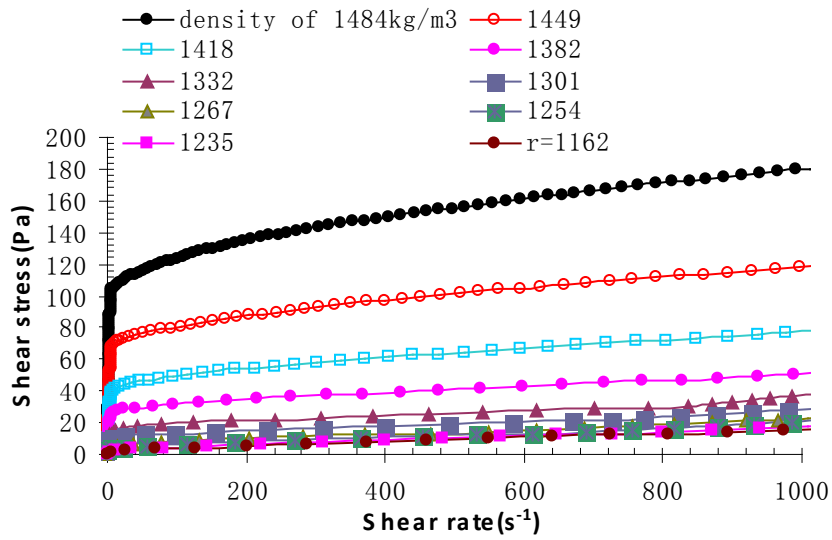


Fig. 1. Relations of shear stresses and shear rates for different densities of mud sample.

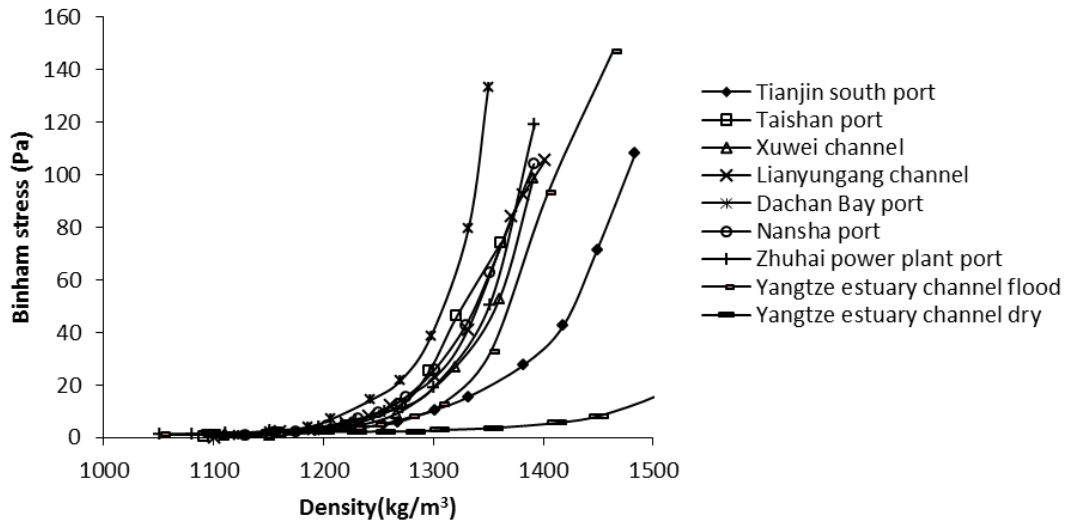


Fig. 2. Bingham stresses of different densities of mud sample collected from different ports.

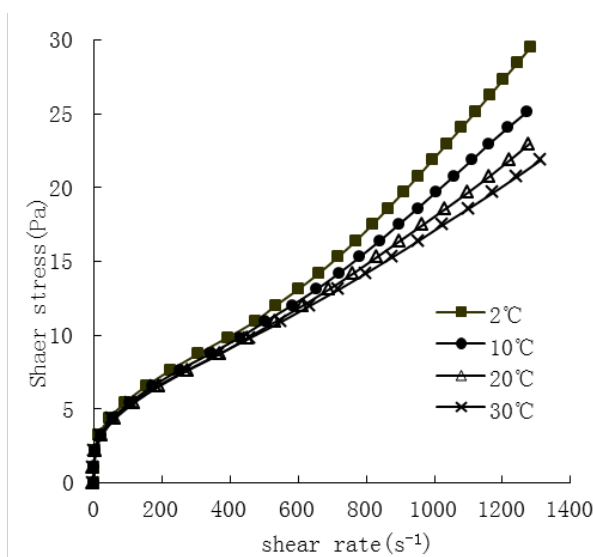


Fig. 3. Effect of temperature on the rheological characteristics of mud with density of 1200kg/m³.

References

- Bai Y.C., C.O. Ng, H.T. Shen and S.Y. Wang. 2002. Rheological properties and incipient motion of cohesive sediment in the Haihe Estuary of China. *China Ocean Engineering* 16:483-498.
- Chou Hsienter. 1989. Rheological response of cohesive sediments to water waves. PhD. Dissertation, University of California.
- Zhenhua Huang and Aode Huhe. 2010. Laboratory study of rheological properties of mudflows in Hangzhou Bay, China. *International Journal of Sediment Research*.

Measuring mud properties with a tuning-forks device

Pedocchi Francisco¹, Valentina Groppo¹, Rodrigo Mosquera¹, Marcos Gallo² and Susana Vinzón²

¹ Instituto de Mecánica de los Fluidos e Ingeniería Ambiental, Facultad de Ingeniería, Universidad de la República, Uruguay
E-mail: kiko@fing.edu.uy

² Área de Engenharia Costeira & Oceanografia, Universidad Federal de Rio de Janeiro, Brasil

The use of tuning forks for measuring and estimating mud properties appears as a very promising alternative to other available technologies. However, the physical principles governing their operation remain to be fully documented. In this work we present a theory that explains the response of an externally forced tuning fork when vibrating inside fluid mud.

Introduction

Following PIANC (2014) the nautical bottom is defined as ‘the level where physical characteristics of the bottom reach a critical limit beyond which contact with the ship’s keel causes either damage or unacceptable effects on controllability and manoeuvrability’. If the bed is composed of cohesive sediments the transition from water to a consistent bed is progressive and diffuse, making the above definition ambiguous. This progressive change, from water to sediment, complicates the interpretation of sonar returns, as the acoustic return depends on both the sound frequency and the density gradient. It is therefore necessary to use intrusive techniques, which allow for direct contact of the measuring device with the mud, in order to determine its properties (density, shear strength, yield strength, viscosity). The RheoTune developed by Stema Survey Services, the Netherlands (Stema, 2013) is based on the tuning-fork technology. The authors have used the RheoTune during nautical bottom surveys in the Rio de la Plata and Amazon River.

Theory

The tuning fork tine oscillation is forced with an adjustable frequency by a piezoelectric element placed on its base, while the tine motion/deformation is measured by another piezoelectric element. The instrument forcing frequency ω is adjusted in order to produce a given phase shift between the forcing and the tine displacement.

Generalizing the results of Allwright (2002), the tine motion can be represented as a forced oscillator moving with a frequency ω

$$F = -M_0\omega^2 x - \rho V_0\omega^2 x + B_0 i\omega x + (1-\alpha)(i\omega)^{3/2} \sqrt{\mu\rho} A_0 x + K_0 x + \alpha A_0 k x . \quad (1)$$

Here F is the amplitude of the external forcing $F \exp(i\omega t)$; x is the complex amplitude of the sensed displacement $x \exp(i\omega t)$, with i the complex unit and t the time; M_0 , V_0 , B_0 , K_0 and A_0 are the mass, volume, damping, elasticity, and surface area of the tuning-fork; ρ , μ , and k represent the density, viscosity, and elasticity of the mud; α is a parameter that may take any value between 0 and 1, and represents the type of response of the mud. If $\alpha=0$ the mud is behaving as a viscous fluid, if $\alpha=1$ the mud is behaving as an elastic material, while values of α between 0 and 1 represent that a part of the mud $(1-\alpha)$ that has a viscous behavior and the rest (α) that has an elastic behavior.

It is possible to adjust the frequency of the external forcing to a value ω_B such that the forcing is $3/4\pi$ ahead of the tine displacement, in other words, in phase with the mud viscous damping. This gives equations for the frequency ω_B and modulus $A_B = |x/F|$ of the displacement.

$$\omega_B = \frac{B_0 + \sqrt{B_0^2 + 4(M_0 + \rho V_0)(K_0 + \alpha k A_0)}}{2(M_0 + \rho V_0)}, \quad A_B = \left[\sqrt{2} B_0 \omega_B + (1-\alpha) \omega_B^{3/2} \sqrt{\mu\rho} A_0 \right]^{-1} . \quad (2)$$

Note that ω_B depends on the elastic response of the mud $(\alpha k A_0)$, and A_B depends on the mud viscosity, density, and elasticity both explicitly and implicitly through ω_B .

Results

The values of ω_B and A_B recorded as the tuning-fork moves inside a uniform mud with a particular density, viscosity and elasticity, but under different strains states (represented by different values of α), may be used to calibrate the tuning-fork response (Fig. 1). The field recorded pairs of ω_B and A_B values can be used to determine the mud density.

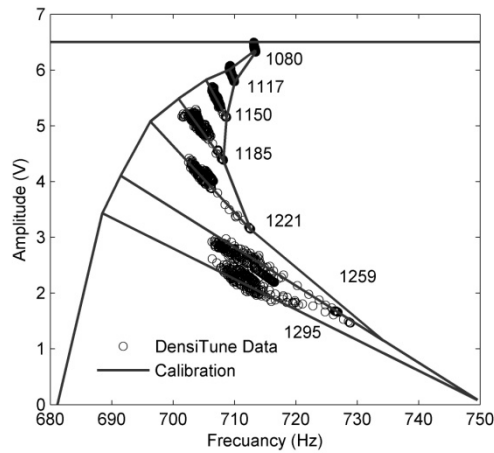


Fig. 1. RheoTune calibration diagram, numbers refer to densities in kg/m³.

Discussion

Equation (2) for A_g shows that it is possible to detect the location of the nautical bottom from the tuning-fork raw amplitude readings as it would be strongly reduced when the instrument penetrates into the bed, and the density and viscosity rapidly increase. In the above result a viscoelastic response of the mud has been assumed which certainly is an oversimplification. It is also clear that the mud properties measured by the tuning-fork correspond to the mud directly surrounding the tine. Mud is actually a two phase material (or three if gas is present), since the tine vibration frequency is on the order of 1 kHz, the effect of the water compressibility and permeability may affect the tuning-fork response as the water can flow in the pores inside fine sediment matrix.

Conclusions

The above results showed that the tuning-fork should be calibrated with local samples of the mud as little disturbed as possible, and if possible, dilution or drying of the samples used for calibration should be avoided. Additional theoretical developments, not included here, showed that it is possible to directly obtain an estimation of the mud viscosity from the tuning fork calibration procedure.

References

- Allwright D. 2002. The vibrating tuning fork fluid density tool. Report, Smith Institute <http://www.smithinst.ac.uk/Projects/ESGI43/ESGI43-NanGall/index.html>.
- PIANC-IAPH. 2014. Harbour Approach Channels Design Guidelines. Report 121, Maritime Navigation Commission, PIANC Secrétariat Général. Brussels, Belgium.
- Stema-Systems 2013. <http://www.stema-systems.nl/>

High resolution bed level changes on an intertidal mudflat

Qin Zhu¹, Bram C. van Prooijen² and Cynthia D. Maan²

¹ State Key Laboratory of Estuarine and Coastal Research
East China Normal University, Shanghai 200062, P.R. China
E-mail: zhugin0612@msn.cn

² Department of Hydraulic Engineering
Delft University of Technology, 2628 CN Delft, the Netherlands

Introduction

Intertidal flats play a key role in estuarine ecosystems and are important buffers against coastal flooding. Many intertidal flats (e.g. the Westerschelde, and Waddenzee in the Netherlands and the Yangtze Estuary in China) are therefore protected. The flats are however threatened by anthropogenic interventions (like deepening of the navigation channels) and by climate change (like accelerated sea level rise). The morphological evolution of the flats is however still difficult to predict, as the interaction between forcings (tides, waves, wind-driven flow) and sediment response (erosion and deposition rates) are not fully understood.

To improve the insights on the sediment processes on muddy intertidal flats a joint campaign between TU Delft and SKLEC is set up on a flat in the Westerschelde (the Netherlands). In this paper, we show the response of the flat to mild conditions and strong wind conditions. Furthermore, the spatial variation of the response is analysed.

Study area and experimental setup

We consider the Kapellebank, a semi-enclosed tidal flat along the north bank of the Westerschelde Estuary in the Netherlands. It faces a channel on the south. The tidal wave is semi-diurnal, with a mean tidal range around 4.5m, indicating a macrotidal flat. The bed slope of the flat is mild (ca. 3/1000). The bed sediment is cohesive (clay component over 8%, around 20%) with a median grain size less than 50 μ m. Parts of the flat were covered with diatoms, forming a biofilm.

A range of measurements with *in situ* instruments on frames, tracking path lines with GPS-drifters and visualization by areal pictures made with a UAV (drone). In this paper, we focus on the results of the instruments at the three frames (A1–A3, see Fig. 1) along a cross shore transect. At these frames, waves, currents, SSC, and bed level changes were measured. Wave height and period were obtained by high frequent pressures sampled by wave-logger every 20min. Current velocity profiles within 50cm above the bed was measured by downward looking ADCP (Nortek 2.0MHz HR-Profiler). Turbidity, for being calibrated into SSC, was recorded by OBS-3+, on the height(s) of 15 and/or 30cm above the bed. An ADV (Nortek 6.0MHz Vector) was used to obtain both turbulent velocities at 15cm above the bed, and bed level changes. This setup provides to study the spatial variation over the flat and to analyse variation in time.

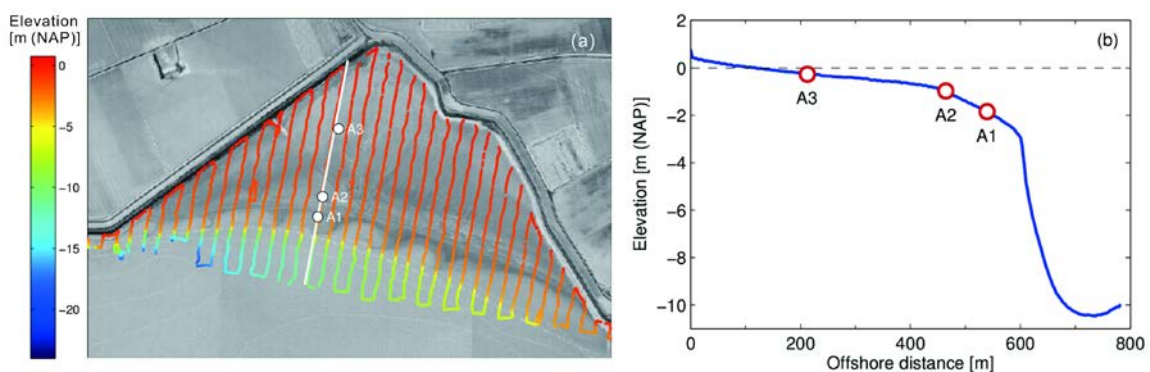


Fig. 1. (a) Areal picture of Kapellebank, the Netherlands, shows the measured bathymetry and observation sites A1–A3. Profile shape along the white line in panel (a) is presented in panel (b).

Results and conclusions

A 23-day record, covering more than a spring-neap cycle, of water level variation, orbital velocities and bed level changes is shown in Fig. 2. Increased wind speeds were found in the period between May 6 and May 13. This is directly affecting the orbital velocity at frame A, as shown in Fig. 2b. During the strong wind period, wave heights increase and oscillate in time by the tidal variation of the water depth. Maximum orbital velocities are found during shallow water as a consequence of smaller ratios of wave length over water depth and as a consequence of shoaling. Significant bed level degradation events are found during shallow water depth periods at A1, see Fig. 1d. The bed level lowered more than 2cm during the low water at the 11th of May. At this low water period, the bed at frame A did not fall dry, implying a relatively long period of severe conditions. After the strong wind period, the bed level almost recovered within a period 10 days.

The sites at A2 and A3 do not show a similar significant response. Almost no bed level variation was found during the strong wind period. The difference between site A1 on the one hand and sites A2 and A3 on the other hand can be explained by the exposure to waves at low tide. Locations A2 and A3 are not flooded during low tide, while A1 is flooded during the full tidal cycle during neap tide. A similar strong wind during spring tide would have had much less impact on site A1, as it would have fallen dry during low tide.

Furthermore, it is noticed that significant sediment transport takes place during shallow water conditions. Not only high concentrations occur, but also significant bed level changes. It is concluded that the sensitivity to erosion is maximum at the elevation just below the low water level. These conditions, however, are generally not well simulated by numerical models.

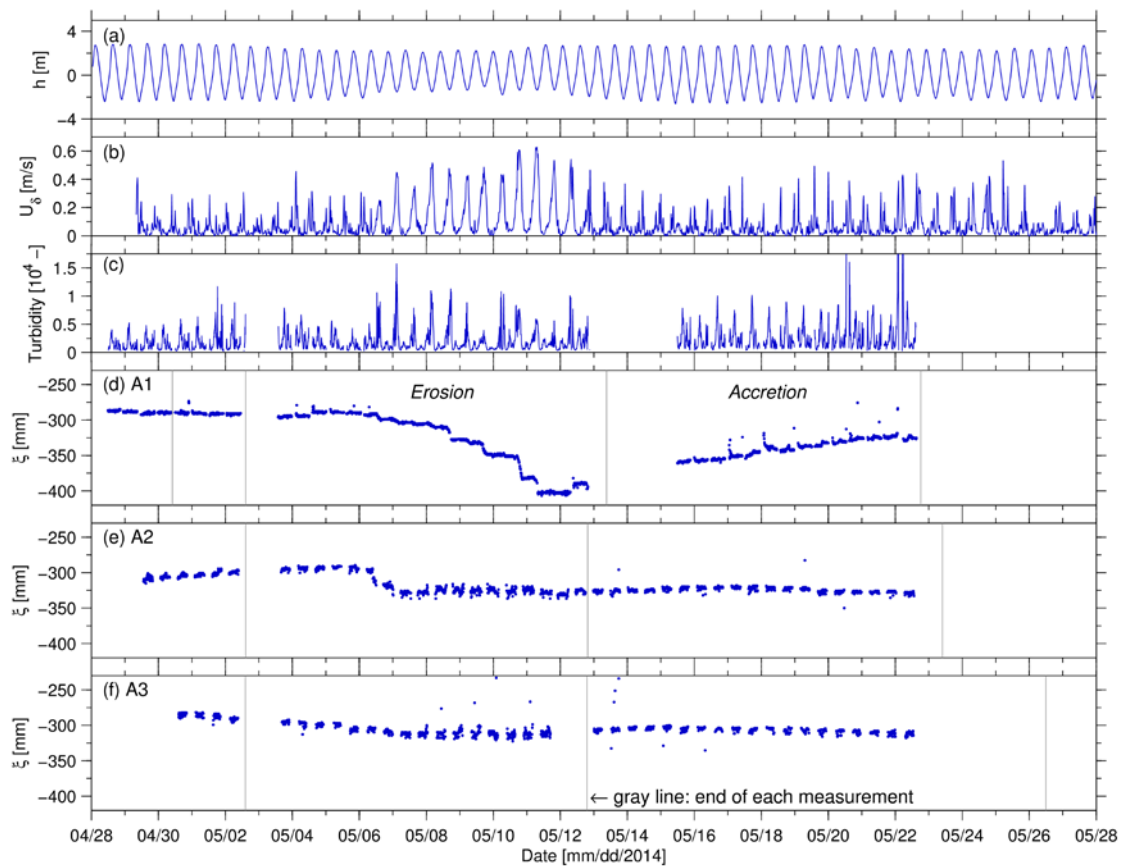


Fig. 3. Time series of (a) water level (h) gauged at Hansweert, which is close to our study area, by Rijkswaterstaat, the Netherlands, (b) significant wave height (H_s) at site A1, (c) turbidity obtained by OBS attached on Vector, and (d)–(f) bed level changes measured by ADV at site A1, A2 and A3. Negative ξ in panels (c)–(e) means the distance between ADV transmitter and bed surface.

Traces of sediment origin in rheological behaviour of mud samples taken from the North-Western Persian Gulf

Razavi Arab Azadeh¹, S. Abbas Haghshenas¹, Farzin Samsami³ and Michael John Risk²

¹ Institute of Geophysics, University of Tehran
North Kargar Ave., Tehran PC 1439951113, Iran
E-mail: sahaghshenas@ut.ac.ir and azadeh_razavi_1981@yahoo.com

² School of Geography and Geology, McMaster University
N0G 1R0, Canada

³ Department of Civil Engineering, West Tehran Branch, Islamic Azad University
Tehran, Iran

Introduction

The Persian Gulf is the text book example of sediments which have directly precipitated from the water. The north-western part of this important body of water is covered with mud deposits which were believed to be mainly originating from the Arvand River catchment area. However, recent findings show that precipitated aragonite needle mud forms a considerable portion of fine sediments in the mentioned area. This study aims to correlate sediment origin, mineralogy and physical properties to the general rheological behaviour of mud deposits in the study area.

Sediment origin in the North-West Persian Gulf

Mud deposits up to 20 metres thickness are observed at the very shallow coasts extending from Shah-Abdollah and Hendijan Fishery Ports in the east towards the Arvand River mouth and surrounding area of Kuwait Bay in the west. Aragonite needles and oolites are found in certain locations in the north-western part of the Persian Gulf. Oolites are a chemically-precipitated type of sediment, getting their name from the fact that they are well-rounded and resemble little eggs ("ooids"). True aragonite needle muds are another chemically-precipitated type of sediment whose aggregation may result in oolite formation through a complicated process. These types of sediments are found in warm, shallow, saline, agitated water, usually where strong currents exist. They are chemically-precipitated from water that becomes oversaturated with CaCO₃. The solubility of carbonate in warm water is already low, and wave agitation blows off more CO₂. This leads to an increase in pH. Small particles are picked up from the bottom, and carried up into surface waters of high pH. Carbonate precipitates around these particles as coatings of aragonite. Tidal deltas in warm waters provide ideal environments in which a grain can be moved periodically and still stay within the same depositional setting for a sufficiently long period of time to develop a thick oolitic coating. Typical habitats for oolites and aragonite needle muds in the modern oceans are the Bahamas, Shark Bay, and the Persian Gulf. There is very limited information on the rate of accumulation of these sediments, but the shoals of the Bahama Banks are presently accreting at the rate of 1mm/year (or 1m/1,000 years). Little has been published on the carbonate mud and oolites of the Iranian coastline.

The true aragonite needle muds are too fine grained to be studied with a light microscope. Hence, Fig. 1 shows photographs of mud samples from nearshore and offshore Hendijan Port taken by a scanning electron microscope (SEM). As it is obvious, the sediment texture consists of ordinary clay flakes together with a considerable amount of aragonite needle mud. Here the aragonite appears as needles with a length/breadth ratio of 5/1 to 8/1. The dimension of the figured needles vary from 0.1 × 0.5μ to 0.2 × 1.7μ. The aragonite fraction in the sediment constituents is estimated to be 40 and 60 percent in the nearshore and offshore samples, while the water content ratio of sediment mixture is measured 100 and 80 percent, respectively. Primary zeta potential measurements show incipient instability in the sediment suspension and high potential of aggregation and flocculation.

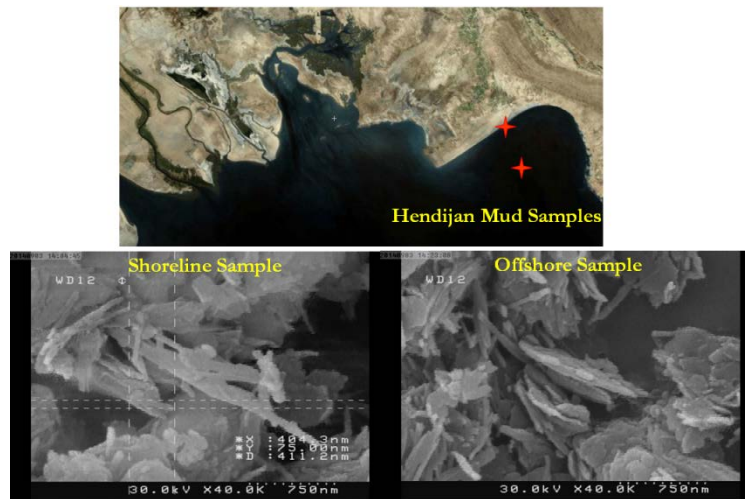


Fig. 1. SEM photographs of mud samples from nearshore and offshore Hendijan Port.

Rheometry investigations

The selected samples from the Hendijan Coast of the Persian Gulf were analysed using an Anton Paar Physica MCR300 rheometer capable of performing oscillatory tests. Concentric cylinder geometries were used as the measuring system at a constant temperature of 25 °C. The oscillatory tests can be operated in terms of controlled shear deformation (CSD) or controlled shear stress (CSS) in the form of sinusoidal functions. To determine the flow stress from the oscillatory tests, the amplitude sweeps tests (keeping the frequency at a constant value; usually the angular frequency sets as 10rad/s) were performed in controlled-strain deformation ramp mode with a strain range of 0.01 to 100 (%). The measured results are storage modulus G' and loss modulus G'' . At low stress amplitudes both G' and G'' have nearly constant values and almost parallel straight lines (linear viscoelastic zone). We note that $G' > G''$ implies a gel-like character of the mud in the respective stress amplitude range. After the crossover point at $G' = G''$, in the stress range in which $G'' > G'$ the behaviour is that of a liquid (Mehta *et al.*, 2014). The flow stress point (Metzger, 2006). Fig. 2 shows sample results of the natural Hendijan mud with two different water contents, relevant to nearshore and offshore samples.

tf is the stress

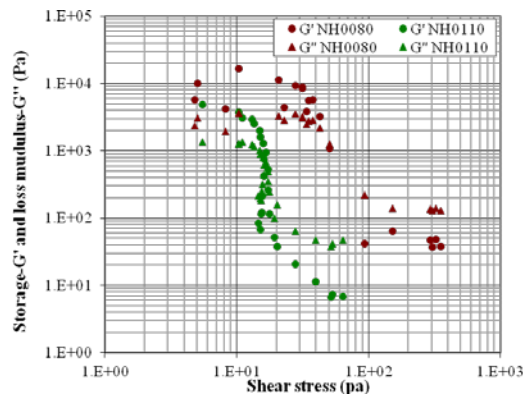


Fig. 2. Sample measured results from oscillatory test.

Summary

A considerable amount of precipitated aragonite needle mud is observed in sediment constituents over the shallow coasts of the North-Western Persian Gulf. This carbonate fraction seems to play an important role in mud rheological behaviour, something which is tried to be investigated in this study.

References

- Mehta A., F. Samsami, Y. Khare and C. Sahin. 2014. Fluid mud properties in nautical depth estimation. *J. Waterway, Port, Coastal, Ocean Eng.* 140(2):210–222.
- Metzger T.G. 2006. *The rheology handbook: for users of rotational and oscillatory rheometers.* Vincentz network GmbH & Co. KG, Hannover, Germany.

Numerical simulation of sediment transport in shallow-water flows

Rehman Khawar¹ and Cho Yong-Sik^{2*}

¹ Department of Civil and Environmental Engineering
Hanyang University, 222 Wangsimni-ro, Seongdong-gu, Seoul 133-791, Korea
E-mail: khawarrehman@hanyang.ac.kr

² Department of Civil and Environmental Engineering
Hanyang University, 222 Wangsimni-ro, Seongdong-gu, Seoul 133-791, Korea
*Corresponding author
E-mail: ysc59@hanyang.ac.kr

A numerical approximation for modelling sediment routing in gradually and rapidly varying flows is presented in this study. A coupled approach is adopted to solve the Saint Venant and sediment transport equations that are able to model influence of flow on sediment transport and bed evolution. The effects of both suspended load and bed load are considered in the numerical scheme, as the former plays an important role in bed evolution under rapidly varying flows. A Godunov-type finite volume technique is used to solve the system of coupled equations. The fluxes through cell interfaces which carry the flow information are computed by Harten-Lax-van Leer-Contact (HLLC) approximate Riemann solver method at each time step, which has the ability to capture shocks resulting from discontinuities. A Second-order temporal and spatial accuracy is confirmed by employing Henn's method and high-order reconstruction technique with limited gradient, respectively. The C-property of the model is satisfied by maintaining well-balanced condition between conservative and non-conservative terms to preserve stability of the numerical scheme. The computational domain is discretized by triangular grids which facilitates local grid refinement in case of abrupt bed discontinuities and obstacles in flow path. Lastly, the numerical scheme is applied to some benchmark test cases to evaluate its adaptability and results are compared with previous studies.

Keywords

Sediment-transport; Finite volume method; Approximate Riemann Solver; Bed dynamics; Hydrodynamics.

Sensitivity analysis for suspended load formulae in sediment transport

Ruiz Gerardo

Facultad de Ingeniería, Universidad Nacional Autónoma de México
Circuito escolar s/n, Edificio U, Ciudad Universitaria, 04510, México, D.F., México
E-mail: gerardrui@hotmail.com

A phenomenon of considerable interest in river mechanics is the suspended sediment that differs from bed load sediment in that it may be diffused throughout the vertical column of fluid. The suspended sediment transport models are often based on semi-empirical formulae that relate to physical properties. In engineering applications, error in these physical properties affects the accuracy of the total sediment fluxes. The present analysis quantifies error propagation from the physical properties to the sediment transport, determines which one controls the errors, and provides the relative strengths, weaknesses and limitations of eight formulae (Rouse, 1937; Lane, 1941; Hunt, 1954; Zagustin, 1968; Van Rijn, 1984; Ni, 1991; Umeyama, 1992 and Wright, 2004). Sensitivity analysis is well recognized as being an important aspect of the responsible use of sediment transport and can help in identifying critical control points, prioritizing additional data collection or research, and verifying and validating a model. Uncertainty is individually tested to see the influence of the physical properties with the method of propagation of errors and the Monte Carlo method for comparison and validation and reviews a range of methods for sensitivity analysis in a number of relations for estimating the entrainment rate of sediment into suspension. The use of global variance-based sensitivity analysis is shown to be more general in its applicability and in its capacity to reflect nonlinear processes and the effects of interactions among variables. The combined effect of errors in all the physical properties is then compared to an estimate of the errors due to the intrinsic limitations of the formulae.

References

- Rouse H. 1937. Modern conceptions of the mechanics of turbulence. *Transactions American Society of Civil Engineering* 102:463-505.
- Lane W. and A. Kalinske. 1941. Engineering calculations of suspended sediment. *Transactions American Geophysical Union* 20(3):603-607.
- Hunt J. 1954. The turbulent transport of suspended sediment in open channels. *Proceedings of the Royal Society* 224(1158):322-335.
- Zagustin K. 1968. Sediment distribution in turbulent flow. *Journal of Hydraulic Research* 6(2):163-172.
- Van Rijn C. 1984. Sediment transport, part II: suspended load transport. *Journal of Hydraulic Engineering* 110(11):1613-1641.
- Ni R. and Q. Wang 1991. Vertical sediment distribution. *Journal of Hydraulic Engineering* 117(9): 1184-1194.
- Umeyama M. 1992. Vertical distribution of suspended sediment in uniform open-channel flow. *Journal of Hydraulic Engineering* 118(6):936-941.
- Wright S. and G. Parker 2004. Flow resistance and suspended load in sand-bed rivers: simplified stratification model. *Journal of Hydraulic Engineering* 130(8):796-805.

Experimental investigation of flocculation in mixed sediments

Samsami Farzin, Alan Cuthbertson and Olugbenga Ibikunle

Infrastructure and Society, Geoscience, School of Energy
Heriot-Watt University, William Arrol Building, Edinburgh, EH14 4AS, UK
E-mail: a.cuthbertson@hw.ac.uk, f.samsami@hw.ac.uk,

Introduction

Many estuaries and near-shore coastal regions have bed sediments consisting of mixtures of cohesive mud and non-cohesive sands. Whilst extensive studies have been conducted on transport processes associated with sand- or mud-only sediments, there remains limited knowledge on the physical behaviour of sand-mud mixtures in suspension. Due to important differences that exist in cohesive and non-cohesive sediment behaviour, it is essential to gain improved understanding of small-scale processes (e.g. flocculation and settling) associated with mixed sediments, many of which are known to have a strong influence on larger scale sediment transport and morphodynamic evolution. In relation to flocculation, particle aggregation and disaggregation processes result from complex interactions which include inter-particle collisions due to Brownian motion, turbulent shear and differential settling (Winterwerp, 2002). These flocculation processes can vary significantly, both spatially and temporally, depending on factors such as wave/tidal-induced turbulent stresses and suspended particulate matter (SPM) concentration and composition (i.e. clay, silt, and organic matter). This variability often results in continually-changing floc properties (e.g. floc size and density), and hence sediment settling fluxes and suspended sediment load. Previous research in this field has included studies of the flocculation properties for sand-mud mixtures under so-called *equilibrium* and *non-equilibrium* conditions (e.g. Cuthbertson *et al.*, 2010; Manning *et al.*, 2011). However, to-date, there have been very few systematic studies conducted to determine the parametric influences on flocculation processes for sand-mud mixtures. The current study presents results from a series of settling column experiments within which the temporal variability in flocculation behaviour is examined for different sand-mud mixtures under controlled zero-mean-shear turbulent flow conditions generated within the column. Ongoing work to establish the important linkages between fluid-sediment interactions within mixed sediment suspensions through development and application of a population balance modelling approach is also discussed.

Settling column experiments

The experimental study was performed in a 2.1m long by 0.25m diameter settling column (Fig. 1). Controlled hydrodynamic forcing conditions (i.e. near-isotropic, zero-mean-shear turbulence) were generated in the column through the oscillation of a fixed, regular array of grids. Pure kaolin clay ($D_{50} = 2\mu\text{m}$) and well-sorted silica sand ($D_{50} = 150\mu\text{m}$) were used to represent the cohesive and non-cohesive sediment fractions, respectively. The sand and clay fractions were added separately to the upper buffer mixing tank of the column using a calibrated vibration (dry) feeder and peristaltic pump dosing system, respectively. Input concentrations for the clay suspension varied between $C_m = 1.2 - 2.4\text{g l}^{-1}$ (at a constant pump feed rate of 5ml s^{-1}), while the sand feed rate ranged from $I_s = 0 - 70\text{mg s}^{-1}$. Non-intrusive measurements of the flocs generated within the column were obtained in the floc viewing chamber (Fig. 1) with a digital CCD Camera and 3.3X macro lens [image resolution 1932×1452 pixels (1 pixel $\equiv 3.78\mu\text{m}$), [see Fig. 2(a)]. Individual flocs were identified and their geometric properties measured using the image analysis software package *ImageJ* [Fig. 2(b) and (c)]. Within each run, the significant $D_{f,sign}$ and maximal $D_{f,95}$ floc sizes were obtained from ensemble averages of the largest 33% and 5% of all identified flocs, respectively. Manual validation of flocs included in the ensemble-averaging procedure ensured that floc were singular (i.e. non-overlapping) and focussed fully in the laser light sheet (i.e. no distortion through blurring). The suspended sediment concentration was measured at the mid-elevation of the main column section and directly below the oscillating grid array using Optical Backscatter (OBS300) sensors. Detailed calibration of these OBS probes was conducted to convert measured NTU values into total suspended sediment (TSS) loads generated for the range of sand-mud mixture compositions tested.

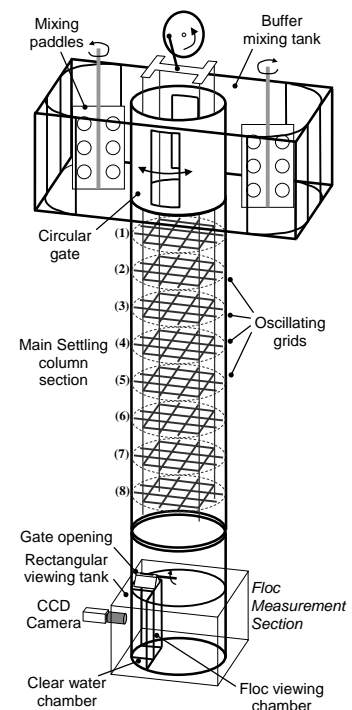


Fig. 1. Schematic of settling column, oscillating grid array and in-situ floc measurement section.

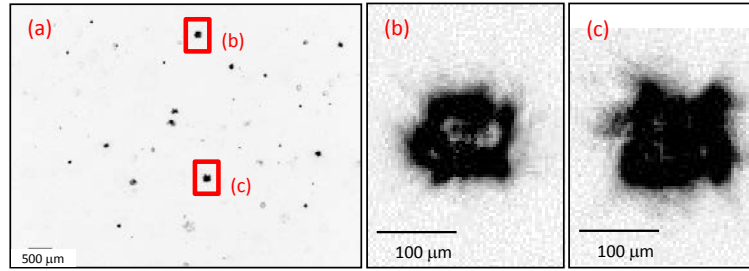


Fig. 2. (a) Image of settling kaolin flocs, (b)(c) enlarged images of individual flocs.

Results and discussion

Fig. 3 shows example time series plots of the total suspended sediment (TSS) variation measured at the two OBS positions, along with corresponding measurements of the significant $D_{f,sign}$ and maximal $D_{f,95}$ floc sizes at specific times (note: error bars on $D_{f,95}$ values represent the standard deviation in floc sizes used in the ensemble averaging). Results typically show that for mud-only runs [i.e. no sand fraction, Figs. 3.(a) and (c)], floc sizes attained are generally larger than those attained for equivalent sand-mud mixture conditions [i.e. equivalent mud concentrations C_m and grid-generated shear rates G , Fig. 3(b) and (d)]. It is interesting to note that, at lower shear rates G , the TSS concentration within the column continues to increase over the duration of the run [Figs. 3.(a) and (b)], whilst it is shown to reach an *equilibrium* concentration under higher G values [i.e. TSS \rightarrow 0.95 g l^{-1} at $t > \sim 275$ min, Fig. 3(c)]. Equivalent floc measurements are shown to indicate a non-linear increase in $D_{f,sign}$ and $D_{f,95}$ floc sizes with these TSS values, particularly noticeable for the sand-mud mixtures [Fig. 3(b) and (d)]. This may be due partly to (i) the temporal lag in response of flocculation processes to changes in TSS levels within the column (i.e. *non-equilibrium* conditions), and (ii) the additional effect of the sand fraction in inhibiting floc growth through differential settling processes and direct particle-floc collisions (Cuthbertson *et al.*, 2010). In this regard, results from the ongoing development and application of a population-balance modelling approach, aimed at simulating the additional floc break-up mechanisms associated with sand-mud mixtures, will also be reported.

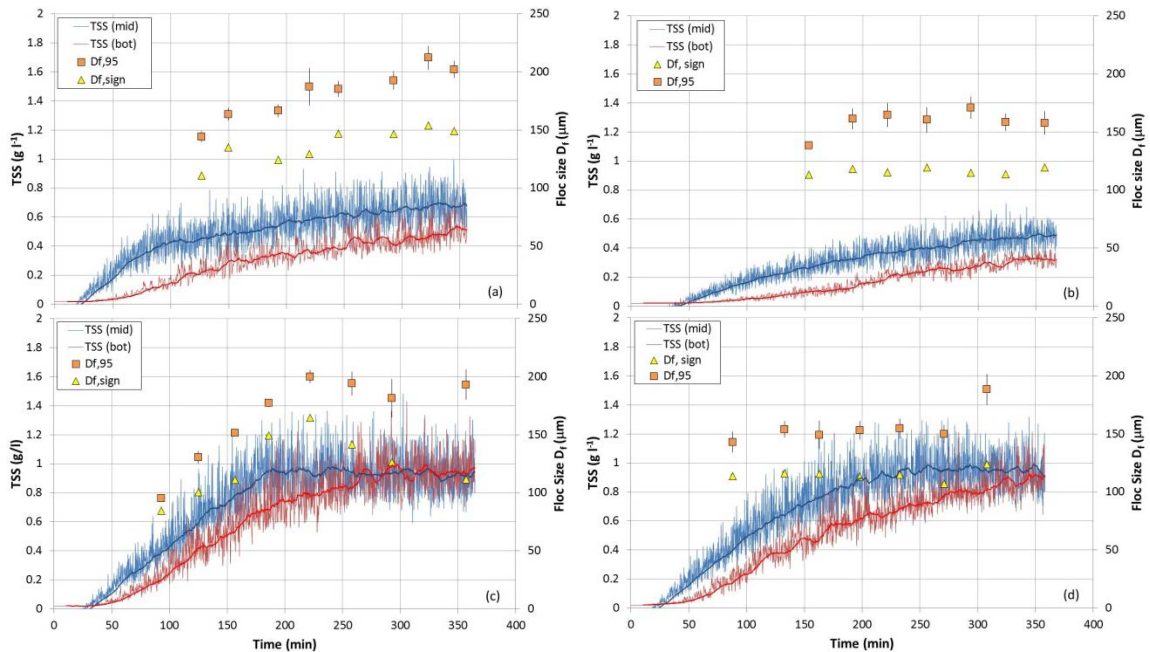


Fig. 3. Time series plots of total suspended sediment (TSS) and measured floc sizes ($D_{f,sign}$ & $D_{f,95}$) for runs with C_m (g l^{-1}): I_s (mg s^{-1}): G (s^{-1}) of (a) 1.8:0:0.81, (b) 1.8:70:0.81, (c) 1.8:0:2.31, (d) 1.8:70:2.31.

References

- Cuthbertson A., P. Dong and P. A. Davies. 2010. Non-equilibrium flocculation characteristics of fine-grained sediments in grid-generated turbulent flow. *Coastal Engineering* 57(4):447-460.
- Manning A.J., J.V. Baugh, J.R. Spearman, E.L. Pidduck and R.J.S. Whitehouse 2011. The settling dynamics of flocculating mud-sand mixtures: Part 1—Empirical algorithm development. *Ocean Dynamics* 61(2-3):311-350.
- Winterwerp J.C. 2002. On the flocculation and settling velocity of estuarine mud. *Continental Shelf Research* 22:1339-1360.

In situ observations of sediment dynamics in Tongzhou Bay, China: in response to wave-current interaction and strong wind forcing

Shao Y.Y.¹, Z.L. Zhu¹ and X.T. Shen²

¹ College of Harbour, Coastal and Offshore Engineering, Hohai University, Nanjing, P.R. China
E-mail: syy@hhu.edu.cn

² Virginia Institute of Marine Science, College of William and Mary, USA

Introduction

Tongzhou Bay connects with the margin of Southern Yellow Sea, China, and is adjacent to the mouth of Changjiang River Estuary (Fig. 1). About 50% of the sediments in the bay are silt and clay particles that originated from the Old Changjiang River and Old Yellow River (Milliman *et al.*, 1986). According to the measurement under the normal weather, the average tidal range in Tongzhou Bay is about 3~4m; the max current velocity in the spring and neap tide are about 1.3m/s and 0.7m/s respectively; the maximum suspended sediment concentration is 1.2g/L; the suspended sediment median size D_{50} is about 0.004~0.016mm; and the bed sediment D_{50} is about 0.02~0.07mm. However, few studies are conducted to illustrate the complex local sediment dynamics under the interaction of waves and currents, especially during the strong wind period. The depth of deep-water channel may change after the period of strong wind. The sediment load during this period may increase dramatically in the harbour and cause severely sudden siltation in the navigation channels. Thus, it has a realistic significance to understand the sediment dynamics under the impacts of wave-current interaction and strong winds, and make it applicable to solve scientific and engineering issues such as sudden siltation in Tongzhou Bay.

Methodology

A quadruped bottom observation system with various instruments (e.g., Nortek ADP, OBS-3A, and LISST-100) will be mounted near the bed of the bay to illustrate the patterns of the bottom sediments under the effects of wave, tidal currents, and strong winds. As shown in Fig. 2, a downward, 1MHz Nortek ADP will be used to find the time-averaged current velocity of the measuring point 120cm above bed. The ADP will record Suspended Sediment Concentrations (SSC) as well by using an OBS-3A (Downing, 1983). The OBS-3A will be calibrated both *in situ* and in the laboratory. The grain-size distributions of suspended sediments will be observed by using a LISST-100 instrument (Type C) (Agrawal and Pottsmith, 2000). In addition, the current velocity profile will be obtained using an upward 600kHz RDI broadband ADCP, with wave gauge assembled to measure the wave height and wave period (Van Haren, 2001). The ADCP also records SSC results using another two OBS-3As. Key parameters that influence sediment dynamics such as bed erodibility and settling velocity will also be estimated from the collected data to understand 'how much sediment is suspended' and "how far that sediment is transported" (Friedrichs *et al.*, 2008).

Results and conclusions

The following results can be expected according to the collected data using this bottom observation system:

- 1) The vertical structure of suspended sediment concentration in response to wave-current interaction and strong wind forcing can be measured with high temporal and spatial resolution.
- 2) The available data can also be processed to find various sediment parameters such as settling velocity and erosion rate that valuable to develop and verify a mathematical model, and even more important, to understand the sediment processes under complex hydrodynamic conditions in Tongzhou Bay.

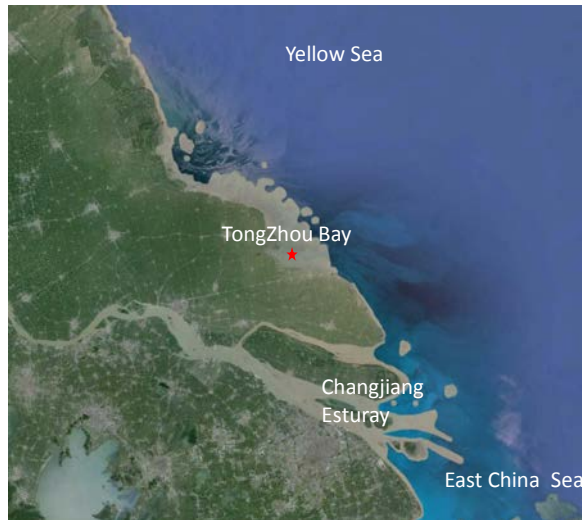


Fig. 1. Map of Tongzhou Bay, China. The location is marked in red pentagram.

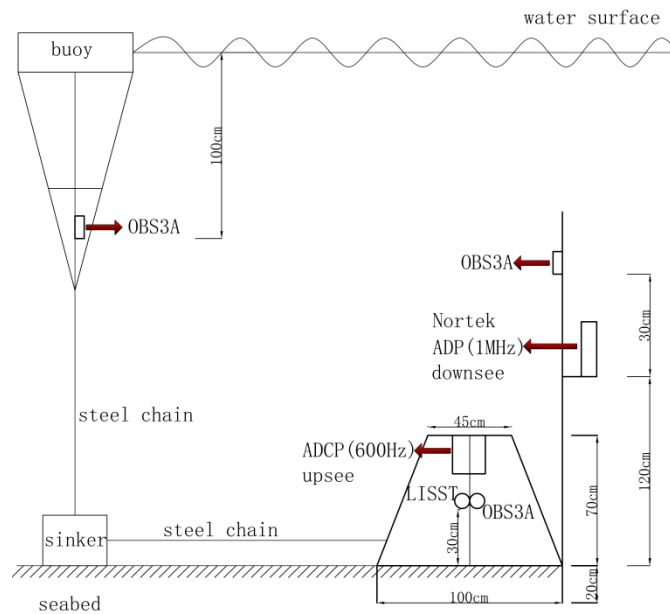


Fig. 2. Bottom observation system with mounted ADCP, ADP, OBS, and LISST.

References

- Agrawal Y.C. and H.C. Pottsmith. 2000. Instruments for particle size and settling velocity observations in sediment transport. *Marine Geology* 168:89-114.
- Downing J.P. 1983. An optical instrument for monitoring suspended particles in ocean and laboratory. p. 199-202. *Proceedings of Oceans' 83* (San Francisco, CA).
- Friedrichs C.T., G.M. Cartwright and P.J. Dickhudt. 2008. Quantifying benthic exchange of fine sediment via continuous, noninvasive, measurements of settling velocity and bed erodibility. *Oceanography* 21:168-172.
- Milliman J.D., F. Li, Y.Y. Zhao, T.M. Zheng and R. Limeburner. 1986. Suspended matter regime in the Yellow Sea. *Progress in Oceanography* 17:215-227.
- Van Haren H. 2001. Estimates of sea level, waves and winds from a bottom-mounted ADCP in a shelf sea. *Journal of Sea Research* 45:1-14.

Mud siltation in the north harbour of Incheon, Korea

Shin Hyun-Jung¹, Guan-hong Lee¹, Soongji Lee¹, Jeong Shin Lee², Tim Dellapenna³, Josh Williams³, Young Taeg Kim⁴ and Ho Kyung Ha¹ and Jae Il Kwon⁵

¹ Department of Oceanography, Inha University, 100 Inharo, Incheon, 402-751, Korea
E-mail: hyunjung@inha.edu

² Department of Environmental Engineering, Kwangwon University, Seoul, Korea

³ Department of Marine Sciences, Texas A&M University, Galveston, TX, 77554, USA

⁴ Ocean Research Division, Korea Hydrographic and Oceanographic Administration, Korea

⁵ Korean Institute of Ocean Science and Technology, Korea

The development of North Harbour was initiated at a macro-tidal flat within the Harbour Complex of Incheon, Korea in 1997 (Fig. 1). To maintain the design depth of -14m below LLW (Low LowWater) from the tidal flat of 2m above LLW, dredging operation has been repeated over the last 13 years within the unbalanced (disequilibrium) North Harbour. In efforts to reduce the siltation within the harbour, this paper attempts to estimate siltation rate and then determine dominant mechanisms for the siltation within the North Harbour. The siltation rate was estimated and then confirmed by the following two independent methods: comparison of available hydrographic sheets and radioisotope analysis of gravity cores. The sedimentation rate varied from 10cm/yr in the far end of the harbour to about 100cm/yr at the entrance (Fig. 2). In order to determine dominant mechanisms for siltation, two ADCPs and two CTDs were deployed at the entrance and the far end of the harbour over a month, and examined flow mechanisms for a harbour basin (Fig. 3). Moreover, the EFDC model simulation indicated that the eddy forms during the flood of spring tide and it appears to be responsible for the high siltation at the harbour entrance (Fig. 4).



Fig. 1. Location map of North Harbour.



Fig. 2. Sedimentation rate in the North Harbour. The rate was evaluated with the core length divided by the year of sedimentation.

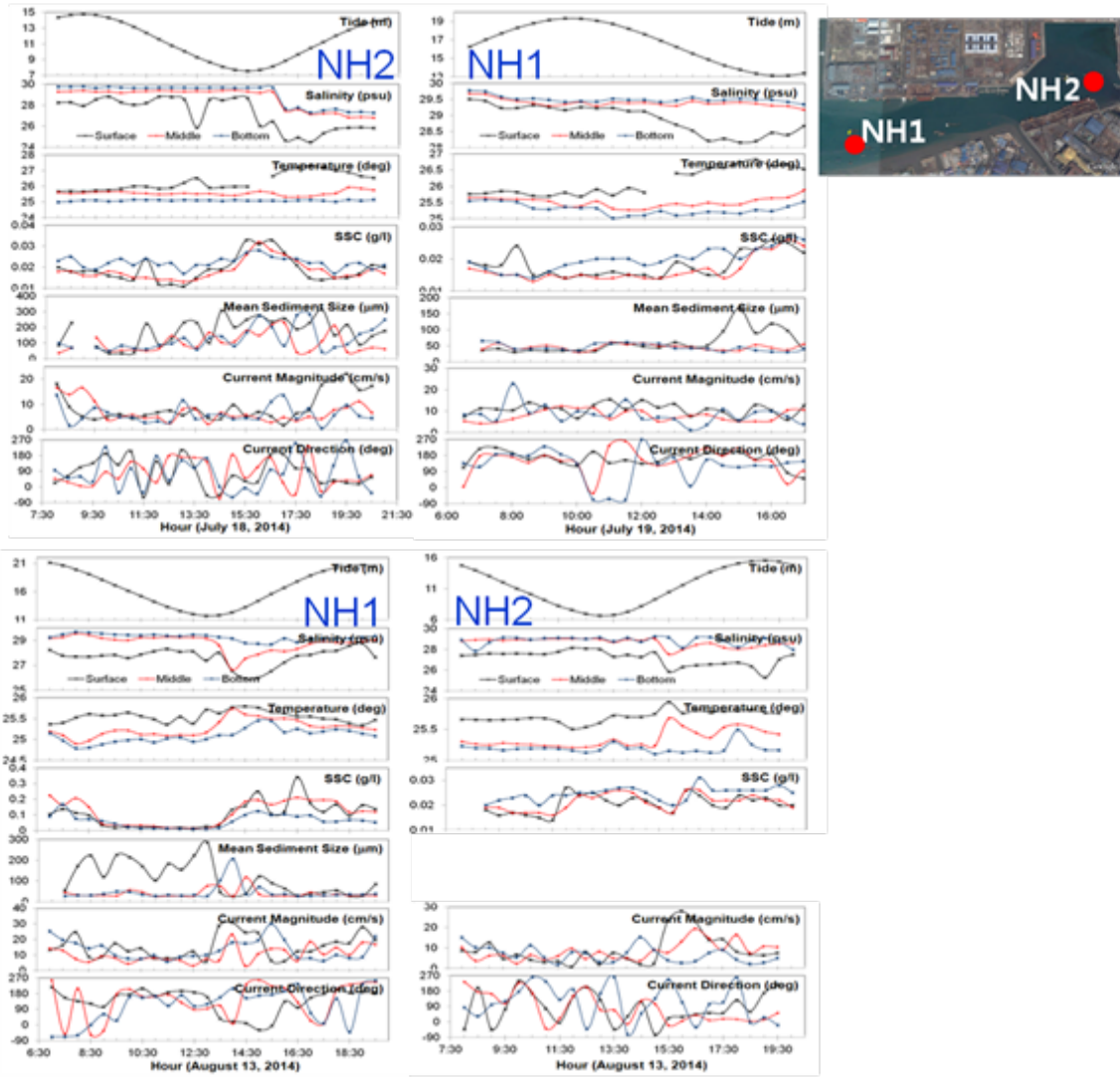


Fig. 3. Time-series of flow and suspended sediment concentration at two stations (NH1 and NH2) during two tidal stages.

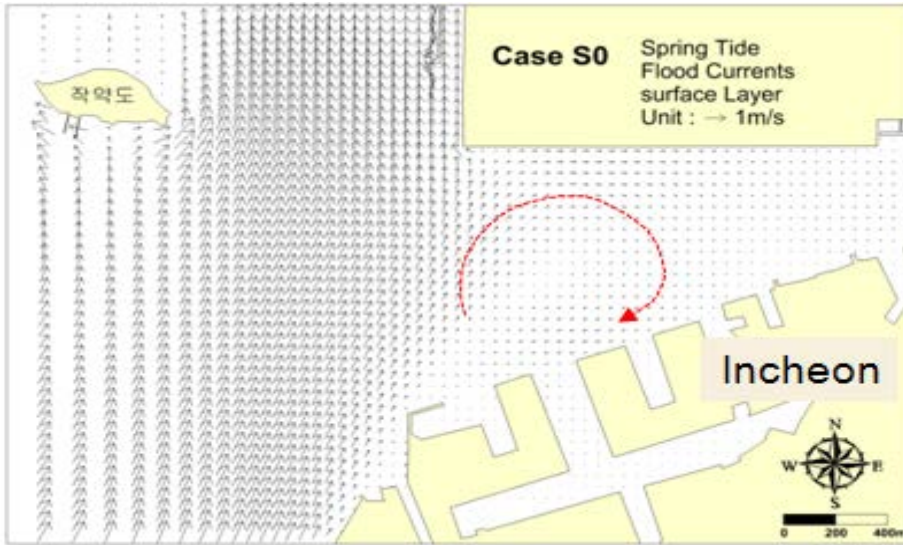


Fig. 4. The model simulation indicates that the eddy is responsible for high siltation at the harbour entrance.

Extreme values of suspended particulate matter concentration and their relation to swell and wind sea in the Belgian coastal zone

Thant Silvy¹, Matthias Baeye², Michael Fettweis², Frederic Francken², Jaak Monbaliu³ and David Van Rooij⁴

¹ MSc student Marine and Lacustrine Sciences and Management, Ghent University
E-mail: Silvy.Thant@gmail.com

² Operational Directorate Natural Environment (OD Nature), Royal Belgian Institute of Natural Sciences (RBINS), Gulledele 100, B-1200 Brussels, Belgium

³ Department of Civil Engineering, Katholieke Universiteit Leuven (KUL), Kasteelpark Arenberg 40, B-3001 Leuven

⁴ Department of Geology and Soil Science, Renard Centre of Marine Geology (RCMG), Ghent University (UGENT), Krijgslaan 281 S8, B-9000 Gent

SPM concentration is one of the key parameters to describe the environmental status, and to evaluate and understand the impact of human activities in both nearshore and offshore areas (Fettweis and Van den Eynde, 2003; Dobrynin *et al.*, 2010). Long-term measurements are needed in order to resolve all variations in SPM concentration. Processes affecting SPM concentration are turbulence, tides, neap-spring cycles, meteorological events, season, and other long-term fluctuations. SPM concentration has been measured since 2005 at two coastal observatory sites in the high-turbidity zone off the Belgian coast. The measurements have been carried out using a benthic tripod that allowed measuring during all meteorological conditions, including storms.

The effects of storms on sediment re-suspension and SPM concentration have been investigated using meteorological and wave data from IVA MDK (afdeling Kust - Meetnet Vlaamse Banken). SPM concentration data from MOW1 (51.358°N, 3.098°E) and Blankenberge (51.329°N, 3.107°E) were estimated using the backscatterance data from a 3MHz acoustic Doppler profiling current meter. Because of the large amount (about 1500 days) of SPM concentration data, a detection algorithm for identifying extreme events was developed. This peak detection function allowed eventually cataloging the extreme SPM concentrations and relating them to storm events and wave system data.

Many events of extreme SPM concentration were detected and were related to one of the following specific extreme weather conditions: 1) NNW storms with high swell activity, 2) SW storms and 3) strong NE winds. The wave systems responsible all have a distinct effect on the degree of erosion of the seafloor bed sediments, the re-suspension of SPM concentration and the upward mixing of SPM through the water column. A NNW storm, characterized by swell waves, will cause a stronger erosion of bed sediments forming a high-concentrated suspension layer of SPM near the bottom in comparison to SW storms. The latter, characterized by wind sea, results in the absence of the benthic suspension layer. However, an enhanced upward mixing of SPM through the water column can be observed in contrast to the situation during NNW storms (Fig. 1). This is a consequence of the occurrence of a hindered re-suspension and settling of SPM due to the increased concentration (saturation concept), leading to a dense suspension and a reduced turbulence energy level. In this case, an upward mixing of SPM is attenuated since this is directly related to turbulent energy levels (Winterwerp, 2002; McAnally *et al.*, 2007; Winterwerp *et al.*, 2002, 2012). The SPM processes in the case of strong NE winds is different. Extreme SPM concentrations are mainly caused by advection of SPM from a more remote SPM source (e.g. Scheldt River).

Additionally, the interaction of different wave systems, together with water depth and sediment type will play an important role in understanding this variation in impact of different extreme weather conditions and the presence of extreme values of SPM concentration.

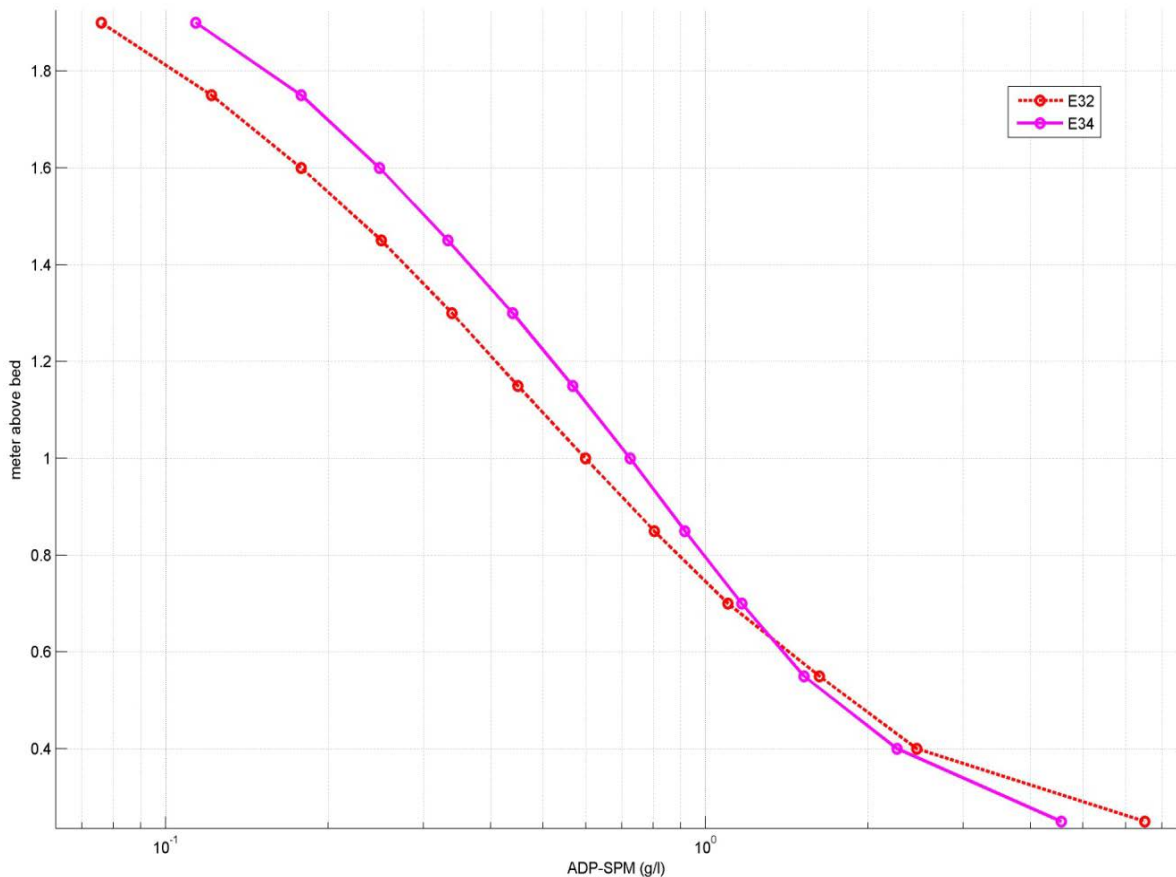


Fig. 4. Vertical profile of the averaged SPM concentration for a NNW storm event (E32, 10/10/2013) and a SW storm event (E34, 28/10/2013). SPM concentrations of E32 are higher at 0.3mab compared to E34, due to the higher erosion capacity of NNW storms. Concentrations at 1.8mab are higher for the SW event that is characterized by enhanced vertical mixing of SPM.

References

- Dobrynin M., G. Gayer, A. Pleskachevsky and H. Günther. 2010. Effect of waves and currents on the dynamics and seasonal variations of suspended particulate matter in the North Sea. *Journal of Marine Systems* 82(1-2):1-20.
- Fettweis M. and D. Van den Eynde. 2003. The mud deposits and the high turbidity in the Belgian-Dutch coastal zone, southern bight of the North Sea. *Continental Shelf Research* 23(7):669-691.
- McAnally W.H., F. Asce, C. Friedrichs, D. Hamilton, E. Hayter, P. Shrestha, H. Rodriguez, A. Sheremet and A. Teeter. 2007. Management of fluid mud in estuaries, bays, and lakes. I: Present state of understanding on character and behavior. *Journal of Hydraulic Engineering* 133(1):9-22.
- Winterwerp J.C. 2002. On the flocculation and settling velocity of estuarine mud. *Continental Shelf Research* 22(9):1339-1360.
- Winterwerp J.C., A.W. Bruens, N. Gratiot, C. Kranenburg, M. Mory and E.A. Toorman. 2002. Dynamics of concentrated benthic suspension layers. *Proc. 6th International Conference on Cohesive Sediment Transport, INTERCOH*. Delft, the Netherlands.
- Winterwerp J.C., G.J. de Boer, G. Greeuw and D.S. van Maren. 2012. Mud-induced wave damping and wave-induced liquefaction. *Coastal Engineering* 64:102-112.

Seasonal variations in SPM and floc characteristics in a hypertidal estuary

Todd David¹, Alex J. Souza² and Colin F. Jago³

¹ HR Wallingford, Howbery Park, Wallingford, Oxfordshire, OX10 8BA, UK
E-mail: d.todd@hrwallingford.com

² National Oceanography Centre, Joseph Proudman Building, 6 Brownlow Street, Liverpool L3 5DA, UK

³ School of Ocean Sciences, Bangor University, Askew Street, Isle of Anglesey LL59 5AB, UK

Suspended particular matter (SPM) is a highly variable and important aspect of estuarine systems. It determines turbidity; impacting water quality, generates benthic fluff, modifies biogeochemical exchanges, and constrains primary productivity. Further, SPM carries biogeochemical components (e.g. carbon, nitrogen), deciding the fates of anthropogenic system inputs. Most SPM is in the form of flocs (aggregates of dead and living organic matter, cohesive inorganic matter, and water) that are easily ruptured and/or may aggregate during sampling. Reliable information on floc behaviour is scarce particularly since floc properties change over tidal (suspension/advection), lunar (spring-neap cycle), and seasonal (storm resuspension and biological production) time scales.

The results of an extensive field campaign in the Dee Estuary (NW United Kingdom) are presented, investigating the fates of SPM. Using data from a combination of acoustics, optics, moored deployments and CTD stations particle characteristics varied across tidal, spring-neap, and seasonal time-scales. This was due to seasonal changes in both river input and levels of biological activity. During winter, turbulence-mediated flocculation and breakup dominated, with particles coming together under quiescent conditions, and breaking up during high turbulence conditions. By contrast, stronger, more shear-resistant flocs were present during summer with increased yield strength providing significant resistance to breakup. These changes significantly altered the W_s of SPM within the estuary, which would affect particle flux as W_s for similar density particles in summer may be much greater during summer than in winter.

The main channel bifurcates 12km seaward of the canalized section into two deep channels, extending into Liverpool Bay. The present study centres on observations from the easternmost channel, the Hilbre Channel, and presents a subset of results from two moored deployments of the STABLEIII benthic tripod and accompanying CTD stations undertaken in February-March and May-June 2009. Stokes' settling velocities were calculated using LISST data, while a modified version of the method of Ramirez-Mendoza *et al.* (2014).

During February-March chlorophyll and biological polysaccharide levels were found to be low and flocculation was controlled by the natural attractive forces between clay particles and levels of turbulent shear. Weak flocs were produced under low turbulence conditions during low and high water and were broken up into smaller microflocs during high turbulence conditions on the flood and ebb tides.

During May-June chlorophyll and biological polysaccharide levels were found to be higher. Two particle populations were identified: population B and population X. Floc size showed no relationship with turbulence for either population. Population B flocs were denser and settled faster than similarly-sized flocs during February-March. These flocs were resuspended on each tide without breakup. Population X particles occurred predominantly during current speeds in excess of 0.4ms^{-1} and did not change density with changing size.

It is thought that the settling velocity of SPM within the estuary was changed by these altering characteristics, emphasising the importance of modelling not only the physical, but the biological aspects of estuarine SPM in order to parameterize particle characteristics correctly. Modelling estuarine SPM with a constant settling velocity, or with a relationship based on shear alone, will be highly inaccurate for time periods in which biological processes have an impact upon SPM particle characteristics.

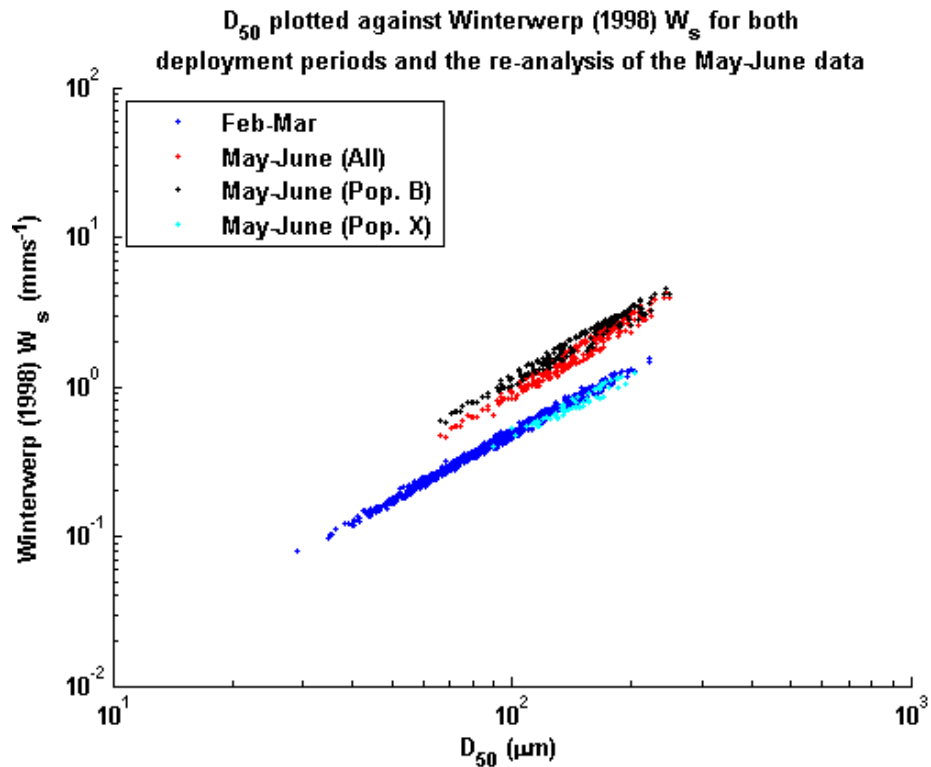


Fig. 1. D_{50} plotted against settling velocities (Winterwerp, 1998) for the February-March data, original May-June analysis and the re-analysed May-June data split into populations B and X.

References

- Ramirez-Mendoza R., A.J. Souza and L.O. Amoudry. 2014. Flocculation in hypertidal estuaries. *Ocean Dynamics*: 1-13.
- Winterwerp J.C. 1998. A simple model for turbulence induced flocculation of cohesive sediment. *Journal of Hydraulic Research* 36:309-326.

Observed residual transport of SPM within a coastal turbidity maximum zone

van der Hout Carola, Rob Witbaard, Theo Gerkema

Royal Netherlands Institute for Sea Research (NIOZ)
PO Box 59, 1790 AB Den Burg (Texel), the Netherlands
E-mail: cvanderhout@gmail.com

Introduction

The research presented here has been done to investigate the residual longshore and cross-shore transport of SPM along the Dutch coast borders of the Southern North Sea. This coast is a transport route of SPM in the order of 7-25Mton/yr (Fettweis *et al.*, 2007). The origin of the material is mainly erosion at the Strait of Dover and sources further upstream. Deposition of the SPM occurs in the ecologically important Wadden Sea and further north beyond the German Bight. As the Dutch coast is heavily engineered, it is important to understand where and how the SPM is transported in order to understand the consequences of the interventions. SPM is retained close to the coast due to the River Rhine discharge, which creates the Rhine ROFI with large longshore and cross-shore salinity differences along the Belgian and Dutch coast (Lacroix *et al.*, 2004; De Boer *et al.*, 2009). Recent spatial observations of the SPM distribution in the nearshore inner shelf have identified a near bottom turbidity maximum zone (TMZ) at 1 - 2km from the coastline. The maximum observed concentrations were about 200mg/l (Van der Hout *et al.*, *subm.*). In the same period a measurement platform was deployed in this TMZ near the village of Egmond amongst others to monitor sediment SPM transport. This time-series will give an estimate of the magnitude of the longshore transport in the TMZ. But also, it will help to identify the longshore and cross-shore processes responsible for the SPM transport.

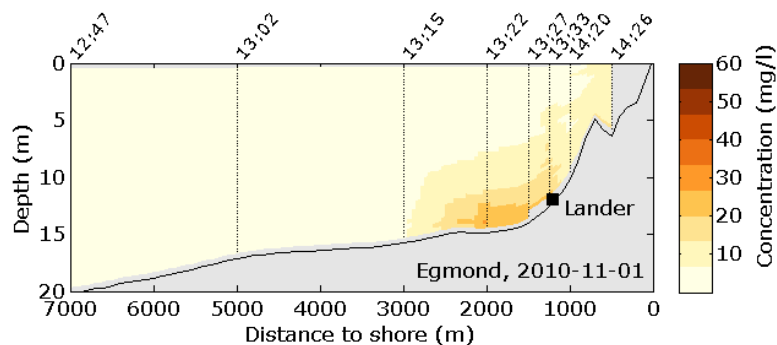


Fig. 1. Location of the lander with reference to one of the spatial observations of the TMZ at the Egmond transect.

Observations

At 1.2 kilometre off the coast of Egmond a bottom lander was placed at a local water depth of 11 metres from March 2011 until November 2012. This location was within the 2.5km wide TMZ, and on the inshore side of the area where a persistent peak concentration of SPM is found (Fig. 1). The lander platform consisted of a triangular aluminium frame, with 2m width and 2m height. Depending on the season, the measurement platform was replaced every three to six weeks and data from the instruments was retrieved. The lander platform was equipped with a series of sensors measuring the following parameters: current velocity, turbulence, temperature, salinity, turbidity (at 4 heights) and fluorescence (at 4 heights). All data was gathered with a frequency interval of 10 minutes. Current velocity was measured at 140cm above the seabed with a Nortek Aquadopp Doppler current meter. At the top of the frame, an upward looking RDI ADCP was placed to measure the current velocity in the upper water column. A Nortek Vektor current meter was mounted at the lander at a height of 30cm above the seabed. The instrument was set to record a burst interval of 2 minutes at 1Hz every 10 minutes. Temperature and salinity were measured with a pumped version of the Seabird SM37 CTD system at 140cm above the seabed. Turbidity and fluorescence were measured optically at four heights above the bottom, i.e. 30, 80, 140 and 200cm, using ALEC Compact-CLW's. All ALEC sensors have been calibrated in the lab over a range of local SPM and chlorophyll-a concentrations.

Results

The SPM concentrations are larger than 1g/l during 1.8% of the time at 0.3 metres above the seabed. At the sensors higher up the water column almost no observations of 1g/l are observed. On average the SPM concentration at 2.0m above the seabed is 2.5 times lower than the SPM concentration at 0.3m above the seabed. The high concentrations occur during storms with TKE larger than 50N/m². A first analysis of the alongshore SPM transport indicates that the transport during storms dominates the residual longshore transport over the tidal residual transport (Fig. 2). This is an effect of both the higher SPM concentrations throughout the water column and the large effect of the storm on the direction of the residual water transport. Most of the time the tidal residual transport is northward, except for northerly storms. Peaks of northward transport are related to southerly and westerly storms. The balance between northerly and southerly/westerly storms during a certain year seems to determine the residual transport of SPM. For the transport in the cross-shore direction, upwelling and downwelling due to wind and tidal straining are possibly important processes (De Boer *et al.*, 2009). The 2-years time-series will be used to identify the upwelling and downwelling events, and their effect on the cross-shore transport. The question is, are these processes in balance at this location, or is there still accumulation of SPM occurring in the TMZ at this distance far from both the SPM source and the River Rhine outflow? In the presentation, we will further examine the role of these processes.

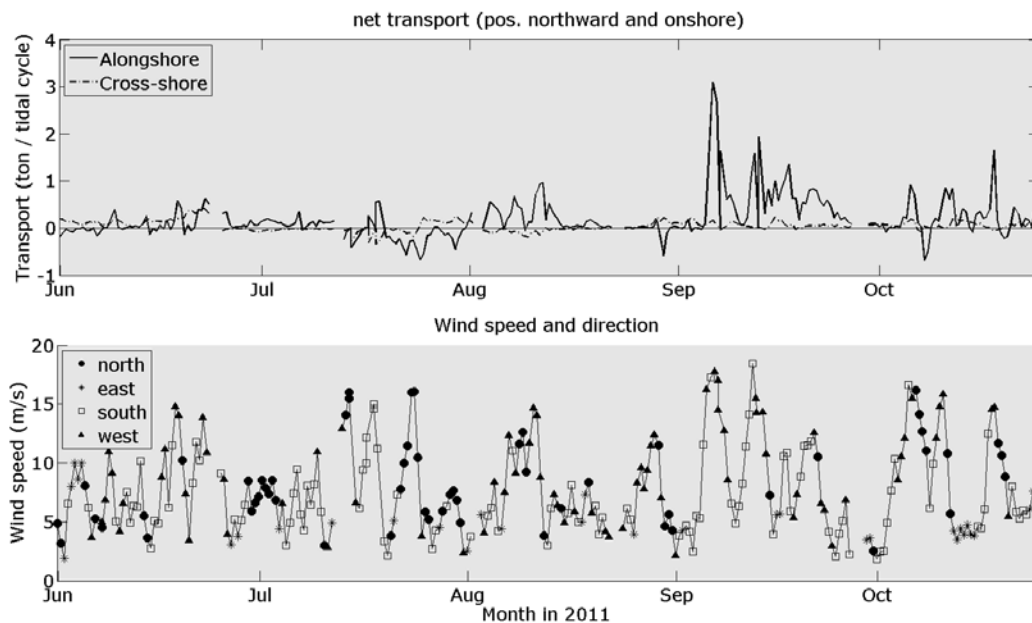


Fig. 2. Top: First results of tidal net longshore and cross-shore transport in the near bed layer at the lander location for a 5-month period. Bottom: Tidally averaged wind speed (vertical axis) and direction (various markers).

Acknowledgements

The authors would like to acknowledge Rijkswaterstaat, Foundation LaMER and Ecoshape for financial support of the monitoring program. The captains and crews of the research vessel Pelagia and of the Coast Guard Vessel Hr. Ms. Terschelling are thanked for their contribution to the data collection.

References

- De Boer G.J., J. Pietrzak and J.C. Winterwerp. 2009. SST observations of upwelling induced by tidal straining in the Rhine ROFI. *Continental Shelf Research* 29:263-277.
- Fettweis M., B. Nechad and D. Van Den Eynde. 2007. An estimate of the suspended particulate matter (SPM) transport in the southern North Sea using SeaWiFS images, *in situ* measurements and numerical model results. *Continental Shelf Research* 27(10-11):1568-1583.
- Lacroix G., K. Ruddick, J. Ozer and C. Lancelot. 2004. Modelling the impact of the Scheldt and Rhine/Meuse plumes on the salinity distribution in Belgian waters (southern North Sea). *Journal of Sea Research* 52:149-163.
- Van der Hout C.M., T. Gerkema, J.J. Nauw and H. Ridderinkhof. (subm.). Observations of a narrow zone of high suspended particulate matter (SPM) concentrations along the Dutch coast. In revision at *Continental Shelf Research*.

A glider in the plume: an innovative approach to investigate and simulate the fate of Rhône River sediment in the Gulf of Lions during the 2014 winter flood

Verney Romaric¹, Gael Many², Aurelien Gangloff¹, François Bourrin², David Doxaran³, Ivane Pairaud⁴, Matthias Jacquet¹ and David Le Berre¹

¹ Laboratoire DYNECO/PHYSED, IFREMER, PO Box 70, 29280 Plouzané, France
E-mail: romaric.verney@ifremer.fr

² CEFREM, UMR CNRS 5110 - UPVD, 52 Avenue Paul Alduy, 66860 Peprignan Cedex, France

³ Observatoire Océanologique, Laboratoire d'Océanographie de Villefranche, UMR 7093 - CNRS/UPMC, 181 Chemin du Lazaret, 06230 Villefranche sur Mer, France

⁴ LERPAC, IFREMER, Zone Portuaire de Bregailon, CS20330, 83507 La Seyne sur Mer, France

Context

The fate of riverine sediments in Mediterranean coastal environments is driven by two mechanisms: direct transfers associated to the plume dynamics and indirect transfers related to sediment resuspension by storms. Quantifying and modelling sediment fluxes in the Gulf of Lions first require to better observe and understand these mechanisms. Usual but not trivial observations have been collected over the last decades in the Gulf of Lions, and especially close to the Rhône River prodelta: the deployment of the MESURHO fixed observatory, many *in situ* optical and physico-chemical profiles operated from research vessels, towed instrumented vehicles or autonomous floats, the analysis of remote sensing ocean colour data. While all these observations are fully complementary and crucial for our understanding of coastal dynamics, they fail to provide necessary repeated observations, over the full water column, along cross shore or longshore transects. The TUCPA project aimed to i) investigate the interest in deploying gliders within the Rhône River plume, ii) examine with an innovative approach the plume dynamics during a significant flood event ($Q > 5000 \text{m}^3 \cdot \text{s}^{-1}$), iii) improve our modelling results on the area.

Methods

A SLOCUM coastal glider, equipped with a CTD, O₂ sensor and optical backscatter sensors at 532, 700 and 880nm, was deployed for two weeks from January, 30th to February 14th 2014, undulating from top to bottom along a North/South transect from the Rhône River mouth to the continental shelf break (a full transect is completed in 2 days approximately). In parallel to these autonomous real time measurements, two field campaigns were conducted at the beginning and end of the glider deployment to measure additional SPM features and validate glider observations. Profiles with an optical grape (optical backscattering sensors, LISST100X and LISST HOLO and CTD) were realized along the glider transect and also further within the plume. Meantime water samples were also collected close to the bed and near the surface for SPM characterization (microfloc / primary particle distribution, mass concentration, chlorophyll a concentration).

The MARS3D hydrodynamic and sediment transport model was implemented in the Gulf of Lions in order to investigate and quantify SPM fluxes and the role of extreme meteorological and hydrological events. This model is based on a regular 1.2km grid, and is forced by daily measured water and solid river discharges, METEOFRACTANCE ARPEGE model wind results and WAVEWATCH3 wave fields. This model reproduces the coastal circulation, and especially the surface plume dynamics. The sediment processes are simulated using the MIXSED module (Le Hir *et al.*, 2011) with 4 sediment classes (2 sands, 2 muds). Flocculation processes are reproduced using the Krone/Van Leussen formulation, with variable settling behaviour for each mud class. The bed sediment distribution is initialized from grab samples collected over the last decades.

Results and conclusions

The glider was operated during the largest flood event measured during winter 2014, reaching $5000 \text{m}^3 \cdot \text{s}^{-1}$ on February, 11th. This flood generated a well-defined surface plume, up to 20m thick close to the coast (against few meters during low river discharge), characterized by usual decreasing suspended solid concentrations from coast to shore. Moreover, this plume was observed 50km off shore, with significant concentrations (above $10 \text{mg} \cdot \text{l}^{-1}$) 20km off shore. A nepheloid benthic layer was also observed on the entire continental shelf, featured by strong temporal and cross-shore thickness variability. These preliminary results are confronted with the model results, both in terms of surface concentration, plume metrics (covered area, central position, distance to the coast, plume thickness) evaluated from glider and MODIS ocean colour observations. The model

is also used to evaluate fluxes through embedded zones from the prodelta region to the Gulf of Lions.

The TUCPA experiment demonstrated the feasibility of tracking sediment dynamics in coastal regions from gliders, and the great potential of such measurements to observe sediment patterns in coastal seas. This approach will be further investigated in the MATUGLI project (2014-2017) combining optical and acoustic approaches to evaluate sediment structures and sediment fluxes.

References

Le Hir P., F. Cayocca and B. Waeles. 2011. Dynamics of sand and mud mixtures: A multiprocess-based modelling strategy. *Continental Shelf Research* 31(10):S135-S149.
doi:10.1016/j.csr.2010.12.009.

Influence of hydrodynamics on sediment characteristics: comparison between two tidal flats

Wang Xianye¹, Bram van Prooijen², Qin Zhu¹ and Qing He¹

¹ State Key Laboratory of Estuarine and Coastal Research
East China Normal University, Shanghai 200062, P.R. China
E-mail: xywang@sklec.ecnu.edu.cn

² Department of Hydraulic Engineering
Delft University of Technology, Stevinweg 1, 2628 CN Delft, the Netherlands

Introduction

Interaction between hydrodynamics and sediment is a complex issue in tidal flat. The various tidal processes can influence the sediment transport (Winterwerp, 2011), and also the sediment behaves differently in settling and consolidation aspects (te Slaa *et al.*, 2013). In this study, combined with the methods of field measurements and laboratory tests, a series of experiments have been carried out in two different tidal flats, i.e. Kapelle bank in Western Scheldt, the Netherlands and the Chongming Dongtan in Yangtze River, China.

Methods

First, through arranging instrument in field to investigate the in-situ hydrodynamics, such as: velocity, wave, suspended sediment concentration etc. Secondly, collect sediment of bed surface and carry out laboratory test to obtain the sediment characteristics, such as: water content, grain size distribution, and rheology etc. Finally, combined the results both in field and laboratory, quantifying the influence of hydrodynamics of on sediment characteristics and behaviours.

Results

Field measurements

In this study, the result of the field measurement shows the flow and sediment processes in the tidal flat of Kapelle bank (as shown in Fig. 1). And it is a prerequisite to analyse the sediment characteristics. The rose diagram depicted was measured by an up-looking Nortek Aquadopp, the time interval is 300s, and the sampling positions were 1m above the bed. It shows that the sand component of the sediment close to the shore is more than the others. And the median diameter in west is larger than that in east. This may be caused by the flow and the sediment net transport during the flood and ebb.

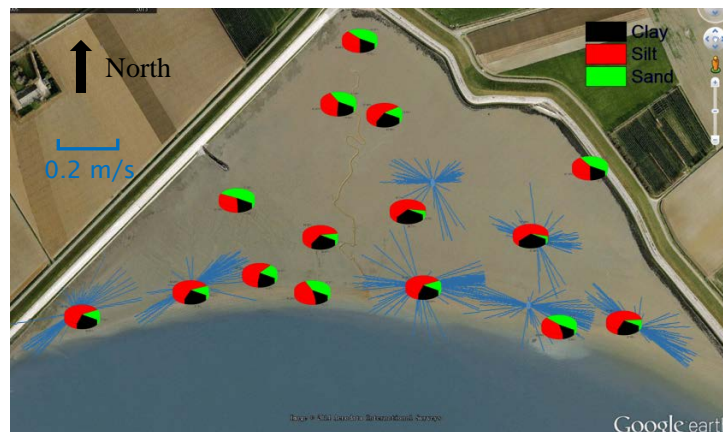


Fig. 1. The flow and sediment distributions in Kapelle bank (May 14, 2014 23:00-May 15, 2014 09:00).

Laboratory experiments

A series of experiments have been conducted to reveal the inherent properties of the sediment, for instance, the settling test of sediment in Kapelle bank has been carried out using the solution of the flocculant of BASF Zetag with the mass concentration 0.25g/L. The solution is mixed with the suspended sediment with the concentration of 60g/L in a cylinder which has the capacity of 250ml. With the time elapses, the settling interface between water and sediment then has been recorded to estimate the settling velocity of the sediment. It can be seen from Fig. 2 that the flocculant can

accelerate the settling when the concentration is less than 0.03g/L, then with the increase of the flocculant it can slow down the settling velocity. In addition, the corresponding experiments using the sediment of Chongming Island are in progress.

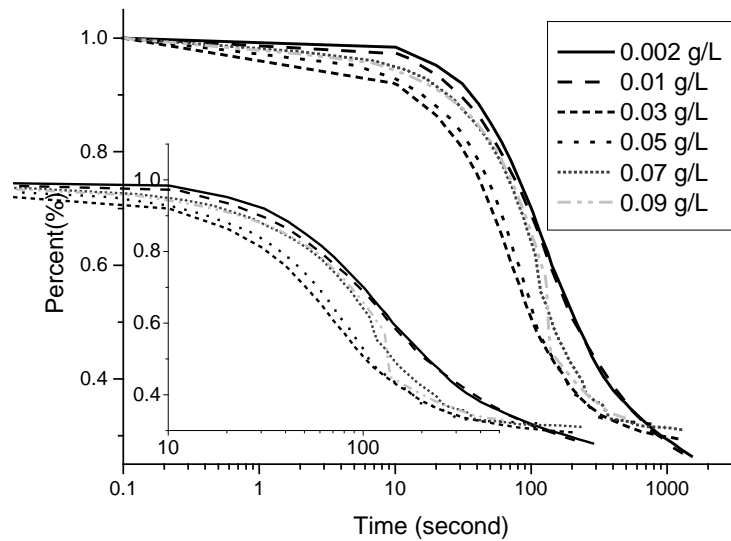


Fig. 2. The effects of different concentrations of the flocculant on sediment settling (Zetag 7587).

Acknowledgements

The first author (X.Y. Wang) is supported by the project 'Fate or Future of Tidal Flats in Estuaries and Tidal Lagoons' (project number: 842.00.007h) which is funded by the Netherlands Organisation for Scientific Research (NWO) within the programme 'Joint Scientific Thematic Research Programme' (JSTP), and also is financially supported by State Key Laboratory of Estuarine and Coastal Research (SKLEC). We also acknowledge Prof. Johan C. Winterwerp, Dr. Claire Chassagne, Dr. Miguel de Lucas Pardo, Ms. Maria Ibanez Sanz, Mr. Leon van Paassen, Mr. Arno Mulder, Mr. Sander de Vree, Mr. Jaap van Duin and Mr. Tonny Schuit for assisting with discussion and measurements in TUDelft.

References

- te Slaa S., Q. He, D.S. van Maren and J.C. Winterwerp. 2013. Sedimentation processes in silt-rich sediment systems. *Ocean Dynamics* 63(4):399-421.
- Winterwerp J.C. 2011. Fine sediment transport by tidal asymmetry in the high-concentrated Ems River: indications for a regime shift in response to channel deepening. *Ocean Dynamics* 61(2-3):203-215.

The paradigm of coagulation processes of polystyrene latex particles

Zhang Jinfeng¹, Qinghe Zhang¹ and Jerome P.-Y. Maa²

¹ State Key Laboratory of Hydraulic Engineering Simulation and Safety Tianjin University, Tianjin 300072, P.R. China
E-mail: jfzhang@tju.edu.cn

² School of Marine Science, College of William and Mary, Department of Physical Sciences, Virginia Institute of Marine Science, Gloucester Point, VA 23062, USA

Introduction

In many industrial processes and natural environments, colloidal particles are coagulated in turbulent flows. While turbulent shear is a primary mechanism by which flocs can form and increase their size, it is also believed that turbulent shear is responsible for limiting the maximum size that aggregates can attain, van Leussen (1994).

Many studies show that there is a critical value on the shear rate, G^* , when $G \leq G^*$, the floc size increases with the shear rate and when $G > G^*$, the floc size decreases as G further increases. The critical value G^* depends on the residence time and flocculation behaviour (Mietta *et al.*, 2009). To explain why the floc size is small at low shear rates (Winterwerp, 1998) suggests that it is due to settling-out of large floc from the study domain which means a limited residence time of floc in low turbulent flows. To verify this hypothesis, i.e. when excluding sedimentation process, the equilibrium floc size should decrease monotonically with increasing shear rate, even when G is small. Mietta *et al.* (2009) carried out a lab experiment that uses latex particles, which has the same density of that for the ambient fluid to eliminate sedimentation, to support this explanation. However, Colomer *et al.* (2005) argued that this would produce very large aggregates at small shear rates with the paradoxical result of huge aggregates at no shear. They also carried out an experimental investigation of coagulation of latex particles and they found that at low shear rate ($0.7 \leq G \leq 27.36s^{-1}$) aggregation dominates over breakup, and thus, the median aggregate size increases with G . This is an opposite finding when compared with that from Mietta *et al.* (2009). The difference between these two sets of lab experiments are the primary particle sizes ($10\mu m$ versus $2\mu m$) and experimental devices (mixing jar versus oscillating grids). To clarify why there is a different conclusion is the objective of this study.

Numerical model

A three-dimensional lattice Boltzmann (LB) model for flocculation processes of fine sediment is adopted. Details of the LB method for flocculation process of cohesive sediment in homogenous turbulent flows can be found in Zhang *et al.* (2013). The aggregate size is a dynamic property depending on the rates of aggregation and breakup. Shear strength of the aggregate is of great importance to the flocculation processes of colloidal particles.

The rate of breakup of flocs and the equilibrium size of flocs in turbulent flows depend on their strength F_c . Winterwerp (1998) suggested:

$$F_c = \frac{\pi}{4} d_f^2 \tau_B \quad (1)$$

where d_f is the floc size and τ_B is the yield stress, which is defined as, Tang *et al.* (2001):

$$\tau_B = 1.1 \frac{(d_f / d_0)^{D_f - 3}}{1 - (d_f / d_0)^{D_f - 3}} \left(\frac{F}{d_0^2} \right) \quad (2)$$

where d_f is the floc size, D_f is the fractal dimension of the floc. F is the binding forces between particles, including the van der Waals attractive force, electrostatic repulsive force, and lubrication force. When the external force, F , such as the shear force of the fluid imposed on the floc is larger than the floc strength F_c , it will break up.

Results and conclusions

A fully resolved simulation of coagulation processes of colloidal particles in aqueous solutions is presented based on the lattice Boltzmann method. In this study, the objective is to simulating what has been done by Colomer *et al.* (2005) with the following conditions: suspensions of latex particles are prepared in a 1.29 M NaCl solution in ultrapure water with an initial particle volume concentration of 5.0×10^{-5} ; Latex particles have a diameter of $2\mu m$ and a density of $1055 kg/m^3$; A shear range between 0.7 and $70s^{-1}$ is selected by means of mimicking an oscillating-grid. An extra

size of latex particles (i.e. 10 μ m) will be added to check if the primary particle size is an affecting factor. The sedimentation mechanism is irrelevant because the density of the solution is the same as that of the particles. This implies an unlimited residence time during the coagulation processes. The interactions between solid particles and turbulence, solid particles and solid particles are considered to directly simulate the collision and cohesion processes of latex particles in the turbulent flows. The development of floc size distribution is simulated at the steady-state of coagulation and breakup processes. An additional simulation by changing the ambient fluid density will be investigated to check the effect of the residence time on the flocculation process.

References

- Colomer J., F. Peters and C. Marras. 2005. Experimental analysis of coagulation of particles under low-shear flow. *Water Res.* 39(13):2994-3000.
- Mietta F., C. Chassagne and J.C. Winterwerp. 2009. Shear-induced flocculation of a suspension of kaolinite as function of pH and salt concentration. *Journal of Colloid and Interface Science* 336(1):134-141.
- Serra T., J. Colomer and B.E. Logan. 2008. Efficiency of different shear devices on flocculation. *Water Res.* 42:1113-1121.
- Tang S., Y. Ma and C. Shiu. 2001. Modelling the mechanical strength of fractal aggregates. *Colloids and surfaces. A: Physicochemical and engineering aspects* 180(1):7-16.
- Van Leussen W. 1994. Estuarine macroflocs and their role in fine-grained sediment transport. *Ph.D. Thesis*, University of Utrecht, the Netherlands.
- Winterwerp J.C. 1998. A simple model for turbulence induced flocculation of cohesive sediment. *Journal of Hydraulic Research, IAHR* 36(3):309-326.
- Zhang J.F., Q.H. Zhang, J.P.Y. Maa and G.Q. Qiao. 2013. Lattice Boltzmann simulation of turbulence-induced flocculation of cohesive sediment. *Ocean Dynamics* 63(9-10):1123-1135.